Fifty Shades of Brown: Variability of Dissolved Organic Matter in Forested Streams across Spatial and Temporal Scales

by

Julia Orlova

A thesis submitted in partial fulfillment of the requirements for the degree of

Doctor of Philosophy

in

Water and Land Resources

Department of Renewable Resources
University of Alberta

Abstract

Dissolved organic matter (DOM) in stream water plays a critical role in shaping aquatic ecosystems, influencing water quality and acting as a food source to microorganisms, and affects drinking water treatment. Understanding variations in the concentration and composition of DOM and environmental controls on DOM is crucial for predicting the effects of climate change and land use on changes in stream DOM. Yet, with so many factors potentially affecting DOM and vast differences among forested regions, our understanding of DOM in streams across the boreal region is incomplete. The three studies (Chapters 2-4) in this thesis were designed to further our understanding of variations in and controls on stream DOM across spatial and temporal scales of heterogeneous forested regions.

Chapter 2 examines stream DOM at a sub-continental scale. Using a combination of analytical techniques, including absorbance and fluorescence spectroscopy, liquid chromatography, mass spectrometry, and flow field-flow fractionation, we analyzed DOM composition in 52 streams across six forested ecozones in Canada. I discovered three primary axes of variation in DOM composition: DOM aromaticity, driven by the abundance of wetlands; DOM oxygenation, related to variations in climate; and biopolymer content, linked to the presence of lakes in catchments. Although DOM composition varied greatly seasonally and among the streams within the same ecozone, inter-site variability in DOM composition was often greater than intra-site and temporal variations, suggesting the profound influence of landscape and climatic characteristics.

Chapter 3 focuses on a single ecozone, the Boreal Plains, which is differentiated from other boreal regions by its flat terrain, subhumid climate and heterogeneity in glacial deposits resulting in complexity of surface water – groundwater interactions and variable hydrologic connectivity of

terrestrial sources to streams. This chapter examined DOM concentration and composition in 17 forested streams. Spatial variations in stream DOM at the regional scale arose from the presence of lakes, as well as coarse-grained surficial geology, associated with reduced DOM concentration and aromaticity. Temporally, distinct trends emerged, including increases in DOM throughout the summer season, likely tied to soil warming that promotes decomposition of organic matter, and short-term dilution or flushing related to storm events, and declines during droughts. The results suggested that even at the regional scale, variations in stream DOM concentration and composition were substantial and could be predicted based on catchment characteristics, hydrology and season.

Finally, Chapter 4 shifts the focus from terrestrial sources of DOM to aquatic processes that transform DOM – photodegradation and biodegradation. Changes in DOM concentration and composition due to these processes were studied in water from five Boreal Plains streams using laboratory incubations. Photodegradation was particularly influential, aligning stream samples more closely with lake DOM composition, revealing the importance of this process for DOM transformation in the Boreal Plains streams, as well as emphasizing the importance of lakes in this landscape.

Collectively, these studies underscore the large variability in stream DOM at sub-continental and regional scales and contribute valuable insights into the controls of stream DOM composition. At all scales, they highlight the importance of lakes and wetlands in a catchment, and temperature. The differences in terrestrial sources of DOM and in-stream processing have implications for carbon cycling, downstream water quality and treatability.

Preface

This thesis is a result of a collaborative effort that advanced our understanding of variations in aquatic dissolved organic matter in forested catchments. The three studies are currently under review or in preparation to submission to peer-reviewed journals. All studies were designed primarily by DO and JO. JO led field data collection, conducted select laboratory analysis, analyzed and visualized data, and prepared draft manuscripts. Other co-authors contributed to water sampling, sample analyses, data interpretation and draft revisions, as well as access to research sites and resources. In particular, several analyses of water samples were possible thanks to FA (DBP-FP), CC (AF4), RH (FT-ICR-MS). The pan-Canadian DOM study (Chapter 2) would not have been possible without ME and US, as well as many partners, who created the *for*Water Network. I'd also like to acknowledge Julie Grant at the University of Waterloo for her assistance with creating the conceptual ecozone figure in Chapter 2 and its Boreal Plains ecozone version in Chapter 3.

Chapter 2: Orlova, J., Amiri, F., Bourgeois, A.K., Buttle, J.M., Cherlet, E., Cuss, C.W., Devito, K. J., Emelko, M. B., Floyd, W. C., Foster, D. E., Hutchins, R. H. S., Jamieson, R., Johnson, M. S., McSorley, H. J., Silins, U., Tank, S. E., Thompson, L. M., Webster, K. L., Williams, C. H. S., and Olefeldt, D. (2024). Composition of stream dissolved organic matter across Canadian forested ecozones varies in three dimensions linked to landscape and climate [manuscript under review by *Water Resources Research*].

Chapter 3: Orlova, J., Devito, K. J., Tank, S. E., and Olefeldt, D. (2024). Seasonal temperature trend overrides the effect of discharge on dissolved organic matter in the Boreal Plains streams. [manuscript in preparation for submission to *Hydrologic Processes*].

Chapter 4: Orlova, J., Tank, S. E., Devito, K. J., Amiri, F., Emelko, M. B., and Olefeldt, D. (2024). The role of aquatic DOM transformations in shaping DOM character and drinking water treatability in boreal streams [manuscript in preparation for submission to a scientific journal].

Acknowledgement

I am most grateful to my supervisor, Dr. David Olefeldt, who entrusted me with several research ideas and resources to make my dream of doing science come true. Working with David and learning from him has been a pleasure and a privilege. I am sincerely grateful to my committee members, Dr. Kevin Devito and Dr. Suzanne Tank, for their generous advice, support, wisdom and numerous reference letters for my scholarship and job applications. I am honored to have conducted my research at the URSA, and my hope is that this long-term research site lives on and produces many more interesting studies.

A profound thank-you to the NSERC's *for*Water Network for funding my research project and allowing me to attend the AGU conference, the HQP training weeks and other meetings, which were great learning and networking opportunities, and significantly enriched my overall PhD experience and inspired me to learn about areas that fall outside of my PhD project, such as forestry and drinking water treatment. I got to meet and collaborate with many researchers across Canada, and feel extremely fortunate to have been a part of the Network.

I am very grateful for the funding I received through the UAlberta North, which helped cover my field work expenses. I am also grateful for the scholarships from the University of Alberta and the Government of Alberta (AGES).

Thank you very much to all current and former undergraduate and graduate students in CAWS lab for the help with field data collection, especially Garret Malishewski, Renae Shewan, Christopher Schulze, Lauren Thompson, Emily Pugh, Becca Frei. A special thanks to Allan Harms with NRAL for analyzing and re-analyzing hundreds of my samples.

Finally, I extend my deepest gratitude to my parents for being there for me throughout my journey. And although I am proud to have [finally] completed my program, my thoughts remain with my two grandmothers, who both passed away while I was working on the thesis, and whom I miss dearly every single day. This thesis is my tribute to their memory.

Table of Contents

List of Tables

List of Figures

1. General Introduction

1.1. Aquatic dissolved organic matter

Dissolved organic matter (DOM) is a complex mixture of organic molecules of varying size and composition (Kellerman et al., 2014). In aquatic ecosystems, DOM is generally derived from allochthonous and autochthonous sources (Thorp & Delong, 2002). The concentration and composition of DOM in surface water vary based on multiple factors, including the source of DOM and aquatic transformations (e.g., Voss et al., 2023). DOM regulates many aquatic ecosystem functions, fuels food webs, and influences drinking water treatability (e.g., Matilainen et al., 2010; Prairie, 2008; Sanders et al., 2015). The flux of DOM from land to ocean is an important component of the global carbon (C) cycle. But climate change and land disturbance have the potential to affect the amount and composition of DOM that is delivered to surface waters and transported downstream (e.g., Davidson & Janssens, 2006; Laudon et al., 2009). Due to differences in terrain, geology and climate among regions where DOM studies have been conducted, findings from one region cannot always be applied to other regions. Despite a large number of studies of DOM conducted in different regions and at different spatial and temporal scales, our understanding of regional variations in stream DOM and controls on it, the effects of climate change and disturbances, and the role of in-stream processes is still incomplete (Ward et al., 2017).

Streams and rivers act both as a conduit of organic and inorganic C from land to the ocean and as a source of carbon dioxide (CO_2) to the atmosphere, providing up to 10% of the global CO_2 emissions (Koehler et al., 2014). During transport DOM is altered or mineralized to CO_2 via microbial respiration and photochemical processes, and it is still unclear which process is more important (Cory et al., 2014; Demars, 2019). Lakes are known as hotspots for organic matter turnover (Evans et al., 2017), but streams historically were referred to as passive pipes. However,

some estimates show that the role of streams and rivers is still significant (Cole et al., 2007), despite their small area, as they contribute 1.8 Pg C per year to the atmosphere (Raymond et al., 2013; Wallin et al., 2013). In comparison, annual riverine export of C to the oceans is approximately 0.95 Pg C, with just over half of it in the organic form (Bauer et al., 2013). Quantification of C fluxes at different scales is ongoing research.

Aside from its importance for global C cycling, DOM has multiple functions in aquatic ecosystems. It is a food source; it controls light and temperature regime, transport and bioavailability of nutrients and contaminants (e.g., Aiken et al., 2011; Rivera Vasconcelos et al., 2018). In drinking water systems, OM affects the performance of treatment processes, contributes to undesirable odor and taste, and is a disinfection by-product precursor (Sillanpää, 2015). We need to characterize and quantify OM, if we want to understand its properties and behavior in surface waters.

Chemical diversity of DOM makes its characterization a complex task. DOM is commonly characterized based on molecular size, but the size boundaries are not formally accepted and vary based on specific applications and analytical techniques used for characterization. In environmental studies, DOM is often distinguished from particulate organic matter (POM) using 0.45 μm filtration (Zsolnay, 2003). At the same time, the OM fraction of 0.001-1 μm is referred to as colloidal, and the one <0.1 μm as nanoparticles (Lead & Wilkinson, 2006). Although different size fractions have different composition and behavior (e.g., bioavailability) in aquatic ecosystems, due to constant interactions between the fractions (that are still poorly understood), the distinction is, perhaps, qualitative. While POM may constitute a significant proportion of stream OM in catchments with high soil erosion (Quinton et al., 2010), most of the organic C pool in surface waters is present as dissolved fraction (Attermeyer et al., 2018), which is the focus of this thesis.

In addition to size, multiple analytical techniques have been developed to describe DOM with respect to its molecular, structural and isotopic composition (McCallister et al., 2018). Different methods provide insights into different properties of DOM, although differences in techniques make comparisons between studies difficult. Optical techniques that assess light absorbing and fluorescing properties of DOM have become increasingly popular in environmental and water treatment research due to their relative simplicity, affordability, and valuable insights into DOM composition (Chen & Yu 2021). In particular, the commonly used algorithms to process 3D excitation-emission matrices (EEMs), peak-picking and parallel factor analysis (PARAFAC), allow identifying fluorescent components with distinct characteristics that can be used to assess the sources and fate of DOM. However, optical spectroscopy has limitations: it only assess DOM that absorbs light (coloured – or chromophoric – dissolved organic matter, CDOM) and/or fluoresces (FDOM), there can be interference from other solutes (e.g., Fe) and it is sensitive to changes in pH (e.g., Groeneveld et al., 2022; Poulin et al., 2014).

Despite the multitude of tools available for DOM characterization, there is still much work to be done in understanding the differences in aquatic DOM concentrations and composition across different physiogeographic regions. DOM is a function of multiple environmental factors (including climate and various stream and catchment characteristics, like topography, landcover, land disturbance) and varies over different scales and seasons. Studies of stream DOM conducted in different regions and at different temporal and spatial scales often examined and found different controls important. DOM studies conducted at larger scales are few and far between (e.g., Aukes et al., 2021; Jaffé et al., 2008, 2012). Many findings may not be directly transferrable to other regions, for instance, due to the differences in study design, methods and environmental conditions, which necessitates more regional studies and comparisons between regions.

The effects of climate change on terrestrial and aquatic ecosystems have been observed in many parts of Canada (Bush & Lemmen, 2019). To predict the response of stream DOM to climate change and land disturbance, we need to characterize its variability across spatial and temporal scales and to identify controls that determine its concentration and composition. Thus, the overarching goal of this thesis is to describe current DOM concentrations and composition using different analytical techniques in a range of streams draining diverse landscapes in Canada. My thesis assesses the importance of environmental controls on stream DOM going from sub-continental to regional scale, and contrasts the Boreal Plains ecozone, which occupies a large portion of Western Canada, to other forested regions, including two boreal regions where DOM has been studied extensively (Scandinavian Shield and Boreal Shield). It continues to build on our knowledge of aquatic DOM in the Boreal Plains (Olefeldt et al., 2013a; Pugh, 2021), and fill the gap with respect to seasonal and spatial variations in stream DOM, as well as DOM lability. The results of my thesis will allow predicting potential shifts in stream DOM as temperatures rise, hydrology and landcover change.

1.2. Aquatic transformations of DOM

Our understanding of variations in stream DOM will be incomplete without consideration of aquatic transformations of DOM. DOM delivered to lakes and streams is partly reactive, and changes in concentration and composition as it moves through the stream network (Berggren et al., 2022). Reactivity can be defined as the rate of transformation or turnover. Based on reactivity potential, DOM is frequently described as labile or recalcitrant (Guillemette & del Giorgio, 2011), although the use of the latter term has been disputed (Kleber, 2010). Headwater streams are considered hotspots for DOM degradation (Palmer et al., 2016). DOM can be lost via mineralization (as a result of sunlight irradiation and microbial respiration), flocculation, sorption

onto mineral particles and sedimentation (e.g., Berggren et al., 2017; von Wachenfeldt & Tranvik, 2008). Water residence time has been used to predict DOM turnover (Catalan et al., 2016). Short residence times in forested headwater streams may allow for little transformation (Kothawala et al., 2015); although fast turnover rates have been reported for unshaded streams (Cory et al., 2014). In regions with flat topography, like the Boreal Plains ecozone, diffuse flow though peatlands over large areas likely allows for long residence time in comparison with primarily channel flow in other regions. As DOM moves downstream, the composition shifts from more aromatic in the headwaters to more aliphatic in larger rivers, and variability in DOM composition decreases (Creed et al., 2015). To predict the fate of aquatic DOM in surface waters, we need to understand its reactivity.

Aquatic DOM processing is dependent on a range of intrinsic (i.e. composition) and extrinsic (i.e. environment) controls (Berggren et al., 2022). The composition of DOM is a function of its source. While DOM is an energy source for heterotrophic microbes (Wetzel, 1995), not all DOM is biolabile. Microbes preferentially utilize low-molecular-weight molecules, like sugars and organic acids (e.g., Amado et al., 2015; Benner & Kaiser, 2011), but photochemical transformation of DOM can change DOM bioavailability (Vähätalo & Wetzel, 2004). Coloured DOM is photolabile, although non-coloured DOM can be phototransformed indirectly via photosensitized reactions (Sulzberger & Durisch-Kaiser, 2009). The loss of colour is called photobleaching. The rate of DOM degradation cannot be explained just by its composition, and environmental conditions have to be considered (Catalán et al., 2021). Intrinsic and extrinsic controls are interdependent; for example, potential reactivity of DOM may not be realized due to environmental limitations (e.g., temperature, suitable microbial community, nutrient and light availability). We should expect to see differences in aquatic DOM degradability in contrasting

environments. Thus, regional studies can provide insight into the importance of different controls for instream transformation of DOM.

To quantify the rate of DOM photodegradation, researchers measure absolute and relative changes in dissolved organic carbon (DOC), mineralization of DOC per unit of absorbed light energy (Bertilsson & Tranvik, 2000), and the apparent quantum yield (AQY), which quantifies wavelength effect on dissolved inorganic carbon (DIC) photoproduction (Johannessen & Miller, 2001). By removing the effect of optical density, the latter two approaches allow comparing photolability of DOM from different sources, and can be used to model CO_2 emissions across large areas. Microbial uptake and mineralization of DOM is often assessed through dark incubation experiments over periods ranging from hours to days to months (Vonk et al., 2015); biofilm reactors have been used to accelerate the process (Volk et al., 1997, Bowen et al., 2020). Biodegradable DOC (BDOC) can be assessed using DOC and O_2 consumption and DIC production (Vonk et al., 2015). It can be hard to compare bioavailability of DOM between incubation studies that are designed differently, e.g., use different temperature, duration, filtration (0.2-0.7 μm, or no filtration) and inoculum. Although laboratory incubations do not accurately represent field conditions, the results can be a useful measure of DOM photo- and bioreactivity, and can answer questions about the role of different transformation processes and potential responses to changing environmental conditions, which is particularly important for regions that may be vulnerable to climate change and land disturbance.

1.3. Regional studies of DOM

A large portion of aquatic DOM research in forested catchments has been conducted in in Scandinavia (especially the Krycklan Catchment Study; Laudon et al., 2021), the UK, Ontario and Quebec (e.g., de Melo et al., 2023; Eimers et al., 2008; Worrall et al., 2012). Most of these regions

are characterized by relatively humid climate, high relief, igneous or metamorphic bedrock and shallow soils. Differences in aquatic DOC concentration and composition, and multiple controls on DOM across different spatial and temporal scales have been observed in these regions. One of the most significant discoveries is that wetland-dominated and forest-dominated catchments behave differently during hydrologic events (snowmelt and rain events). A negative relationship exists between DOM concentration and discharge in wetland-dominated streams, as organic-rich wetland water is diluted by rain water, and a positive relationship exists in forest-dominated catchments, where DOM is flushed from riparian areas into streams during rain events (Laudon et al., 2011). Although the physics of the processes are the same everywhere, their relative importance may vary. These variations may influence the functioning of aquatic ecosystems, downstream water use (e.g. drinking water treatment), and sensitivity to land disturbance and climate change.

The influence of landcover is not limited to hydrologic events. Wetlands are known as major sources of aromatic DOM to streams (e.g., Ågren et al., 2008; Creed et al., 2008), while upstream lakes typically reduce the concentration and aromaticity of DOM (e.g., Kothawala et al., 2014; Larson et al., 2007). Some studies also reported relationships between DOM and various catchment properties, such as area and slope (e.g., Frost et al., 2008; Kothawala et al., 2015). Antecedent moisture conditions and temperature influence seasonal changes in DOM concentration (Tiwari et al., 2022; Wallin et al., 2015). At larger scales, differences in climate may come into play (Winterdahl et al., 2014). The strength of relationships between DOM and various controls may vary for regions with different climates and physiogeography. Therefore, site comparisons are important as they help us understand the role of different processes and controls on aquatic DOM.

In Canada, forests occupy 3.47 million km^2, or 38% of the total land area (Natural Resources Canada, 2020). Profound variations in climatic and physical conditions (including temperature and moisture regime, geology and topography) across Canada have created diverse forested regions (or ecozones), characterized by distinct soils, tree species, prevalence of wetlands and lakes (Ecological Stratification Working Group, 1996), as well as water quality and quantity in lakes and streams draining the forests. Forests store large amount of carbon in biomass, dead plant material and soils, especially deep organic soils (Kurz et al., 2013). Healthy forests support diverse aquatic life and are sources of high-quality drinking water to communities across Canada (Emelko et al., 2011). But climate change, natural disturbance and land use may lead to more variable or deteriorated surface water quality, including altered concentration and composition of aquatic DOM. Thus, studying variations in water quality and controls on it across different regions is crucial not only to fill the gap in our understanding of carbon cycling, but also to predict and mitigate the effects on aquatic DOM and inform land management and water use.

The Boreal Plains ecozone is one of the regions where variations in DOM concentration and composition in stream water have been understudied. The Boreal Plains is a water-limited, low-relief landscape characterized by heterogeneous surficial geology and land cover, which separate it from other boreal regions (Devito et al., 2005, 2023; Hokanson et al., 2019; Stralberg et al., 2020). Sedimentary bedrock is overlain by thick glacial deposits ranging from till and clay to sand, which provide large water storage capacity. The glacial sediments are blanketed by deciduous, mixedwood or coniferous forests, which often act as water sinks, and peatlands, which are the sources of water to regional lakes and streams due to reduced evapotranspiration compared to forest stands. Low and highly variable water availability, largely flat topography, abundance of wetlands, and complex surface water – groundwater interactions in the Boreal Plains provide a

stark contrast to other boreal and temperate forested regions in Canada, including the Boreal Shield, Atlantic and Pacific Maritimes, and Montane Cordillera. Boreal forests will likely be susceptible to climate warming and climate-induced disturbances like wildfires, and we are currently unable to confidently predict changes in hydrology and water quality (Price et al., 2013; Ireson et al., 2015; Schindler & Donahue, 2006). In addition to climate change, significant industrial development (e.g., oil sands mining and *in situ* recovery, infrastructure construction, forestry and pulp mill operations), some agriculture and urban development add pressure on surface waters, and increase uncertainty about the future of surface water quantity and quality in the Boreal Plains ecozone (Squires et al., 2010). Field studies can help improve our understanding of the processes and factors that determine the hydrology and water quality on the Boreal Plains, and reduce the uncertainty associated with the climate change and land disturbance predictions across the boreal forest.

1.4. Research objectives

The overarching goal of the project was to understand seasonal and spatial variations of DOM in forested streams in Canada, and in the Boreal Plains ecozone in particular. Three studies were designed to achieve this goal. Variations in stream DOM were assessed at a range of scales – from national/sub-continental to regional, and with the changing scales changed environmental controls.

The objective of the first study (**Chapter 2**) was to characterize DOM in streams of six forested ecozones in Canada, including the Boreal Plains ecozone, using a range of analytical techniques, and to determine the drivers of DOM variability at the sub-continental scale. After learning how stream DOM compared across various Canadian ecozones, the second study (**Chapter 3**) focused on the Boreal Plains streams. The objective was to understand spatial and

temporal variations in DOM concentrations and composition in 17 streams with catchments of different size, landcover and surficial geology, sampled over 4 years. The study assessed the importance of different environmental controls on stream DOM, as well as seasonal and short-term/event changes in DOM. Variations in catchment characteristics, hydrology and climate are insufficient to explain downstream changes in DOM. Therefore, using laboratory experiments, the third study (**Chapter 4**) examined the importance of photodegradation and biodegradation for DOM loss and transformation at five Boreal Plains streams, with the objective to quantify relative and absolute changes in DOM concentrations and composition due to aquatic transformations. In addition, this study assessed the effect of the photodegradation on formation potential of several disinfection by-products. **Chapter 5** provides a synthesis of findings from the three data chapters, including the importance of different controls on variations in DOM in headwater streams, and the implications for drinking water treatability, and discusses the potential impacts of climate change and land use on stream DOM.

2. Composition of Stream Dissolved Organic Matter across Canadian Forested Ecozones Varies in Three Dimensions Linked to Landscape and Climate

Abstract

Dissolved organic matter (DOM) is a principal variable influencing aquatic ecosystem processes. The concentration and composition of DOM in streams depend on both the delivery of DOM from terrestrial sources and on aquatic DOM production and degradation. However, there is limited understanding of the variability of stream DOM composition at continental scales and the influence of landscape characteristics and disturbances on DOM across different regions. We assessed DOM composition in 52 streams at seven research sites across six forested ecozones in Canada using 25 indices derived from five analytical approaches; absorbance and fluorescence spectroscopy, liquid chromatography – organic carbon detection, Fourier-transform ion cyclotron resonance mass spectrometry, and asymmetric flow field-flow fractionation. Combined analyses showed clear clustering and redundancy across analytical techniques, and indicated that compositional variations were primarily related to three axes of DOM composition: a) aromaticity, which was greater in low-relief, wetland-dominated catchments, b) oxygenation, which was greater in colder and drier ecozones, and c) biopolymer content, which was greater in lake-influenced catchments. Variability in DOM composition among research sites was greater than variability of streams within a site and variability over time within a stream. Disturbance (forest harvesting and wildfire) had no common influence on DOM composition across research sites, emphasizing the need for regional studies. Overall, our study is a unique assessment of the variability of stream DOM composition and its drivers at a subcontinental scale, and it provides key insights for the choice and interpretation of DOM indices from various analytical approaches.

2.1. Introduction

The concentration and composition of dissolved organic matter (DOM) in surface waters influence core ecosystem functions and serve as key drivers of drinking water treatment needs and challenges. For example, in aquatic ecosystems, DOM controls temperature and light penetration (Reitsema et al., 2018), protects organisms from harmful ultraviolet (UV) radiation (Williamson et al., 1996), governs the bioavailability and mobility of trace metals, nutrients and contaminants (Aiken et al., 2011; Cuss et al., 2020; Kohler et al., 2014; van Leeuwen & Buffle, 2009), and is a primary energy source in food webs (Wetzel, 1995). In drinking water treatment, DOM typically dictates the charge of suspended particles and associated chemical coagulant demand and serves as a precursor of disinfection by-products of health concern; if it is not sufficiently removed, it can foul membranes, contribute to unpleasant taste and odor, and increase the potential for bacterial regrowth in distribution systems (Emelko et al., 2011). The concentration and composition of DOM in streams result from a mixing of distinct terrestrial DOM sources and are further influenced by the production, degradation and transformation of DOM within aquatic networks (Ward et al., 2017). The spatial and temporal variability of riverine DOM composition is thus linked to catchment characteristics, such as landcover, topography, size, and disturbances (Kothawala et al., 2014; Laudon et al., 2011). However, most studies of stream DOM composition focus on variability within specific physiogeographic regions, and less is known about controls on DOM composition between regions at continental scales, including influences of climate, geology, soil, and forest types.

DOM is a complex mixture of organic molecules that can be characterized using a variety of approaches that describe molecular size, class (proteins, carbohydrates, lipids, amino acids), structure, reactivity (aromaticity, hydrophobicity, polarity, acidity, functional groups), and

humification. Each approach for DOM analysis has different costs and complexity. Relatively simple and low-cost approaches for DOM characterization include biological and chemical oxygen demand (Erlandsson et al., 2008), elemental carbon (C), nitrogen (N) and phosphorous (P) ratios (Aitkenhead & McDowell, 2000), and indices derived from ultraviolet-visible (UV-vis) absorbance and fluorescence spectra. The molecular and structural composition of the DOM pool can also be characterized using fluorescence excitation-emission matrix (EEM) spectroscopy (Coble, 1996), mass spectrometry (Stenson et al., 2002), field-flow fractionation (Guéguen & Cuss, 2011), and size-exclusion chromatography (Chin et al., 1994; Huber et al., 2011). These techniques allow for similar or more detailed insights into the source and reactivity of DOM in aquatic systems and can help advance our understanding of the diversity and variability of riverine DOM composition. The use of multiple analytical approaches enables assessment of overlapping and unique information about DOM composition, which can inform the choice of approaches for future studies based on needs for both DOM interpretation and analysis cost/complexity (Stubbins et al., 2014).

Approximately 9% of the world's forested area is found in Canada, with distinct regions (known as ecozones) differentiated based on vegetation type, soils, geology, topography, and hydro-climate (Ecological Stratification Working Group, 1996). Each of these factors can potentially influence the concentration and composition of riverine DOM. Vegetation type is known to influence the composition of DOM in soil litter leachates, e.g., with distinct differences between coniferous and deciduous litter (Cuss & Guéguen, 2015; Thevenot et al., 2010). As DOM moves through mineral soils, there is preferential sorption, transformation and desorption, which generally leads to the loss of DOM fractions with high molecular weight, hydrophobicity and aromaticity; but these processes can be affected by soil texture, mineralogy and pH (Kalbitz et al.,

2000; Kleber et al., 2015). Wetlands are diverse ecosystems, and often deliver high concentrations of colored, aromatic DOM to streams from hydrologically connected organic-rich soils (Kothawala et al., 2015; Laudon et al., 2011), yet the extent to which they influence stream DOM is not well understood, especially with respect to regional differences. Topography and surficial geology can also influence stream DOM by influencing the relative contributions to streamflow from near-surface and deeper groundwater flowpaths (Battin et al., 2008; Jankowski & Schindler, 2019). Lakes may have regional differences in their influence on riverine DOM, as water residence times, bathymetry and trophic status change the balance between autotrophic DOM production and DOM degradation through microbial and photochemical processes (Evans et al., 2017; Larson et al., 2007; Vähätalo & Wetzel, 2004). Lastly, regional differences in climate may result in differences in production, degradation and delivery of DOM among regions. Climate influences hydrologic connectivity of terrestrial DOM sources to surface waters and aquatic processing through water residence times (Kothawala et al., 2015), as well as microbial activity (Freeman et al., 2001; Jankowski & Schindler, 2019; Pietikäinen et al., 2005),. A comparison of stream DOM across climatic regions in the United States revealed compositional differences (Jaffé et al., 2008, 2012). The diversity of forested landscapes across Canada presents an excellent opportunity to assess regional differences and controls on stream DOM composition.

Water originating in forested catchments is threatened by both natural and anthropogenic landscape disturbances in these regions (Baker, 2003; Emelko et al., 2016; Huntington et al., 2009). Forest harvesting and wildfire are the two most widespread disturbances in Canadian forests (Brandt et al., 2013); both can affect hydrology (Moore et al., 2005; Shakesby & Doerr, 2006) and downstream water quality and treatability (Carnigan et al., 2000; Emelko et al., 2011). The loss of vegetation and the surface organic layer after disturbance can alter both DOM sources and the

hydrologic processes that mobilize and deliver DOM to streams (Rhoades et al., 2019). Impacts on stream DOM concentrations and composition following disturbances can be short-lived, restricted to periods of high flow, or last for decades (Carignan et al., 2000; Emmerton et al., 2020; Webster et al., 2022; Yamashita et al., 2011). While effects on stream DOM from disturbances have been evaluated at local scales, less is known about commonalities of these effects across diverse physiogeographic settings.

Stream DOM concentration and composition and their linkages to landscape characteristics have not been systematically evaluated at the continental scale in Canada. By analyzing DOM in samples from 52 streams located at seven watershed research observatories (henceforth referred to as research sites) across six major Canadian forested ecozones using several analytical techniques, our objectives were to: 1) describe differences in stream DOM composition between regions and assess whether major sources of variability are regional (among-site), local (within-site), or temporal (within-stream); 2) determine how DOM composition relates to various regional landscape and local catchment characteristics and disturbances; and 3) compare DOM information generated from different analytical techniques, to assess which metrics best describe key dimensions of DOM variability. As such, this study provides insights needed for our understanding of terrestrial-aquatic linkages and aquatic functions and for land management and drinking water treatability.

2.2. Materials and Methods

2.2.1. Research sites, stream catchment characterization, and water sampling

We collected water samples from creeks and rivers at seven research sites located in six Canadian ecozones (Figure 1, Table 1). An ecozone is the highest level in an ecological land classification, where geologic, landform, soil, vegetative, climatic, water, wildlife and human

factors determine the broad characteristics of each ecozone on a sub-continental scale (Ecological Stratification Working Group, 1996). Most of Canada's predominantly forested ecozones were represented by a research site, and we henceforth refer to the research sites by their respective ecozone names (Figure 2-1). Broad differences in topography, vegetation and forest types, soils, surficial geology and climate among the seven research sites are summarized in Table 2-1.

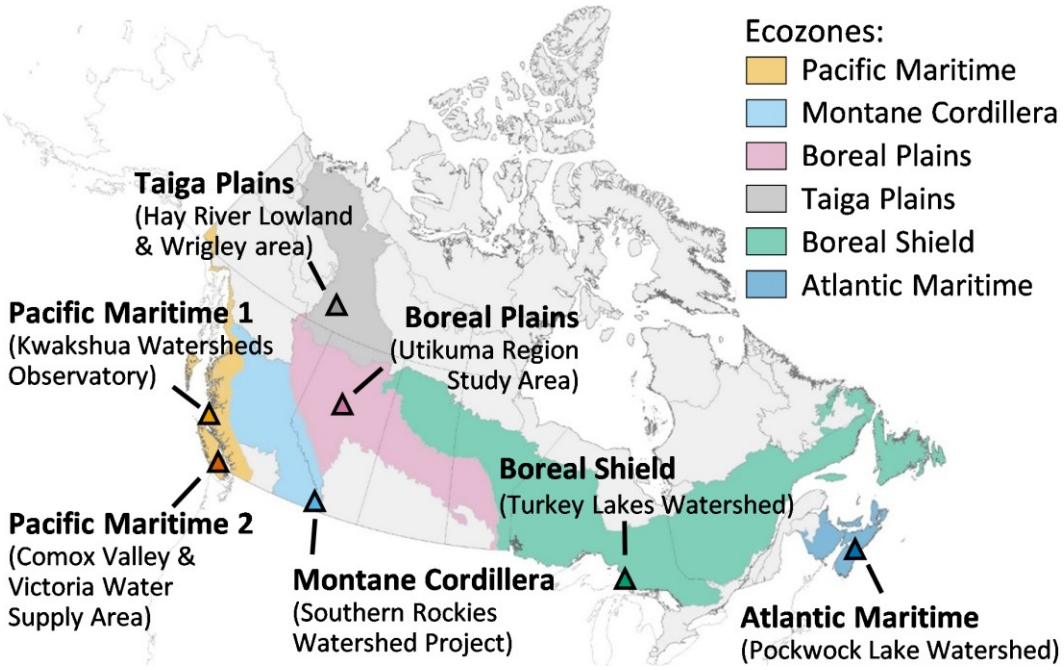

Figure 2-1. Location of the research sites within Canadian ecozones.

Between three and six streams from each research site were sampled, except for the Taiga Plains where 19 streams were sampled (Table A1). Each stream was sampled between two and ten times in 2019-2021 to capture different seasons and flow conditions, with the exception of 16 Taiga Plains streams that were sampled only once in the summer of 2019 (Figure A1). Samples were usually collected during open-water conditions; under-ice samples were only collected at the Boreal Plains site.

Streams were selected to capture the variability in landcover and surficial geology within each research site, and at least one stream from each research site (except Pacific Maritime 1) had

been extensively affected by either wildfire or forest harvesting in the last 30 years (Table A1). Catchment sizes varied between 0.05 and 1,260 km^2, with half of the catchments between 3.2 and 56 km^2. Each catchment was further characterized with respect to climate, slope, stream order, and the proportions of wetlands, open water, various soil and forest types (Tables A1 and A2). Climate parameters along with soil and forest types were extracted at the ecodistrict level from the National Ecological Framework dataset (Marshall et al., 1999). Climate variables included mean annual temperature (MAT) and climate moisture index (CMI), which was calculated as the difference between mean annual precipitation and potential evaporation (Hogg, 1997). Soil types were grouped into four broad categories: organic (humisol, mesisol, fibrisol, gleysol, organic and gleysolic cryosol), podzols (ferro-humic and humo-ferric podzols), brunisols/luvisols, and rock (bare rock and regosol). Forests were categorized as coniferous, mixed or broadleaf. For bedrock geology, we differentiated between carbonate sedimentary (Boreal Plains, Taiga Plains and Montane Cordillera) and igneous/metamorphic (Pacific Maritime, Boreal Shield and Atlantic Maritime). We classified catchments as "lake-dominated" when lake area was >4% of catchment area, and as "wetland-dominated" when wetland area was >20%. These cut-offs are similar to those used at local scales to assess the influences of lakes and wetlands on boreal stream water chemistry (Kasurinen et al., 2016; Laudon et al., 2011; St. Amour et al., 2005). Proportions of harvested (clear-cut or partial-cut) or burned areas were determined for each stream catchment based on publicly available, published or unpublished data (Table A1). Streams were classified as "disturbed" when >25% of the catchment area was burned or harvested in the last 30 years (Yamashita et al., 2011).

Table 2-1. Climatic, topographic, geologic and landcover characteristics of research sites.

Research site ID	Research site name	Topography[1]	Vegetation zone[2]	Dominant forest type[3]	Dominant soil type[3]	Surficial geology[3]	MAT[4] (°C)	MAP[4] (mm)
Pacific Maritime 1	Kwakshua Watersheds Observatory[5,6]	hilly	Pacific Cool Temperate Forest	coniferous	ferro-humic podzol (folisol)	alpine complexes, colluvial blocks	9.2	3262
Pacific Maritime 2	Comox Valley and Victoria Water Supply Area[7,8]	mountainous	Pacific Cool Temperate Forest	coniferous (mixed)	humo-ferric podzol (dystric brunisol, ferro-humic podzol)	alpine complexes, till veneer/blanket, colluvial blocks	9.7	1476
Montane Cordillera	Southern Rockies Watershed Project[9]	mountainous	Cordilleran Cool Temperate Forest and Alpine Tundra	coniferous (mixed), alpine /barren land	dystric brunisol (gray luvisol, regisol)	alpine complexes, till veneer/blanket, colluvial rubble	1.6*	1137*
Boreal Plains	Utikuma Region Study Area[10]	flat to undulating	Boreal Forest & Woodland	coniferous (mixed and broadleaf)	gray luvisol (mesisol, dystric brunisol)	till blanket, fine grained, glaciolacustrine	1.7	462
Taiga Plains	Hay River Lowland and Wrigley areas[11,12]	flat to undulating; hilly to mountainous	Boreal Forest & Woodland	coniferous (mixed and broadleaf)	eutric brunisol (organic cryosol, gray luvisol, mesisol, brunisolic turbic cryosol)	till blanket, till veneer, fine grained (glacio)lacustrine	-1.0 to -4.3	320 to 388
Boreal Shield	Turkey Lakes Watershed[13]	hilly	Eastern Cool Temperate Forest	broadleaf (mixed)	humo-ferric podzol	till blanket, till veneer, glaciofluvial plain	5.3	1041
Atlantic Maritime	Pockwock Lake Watershed[14,15]	undulating	Eastern Cool Temperate Forest	coniferous (mixed, broadleaf)	humo-ferric podzol (gleysol and mesisol)	till blanket, till veneer, rock with minor quaternary deposits	6.5	1513

Notes:

[1]Gruber (2012); [2]Baldwin et al. (2019); [3]Marshall et al. (1999);

[4]MAT = mean annual temperature, MAP = mean annual precipitation based on Canadian climate normals 1981-2010 data for the following climate stations: Addenbroke Island, Courtenay Meadowbrook, Sooke Lake North, Shawnigan Lake, Victoria Highland, High Level A, Fort Simpson A, Wabasca RS, Sault Ste Marie 2, Pockwock Lake and monthly data from 1981-2007 for Wrigley A climate station (ECCC, 2023a)

*Montane Cordillera research site climate station data (Williams et al., 2019)

[5]Oliver et al. (2017); [6]Giesbrecht et al. (2021); [7]Jackson & Blecic (1996); [8]Riddell & Bryden (1996); [9]Silins et al. (2016); [10]Devito et al. (2016); [11]Ecosystem Classification Group (2009); [12]Quinton et al. (2019); [13]Webster et al. (2021a); [14]Gorham et al. (1998); [15]Jutras et al. (2011)

2.2.2. General water chemistry analysis

Water samples for most analyses were collected in 60-mL amber glass bottles, unless stated otherwise below. These bottles were cleaned by soaking in 10% hydrochloric acid (HCl) for at least 24 hours and rinsed thoroughly with ASTM Type I (MilliQ®) water, and/or combusted at 500°C for at least 4 hours. Samples for anion analysis were collected in 60-mL plastic bottles. All bottles were rinsed with sample water prior to filling. Samples were typically filtered in the field using 0.45 µm polyether sulfone (PES) syringe filters, and then shipped in coolers with ice packs to the laboratory, where they were received within 1-5 days. Samples for elemental analyses, including dissolved organic carbon (DOC), total dissolved nitrogen (TDN) and cations (Na, K, Ca, Mg, Fe, Mn), were preserved with HCl. Samples were stored cool (4°C) prior to analysis.

The analyses of DOC, TDN, major ions and inorganic nutrients were performed at the Natural Resources Analytical Laboratory, University of Alberta. Concentrations of DOC and TDN were measured on a Shimadzu TOC-L_{CHP} Analyzer (Shimadzu Corporation, Jiangsu, China). Low DOC concentrations (<2 mg L^{-1}) were reanalyzed using the persulfate wet oxidation method on Aurora 1030W TOC Analyzer (OI Analytical, College Station, Texas, USA) with a detection limit of 0.05 mg L^{-1}. The carbon-to-nitrogen ratio (C/N) was calculated as the concentration ratio of DOC to TDN (TDN values were not corrected for inorganic nitrogen concentrations). Ammonium (NH_4^+), nitrate and nitrite ($NO_2^- + NO_3^-$), soluble reactive phosphorus (SRP), chloride (Cl^-) and sulfate (SO_4^{2-}) were determined by colorimetry (Gallery Beermaster Plus Photometric Analyzer, Thermo Fisher Scientific Inc., Vantaa, Finland). Concentrations of dissolved sodium (Na), calcium (Ca), magnesium (Mg), iron (Fe), and manganese (Mn) were measured on a Thermo Scientific™ iCAP™ 6300 Duo ICP-OES Analyzer (Thermo Fisher Scientific Inc., Cambridge, United Kingdom). Detection limits are provided in Table A3. In addition to standard laboratory quality

control checks, duplicates and MilliQ® water blanks were submitted for analyses as blind samples periodically to assess the uncertainty associated with the sampling and laboratory analysis. The pH was measured either *in situ* using different field pH meters (Boreal and Taiga Plains, and Atlantic Maritime sites) or in the laboratory at the University of Waterloo using a Fisherbrand™ accumet™ AB250 benchtop pH meter.

2.2.3. Analysis of DOM composition

We used several analytical approaches to assess stream DOM composition, including UV-vis absorbance and fluorescence spectroscopy, Fourier-transform ion cyclotron resonance mass spectrometry (FT-ICR-MS), asymmetric flow field-flow fractionation (AF4), and liquid chromatography – organic carbon detection (LC-OCD). Each method yields indices of DOM composition (Table A4) that represent either direct or indirect measures of bulk DOM properties, such as aromaticity, degree of humification, hydrophobicity, average molecular size or elemental ratios, or the relative abundance of specific DOM moieties (Chen & Yu, 2021). Not all samples were analyzed using all approaches; out of the 229 samples, 219 were analyzed for UV-vis absorbance and fluorescence, 194 for AF4, 95 for LC-OCD, and 46 for FT-ICR-MS (Figure A2).

Absorbance and fluorescence

The absorbance spectra between 200 and 700 nm were measured using a Shimadzu UV-1280 spectrophotometer (Shimadzu Corporation, Kyoto, Japan). From the absorption spectra we determined the absorbance at 254 nm (A_{254}; Dobbs et al., 1972), specific UV absorbance at 254 nm (SUVA; Weishaar et al., 2003), the ratio of absorbance at 250 and 365 nm (E2:E3; de Haan & de Boer, 1987), the spectral slope between 275 and 295 nm ($S_{275\text{-}295}$), and the ratio of slopes $S_{275–295}$ and $S_{350–400}$ (S_R; Helms et al., 2008). Iron concentrations at the research sites varied on average from 0.01 to 0.884 mg L^{-1} (Table A5). We assessed the need to correct SUVA for interference

from iron absorbance (Poulin et al., 2014), but the correction did not change SUVA values or ranking among samples sufficiently to impact our results, and we thus report uncorrected SUVA values.

Fluorescence excitation-emission spectra were measured using a benchtop fluorometer (Aqualog®, Horiba Scientific, Edison, New Jersey, USA) across excitation wavelengths of 250-480 nm (5-nm increments) and emission wavelengths of 280-500 nm (2.33-nm increments). Due to large variations in DOM concentrations and absorbance, samples with high absorbance were diluted with MilliQ® water using a maximum dilution of 2x (Kothawala et al., 2013), and with integration times adjusted to be between 0.5 and 10 s. Water Raman signal-to-noise and emission calibration validations were performed upon every run. Parallel factor analysis (PARAFAC) was performed in MATLAB® R2020a (The Mathworks, Inc.) using the drEEM-0.6.3 toolbox (Murphy et al., 2013). Sample excitation emission matrices (EEMs) were blank-subtracted, corrected for inner-filter effects, and Raman normalized. Noisy segments of EEMs (e.g., the region below the 1st order Rayleigh scatter) and outliers were removed, leaving 216 samples to develop the PARAFAC model, which was successfully split-half validated for five components (C1-C5) and matched in OpenFluor database (Murphy et al., 2013, 2014). Components C1 to C4 have been described as humic-like components, with C1 and C2 described as derived from terrestrial sources while C3 is described to be derived from microbial sources. Component C5 is associated with protein-like DOM (Table 2-2 and Figures A3 and A4).

Fluorescence data were also used to estimate the biological index (BIX) and humification index (HIX) using the drEEM-0.6.3 toolbox. The BIX is a proxy of the recent autochthonous production of DOM, and is calculated as the ratio between emission at 380 nm (β peak representing recently derived DOM), and the emission maxima between 420 and 435 nm (α peak representing

highly decomposed DOM), at an excitation of 310 nm (Huguet et al., 2009). The HIX is a measure of the degree of humification (associated with lower H/C ratios in humified organic matter), and is the ratio of fluorescence intensity at 435-480 nm and the total of fluorescence intensity at 300-345 nm and 435-480 nm, at 254 nm excitation (Ohno, 2002).

Table 2-2. Description of validated PARAFAC components

PARAFAC component	Excitation maximum (nm)	Emission maximum (nm)	Probable source and/or reactivity	Select studies in OpenFluor with spectrally similar components (Tucker congruence ≥0.95 for excitation and emission)
C1	<250, 345	456	terrestrial, humic-like; photolabile	Eder et al., 2022 (C2); Osburn et al., 2018 (C1); Wauthy et al., 2018 (C1); Kothawala et al., 2014 (C1/C4)
C2	<250	424	terrestrial, humic-like; refractory	Eder et al., 2022 (C3); Lapierre & del Giorgio, 2014 (C1), Olefeldt et al., 2013 (C_A), Osburn et al., 2011, 2015 (C3)
C3	<250, 310	391	microbial humic-like	Harjung et al., 2019 (C2); Wauthy et al., 2018 (C4); Kothawala et al., 2014 (C2); Osburn et al., 2011 (C2)
C4	275, 405	495	humic-like; dark-coloured, highly aromatic and photolabile	Kothawala et al., 2014 (C3); Guéguen et al., 2014 (C3)
C5	280	309	protein-like	Harjung et al., 2019 (C4); Wauthy et al., 2018 (C5); Kothawala et al., 2014 (C6); Osburn et al., 2011 (C5)

AF4 and FT-ICR-MS

We used AF4 to measure the mass-average molecular mass of DOM, reported as the molecular mass at the peak maximum of the fractogram (M_p). Samples were analyzed using a Postnova AF2000 Multiflow FFF fractionation system (Postnova Analytics, Salt Lake City, Utah, USA) equipped with a 300 Da PES membrane (Cuss et al., 2017). The instrument was calibrated over a molecular mass range of 0.69–20.7 kDa before and after every ten samples using a mixture of bromophenol blue (Sigma-Aldrich, St. Louis, Missouri, USA) and polystyrene sulfonate (PSS) size standards (PSS-Polymer Standards Service – USA Inc., Amherst, Massachusetts).

Samples for the FT-ICR-MS analysis were collected in 60 mL plastic bottles and stored frozen. Prior to the analysis, samples were acidified using trace-metal grade HCl, de-salted and concentrated using solid phase extraction, and then passed through 100 mg Bond Elut PPL cartridges (Agilent Technologies) (Dittmar et al, 2008). Samples were eluted with 1 mL of methanol and injected into a Bruker 9.4T Apex-Qe mass spectrometer (Bruker Daltonics, Billerica, MA, USA) with an Apollo II electrospray ionization source in negative mode using a flow rate of 120 μL hr^{-1} to acquire 600 spectra scans. Molecular formulae were assigned using the ICBM-OCEAN tool and the following constraints: $C_{1\text{-}50}$, $H_{1\text{-}200}$, $O_{1\text{-}50}$, $N_{0\text{-}4}$, $S_{0\text{-}2}$, $P_{0\text{-}1}$ (Merder et al., 2020). Oxygen-to-carbon ratio (O/C), hydrogen-to-carbon ratio (H/C), and modified aromatic index (AI_{mod}) were calculated from the molecular formulae (Koch & Dittmar, 2006). Each formula was classified as Aliphatic ($H/C \geq 1.5$), Aromatic ($0.5 \leq AI < 0.67$), Condensed Aromatic ($AI \geq 0.67$), and for $H/C < 1.5$ and $AI < 0.5$, Low-O Unsaturated ($O/C \leq 0.5$) or High-O Unsaturated ($O/C > 0.5$). Aliphatic compounds include lipids, proteins and carbohydrates; unsaturated compounds include lignins and tannins; aromatic compounds include phenols; and the condensed aromatic class includes black carbon. Signal intensity for each formula was normalized and the relative abundance of compounds within each class was used to determine the proportion of each class in each sample. Sample H/C and O/C were also estimated as intensity weighted averages.

LC-OCD

Water samples for LC-OCD analysis were collected unfiltered in 1-L HDPE or LDPE bottles and shipped to the University of Waterloo. LC-OCD analysis used a Model 8 LC-OCD analyzer (DOC-Labor GmbH, Karlsruhe, Germany). A size exclusion column, weak cation exchange column on a polymethacrylate basis (Toyopearl HW 50S, 250 mm x 20 mm, 30 μm from TOSOH Bioscience) was used for separation. Two detectors—a nondestructive, fixed wavelength UV

detector (UVD 254 nm, type S-200, Knauer, Berlin, Germany) and an organic carbon detector (OCD, Huber and Frimmel, 1991)—were used for carbon detection and characterization after chromatographic separation. OCD and UVD calibrations were based on potassium hydrogen phthalate. For data acquisition and data processing a customized software program was used (ChromCALC, DOC-LABOR, Karlsruhe, Germany). Using LC-OCD, chromatographic DOM was separated into five size fractions based on the hydrodynamic radii (Huber et al., 2011). The biopolymer (BP) fraction is very high molecular weight (100,000–2,000,000 g mol^{-1}), hydrophilic, not UV-absorbing compounds, which include polysaccharides, amino sugars, polypeptides and proteins. Humic substances (HS) fraction consists of humic and fulvic acids with molecular weight of 400-1100 g mol^{-1}. Building blocks fraction includes HS-like material of lower molecular weight (300-500 g mol^{-1}). All aliphatic organic acids with weights <350 g mol^{-1} co-elute in the LMW acids (LMWA) fraction, and weakly charged hydrophilic or slightly hydrophobic compounds like alcohols, aldehydes, ketones, amino acids appear in LMW neutrals (LMWN) fraction. These fractions were expressed as a percent of the overall chromatographable DOC.

2.2.4. Statistical analysis

Statistical analyses were performed in RStudio version 1.2.5042 (RStudio Team, 2020). Data were processed and summarized using the R packages *dplyr*, *tidyr*, *plyr*, *PerformanceAnalytics*, *corrplot*, *ggdendro*, *factoextra* and *tibble* (Wickham et al., 2020; Wickham & Girlich, 2022; Wickham, 2011; Peterson & Carl, 2020; Wei & Simko, 2017; Kassambara & Mundt, 2020; Müller & Wickham, 2020) and illustrated with the *ggplot2* package (Wickham, 2016).

To assess variations in water chemistry and DOM composition among the sites, we performed a principal component analysis (PCA) using the `prcomp` function in the *vegan* package (Oksanen et al., 2022). Many variables did not meet the PCA assumption of linear correlations

between the original variables; these variables were transformed using the `bestNormalize` function to reduce the nonlinearity (Peterson and Cavanaugh, 2020). Since not all samples were run using all analytical approaches, we first ran separate PCAs using different subsets of data. To combine DOM composition indices from all approaches in a single PCA, we reduced the dataset to include average DOM composition indices across all sampling events for each stream. To maximize the number of streams in the PCA, we used the `rfImpute` function from the *randomForest* package (Liaw & Wiener, 2002) to impute the missing values for four streams (S3, S5, S16 and JMR) that had no FT-ICR-MS data. To assess which catchment characteristics (including size, landcover, soil type, climate, and disturbance) influenced DOM composition, PCA scores for the first three principal components were used in a random forest analysis performed using the `randomForest` function.

2.3. Results

2.3.1. General water chemistry

We found clear differences in general water chemistry among most research sites, despite substantial temporal variability for individual streams and spatial variability among streams within each research site (Figure 2-2a, Table A5). A PCA was performed using 211 samples and 11 general water chemistry variables, including pH, major ions, SRP, TDN and DOC concentration. There were strong correlations between concentrations of Ca and Mg and of Fe and Mn, and thus only Ca and Fe were included in the PCA. The PCA identified three components with eigenvalues >1 (Figure 2-2a, A6, Table A6). Streams from the Boreal Plains and Taiga Plains sites generally clustered together, with high PC1 scores (high DOC, Fe, TDN, Cl^- and SRP). Pacific Maritime 2, Boreal Shield and Montane Cordillera streams had low PC1 scores. The Montane Cordillera and

some Boreal Plains and Taiga Plains streams had high PC2 scores (high NO_2^- + NO_3^-, pH, SO_4^{2-}, and Ca), while Atlantic Maritime and Pacific Maritime 1 streams had low PC2 scores.

The highest DOC concentrations were found in Boreal Plains, followed in order by Taiga Plains, Atlantic Maritime, and Pacific Maritime 1 streams (Figure 2-3), although there was substantial seasonal variation. The lowest DOC concentrations, typically <3 mg L^{-1}, were measured in the Montane Cordillera, Pacific Maritime 2 and Boreal Shield streams. The concentration of DOC was positively correlated with TDN and Fe. Despite the overall correlation between DOC and TDN, the C/N ratio differed among research sites with the highest C/N in Atlantic Maritime streams and the lowest in Mountain Cordillera streams (Figure 2-3b). The concentration of DOC was not correlated with pH. Nitrate-nitrite concentrations were high in the Montane Cordillera, Boreal Shield and Pacific Maritime 2 streams, which were also the streams with the lowest DOC concentrations. Concentrations of NH_4^+ and SRP were correlated and were highest in Boreal Plains and Atlantic Maritime streams.

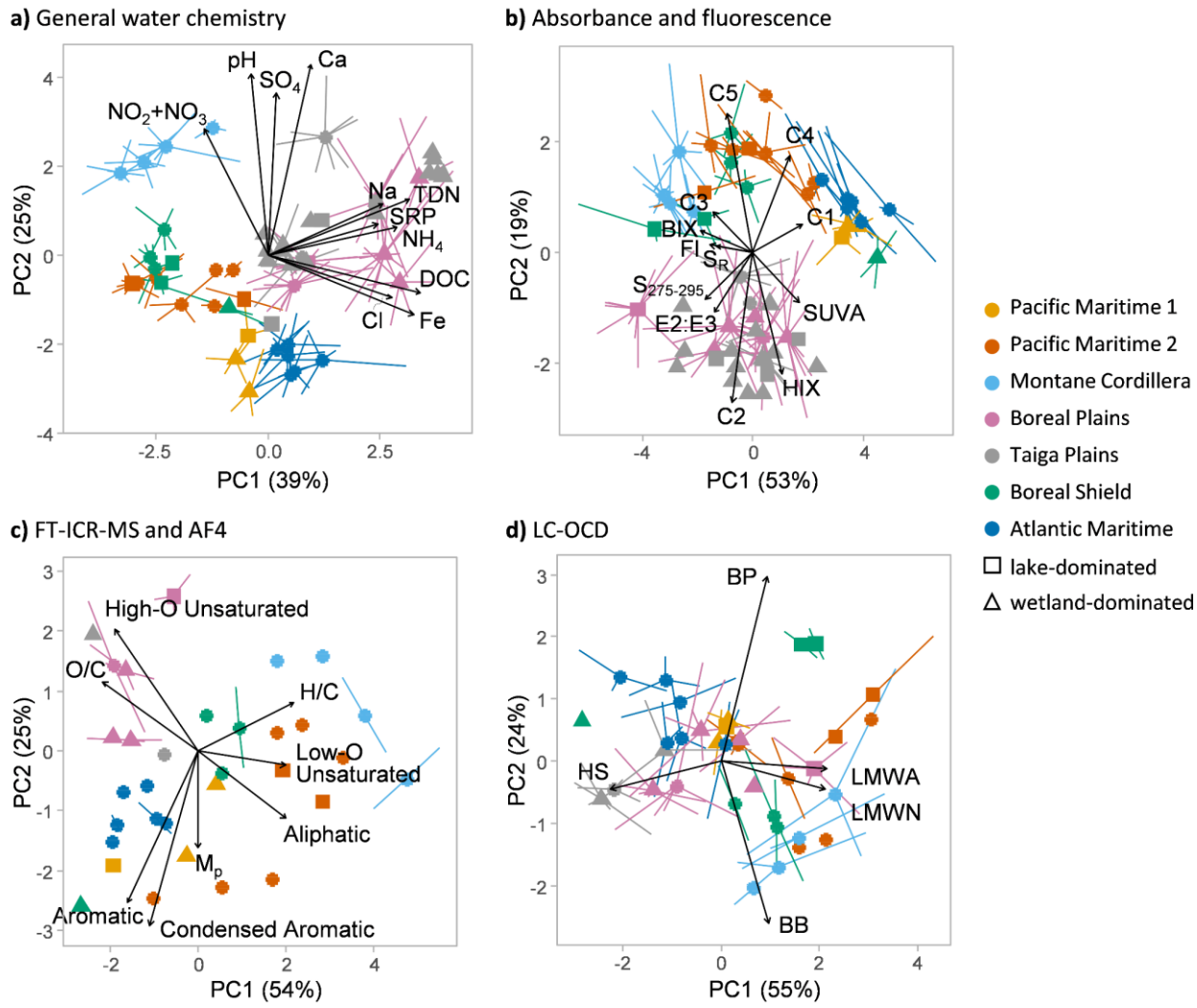

Figure 2-2. General water chemistry (a) and DOM composition based on different analytical approaches (b-d) for stream water samples from seven research sites located in six Canadian forested ecozones. Symbols represent average PCA scores for each stream, and whiskers point to individual samples, where multiple samples were available (i.e. temporal variability). Streams with catchments dominated by wetlands (squares) and lakes (triangles) are highlighted. The scale of variable loadings (arrows) was stretched for clarity.

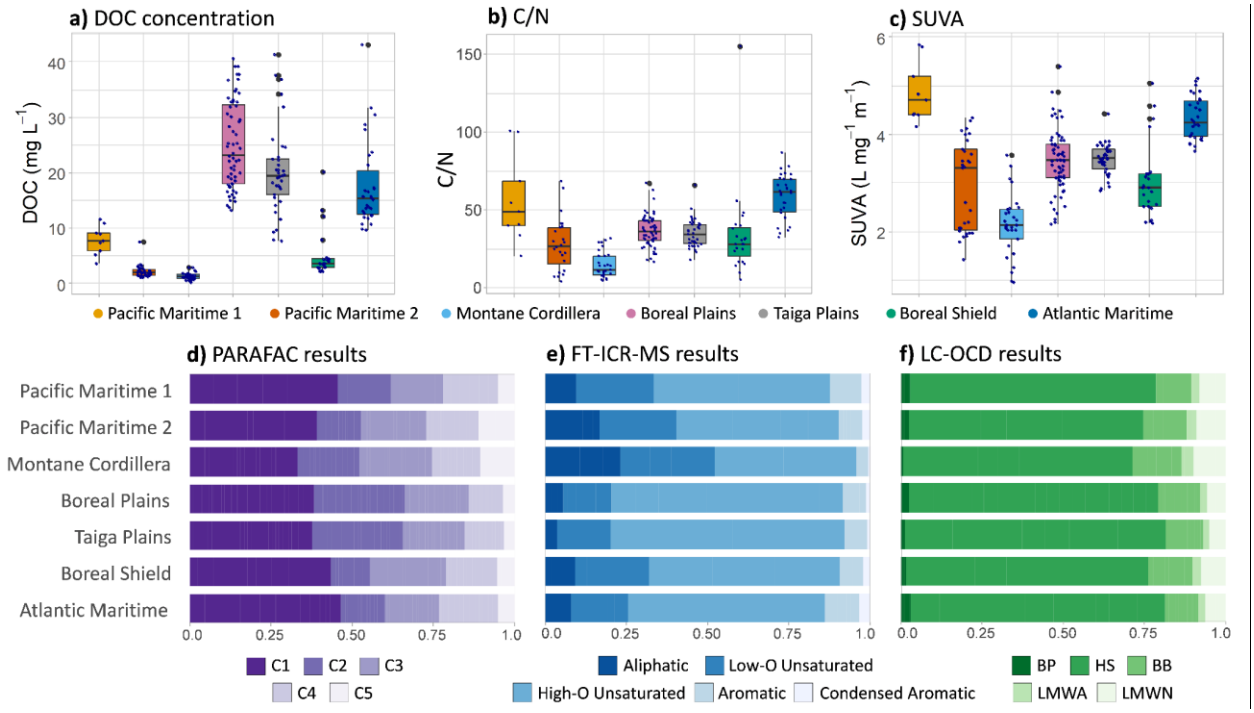

Figure 2-3. Comparison of stream DOC concentration and DOM composition for seven research sites across six Canadian forested ecozones. Boxplots of DOC concentration (a), C/N ratio (b), and SUVA (c) show individual measurements (blue dots). PARAFAC (d), FT-ICR-MS (e), and LC-OCD (f) plots show average fractional DOM composition of various DOM moieties (data for nine streams with lake-dominated catchments excluded).

2.3.2. DOM composition

Absorbance and fluorescence

The highest SUVA was found in Pacific Maritime 1 (3.6-5.8 L mg^{-1} m^{-1}) and Atlantic Maritime (3.6-5.2 L mg^{-1} m^{-1}) streams, while the lowest was found in Montane Cordillera streams (1.0-3.6 L mg^{-1} m^{-1}) (Figure 2-2b, Figure 2-3c). Higher values (and greater range) of absorbance slope parameters were seen in Montane Cordillera for S_R, and Montane Cordillera and Boreal Plains for E2:E3 and $S_{275\text{-}295}$, and lower values in Atlantic Maritime and Pacific Maritime 1 (Figure A5a-c). The highest BIX was measured in Montane Cordillera and several lake-dominated streams (Boreal Plains and Boreal Shield), and the lowest in Atlantic Maritime and Pacific Maritime 1. The HIX values were generally higher in Boreal and Taiga Plains, and lower in Pacific Maritime

2, Montane Cordillera and lake-dominated streams (Figure A5d-e). PARAFAC component C1 had the greatest contribution to the EEMs (Figure 2-3d) and was especially high in Pacific Maritime 1, Atlantic Maritime, and Boreal Shield streams without lake influence, but relatively low for Mountain Cordillera streams. Component C4 had a similar pattern to C1 among research sites. Component C2 was especially high for Boreal Plains and Taiga Plains streams, while component C3 had the least variability among research sites. Component C5, associated with protein-like compounds, was highest in Pacific Maritime 2 and Mountain Cordillera streams and lowest in Boreal Plains and Taiga Plains streams (Figure 2-3d).

The PCA of absorbance and fluorescence data identified three components with eigenvalues >1 (Figure 2-2b and A7, Table A7). In this PCA, Atlantic Maritime and Pacific Maritime 1 streams and a wetland-dominated Boreal Shield stream had high PC1 scores (high SUVA, C1 and C4, low BIX, $S_{275\text{-}295}$), Boreal Plains and Taiga Plains streams had low PC2 scores (high C5, C4, low C2 and HIX), and Pacific Maritime 2 and Boreal Shield streams had high PC2 scores. Lake-dominated streams generally had relatively low SUVA and HIX, and high C5, C3, BIX, S_R, E2:E3, and $S_{275\text{-}295}$, and thus lower PC1 scores compared to other streams from the same research site (Figure 2-2b). Wetland-dominated streams generally had relatively high SUVA, HIX and C2, and thus high PC1 scores. Variability for individual streams showed that Atlantic Maritime streams had seasonal co-variance in PC1 and PC2 scores, while other streams had no seasonal co-variance between PC1 and PC2 scores.

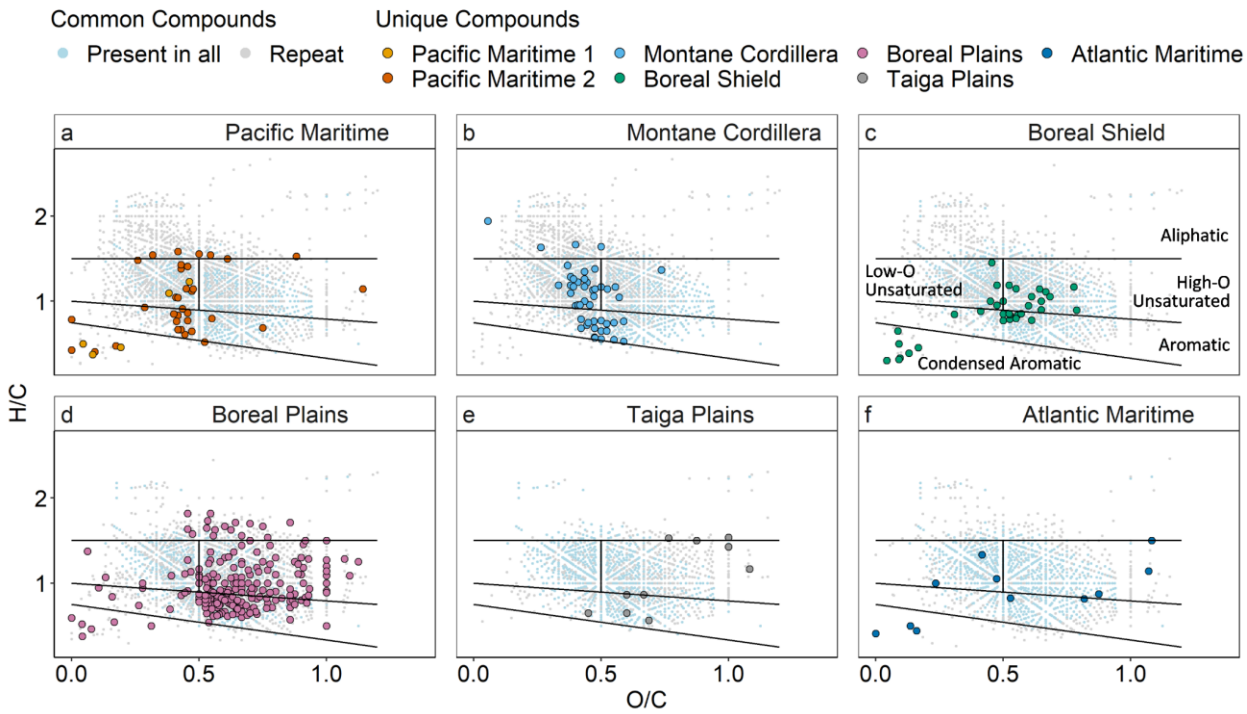

Figure 2-4. Van Krevelen diagrams showing common and unique DOM compounds at each research site. Five fractions used in analysis are separated by black lines and labelled in panel c. Repeat compounds (grey) are present in more than one research site.

AF4 and FT-ICR-MS

The AF4 analysis showed that M_p did not vary among research sites, but was lower in lake-dominated streams, which often had M_p <1125 Da. The highest M_p (>1,500 Da) was found in several Taiga Plains streams and a wetland-dominated Boreal Shield stream (Figure A4f).

The FT-ICR-MS analysis showed that most molecular formulae were not unique to individual research sites; what varied among samples and research sites was primarily the relative abundance of specific formulae (Figure 2-4). The Boreal Plains streams had the greatest number of unique formulae, primarily compounds with high O/C, while the Pacific Maritime 1 and 2 and Montane Cordillera streams primarily had unique compounds with low O/C. The Pacific Maritime, Montane Cordillera, and Boreal Shield streams had a greater abundance of high H/C formulae compared to Boreal Plains, Taiga Plains, and Atlantic Maritime streams (Figure 2-4). The

proportion of Aliphatic compounds was high in Montane Cordillera and Pacific Maritime 2 streams, while the proportions of Aromatic and Condensed Aromatic compounds were high in Atlantic Maritime, Pacific Maritime 1 and several Pacific Maritime 2 streams. The Boreal Plains and Taiga Plains streams had the highest proportion of High-O Unsaturated compounds (Figure 2-3e).

The PCA performed on FT-ICR-MS and AF4 data identified three components with eigenvalues >1 (Figures 2c and A8, Table A8). Similarities among research sites mimicked those found in the PCA using UV-vis absorbance and fluorescence data (Figure 2-2b-c). Wetland-dominated streams generally had relatively low PC1 scores, i.e. high Aromatic and O/C. There was no consistent pattern for lake-dominated streams to have higher or lower PC1 or PC2 scores compared to streams within the same research site.

LC-OCD

Across all sites, stream DOM was dominated by the HS fraction (55-80% on average), followed by BB (10-14%) and LMWN (5-9%) (Figure 2-3f). Proportions of BP and LMWA were generally <3%. Proportions of LMWA and LMWN fractions were relatively high in the Montane Cordillera and Pacific Maritime 2 streams and in some Boreal Shield and Pacific Maritime 1 streams (Figure 2-3f). Proportion of HS fraction was high in the Boreal Plains, Taiga Plains, Atlantic Maritime streams, and the wetland-dominated Boreal Shield stream, while proportion of BB fraction was high in the Montane Cordillera. Two lake-dominated Boreal Shield streams had the highest proportion of BP fraction.

The PCA of the LC-OCD data identified two principal components with eigenvalues >1 (Figure 2-2d, Table A9). The PC1 axis differentiated streams with high proportion of HS fraction (Taiga Plains, Atlantic Maritimes and wetland-dominated streams) and streams with high

proportions of LMWA and LMWN fractions (Montane Cordillera, Pacific Maritime 2). The PC2 axis separated streams with high proportion of BB fraction (Montane Cordillera) and streams with high proportion of BP fraction (including several lake-dominated streams). Overall, there was more overlap among the research sites in the LC-OCD PCA plot compared to PCAs using other approaches (Figure 2-2b-d), and wetland- and lake-dominated streams showed more consistent trends, similar to Aukes et al. (2021).

2.3.3. Correlations among DOM composition indices

A correlation matrix using data from all stream samples was generated for the 25 DOM composition indices (qualitative indicators of DOM composition), along with DOC concentration and A_{254} (quantitative measures) (Figure 2-5). Hierarchical clustering yielded four broad groups of DOM composition indices (Figure A9), with each group including DOM indices from at least three different analytical approaches. The first group of DOM indices was associated with humic, high-oxygen DOM compounds (HIX, HS, O/C, and High-O Unsaturated). The second group was associated with aromatic, low-nitrogen DOM compounds (M_p, SUVA, C1, C4, C/N, Aromatic and Condensed Aromatic). The third group of DOM indices was associated with autochthonous, low molecular weight, aliphatic DOM compounds (Low-O Unsaturated, Aliphatic, H/C, LWMA, LMWN, BP and C5), while the fourth group included DOM indices that are likely associated with photodegraded or autochthonous DOM compounds (BB, BIX, C3, C2, E2:E3, S_R and $S_{275\text{-}295}$). The analysis showed that stream DOC concentration (and A_{254}) was strongly positively correlated with DOM indices in the first group, weakly positively correlated with the second group, strongly negatively correlated with the third group, and weakly negatively correlated with the fourth group of DOM indices (Figure 2-5).

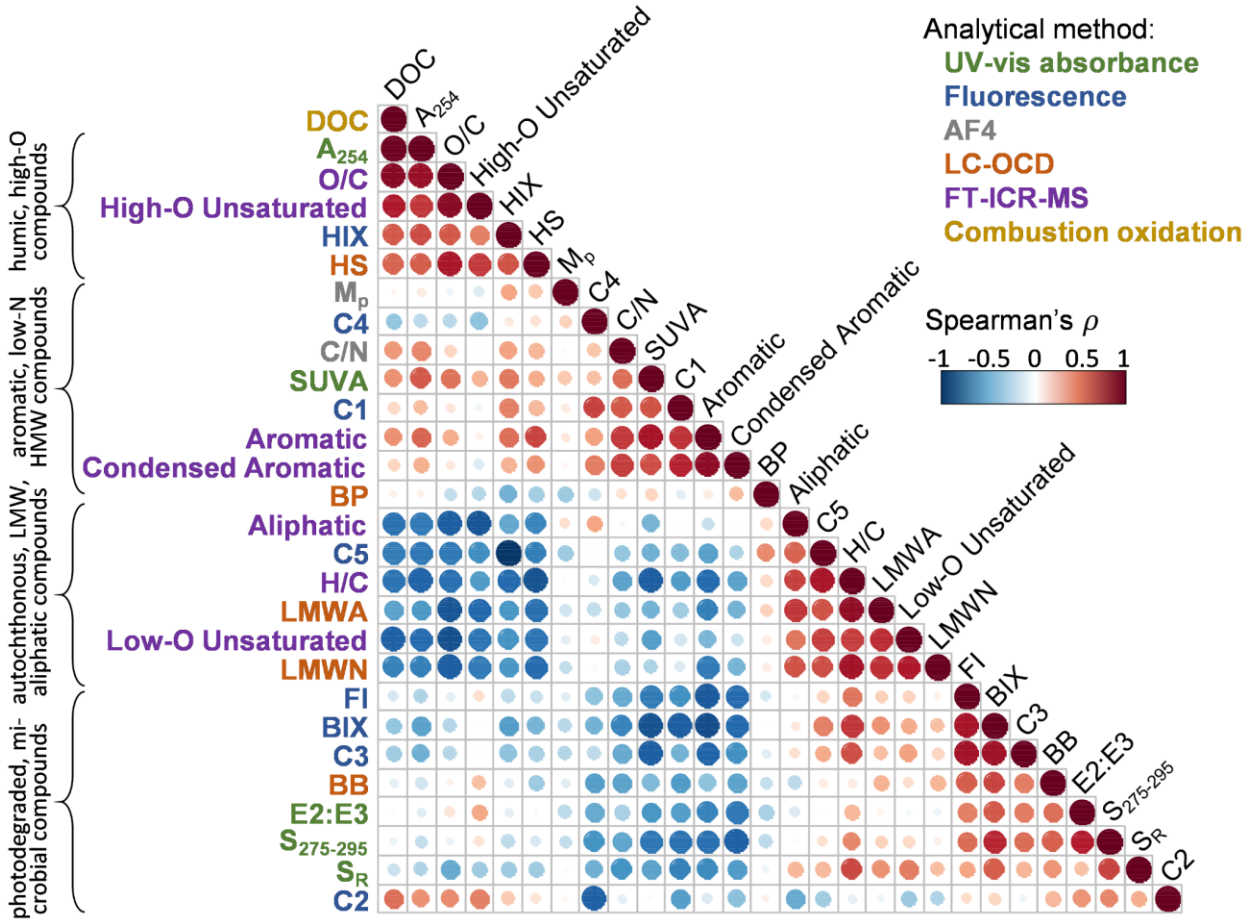

Figure 2-5. Correlation matrix of DOM indices used in the study. Circle colour and size indicate Spearman's rank correlation coefficient (ρ). Insignificant correlations ($p \geq 0.05$) are left blank. The groupings on the left are based on a cluster analysis (Figure S9). The colour of the text for each index corresponds to the DOM analytical approach used.

2.3.4. Environmental controls on DOM composition

We combined all DOM indices into a single PCA (Figure 2-6a-b, A10, A11), which required us to use average values of DOM indices for each stream since not all DOM indices were analyzed for all samples. A total of 32 streams had all DOM indices analyzed for some samples, and an additional four sites had all DOM indices except indices from FT-ICR-MS analysis which were imputed for this PCA. The PCA had four components with eigenvalues >1; the first two components explained 52% and 21% of the variability, respectively; the third component explained an additional 11%, and the fourth only 5% (Table A10). Positive scores on the PC1 axis

(i.e. high H/C, LMWA, BIX, Low-O Unsaturated, S_R and $S_{275-295}$) were associated with streams from the Montane Cordillera, Pacific Maritime 2, and a few lake-dominated streams. Negative scores on the PC1 axis (i.e. high SUVA, Aromatic, C/N, O/C, Condensed Aromatic, C1, HS and HIX) were associated with Atlantic Maritimes, Pacific Maritime 1, and a wetland-dominated Boreal Shield stream. Positive scores on the PC2 axis (i.e. high C2, High-O Unsaturated, E2:E3, $S_{275-295}$ and O/C) were associated with Boreal Plains and Taiga Plains streams. Negative scores on the PC2 axis (i.e. high C4, Aliphatic, C5 and LMWN) were associated with Pacific Maritime 2 and Pacific Maritime 1 streams. High scores on the PC3 axis (i.e. high BP and C5, and low M_p) were primarily associated with lake-influenced streams.

Random forest analyses showed which climatic and catchment characteristics influenced each of the three principal components in the PCA (Figure 2-6c-e). The components were influenced primarily by wetland soils (PC1), climate (PC2), and lakes (PC3). Scores for PC1 decreased with greater presence of wetland soils (% wetland soils from ecodistrict dataset in Table A2 (Marshall et al., 1999) and % wetland area in Table A1 were strongly correlated; therefore, only wetland soils were included in random forest analysis), lower slope (slope was negatively correlated with wetland abundance), and lower stream pH. Scores for PC2 increased with lower CMI and MAT, and lesser presence of podzolic soils. Scores for PC3 increased with greater presence of lakes, and to a lesser degree higher stream pH, lower slope, and greater catchment area, all of which were in turn related to the presence of lakes.

Disturbance was a poor predictor for each principal component in the PCA (Figure 2-6c-e), regardless of whether it was expressed as a numerical variable (proportion of disturbed area in the catchment) or as a categorical variable (disturbed vs. undisturbed catchment). Disturbed streams plotted generally near the undisturbed streams within the same research site.

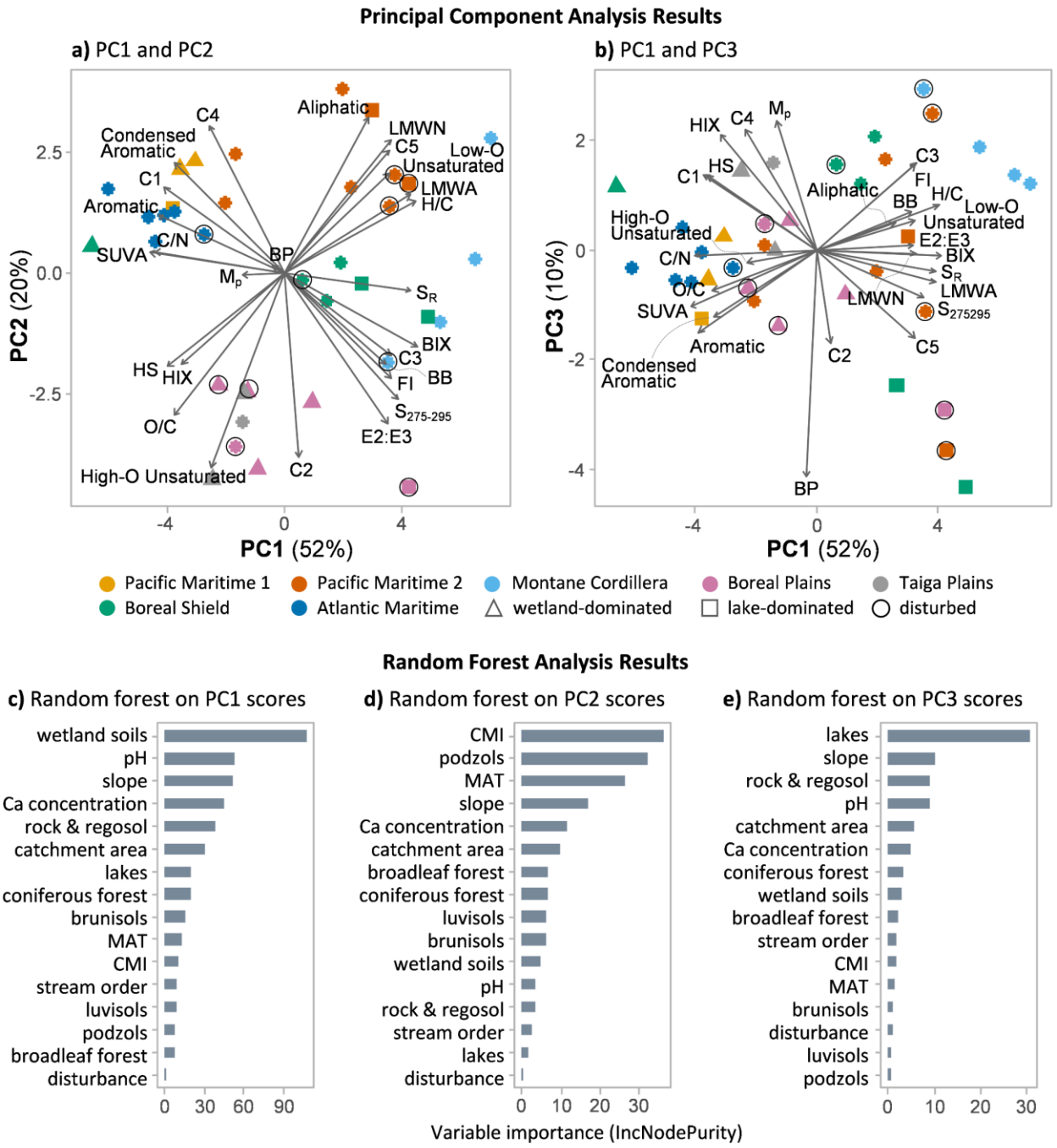

Figure 2-6. PCA using averages for each stream for all DOM indices for the first three principal components (a-b). Points (circles/triangles/squares) represent parameter averages (where multiple samples are available) for each stream; open black circles indicate disturbed streams (% catchment area harvested or burned >30%). The scale of variable loadings (arrows) is increased for clarity. Random forest results using PCA scores for the streams with catchment characteristics as factor variables (c-e).

2.4. Discussion

Our study compared DOM composition from streams draining forested headwater catchments (<1-1260 km^2) at seven research sites across six Canadian ecozones. Each research site was characterized by different climate, geology, soils, vegetation, and six of seven included streams with forest harvesting or wildfire disturbances within the last 30 years (Figure 2-7). The combination of multiple analytical approaches allowed for discrimination between the research sites and individual streams. There was generally little overlap in DOM composition between most research sites. While the repeated sampling of individual streams in this study may not have been sufficient to fully characterize the temporal variability in DOM composition for individual streams (e.g., McSorley, 2020; Oliver et al., 2017), our study still provided robust evidence showing that regional landscape characteristics are the dominant control on DOM composition at large geographical scales. Below we describe and discuss the differences in stream DOM composition among regions, the three main axes of variation in DOM composition, their links to catchment characteristics, and implications for our understanding of potential impacts from climate change, land use and disturbances.

2.4.1. Three axes of DOM composition

Our study used several approaches to describe DOM composition, yielding 25 indices. Many indices were strongly correlated to one another, and a majority of them differentiated between two main axes of DOM composition, while a few distinguished a third axis (Figure 2-5 and Figure 2-6a-b).

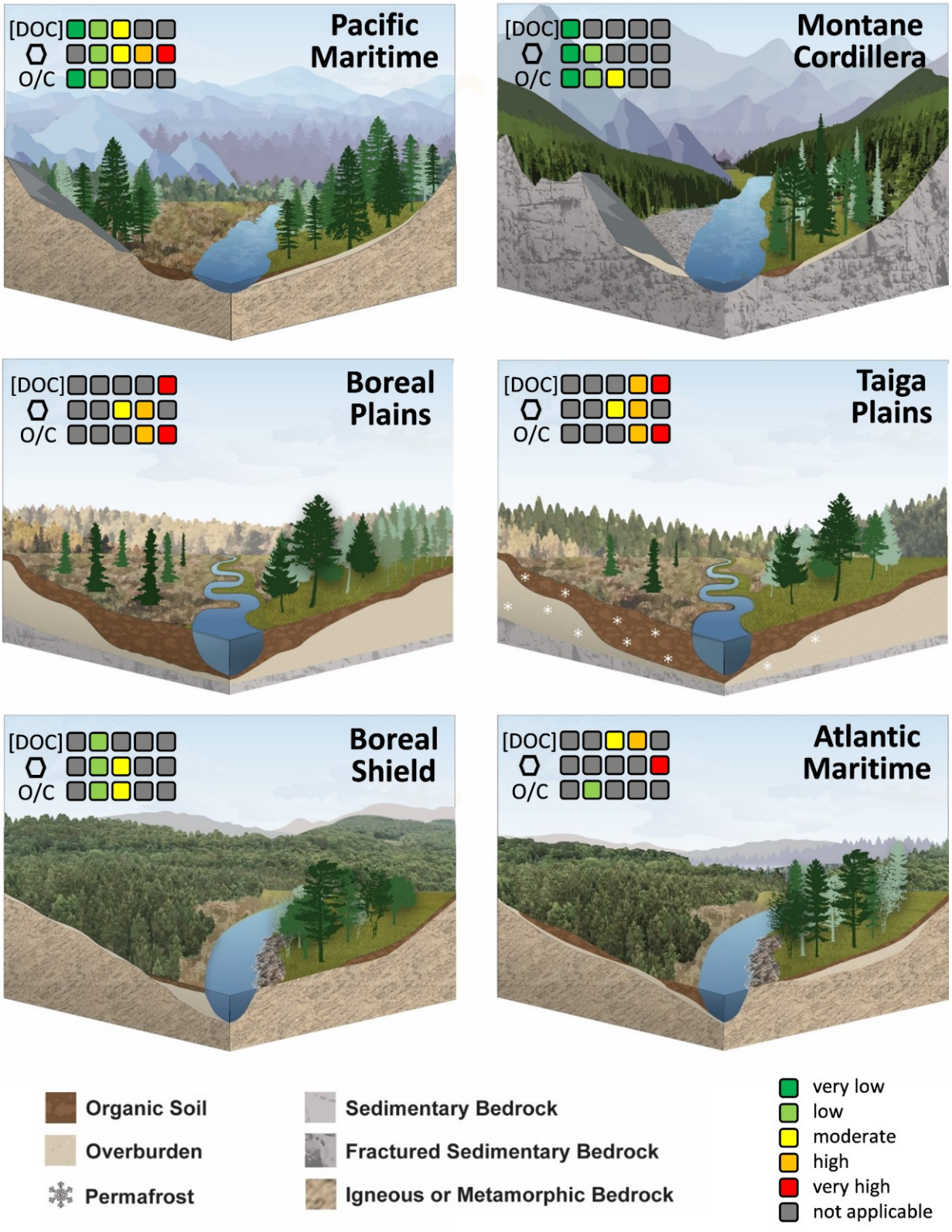

Figure 2-7. Conceptual illustration of the differences in surficial geology and landcover among the ecozones, as well as observed variations in DOC concentration ([DOC]), DOM aromaticity (⎔) and O/C ratio.

The first axis, which we refer to as the *aromaticity axis*, differentiated DOM with high aromaticity from DOM compounds that are known to be preferentially produced through autochthonous or photochemical processes (PC1 in Figure 2-6a). Hence studies interested in assessing DOM aromaticity can use indices such as SUVA (absorbance), HIX and PARAFAC component C1 (fluorescence), C/N (combustion oxidation analysis or FT-ICR-MS), HS (LC-OCD) or Aromatic and Condensed Aromatic (FT-ICR-MS). These indices increase with an increase in humified, plant-derived DOM of terrestrial origin, with high molecular weight and aromaticity (Kothawala et al., 2014; Marín-Spiotta et al., 2014). The DOM indices that were negatively correlated with the *aromaticity axis* were $S_{275\text{-}295}$ and S_R (absorbance), BIX (fluorescence), LMWA (LC-OCD), and H/C and Low-O Unsaturated (FT-ICR-MS). These indices thus describe DOM of lower molecular weight, a lower degree of humification and of autochthonous origin (e.g., Liu et al., 2020). Several indices on the *aromaticity axis* have been found to preferentially increase ($S_{275\text{-}295}$) or decrease (SUVA, HIX) during photodegradation (Helms et al., 2014) and during selective sorption as DOM passes through mineral soil (McDonough et al., 2022).

The second axis, which we refer to as the *oxygenation axis*, differentiated humic DOM with high oxygen content from aliphatic, low molecular weight DOM (PC2 in Figure 2-6a). Scores on the *oxygenation axis* increased with E2:E3 (absorbance), PARAFAC component C2 (fluorescence), BB (LC-OCD), O/C and High-O Unsaturated fraction (FT-ICR-MS), and decreased with PARAFAC components C4 and C5 (fluorescence), LMWN (LC-OCD), and Aliphatic fraction (FT-ICR-MS). High-O Unsaturated compounds are often described as tannins (D'Andrilli et al., 2015), which are abundant terrestrially derived compounds with large molecular size, polyphenolic structure, and varying reactivity (Kraus et al., 2003). Compounds with O/C>0.9

are classified as sugar-like (Fellman et al., 2020). Higher O/C values were associated with the research sites characterized by higher DOC concentrations and A_{254}.

The third axis, referred to as the *biopolymer axis*, explained less of the overall DOM variability, but corresponded with higher BP (LC-OCD) and PARAFAC component C5 (fluorescence), and lower M_p (AF4), which are associated with biologically labile, autochthonous DOM, such as polysaccharides, proteins and amino acids (Huber et al., 2011; Kothawala et al., 2014). Biopolymers represent large DOM molecules, but were negatively correlated with M_p. However, given that M_p was most useful in distinguishing lake-dominated streams, which had lower M_p, and larger BP fraction, this negative correlation indicates elevated biopolymer content but smaller average molecular mass in lake-dominated streams.

Each PCA on DOM composition using different analytical approaches (UV-vis absorbance + fluorescence, LC-OCD, and FT-ICR-MS + AF4) was able to differentiate DOM composition between research sites in a similar manner (Figure 2-2b-d). In particular, the Boreal Plains and Taiga Plains streams cluster together in all figures, and across from them are the Pacific Maritime 2 streams. The Atlantic Maritime and Montane Cordillera plot at the opposite ends from each other. The Pacific Maritime 1 streams are most similar to Atlantic Maritime and several Pacific Maritime 2 streams, while the Boreal Shield streams are similar to Montane Cordillera and some Pacific Maritime 2 streams. Thus, it appears that many goals of DOM characterization could be achieved using simpler UV-vis absorbance and fluorescence analyses instead of more complex and expensive techniques. At the same time, the more complex analytical techniques like FT-ICR-MS, LC-OCD and AF4 give us more detailed information about variations in DOM composition, including direct information on DOM size, elemental composition, and quantity of specific DOM fractions.

2.4.2. Comparison of DOM composition among research sites and ecozones

Our seven research sites spanned six forested ecozones (Figure 2-7). The research sites were characterized by major differences in slope, where sites with flat terrain (Boreal and Taiga Plains) had extensive wetlands. Forests ranged from predominantly coniferous (Montane Cordillera, Pacific Maritimes, Taiga Plains) to mixed (Boreal Plains) and broadleaf (Atlantic Maritime, Boreal Shield), and soils from thick organic deposits (Boreal and Taiga Plains, Pacific Maritime 1) and gleysolic soils in depressions or poorly-drained areas (Atlantic Maritime) to brunisols, luvisols (Boreal and Taiga Plains, Montane Cordillera) and podzols (Pacific Maritimes 1 and 2, Atlantic Maritime, Boreal Shield). Surficial geology varied from sedimentary bedrock with thick heterogeneous glacial deposits (Boreal and Taiga Plains), to fractured sedimentary bedrock with thick deposits in valleys or till veneers at higher elevations (Montane Cordillera) to poorly-weathered or fractured igneous or metamorphic bedrock overlain by relatively thin to absent glacial deposits (Pacific Maritimes 1 and 2, Atlantic Maritime, and typically Boreal Shield). While the research sites and specific catchments included in this study do not represent the full variability of catchment characteristics within an ecozone (e.g., the differences between Pacific Maritime 1 and 2 discussed below), our dataset allowed for a unique assessment of how landscape and climate influence stream DOM concentrations and composition.

Despite being located furthest apart, streams in Pacific Maritime 1 and Atlantic Maritime were found to have many similarities in DOM composition. Both research sites had moderate to high DOC concentrations and DOM with very high aromaticity and low to moderate O/C (Figure 2-7). Both research sites have relatively warm and humid climates, with coniferous forests on podzolic soils and undulating to hilly topography with a significant presence of wetlands in depressions. Stream water at both research sites had relatively low pH and low concentrations of

Ca and SO_4^{2-} due to the igneous bedrock and influence of wetlands, while the maritime influence led to elevated concentrations of Cl^-. Similar landscapes and climates in other regions and countries seem to follow the broad trends that we observed in Canada. For example, a research site in Alaska further north along the Pacific coast had higher stream DOC concentrations than what we measured at Pacific Maritime 1 (D'Amore et al., 2015; Fellman et al., 2020). The Krycklan research site on the Scandinavian Shield, characterized by a maritime climate, and similar topography, soils, and wetland extent to Canada's Atlantic Maritime ecozone, has comparable DOC concentrations and SUVA (Kothawala et al., 2015).

Streams at the Pacific Maritime 2, Boreal Shield and Montane Cordillera sites showed similarities in DOM composition, but did not completely overlap (Figure 2-6a,b). These three research sites had several landscape characteristics in common, including shallow soils, few wetlands, and relatively steep terrain. They exhibited very low to moderate DOC concentrations and aromaticity, and low to moderate carbon oxidation state. The exception was a wetland-dominated stream at the Boreal Shield with higher DOC concentration and aromaticity, and two Pacific Maritime 2 streams that were more similar to Pacific Maritime 1. Regional studies conducted at other research sites on the Canadian Shield suggest that our Boreal Shield research site may not be representative of the entire Boreal Shield ecozone. In particular, streams at our Boreal Shield research site (Turkey Lakes Watershed) drain catchments with fewer wetlands and more broadleaf forests than some other Boreal Shield sites and, for example, had lower DOC concentrations and aromaticity than streams at the Experimental Lakes Area (Aukes et al., 2021; Creed et al., 2008), and lower DOC concentrations than streams in boreal Quebec (Hutchins et al., 2017). Thus, although our results show clear distinctions in DOM concentrations and composition for most research sites, results for individual sites cannot always be extrapolated to the entire

ecozone. At the same time, our study shows that similarities in landscape characteristics across different ecozones result in commonalities in stream DOM composition.

Lastly, streams in the Boreal and Taiga Plains had many similarities in DOM composition, suggesting that DOM composition at the research sites located in different ecozones may not always be distinguishable. These research sites have some of the highest DOC concentrations, moderate to high aromaticity, and the highest scores on the *oxygenation axis* (Figure 2-7). No large differences in DOM composition were found, likely due to the similarities in landscape (including flat terrain, thick overburden on top of sedimentary bedrock, abundance of wetlands, primarily coniferous or mixed forests) and climate (lower mean annual temperature and precipitation than other research sites). The main difference between these research sites is the presence of permafrost. Some studies observe decreased connectivity in boreal peatlands with permafrost leading to lower DOC concentrations in streams (Frey and Smith, 2005; Olefeldt et al., 2014), which is consistent with our findings of lower DOC in Taiga Plains streams than in the Boreal Plains.

2.4.3. Environmental controls on DOM composition

Variability along the *aromaticity axis* was explained primarily by the proportion of wetlands (or wetland soils) in the catchment. Wetlands had a common influence across ecozones, including elevated SUVA, HS, Aromatic/Condensed Aromatic compounds, and M_p, as indicated by the random forest results. Wetlands often covered more than 50% of Boreal and Taiga Plains catchments, and up to 50% of the Pacific Maritime 1 catchments. Due to reduced evapotranspiration and low storage capacity, wetlands are the runoff-generating areas in the Boreal and Taiga Plains (Devito et al., 2017). Dominance of surface and near-surface flowpaths intersecting organic rich soils at Boreal and Taiga Plains resulted in high DOC concentrations and

aromatic DOM. Although the Atlantic Maritime catchments had fewer wetlands, high aromaticity may be related to a decline in acid deposition and a subsequent increase in solubility of DOM, and brownification seen in some surface waters in Canada's eastern provinces (Redden et al., 2021; Webster et al., 2021b). The type of forest (coniferous vs. broadleaf) was not a strong predictor of stream DOM composition along this axis, possibly due to convergence in DOM characteristics in the mineral soil (Thieme et al., 2019).

Variation along the *oxygenation axis* was explained by climatic factors (MAT and CMI) and podzols. Podzolic soils that had the highest scores in random forest are formed in warm, humid climates through intense weathering. Hence, podzols, as a result of climate, have a common influence along this axis. The PC2 axis separated the two coolest and driest research sites – Boreal Plains and Taiga Plains, which had the highest O/C – from the remaining sites, including Pacific Maritimes 1 and 2, characterized by the warmest climate and the lowest O/C. Temperature affects the rate of degradation of organic matter in soils (Thevenot et al., 2010). The Boreal and Taiga Plains streams are characterized by the largest proportions of wetlands and highest DOC concentrations. According to the enzymic 'latch' theory, anoxic conditions in wetlands promote accumulation of polyphenolic compounds, like tannins (Freeman et al., 2001), although recent evidence suggests degradation occurs under both oxic and anoxic conditions (McGivern et al., 2021). Wetlands in higher latitudes have been found to have greater DOM carbohydrate abundance, potentially due to slower decomposition rates in cooler temperatures (Verbeke et al., 2022). Carbohydrates have a higher carbon oxidation state than aromatic compounds, which may explain higher export of oxygen-rich DOM via predominantly shallow flowpaths in wetland-dominated Boreal and Taiga Plains catchments. Climate warming may accelerate decomposition of carbohydrates in wetlands at higher latitudes (Verbeke et al., 2022). Research sites with the

lowest scores on the *oxygenation axis* were the warmest and wettest – Pacific Maritime 1 and 2 (low O/C and high H/C, LMW, aliphatic compounds), and to some extent Atlantic Maritime (dark-colored, aromatic DOM, but with lower oxygen content). Oxygen-rich DOM may also be lost at research sites with deep flowpaths, like Montane Cordillera, as water percolates through till and fractured sedimentary bedrock, and oxidized and aromatic DOM is preferentially removed by sorption onto mineral particles, producing DOM with a strong aliphatic signal that mimics the effects of photodegradation and microbial DOM production (Hawkes et al., 2018; McDonough et al., 2022). Overall, the separation along the *oxygenation axis* follows the temperature and precipitation gradient, and likely indicated the effect of slowed DOM decomposition in soils, which result in higher concentrations of oxygen-rich compounds like tannins and carbohydrates, and the abundance of wetlands may enhance this effect.

Variation along the *biopolymer axis* was determined by lake influence. The lake effect in our study was indicated by elevated BP fraction, BIX (especially Boreal Shield streams), PARAFAC component C5, S_R, E2:E3, and $S_{275\text{-}295}$, which are indicative of photodegradation and autochthonous DOM production (Helms et al., 2014; Kothawala et al., 2014; Sachse et al., 2012). Although the composition of DOM varied among the lake-dominated streams, likely reflecting the terrestrial DOM source, variable retention time and water chemistry in lakes and climatic factors (Kurek et al., 2022; Kothawala et al., 2014), aquatic processes including autochthonous DOM production and photodegradation appear to cause common shifts in DOM composition. We noticed that lake position in the catchment was also important. For example, at Pacific Maritime 2, one stream had a large lake in the upper reach, while another stream had a smaller lake just upstream of the sampling site (Government of British Columbia, 2021). Although the latter was not classified as lake-dominated (lake area <4% of catchment area), it exhibited a similar lake effect

(greater proportions of LMW compounds, BP fraction, and PARAFAC component C5) due to the lake's proximity to the stream sampling site.

Seasonal variations in DOM composition at a single stream can be large, and occasionally greater than variations among streams within the same research site (Figure 2-2). Variations appear to be the greatest in several streams where we measured low DOC concentrations (Montane Cordillera, Pacific Maritime 2), where a small addition of DOM from a different source may result in large changes to the proportions of different DOM compounds. Large changes in absorbance and fluorescence were also seen in several lake-dominated streams (Boreal Shield and Boreal Plains), where sunlight exposure, respiration and autochthonous DOM production during water residence may significantly alter DOM composition. Our study was not designed to explore controls on temporal variability in DOM, but rather to compare the magnitude of variability within research sites and streams to that between sites. Although there were large temporal shifts in DOM composition (whiskers in Figure 2-2), differences between some research sites were visually greater.

Our study showed that disturbance such as wildfire and forest harvesting had no large common influence on DOM composition and was not an important predictor for DOM composition. Hence, we found no common influence of disturbance on DOM composition across research sites similar to what we found, for example, for lake or wetland cover. The effect of disturbance on DOM composition was thus likely a smaller signal compared to the higher-order physiogeographic controls like climate and landcover. However, our study does not rule out the influence of disturbances on DOM composition, but suggests that detailed, regional studies are required to understand impacts from specific disturbances in specific settings. Several reason likely contributed to the lack of a common effect of disturbances on DOM composition in this study. For

example, we arbitrarily picked a threshold of 25% disturbed area to classify our catchments as disturbed. The disturbances in our catchments differed in age: some occurred three decades ago (Boreal Shield), others as recently as 2019-2020 (Atlantic Maritime), and repeated harvesting took place in Pacific Maritime 2, where all forests are second growth. Although disturbed catchments can take many decades to recover, disturbances older than 30 years were not considered, thus missing much of the historical wildfire and harvest.

In addition, the type and magnitude of disturbances varied among the research sites and individual catchments. We treated forest harvesting (including clear-cut and partial-cut) and wildfires similarly, although they may result in different effects on DOM, as well as different recovery times. Wildfires may lead to the loss of ground cover, decreased surface roughness, reduced infiltration due to soil crust formation and sealing (Larsen et al., 2009), and increased fluvial erosion (Shakesby & Doerr, 2006), and a release of pyrogenic carbon (Rhoades et al., 2019). The effect is a function of wildfire severity and extent, catchment hydrology and geomorphology. For example, wildfires in the Boreal Plains ecozone had a small or no effect on riverine and lake DOC concentrations due to low landscape-stream connectivity (Emmerton et al., 2020; Olefeldt et al., 2013). Higher DOC concentrations were measured in burned catchments at Montane Cordillera (Emelko et al., 2011). Forest harvesting has the potential to change water balance and flowpaths, thus affecting water chemistry and DOM export, as well as species composition, leaf litter quality and quantity, and soil organic matter inputs (Yamashita et al., 2011). Often, the effects of disturbance are best captured at high flows; however, our sampling did not explicitly target storm events. Some studies in the Pacific Maritime ecozone observed an effect of harvesting on DOM concentrations and composition (Mistick & Johnson, 2020), while others showed little apparent effect (Bourgeois, 2021). In the Boreal Plains ecozone, where aspen forest regenerates rapidly after

harvesting, harvest effects on water chemistry may be outweighed by seasonal variability (Petrone et al., 2016). Given these region-specific disturbance effects on DOM concentration and composition, it is not surprising that disturbance was not identified as a key driver. Our study further demonstrates that to understand impacts of disturbances, land managers should not rely exclusively on studies conducted in other regions.

2.4.4. Implications

Our study suggests that it may be possible to anticipate common shifts in DOM composition across different ecozones, e.g., in response to wetland restoration/degradation or reservoir creation/removal, or climate change. The *oxygenation axis* of DOM composition was primarily explained by climate variables (Figure 2-6d), and may thus be particularly sensitive to the effects of climate warming in the future, resulting in less oxygen-rich DOM in streams of northern regions. Further research may be necessary to understand how specific axes of DOM composition influence aquatic functions, including bioavailability and transport of contaminants from soils, DOM lability and greenhouse gas emissions.

Drinking water treatability, in particular coagulant demand and formation of potentially harmful disinfection by-products (DBPs), has been linked to DOM composition (Matilainen et al., 2010). Coagulation has been shown to preferentially remove DOM characterized by high SUVA and molecular weight, low H/C and high O/C ratios, and fluorescent DOM at low emission wavelengths (Lavonen et al., 2015; Marais et al., 2019). Aromatic, high molecular weight compounds are known as precursors of some DBPs (Marais et al., 2019; Parsons et al., 2004), and A_{254} and SUVA have been commonly used as indicators of DBP formation potential (Matilainen et al., 2010), although the relationships are not universal. Based on observed variations in DOM composition in our study, including aromaticity and molecular size, we may expect differences in

treatability; however, they are hard to predict given the large differences in DOC concentrations among the region. Because DOM composition varies in more than one dimension, it may not always be sufficient to only measure SUVA to predict shifts in treatability needs. Overall, the differences in stream DOM concentrations and composition we observed in our study suggest that drinking water treatability should be region-specific. As climate change may affect DOM concentrations and composition, drinking water treatability may also be impacted.

Our study also suggests that monitoring programs may benefit from including DOM composition indices associated with each of the three DOM composition axes. For example, in addition to SUVA even in simple monitoring program, PARAFAC components may give insight into the oxygenation and biopolymer axes. Thus, similar to Jaffé et al. (2008), we found that UV-vis absorbance and fluorescence can provide the lowest effort DOM characterization relative to all three axes and place regional DOM composition in a larger context.

2.5. Conclusions

We analyzed DOM composition in a range of streams from seven research sites located in six forested ecozones in Canada sampled over the course of two years. Using 25 indices obtained from five analytical techniques, we found both distinct differences and some similarities in DOM composition among the research sites. Though widely disparate in analytical approach, cost and ease of use, each technique provided a similar separation of the research sites. Therefore, it may be sufficient to use simpler approaches such as UV-vis absorbance and fluorescence to broadly characterize differences in DOM in surface waters for many research questions.

Stream DOM composition broadly varied along three axes—the aromaticity, oxygenation, and biopolymer axes—which were explained by wetland coverage, climate, and lake presence, respectively. We were not able to detect a consistent effect of land disturbance on stream DOM

composition across our research sites, which may be attributed to the study design, and the vast differences in climate and landscape characteristics among our research sites that conceal the potential effect of disturbances, suggesting the need for region-specific studies of wildfire and forest harvesting effects.

Our results indicate differences in DOM quantity among the research sites, as well as differences in DOM composition, including aromaticity, size and molecular composition, which in turn have the potential to affect chemical regime (e.g., pH, metal and nutrient transport), light penetration, thermal stratification, and thus create distinct habitats for aquatic plants and organisms. The differences in stream DOM composition will influence the rate of DOM turnover as water moves downstream. Our study provides a description of the range of DOM composition across Canadian headwaters, which will be useful for future studies attempting to put the aquatic DOM composition in their study regions into a larger context and to understand the likely controls on their DOM composition. Our findings will be key to understanding the differences in drinking water treatability among different regions and the effects of disturbances and climate change on DOM composition in surface waters.

3. Seasonal Temperature Trend and Groundwater Connectivity Control Dissolved Organic Matter in Wetland-Rich Catchments of the Boreal Plains, Canada

Abstract

Stream dissolved organic matter (DOM) is a key link between terrestrial and aquatic ecosystems and controls many aquatic functions. Spatial and temporal variability of stream DOM differs among forested regions due to interactions between climate and physiogeography. In Canada, most studies of stream DOM have focused on humid shield environments with shallow soils, modest wetland coverage and hilly terrain. In contrast, the Boreal Plains ecozone in western Canada has sub-humid climate, flat terrain, widespread wetlands and thick heterogeneous glacial deposits underlain by sedimentary bedrock, leading to complex landscape-to-stream connectivity and variable stream DOM. Here we monitored dissolved organic carbon (DOC) concentration and DOM composition (UV-vis and fluorescence spectroscopy) in 17 streams over three years (2018-2020) to examine variability in and controls on the concentration and composition of DOM. Differences in DOM concentration and composition among the Boreal Plains streams, most of which were wetland-dominated (catchment wetland cover >40%), were primarily related to two factors. First, the presence of lakes led to reduced concentration and aromaticity of DOC. Second, the type of glacial deposits (fine-grained or coarse-grained) and landscape position determined surface water and groundwater contribution to streams. Seasonally, we found stream DOC concentration and aromaticity to increase as water temperature increased throughout the summer, likely reflecting increased organic matter decomposition and DOC production in hydrologically connected wetlands. Similar to studies conducted in other forested regions, wetland-dominated streams showed DOC dilution during summer storms, but this was secondary to the seasonal temperature trend. During very dry periods, in a larger stream catchment, wetlands appeared to

become hydrologically disconnected, causing a relative increase in the contribution of mineral sourced groundwater with low DOC concentration and aromaticity. Our results suggest that DOC concentration and aromaticity in small Boreal Plains streams may increase with further climate warming, although hydrological thresholds may cause a shift towards low DOC concentration and aromaticity during droughts.

3.1. Introduction

The concentration and composition of dissolved organic matter (DOM) in surface waters are highly variable across forested regions (Chapter 2). The flux of DOM from terrestrial sources to streams is a function of many variables, including climate, surficial geology and soil types, and land cover (Creed et al., 2008; Frost et al., 2006; Kothawala et al. 2015), and different spatial and temporal patterns in stream DOM have been reported in different regions (Laudon et al., 2011; Moore, 2003). Thus, impacts on stream DOM from climate change and land use may differ among physiogeographic regions, which necessitates regional studies. Of all the DOM studies conducted in forested regions, few have been done in the Boreal Plains ecozone of Canada, and it is not known whether its unique characteristics affect variations in and controls on stream DOM.

The concentration and composition of DOM in stream water can be determined to a large degree by the surrounding terrestrial environment (Kothawala et al., 2015). For example, high proportion of wetlands in a watershed is often linked to a high DOC flux, and wetland cover is often the strongest predictor of dissolved organic carbon concentration ([DOC]) in various regions (e.g., Mulholland and Kuenzler 1979; Creed et al., 2008). However, wetland cover alone may be insufficient to accurately predict stream [DOC] (Frost et al., 2006). Catchment morphology, including slope, vegetation type, soil properties, and the presence of lakes and permafrost have also been shown to affect [DOC], for example, by influencing the source, flowpath and residence

time of water (Harms et al., 2016; Jankowski & Schindler, 2019; Tranvik et al., 2009). In lakes, depending on the residence time and trophic status, DOM can be altered or lost via photo-oxidation, sedimentation and respiration, or produced by algae, thus altering the concentrations and composition of DOM transported downstream (Evans et al., 2017). At a larger scale, predictors of [DOC] include climatic variables, such as annual air temperature and runoff (Köhler et al., 2009; Winterdahl et al., 2014), and soil carbon-to-nitrogen ratio (Aitkenhead and McDowell, 2000). While we know what factors may influence variation in [DOC] and DOM composition, their importance is likely region-specific (Chapter 2; Kothawala et al., 2021). It is unclear how important these factors are for stream [DOC] and DOM composition in the Boreal Plains ecozone.

In addition to spatial variations, temporal changes in stream DOM can also be substantial and are driven by hydrologic and climatic factors. Several studies observed correlations between [DOC] and stream discharge. The relationship observed in the humid shield regions (e.g. Sweden and Ontario) is determined by terrestrial sources of DOM to streams. In wetland-dominated catchments, [DOC] decreases during storm events as a result of dilution by rainwater; in forest-dominated catchments, [DOC] increases as groundwater table rises and intersects with the organic soil in riparian areas, resulting in a flush of DOM to streams (Eckhardt and Moore, 1990; Hinton et al., 1998; Laudon et al., 2011). Seasonal fluctuations in runoff, however, explain only a minor proportion of variability in the DOM composition in shield region streams (Kothawala et al. 2015). A positive correlation with discharge has been observed in the arctic rivers, where [DOC] peaks during spring snowmelt (Finlay et al. 2006; Townsend-Small et al., 2011). A poor relationship with discharge but an increase in [DOC] in the summer was seen in northern Manitoba (Boreal Shield ecozone), (Moore, 2003). A similar increasing trend was seen in the Northwest Territories (Taiga Plains ecozone), and explained by a change in water sources (Burd et al., 2018). In northern

Quebec (Taiga Shield ecozone), most of the sampled peatlands and streams had an increase in [DOC] in the summer, followed by a decrease in the fall, which was explained by increased decomposition and evapotranspiration (Moore, 1987). At the same time, some of the streams showed no seasonal trend in [DOC] or a positive relationship with discharge (Eckhardt and Moore, 1990; Koprivnjak & Moore, 1992; Moore, 1987), suggesting that different streams within the same region may exhibit different seasonal trends in [DOC] or relationships with discharge (Winterdahl et al., 2014). Studies conducted in temperate regions saw a positive relationship between [DOC] and discharge (Raymond and Saiers, 2010), and a clockwise or counterclockwise hysteresis (Moore, 1989; Strohmeier et al., 2013). A fall peak in [DOC] can be related to leaching of fresh leaf litter entering the stream (Grubaugh and Anderson, 1989; Mulholland and Hill, 1997; Oswald and Branfireun, 2014). With differences in climate and potential water flowpaths, it is not clear which temporal patterns in DOM exist in the Boreal Plains and how they vary among the streams.

The Boreal Plains ecozone is different from many other regions, where stream DOM dynamics have been studied. The Boreal Plains occupy a large portion of Western Canada, and is characterized by sub-humid climate, with the average annual precipitation slightly less than the potential evapotranspiration, low annual runoff, spatially diverse landscape, large wetland extent and thick overburden (Devito et al., 2016, 2017; Natural Regions Committee, 2006). The weak relationship between precipitation and runoff (due to thick glacial deposits providing large storage), coupled with complex groundwater flowpaths, can result in a long-term delay between a hydrologic event and lake water levels and chemistry (Pugh et al., 2021), or mute the effect of disturbance on lake and stream water chemistry (Hillman et al., 1997; Olefeldt et al., 2013a). The highly variable runoff and water quality in the Boreal Plains catchments are hard to predict (Ireson et al., 2015), which may pose a challenge for drinking water treatability and supply in the region.

Since the Boreal Plains ecozone has climatic and physiogeographic characteristics that differ from other boreal regions, it is not known whether it has similar controls on DOM characteristics in streams.

Using DOM concentration and composition data from streams draining a range of small Boreal Plains catchments, we wanted to 1) assess spatial and temporal variability in stream DOM, and whether variations in DOM among streams determined by the differences in catchment characteristics (landcover and surficial geology) were greater than seasonal changes and 2) determine the main controls on stream DOM. Because surficial geology determines groundwater flowpaths and contribution to streams, as well as wetland distribution, we hypothesized that we would see a difference in stream DOM between catchments with the coarse-textured outwash deposits and catchments dominated by the fine-textured deposits (glacial till and clay). The former should have larger groundwater contribution, with lower [DOC] and DOM aromaticity, whereas the latter should have streams fed largely via surface runoff from wetlands, and thus have high [DOC] and higher aromaticity (Devito et al., 2023). Knowledge of variations in and controls on [DOC] and DOM composition in the streams of the Boreal Plains is required to better understand the downstream fate of DOM, the implications for drinking water treatability, and the potential effects of climate change and land disturbance on stream DOM.

3.2. Methods

3.2.1. Study site

The study was conducted at the Utikuma Region Study Area (URSA), a long-term research site north of Slave Lake, Alberta, in the Peace River watershed, within the Central Mixedwood subregion of the Boreal Plains ecozone (Figure 3-1; Ecological Stratification Working Group, 1996). A description of the URSA can be found in Devito et al. (2016).

A stream monitoring program was initiated at the URSA in the spring of 2018. We selected streams that represent different forested landscape types (Figure 3-2) to assess seasonal and spatial changes in DOM. The streams included 15 small unnamed streams (S1 to S22) and two larger watercourses: the Utikuma River (UR) downstream of the large Utikuma Lake and Redearth Creek (REC), which is a source of drinking water for the local community (Figure 3-1). All streams have forested catchments (with little to no human development) that range in size from 2.7 km^2 (S22) to 2,586 km^2 (UR), and eventually drain to the Wabasca and then Peace River. The frequency of monitoring and the number of collected samples varied among the streams. During the open-water season (late April to late October) samples were usually collected monthly or biweekly.

Pressure transducers were installed in several streams to continuously record water levels during the ice-free period. Discharge was measured using either an area-velocity method with an acoustic Doppler velocimeter (Sontek FlowTracker ADV), a simple float method or a manual volumetric method (used during low flow at hanging culverts). Discharge and water level data were used to build a rating relationship to estimate daily flows and to quantify DOC export. Discharge for REC from March to October is publicly available from the Water Survey of Canada hydrometric station 07JC002 (ECCC, 2023b). Precipitation and air temperature data were available for the climate stations Red Earth (3075488; ECCC, 2023a) and Red Earth Auto (Government of Alberta, 2023).

Water temperature, pH and specific conductance (SC) were measured in the field or upon return to the lab using one or a combination of the following handheld instruments: YSI Professional Plus handheld multiprobe (YSI Inc., Yellow Springs, OH, USA), Hanna HI98129 Combo pH/EC/TDS tester (Hanna Instruments Inc., Romania), Ultrapen™ PT1 and PT2

conductivity, pH and temperature pens (Myron L® Company, Carlsbad, CA, USA), ProfiLine pH 3110 meter with SenTix® 41 pH sensor (WTW, Weilheim, Germany).

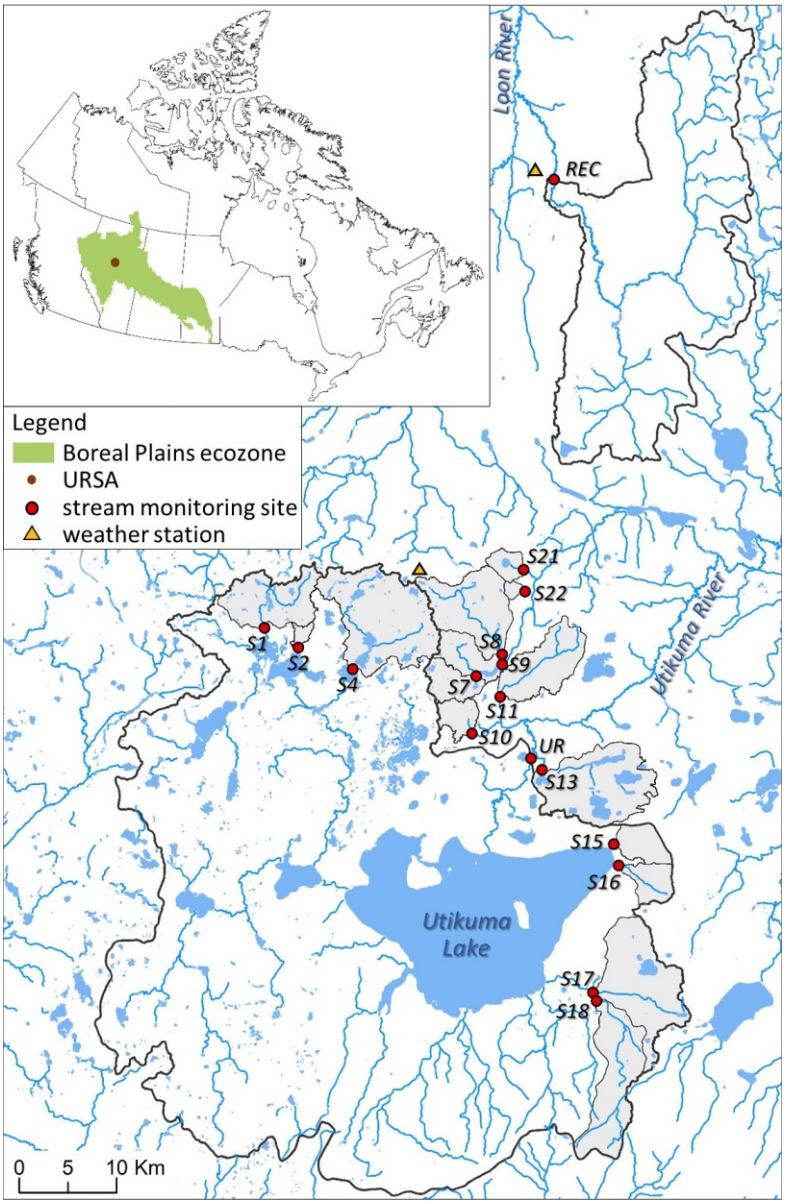

Figure 3-1. Location of the URSA in the Boreal Plains ecozone (inset) and stream catchments at the URSA.

Note:
The FWMIS hydrographic network layer (AEP, 2022) and the Utikuma Lake and REC watershed boundaries (ECCC, 2023c) were constructed at different times and with different data. Hence, some streams cross watershed boundary. There is a lot of potential bias and uncertainty on surface catchment delineations.

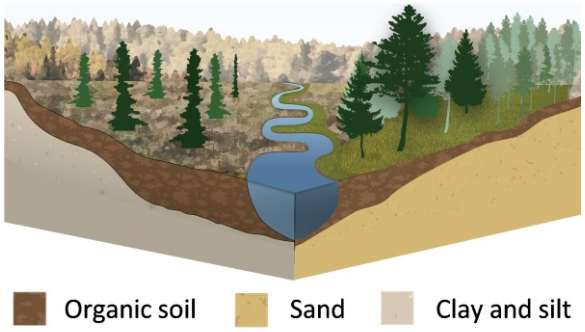

Figure 3-2. Boreal Plains ecozone schematic showing variations in surficial geology (coarse-grained vs. fine-grained glacial deposits), wetland soils and vegetation. Modified from Chapter 2.

At two streams (S2 and S8), autosamplers were installed for event-based sampling in 2019-2020 to collect higher-frequency (e.g., once or twice a day) data during summer rainfall events to assess changes in water chemistry as hydrological connectivity, sources and pathways of water change.

We used ECCC watershed boundaries for REC and UR (ECCC, 2023c). Catchment areas for other streams were delineated in ArcGIS using available satellite imagery and digital elevation models (DEMs). Because the regional topography is generally flat, and the surface and subsurface watershed boundaries may differ greatly, we expect some uncertainty in our catchment delineations (e.g., ±50% or higher for small catchments; watershed boundaries may also vary with annual weather cycles). Proportions of different landscape types, such as wetlands (including bogs, fens, swamps and some marshes), lakes, burned areas, and surficial geology units and other catchment properties (elevation, slope, stream order) were estimated for each catchment using publicly available datasets (Table 3-1).

Table 3-1. Stream catchment characteristics and number of samples analyzed

Site ID	Stream description	Site coordinates		Catchment area (km²)	Strahler order[1]	Elevation[2] (m)	Slope[2] (°)	Surficial Geology[3] (%)			% lakes[1]	% wetland[4,5]	% burn[6] (2011)	# of samples	
		Latitude (° N)	Longitude (° W)					Coarse outwash	Hummocky moraine	Clay plain				[DOC]	Absorbance
S1	Mink River tributary	56.140	115.738	45.0	2	677	1.55	13	63	24	5.74	43.4	31.1	23	37
S2	Mink Lake tributary	56.121	115.683	3.53	1	677	1.02	87	13	0	0	19.6	95.2	32	54
S4	Twin Lake outflow, Mink River tributary	56.101	115.594	91.4	2	681	1.30	53	30	17	8.95	50.4	64.6	33	49
S7	tributary to Artisinn Lake and S9	56.092	115.390	17.4	2	664	1.13	3	64	33	4.30	46.5	65.1	29	46
S8	tributary to Artisinn Lake and S9	56.111	115.346	54.2	3	673	1.17	8	66	27	1.81	62.1	91.9	52	74
S9	Artisinn Lake outflow, Utikuma River tributary	56.102	115.346	92.7	4	669	1.27	10	68	22	3.23	53.5	85.0	30	47
S10	Utikuma Lake tributary	56.039	115.399	13.0	2	657	0.92	0	51	49	0.12	48.3	83.3	24	39
S11	Utikuma Lake tributary	56.072	115.352	42.2	2	653	0.69	4	96	0	0	61.2	85.7	29	45
S13	tributary to Utikuma River	56.004	115.285	74.3	2	655	0.44	0	6	94	15.69	48.4	82.7	23	39
S15	Utikuma Lake tributary	55.934	115.170	17.2	1	658	0.37	22	1	78	0.12	58.6	53.3	34	49
S16	Utikuma Lake tributary	55.914	115.163	16.3	1	657	0.42	0	0	100	1.34	70.3	0	32	48
S17	Utikuma Lake tributary	55.797	115.211	136.6	3	672	0.54	7	27	66	2.77	58.5	0	24	39
S18	tributary to S17	55.790	115.205	61.7	2	691	0.74	5	51	45	0.27	54.7	0	25	40
S21	Utikuma Lake tributary	56.188	115.309	8.97	1	674	0.59	0	38	62	7.18	57.6	92.8	5	5
S22	Utikuma Lake tributary	56.168	115.306	2.74	1	669	0.55	0	67	33	0	72.1	100	5	5
REC	Redearth Creek, tributary to Loon River	56.547	115.240	585	4	615	0.80	15	29	56	0.80	65.5	0.4	37	46
UR	Utikuma River	56.015	115.303	2587	6	676	0.85	30	47	23	16.97	39.2	8.0	23	25

Notes:

– Lakes include all open water, including shallow wetland ponds, included in FWMIS polygon layer (AEP, 2022).

– Catchments were classified as “lake-dominated” when % lakes was >4%, and as “wetland-dominated” when % wetland was >25%.

Sources: [1]AEP (2022); [2]AEP (2017); [3]AER (2016a,b; 2008) and Devito et al. (2005, 2017); [4]Ducks Unlimited Canada (2011); [5]Devito et al. (2017); [6]Government of Alberta (2022)

3.2.2. Laboratory analyses

Water samples were collected in 60-mL amber glass bottles. The bottles were cleaned by soaking in 10% hydrochloric acid (HCl) for at least 24 hours and rinsed thoroughly with MilliQ® water. All bottles were rinsed with sample water prior to filling. Samples were filtered in the field using 0.7 μm GF/F syringe filters (in 2018) or 0.45 μm polyether sulfone (PES) syringe filters (after 2018). Samples for elemental analyses, including DOC, total dissolved nitrogen (TDN) and cations (Na, K, Ca, Mg, Fe, Mn), were preserved with 0.5 mL of 3M HCl. Samples were stored cool prior to analysis.

Collected water samples were analyzed for the concentrations of DOC and TDN, major ions, inorganic nutrients, metals, and DOM optical properties (UV-vis absorbance and fluorescence) in the Department of Renewable Resources and the Department of Biological Sciences at the University of Alberta. Concentrations of DOC and TDN were measured on the Shimadzu TOC-L_{CHP} Analyzer (Shimadzu Corporation, Jiangsu, China) with detection limits of 1 and 0.1 mg L^{-1} for DOC and TDN, respectively. Concentrations of dissolved sodium (Na), calcium (Ca), magnesium (Mg), iron (Fe), and manganese (Mn) were measured on a Thermo Scientific™ iCAP™ 6300 Duo ICP-OES Analyzer (Thermo Fisher Scientific Inc., Cambridge, United Kingdom). Concentrations of soluble reactive phosphorus (SRP), ammonium (NH_4^+), nitrate and nitrite ($NO_2^- + NO_3^-$), chloride (Cl^-) and sulfate (SO_4^{2-}) were determined by colorimetry (Gallery Beermaster Plus Photometric Analyzer, Thermo Fisher Scientific Inc., Vantaa, Finland).

UV-vis absorbance spectra were measured in 2018 using the Ocean Optics Flame spectrometer with direct attach UV-vis sampling system (Ocean Optics, Inc., Florida, USA) and later using the Shimadzu UV-1280 spectrophotometer (Shimadzu Corporation, Kyoto, Japan). From the absorbance spectra we determined absorbance at 254 nm (A_{254}; Dobbs et al., 1972) and

specific UV absorbance at 254 nm (SUVA; Weishaar et al., 2003), the ratio of absorbance values at 250 and 365 nm (E2:E3; de Haan & de Boer, 1987), the spectral slope between 275 and 295 nm ($S_{275\text{-}295}$) calculated using an exponential model, and the ratio of slopes $S_{275–295}$ and $S_{350–400}$ (S_R; Helms et al., 2008).

Fluorescence spectra were measured using a HORIBA Scientific Aqualog® fluorometer (Horiba Scientific, Edison, New Jersey, USA). Due to substantial variations in [DOC] and absorbance among the streams, the integration times were adjusted between 0.5 and 2 s, and samples with high absorbance were diluted with MilliQ® water using a maximum dilution of 2x (Kothawala et al., 2013). The water Raman signal-to-noise and emission calibration validation scans were performed upon every run. We estimated three common indices from the fluorescence excitation-emission matrix (EEM): fluorescence index (FI; Maie et al., 2006), biological index (BIX; Huguet et al., 2009), and humification index (HIX; Ohno, 2002). The FI is a ratio of fluorescence intensities at 470 and 520 nm, obtained at excitation of 370 nm. BIX is a proxy of the recent autochthonous production of DOM and is calculated as the ratio between emission at 380 nm (β peak representing recently derived DOM), and the emission maxima between 420 and 435 nm (α peak representing highly decomposed DOM), at an excitation of 310 nm. HIX is a measure of the degree of humification (lower H:C in humified organic matter), and is the ratio of fluorescence intensity at 435-480 nm and the total of fluorescence intensities at 300-345 nm and 435-480 nm, at excitation 254 nm.

A parallel factor analysis (PARAFAC) and index calculation were performed in MATLAB® R2021b (The Mathworks, Inc.) using drEEM-0.6.3 toolbox (Murphy et al., 2013). Sample EEMs were corrected for the inner-filter effect and MilliQ® blanks, and Raman normalized. A 5-component PARAFAC model was developed using a normalized dataset that included 486

samples after the noisy parts of EEMs and outliers were removed; the model was validated using a split-half analysis. A description of validated PARAFAC components is provided in Table 3-2.

Table 3-2. Description of validated PARAFAC components

PARAFAC component	Excitation maximum (nm)	Emission maximum (nm)	Probable source and/or reactivity	Select studies in OpenFluor with spectrally similar components (Tucker congruence ≥0.96 for excitation and emission)
C1	<250, 335	456	terrestrial, humic-like; photolabile	Kothawala et al., 2014 (C1/C4); Osburn et al., 2011, 2016, 2018 (C1); Thompson et al., 2023 (C1)
C2	<250, 305	391	microbial humic-like	Eder et al., 2022 (C5); Wauthy et al., 2018 (C4); Kothawala et al., 2014 (C2); Osburn et al., 2011, 2016, 2018 (C2); Thompson et al., 2023 (C2);
C3	275, 400	505	terrestrial, humic-like, refractory, photochemical product	Eder et al., 2022 (C1); (C1), Osburn et al., 2011, 2018 (C3); Kothawala et al., 2014 (C3); Wünsch et al. 2021 (C3); Guéguen et al., 2014 (C3)
C4	<250	424		Eder et al., 2022 (C3); Osburn et al., 2011, 2016 (C3); DeFrancesco & Guéguen 2021 (C4)
C5	280	336 (468)	protein-like	Kothawala et al., 2014 (C6); Osburn et al., 2011 (C5), 2016 (C4); Thompson et al., 2023 (C4); Wünsch et al. 2021 (C6); Guéguen et al., 2014 (C4)

3.2.3. Data analysis

Statistical analysis was conducted in RStudio (RStudio, PBC) with R version 4.2.1. Correlation for repeated measures (r_{rm}) was estimated with *rmcorr* package (Bakdash and Marusich, 2017). We used `metaMDS` function in *vegan* package (Oksanen et al., 2019) to conduct non-metric multidimensional scaling (NMDS) analysis. The NMDS used Hellinger-standardized data and Euclidian distance measure. NMDS scores were used in a random forest analysis performed using the `randomForest` function from the *randomForest* package (Liaw & Wiener, 2002) to assess which catchment characteristics influenced DOM composition.

Total annual export of DOC at four streams in 2019-2020 was calculated by interpolating [DOC] between dates with measured [DOC] (Aulenbach et al., 2016); this method was selected due to the lack of a strong relationship between [DOC] and discharge. A year for the calculations

was defined as November 1st to October 31st. Discharge was interpolated for the ice-covered period. Because REC has the longest discharge monitoring period (March 1st to November 1st), we have the most confidence in the interpolated discharge at this stream. Where no data were available, assumptions about [DOC] and discharge were made based on results from other years, spring air temperatures and discharge data from other streams. For example, there was only one winter sampling event (January/February 2021), which was used in the interpolations for other years.

3.3. Results

3.3.1. Hydrologic conditions in 2018-2020

The monitoring period (2018-2020) spanned three hydrologically mesic years (PET/P of 0.9-1.15; Devito et al., 2012) with different precipitation patterns. Total annual precipitation at Red Earth climate station was 673, 618 and 545 mm in 2018, 2019 and 2020, respectively, higher than the long-term average of 402 mm estimated using monthly precipitation for 1996-2022 (with several years having incomplete data). Year 2018 had a distinct spring freshet in late April to mid-May and high flows from mid-June to mid-August. Year 2019 had very low flows in the spring and elevated flows in late summer. Year 2020 also had a spring freshet followed by summer high flows (Figure 3-3).

Generally, there was synchronicity in discharge among the streams (Figure 3-3); however, beaver activity affected flow conditions (and rating curve development) at multiple streams. Several streams dried out during the summer (S1, S7, S16), and some were frozen to bottom during the winter and thus not sampled (S7, S10, S21).

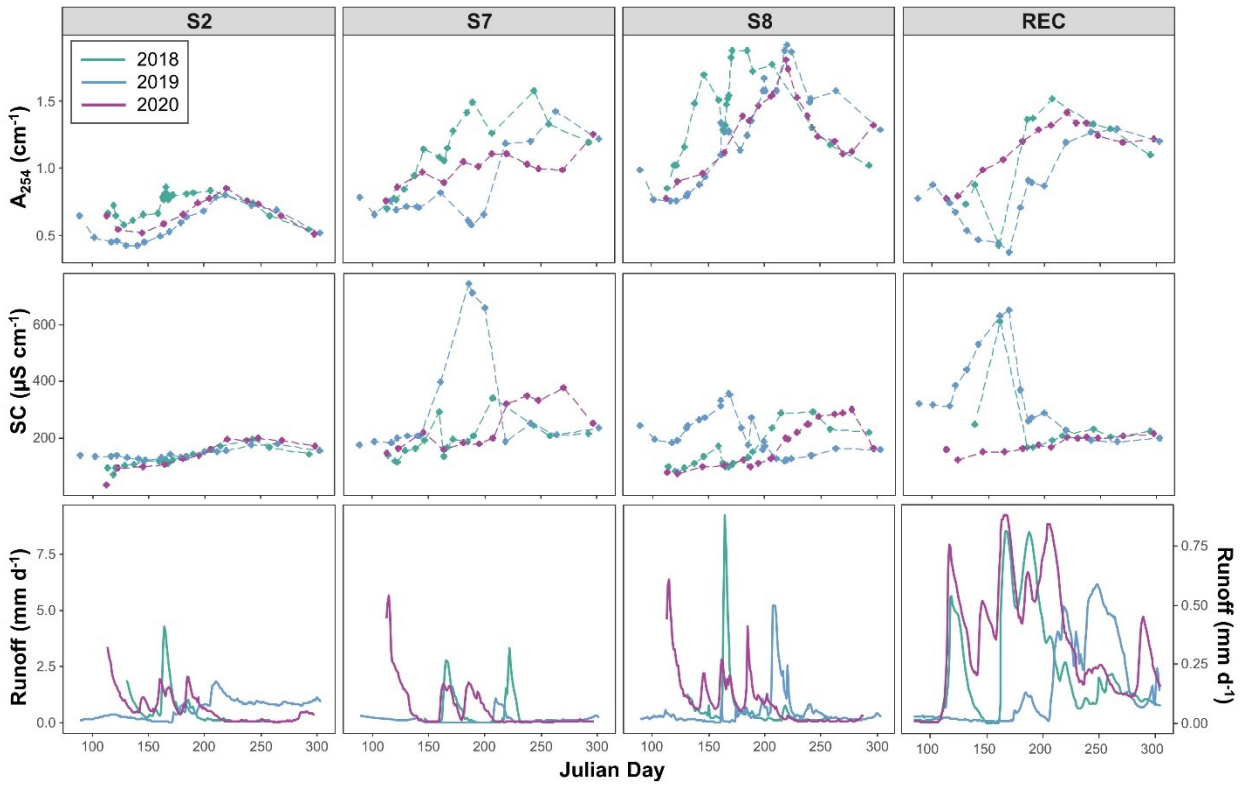

Figure 3-3. Variations in A_{254}, SC and daily runoff at four URSA streams (S2, S7, S8 and REC) in 2018-2020 (excluding winter 2021 samples). Runoff data for REC are from the WSC hydrometric station in Red Earth Creek (ECCC, 2023b). Runoff axis for REC is shown on the right. Points connected by dashed line indicate grab sample data, solid lines indicate continuous data.

3.3.2. Variations in solute concentrations

Most of our streams were characterized by neutral pH (usually between 7 and 8); with lower pH typically seen in S21, S15 and S2, and higher pH in REC and lake-dominated S4 and UR. Average SC was between 100 and 400 µS cm^{-1}, with calcium and carbonate being the dominant ions. Lower and least variable SC and concentrations of major ions were seen in S2 and S4, the two streams with the largest proportion of coarse outwash geology. Major ion concentrations and SC were also low in wetland-dominated S15, S21 and S22. Chloride concentration usually remained below 5 mg L^{-1}, and sulphate below 20 mg L^{-1}, and were lower in streams with coarse outwash geology. Concentrations of several ions, in particular SO_4^{2-} and Cl^-, were significantly higher in S16 compared to the rest of the streams. Average [DOC] was between 16 and 49 mg L^{-1},

and around 30 mg L^{-1} in most streams. Average [TDN] varied between 0.5 and 0.9 mg L^{-1}, and nitrate and nitrite were low and often below the detection limit. Based on DOC and TDN concentrations, average C/N was around 32. Average iron concentration varied between 0.25 and 0.89 mg L^{-1}, but in several wetland-dominated streams, including S8 (and S9 located downstream) and S21, exceeded 1.0 mg L^{-1}, and in UR was only 0.09 mg L^{-1}. Concentrations of major ions and DOC were not correlated (Figure 3-4); [DOC] was correlated with the concentrations of TDN (r_{rm}=0.68) and Fe (r_{rm}=0.37).

Variability in solute concentrations was greater within streams (temporal) than among streams (spatial), with some exceptions (Figure 3-4). Higher SC and concentrations of major ions were measured during prolonged low-flow periods both during the open-water and ice-covered periods. Most solutes, including DOC, TDN, Ca, Na, and SC exhibited chemostatic behavior (Figure B4; Cartwright et al., 2019), and typically no or weak negative relationship with discharge. For several streams, the behavior of solutes was chemodynamic (i.e. relatively larger variations in concentration), but still no clear relationship with discharge.

Intra-annual variations in [DOC] (or its proxy A_{254}) were large but synchronous among most streams, while inter-annual variability was not large (Figure 3-3 and B3a). We observed several trends in [DOC] using both [DOC] and A_{254} as its proxy (Figure B5) due to the absence of [DOC] data for 2018. First, there was an increase in [DOC] throughout the summer, with the peak in late summer, followed by either no change or a slight decrease later in the season. Second, based on autosampler data, there was a decrease in [DOC] during storm events at S8, which is representative of most of catchments in the region. Third, autosampler data for S2 revealed the opposite response – a small increase in [DOC] – during big storms (Figure 3-5). Fourth, during extended low-flow periods (May-June 2018 and 2019), [DOC] decreased at a larger stream (REC); this decrease

coincided with a large increase in SC (Figure 3-3 and B6). This, however, was not the case for smaller streams, where [DOC] slightly increased. At S8, a beaver dam broke during this dry period (June 10, 2019), and caused a small spike in [DOC] (Figure 3-5). Also, at some streams (e.g., S1 and S7), elevated [DOC] was seen in the fall (Figure B3a). Winter concentrations decreased at S8 and REC, but increased at other streams (Figure B3a). Lowest [DOC] was usually seen in coarse outwash-dominated S2, lake-dominated S4 and UR, as well as S11. Highest [DOC] was recorded in REC, S8, S21 and S22. There was a relationship between average [DOC] and proportion of wetlands in a catchment, although a weak one, mainly due to the presence of two outliers, S4 and S11 (Figure 3-6b).

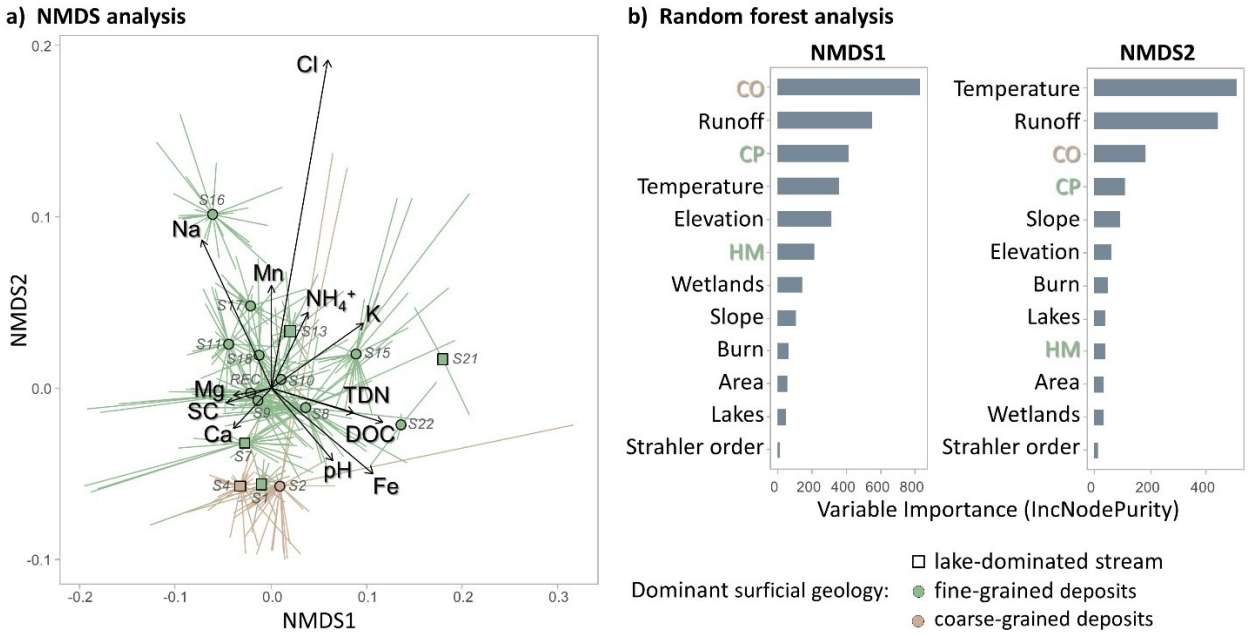

Figure 3-4. Variations in and controls on stream water chemistry, including [DOC]. NMDS analysis (a) and random forest analysis (b). UR is not included. SC = specific conductivity; CO = coarse outwash deposits, HM = hummocky moraine, CP = clay plain; Area = log-transformed catchment area; Burn = proportion of catchment burned during the 2011 wildfire.

Random forest analysis showed that surficial geology (in particular coarse outwash deposits), runoff and water temperature were the best predictors of water chemistry, including

[DOC], based on NMDS results (Figure 3-4b). Catchment properties, such as elevation and wetland cover, stream order were not very important. In comparison, random forest identified temperature as the best predictor of [DOC], followed by runoff, SC, clay plain and coarse outwash surficial geology, and pH (Figure B7), and explained 55.5% of variation in [DOC]. We noticed that day of the year was a better predictor than temperature and runoff in the random forest model. This is likely because it is an interaction term that explains low [DOC] seen early in the season as a result of low water temperatures and low-flow periods when groundwater contribution increases. However, using day of the year may not work well for predicting [DOC] during years with different precipitation patterns or in warmer climate in the future, and therefore, we chose not to use it in our model.

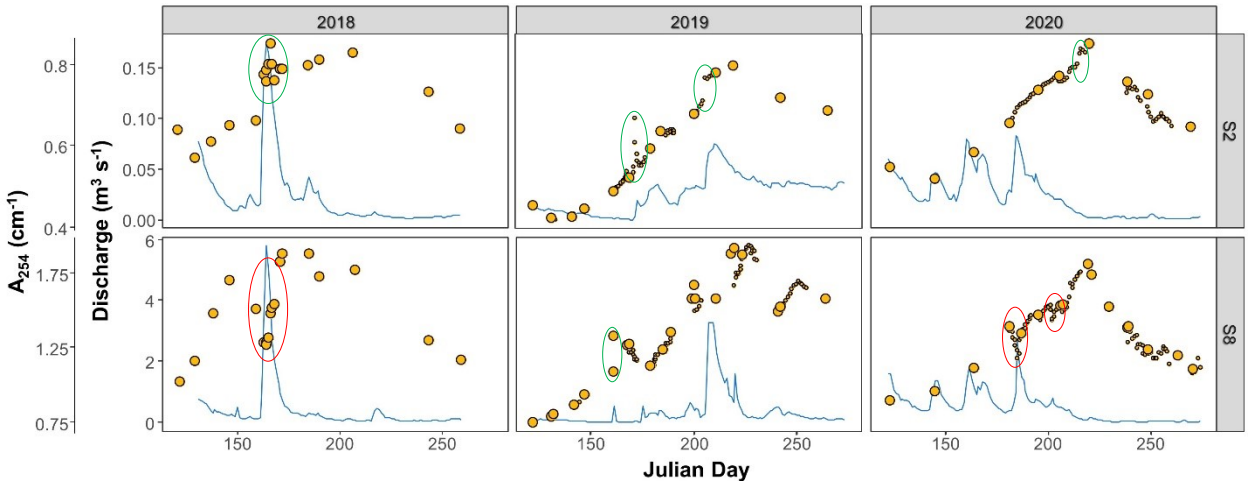

Figure 3-5. Dilution and flushing of A_{254} (circled in red and green, respectively) based on grab sample (large dots) and autosampler (small dots) data at two streams in 2018-2019.

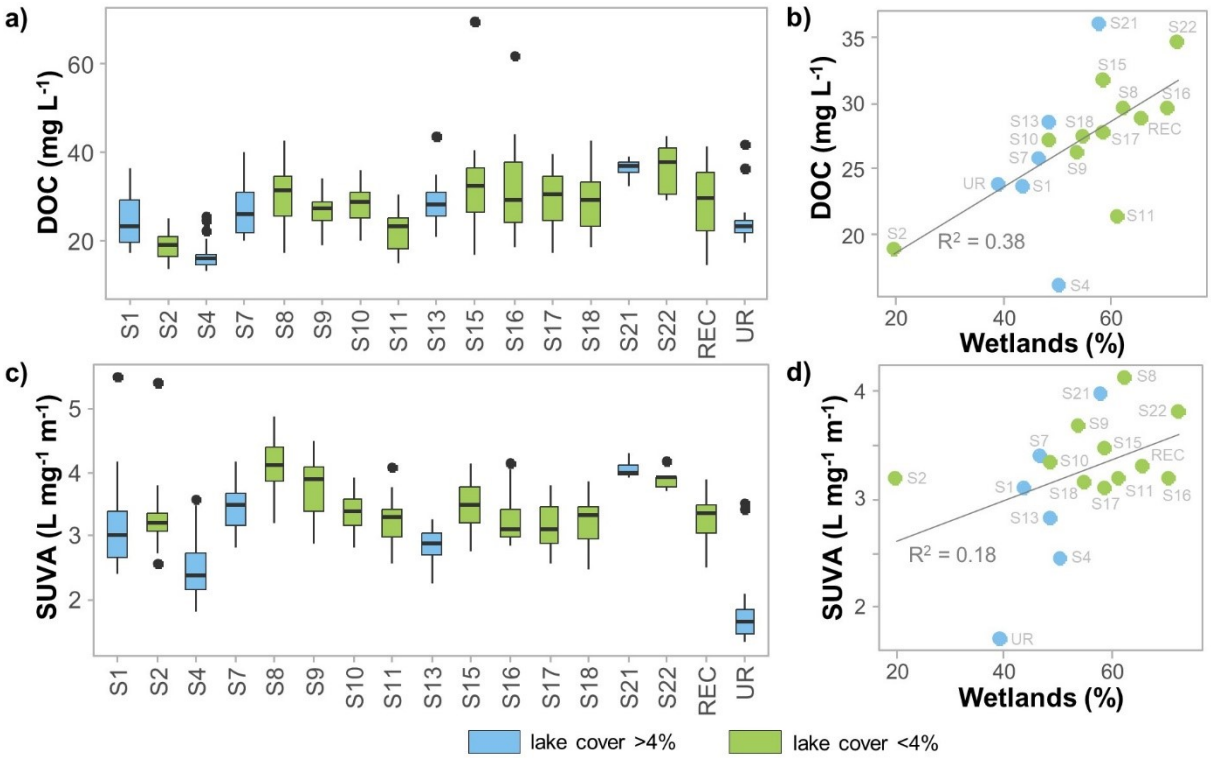

Figure 3-6. Variations in [DOC] (a,b) and SUVA (c,d) among the streams based on catchment lake and wetland cover. One outlier is not shown in a (S21 sample from February 2021). Average [DOC] and SUVA values are presented in b and d.

Our estimates for four streams showed variability in annual runoff among the streams and between the years (Table 3-3). Based on historical data (1987-2021), average March 1st to November 1st runoff in REC was 57 mm (ECCC, 2023a), and equaled 49, 35 and 79 mm in 2018, 2019 and 2020, respectively. Runoff in 2020 was about twice as high as that in 2019, except S2, which had similar runoff in both years. The highest runoff was seen at S8 and S2 in 2020, and the lowest at S7 in 2019, when the stream went dry during the summer. Annual export of DOC varied between 0.9 and 4.9 g m^{-2}, and resembled the variation in runoff. The lowest export was seen at S7 and REC in 2019 and the highest export at S8 in 2020.

Table 3-3. Calculated annual runoff, DOC export and flow-weighted [DOC] at four streams in 2019-2020.

Stream ID	Year	Runoff (mm)	DOC export (g C m^{-2})	Flow-weighted [DOC] (mg L^{-1})
S2	2019	137.6	2.8	20.5
	2020	160.8	2.9	18.2
S7	2019	30.4	0.9	28.9
	2020	135.1	3.5	25.6
S8	2019	103.5	3.5	33.9
	2020	190.9	4.9	25.9
REC	2019	36.1	1.2	33.9
	2020	87.6	2.9	33.1

3.3.3. Variations in DOM composition

Most streams had average SUVA in the range between 3.1 and 4.1 L mg^{-1} m^{-1}, but several lake-dominated streams (UR, S4, S13) had lower values (1.8 to 2.9 L mg^{-1} m^{-1}). E2:E3 was on average between 5 and 7, but higher values were seen in S4 and UR. Average HIX was between 0.90 and 0.96, and a lower HIX at S4 and UR. Average BIX was 0.51-0.65, with a higher HIX at S4 and UR. PARAFAC component C5 and BIX were correlated (r_{rm}=0.80); HIX was most strongly correlated with C1 (r_{rm}=0.66) and C3 (r_{rm}=0.55). Average FI varied from 1.45 to 1.60, suggesting DOM of lower aromaticity and some microbial processing (Kothawala et al., 2015). Overall, most streams were similar in terms of DOM composition based on absorbance and fluorescence indices, and the overlap in sample data in Figure 3-7a reflects that. Only the streams with strong lake influence (UR and S4 and to some extent S13) stood out and were characterized by consistently lower SUVA, HIX, C1 and C3, and higher E2:E3, S_R and BIX, C4 and C5.

The temporal pattern in DOM composition was similar among the wetland-dominated streams. There was a seasonal trend with elevated SUVA early in the season during snowmelt, followed by a small decrease in May, then a progressive increase throughout summer, and finally a decrease later in the season (Figure B3c). SUVA increased in the winter at S2, S4, S13 and S15

and decreased at other streams, based on February 2021 data. Absorbance slope parameters (E2:E3, S_R, $S_{275-295}$) varied little; they were slightly higher during drier periods.

Despite variable discharge patterns in 2018-2021, there were few differences in stream DOM composition between the years (Figures B3c-B3l). There was, however, a pronounced decrease in SUVA at REC under dry conditions in mid-May to early June 2019. Smaller wetland-dominated streams did not respond to this drought similar to REC, and in many cases SUVA slightly increased. At UR in August-September 2019, there was an increase in SUVA, HIX, S_R and E2:E3 and a drop in BIX. This change in DOM composition coincided with elevated water levels in the river and abundant algae and macrophytes in the water.

NMDS on DOM composition data showed overlap among most of the streams (Figure 3-7a), meaning that temporal variability was greater that spatial variability among streams, with some exceptions (S4). NMDS1 separated streams with strong wetland influence, including S22, S21 and S8, but also forest-dominated S2, from those with lake influence. High NMDS1 scores were associated with higher SUVA, C1 and C3, while lower NMDS1 scores indicated higher $S_{275-295}$, E2:E3, S_R, C5. The most distinct stream was lake-dominated S4, which had the lowest scores on NMDS1. Variation along NMDS2 axis was primarily defined by PARAFAC components C4 and C5, and SUVA, with generally smaller differences among the streams. On average, S21, S22 and S8 had higher scores on NMDS2, while lake-dominated S4 and groundwater-dominated S2 and S11 had lower scores. Two streams with coarse-grained surficial geology (S2 and S4) plotted at the opposite ends of the NMDS1 axis, but both had low NMDS2 scores.

Proportion of lakes in a catchment was the best predictor of variability in DOM composition along NMDS1, and water temperature along NMDS2 (Figure 3-7b). Random forest explained 83% and 49% of variation in NMDS1 and NMDS2 scores, respectively. Catchment properties, such as

surficial geology, elevation and wetland cover, were not very important, according to random forest.

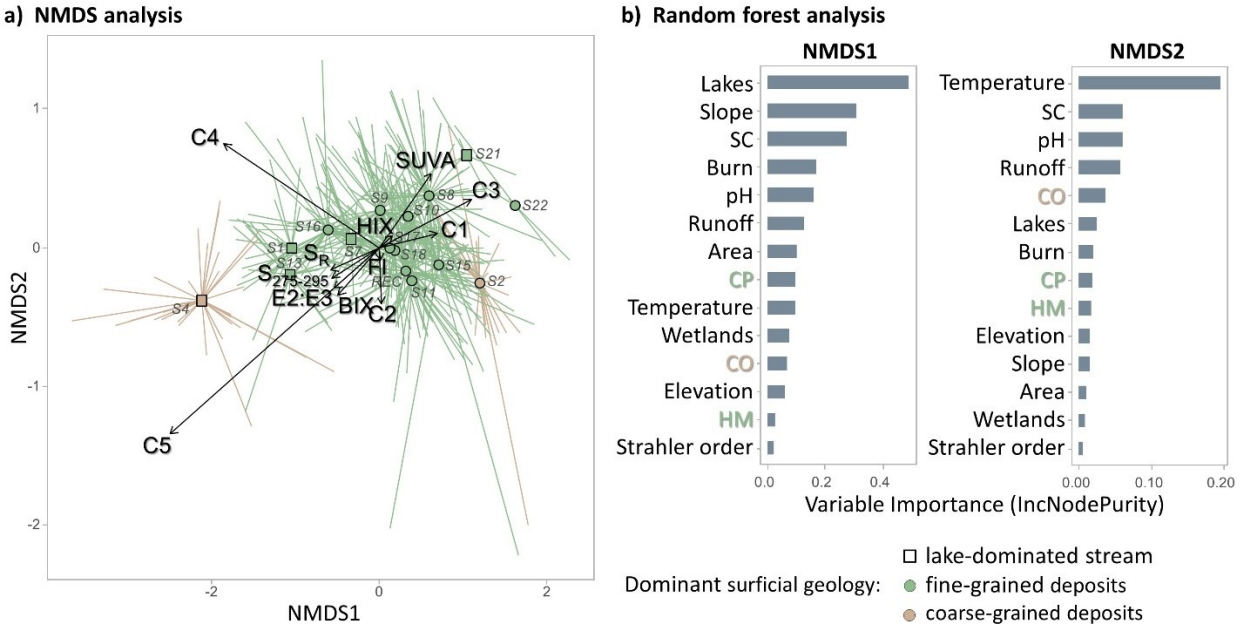

Figure 3-7. Variations in and controls on DOM composition. NMDS analysis (a) and random forest analysis using scores from NMDS (b). UR is not included. SC = specific conductivity; CO = coarse outwash deposits, HM = hummocky moraine, CP = clay plain; Area = log-transformed catchment area; Burn = proportion of catchment burned during the 2011 wildfire.

3.4. Discussion

Data from 17 Boreal Plains streams collected over three years revealed several spatial and temporal patterns in [DOC] and DOM composition, and the main controls on DOM. In particular, we observed a large range of [DOC] concentrations (from <20 to >50 mg L^{-1}), a seasonal trend in [DOC] interrupted by rain events and droughts, and a general synchronicity in seasonal [DOC] and DOM composition changes among the streams, with a few exceptions. Using statistical analysis and time-series plots, we found that these spatial and temporal variations were controlled by catchment characteristics (proportions of wetlands and lakes, surficial geology), hydrology and climate. We will discuss these findings below.

3.4.1. Variations in solute concentrations and DOM composition

The concentrations of DOC, TDN, major ions, metals and inorganic nutrients allowed distinguishing among individual streams, although there was a lot of overlap for most streams. Some of the differences in solute concentrations can be attributed to surficial geology. Most stream catchments are characterized by the clay plain or hummocky moraine (fine-grained till and clay) deposits, and are quite similar in water chemistry. Streams S1, S2 and S4 that have the largest proportion of coarse outwash geology (quartz sand) compared to other streams clustered together (Figure 3-4a). The coarse outwash deposits promote recharge of groundwater by precipitation, and later discharge of groundwater characterized by low concentrations of major ions and DOC to lakes and streams (Devito et al., 2005; Hokanson et al., 2019, 2022). Water chemistry in some clay plain streams, like S16, in particular elevated SO_4^{2-} and Cl^- concentrations, may be related to the presence of marine salts in the sediments rather than different water sources or flowpaths (Devito, *pers.comm.*). Although most streams drain large wetland areas, pH was relatively high (>7), which can be likely explained by the large buffering capacity of carbonate mineral soils.

High [DOC] in stream water was indicative of wetland influence on water chemistry. Wetland-dominated streams are typically defined as those with >25% wetland cover (e.g., Laudon et al., 2011). Most streams in our study had wetland cover >50% (Table 3-1), and are the most common type of catchments in the Boreal Plains. Wetlands are a major control on water chemistry, even though the relationship between average [DOC] and proportion of wetlands in our study was weak overall (Figure 3-6b), and wetlands did not come out as an important predictor on DOM composition (Figure 3-4b and Figure 3-7b). The lack of a strong relationship may be due to the limitations of wetland delineation or the fact that in these truly wetland-dominated catchments, where wetlands are the major source of water to streams, the differences become indistinguishable.

Average SUVA in most streams was similar to or slightly lower than in other boreal regions (e.g., Creed et al., 2008; Olefeldt et al., 2017). In particular, it was lower than in small catchments with similarly high proportion of wetlands (Ågren et al 2008; Kothawala et al., 2015; Oliver et al., 2017). Reduced DOM aromaticity in the Boreal Plains streams compared to other boreal regions may be related to relatively high concentrations of Ca^{2+} and Mg^{2+}, sourced from carbonate-rich mineral soils. These ions are known to cause flocculation and thus decrease the solubility of high molecular weight organic acids (Aiken & Malcolm, 1987; Römkens & Dolfing, 1998).

The streams that fell below the general trend in Figure 3-6b are S4 and S11. Both have a large proportion of wetlands in their catchments. However, S4 is lake-dominated (lakes cover almost 9% of catchment), which resulted in lower [DOC] and less aromatic DOM likely due to photodegradation and autochthonous production. Additionally, S4 has a large proportion of coarse outwash deposits, which could lead to significant contribution of low-DOM groundwater, similar to S2. As for S11, it is located in an area with flowing artesian conditions (Ceroici, 1979), suggesting that groundwater springs may be feeding S11, resulting in lower [DOC]. However, SC was not elevated in this stream (Figure B3m).

3.4.2. Runoff and DOC export

Our annual runoff estimates varied greatly between the two years and among streams, but generally aligned with the regional data (Devito et al., 2017). The large variability in runoff we observed is very characteristic of the Boreal Plains streams, and reflects the regional moisture deficit, large subsurface water storage in thick sediments, and complex surface water-groundwater interactions (Hokanson et al., 2019). Runoff at S8 was greater than at other wetland-dominated streams REC and S7, possibly because large wetlands are located along its channel (which may also explain higher [DOC] and aromaticity in this stream). We saw high and least variable runoff

at S2, one of the smallest streams in our study (3.5 km^2), with catchment characterized by coarse-textured glaciolacustrine deposits and small proportion of wetlands. Groundwater recharge coupled with lower potential evapotranspiration by pine forest in coarse outwash areas makes them water sources (Smerdon et al., 2005). Groundwater feeding S2 also produced the least variable water chemistry and DOM composition. Streams with low groundwater connectivity, like S7, ceased flowing during the dry periods in the summer and in the winter, producing very low annual runoff. Variations in runoff among the streams translated into the differences in DOM export.

Because annual runoff was relatively low in our streams, DOC export in comparison to other boreal regions was also low, despite high [DOC]. For example, our DOC export in 2019-2020 was similar or slightly lower than the export on the Boreal Shield in Ontario and northern Manitoba (e.g., Creed et al., 2008; Eimers et al., 2008; Moore 2003), where stream [DOC] rarely exceeds 10 mg L^{-1}, and in northern Sweden (Olefeldt et al., 2013). It was substantially lower than DOC export from very small almost fully peat-covered catchments in the UK, but not very different from larger streams, similar in size to the ones in this study (Worrall et al., 2012); some of the DOC that accounts for the difference is likely lost in transit (Casas-Ruiz et al., 2017). The estimates of peat-derived DOC mineralization from headwaters to the ocean vary and may be in the range of about 30% (Frei, 2023) to 50% or higher (Moody et al. 2013).

There is some uncertainty in our export estimates due to variable frequency of [DOC] measurements and the lack of winter measurements for both parameters. Additionally, our calculation did not include the autosampler data that revealed decreasing or increasing trends in A_{254} (and thus [DOC]) during high flows, and no [DOC] was measured in autosampler samples, and potential effects on sample quality during storage in the autosampler before the samples were retrieved. However, because runoff during the winter season is very low, and the change in [DOC]

during rain events is short-lived and not very large, we believe the errors are small relative to our estimates, and our calculations remain valid. Based on total annual precipitation data, 2019-2020 were wetter than the long-term average, so our estimates of annual runoff and DOC export are likely higher than the long-term average for the region. Overall, wetland-dominated catchments on the Boreal Plains, despite often higher [DOC], did not have high DOC export compared to other boreal regions.

3.4.3. Controls on DOM composition

The best predictors of DOM composition were lakes (spatial variation) and water temperature (temporal variation). Streams draining catchments with lakes had consistently lower [DOC] and DOM aromaticity. Lakes increase residence time, allowing for photodegradation, microbial respiration and autochthonous DOM production, resulting in lower [DOC] and SUVA, and higher S_R, E2:E3, $S_{275-295}$ and C5, which is commonly observed in other forested regions (Evans et al., 2017; Köhler et al., 2013; Liu et al., 2020). The Boreal Plains have abundant shallow lakes with long residence time, and most streams have to flow through a lake (e.g., Utikuma Lake for most streams at URSA), which emphasizes the importance of lakes in this landscape.

Seasonal changes in [DOC] were pronounced at all streams (except lake-dominated S4 and UR), with the concentrations doubling between the spring and mid-summer. This increase and the range of concentrations are consistent with previous findings from the boreal regions (Burd et al., 2018; Hillman et al., 1997; Moore, 2003), and likely related to overland flow and seasonal frost thaw in wetlands in the spring and early summer (Laudon et al., 2004), and increased microbial processing of organic matter in soils as temperatures increase throughout summer (Pinsonneault et al., 2016). Due to this seasonality, the timing of high flows is important for DOC export. If high flows occur during the spring or early summer, when [DOC] is low, the total export of DOC will

be lower than if high flows occur later in the season. We saw elevated [DOC] in some streams in the fall, which may be explained by leaf fall in catchments with aspen stands (Tank et al., 2010), but in other streams concentrations slightly decreased, as did the temperatures.

Although runoff did not come out as the most important predictor, likely because no high-frequency [DOC] and DOM composition data were available, and because it did not have a consistent effect during rain events across sites, we still saw several patterns in DOM related to runoff. There was evidence of [DOC] dilution (wetland-dominated S8) and flushing (forest-dominated S2) during large rain events, similar to responses seen in other boreal regions. The decrease in [DOC] during high flows can be explained by dilution of DOM-rich wetland water by event water running off as overland and shallow subsurface flow. The increase in [DOC] occurs as a result of rising groundwater table intersecting with organic-rich soil in riparian areas (Laudon et al., 2011). This behavior has not been reported in the Boreal Plains region previously. Interestingly, Hillman et al. (1997) did not observe a change in [DOC] during rain events, despite using a similar sampling approach and frequency. Other studies of stream [DOC] that observed a seasonal trend did not specifically target storm events, so it is possible that the short-term changes in [DOC] were missed (Burd et al., 2018; Moore et al., 2003). Overall, based on our data for two streams (S8 and S2), the change in [DOC] during rain events was short-lived and small relative to the overall increasing seasonal trend, and also in comparison with other wetland-rich boreal regions, where stream discharge is the primary control on [DOC] (e.g., Hinton et al., 1997). Thus, our study showed that the Boreal Plains seem to have some difference in controls on DOM in that the importance of discharge is secondary to temperature.

We also observed reduced [DOC] and a change in DOM composition coupled with increased SC during a summer dry period at our larger stream. These data indicate that some wetlands in the

catchment likely became disconnected, and relative groundwater contribution to streams increased (Frost et al., 2006). Wetlands are the main source of runoff in the Boreal Plains ecozone (Thompson et al., 2015). But our results showed that prolonged dry periods in the summer have potential to limit runoff generation by wetlands. The switch in water sources from wetlands to groundwater, which is characterized by low [DOC] and low-aromaticity DOM (McDonough et al., 2022; Tiwari et al. 2022), was evident in REC, but not in other wetland-dominated streams, where both [DOC] and SUVA slightly increased (Figure 3-3). Tiwari et al. (2022) also discovered that SUVA increased during drought, potentially due to deeper organic soil layers in wetlands contributing more aromatic DOM, and the larger streams had a greater decline in [DOC] compared to smaller streams, as they are father downstream from the wetlands that feed the headwaters. Thus, catchment size may be indicative of the potential effect of drought on stream DOM. Due to the spatial heterogeneity of surficial geology and variations in landscape position, resulting in variations in hydrological connectivity of streams to wetlands and groundwater, the Boreal Plains streams may have different responses of DOM characteristics to droughts.

The reason runoff was still the top four predictor for DOM composition NMDS2 (Figure 3-7d) is likely due to the difference in DOM composition observed during these dry periods compared to high flow periods characterized by high-aromaticity wetland DOM. There are several possible reasons why we did not observe a stronger relationship between runoff and DOM. First, we included streams with different responses to storm flows (wetland-dominated S8 and forest-dominated S2) in the same analysis, and we only had one forest-dominated stream (i.e. wetland cover <20%). We had limited sample data for storm events (we missed many big storms), and we did not include autosampler data in our random forest model (we only measured A_{254} and SC in the autosampler samples). We expect that other URSA streams that we didn't sample as frequently

behaved similarly. It is likely that studies conducted in the boreal regions that did not observe a relationship between DOM and discharge did not have frequent event data. Beaver activity likely also affects the relationship between DOM and discharge. Finally, the effect may not be as obvious compared to the Boreal Shield, because peak flows in the Boreal Plains occur at different times during the season, and there is rarely a big snowmelt event.

Larger streams, like REC, are sources of drinking water to small communities in the Boreal Plains ecozone. Our results suggest that, as [DOC] changes seasonally, so will drinking water treatability. We also found that [DOC] and DOM composition in stream water were predictable based on the time of year, flow conditions, and catchment characteristics (e.g., presence of lakes and wetlands). However, in the subhumid Boreal Plains ecozone, where streams the size of REC (almost 600 km^2) can dry out, water availability in streams may be a more important consideration for the timing of withdrawals for the purpose of drinking water supply.

Our findings also show that climate change may affect [DOC] and DOM composition. As climate warms, soil and water temperature may increase, which will result in an earlier ground thaw and enhance degradation of organics in soil, leading to higher [DOC] earlier in the season. Changes in precipitation pattern and drought frequency may affect the export of DOM. Higher evapotranspiration may result in contraction of lakes and wetlands, although wetlands may exhibit resilience due to reduced evapotranspiration losses (Schneider et al., 2016).

3.5. Conclusion

This study examined variability in DOM concentration, export and composition in a range of streams in the Boreal Plains ecozone, and environmental controls on DOM, and highlighted the complexity of processes that determine stream DOM dynamics. Sampling of 17 streams between 2018 and 2022 revealed several interesting spatial and temporal patterns in [DOC] and DOM

composition. Overall, both [DOC] and DOM composition were highly variable over time in wetland-dominated streams, and less variable in lake-dominated and non-wetland-dominated streams. We saw dilution (wetland-dominated stream) or flushing of [DOC] (forest-dominated stream) during high flows, and a decrease in [DOC] during very low flows (larger wetland-dominated stream). But the main temporal trend was a gradual increase in [DOC] throughout the summer with a July peak, and a subsequent decrease later in the season. It followed the seasonal change in water temperature, which may be related to temperature-controlled DOM production in wetlands, and has implications for DOC export. DOM aromaticity generally followed this increasing seasonal trend. Although similar temporal patterns were reported for other forested regions, we were able to observe and compare both long-term (seasonal) and short-term (event) changes in DOM in a range of streams, which has not been commonly done. Our findings show that despite the large differences in topography, surficial geology, land cover and precipitation, that distinguish the Boreal Plains ecozone from other boreal regions, the same processes govern stream DOM, but their importance varies.

Spatially, the presence of lakes, higher groundwater connectivity (related to surficial geology and landscape position) and smaller proportion of wetland cover in a catchment were associated with lower concentration and aromaticity of stream DOM. However, with most streams characterized by large proportion of wetlands in catchments, [DOC] was high, while SUVA was not as high as in some other boreal regions. Despite the high [DOC], DOC export by streams in the subhumid Boreal Plains ecozone was similar to or lower than in other boreal regions due to low runoff. Understanding the controls on stream DOM allows us to anticipate the effects of climate and land-use change on the concentrations and composition of DOM in the Boreal Plains.

4. The Role of Aquatic DOM Transformations in Shaping DOM Character and Drinking Water Treatability in Boreal Streams

Abstract

Aquatic processes like photodegradation and biodegradation can significantly alter the concentrations and composition of dissolved organic matter (DOM) that is delivered to streams from terrestrial environment; however, we do not know how important these processes are for DOM turnover in streams of the Boreal Plains region of Canada, and what this processing means for downstream water quality and drinking water treatability. We conducted laboratory incubations on water collected from five Boreal Plains streams over different seasons to assess photo- and biodegradation of stream DOM by irradiating water samples in a solar simulator for up to 3 days (photodegradation) and incubating samples in the dark for up to 60 days (biodegradation). We measured changes in dissolved organic carbon (DOC) concentration, and absorbance and fluorescence indices. Most samples responded similarly during incubations, with small loss in DOC concentration but large decreases in aromaticity/humification as a result of photodegradation; and no or little change in aromaticity and an increase in freshness index as a result of dark incubations. There were no clear seasonal patterns, except for winter samples (with lower aromaticity) that had lower dissolved inorganic carbon (DIC) production per A_{254} loss. Spatially, the most distinct stream was the lake-dominated one; it showed little change in DOM concentration and composition during photodegradation. For both types of incubations, there were no strong controls on changes in DOM, although temperature and runoff were identified as potential predictors of the observed changes using mixed-effects modelling. We compared changes in DOM composition during these incubations to samples collected from the regional small lakes, a lake-dominated river and a drinking water reservoir. We saw a strong shift in DOM composition

of photodegraded stream samples (but not of biodegraded samples) toward observed DOM composition in lakes and the reservoir. We also assessed the change in the disinfection by-product formation potential (DBP-FP) as a result of photodegradation. Despite a decrease in absorbance, we did not see a uniform decrease in DBP-FP upon irradiation, confirming a lack of a strong relationship between aromaticity and DBP-FP. These results highlight the importance of both of these processes in transforming DOM as it moves from the wetland-dominated Boreal Plains landscape through the stream network, and especially the strong effect of photodegradation.

4.1. Introduction

Dissolved organic matter (DOM) in headwater streams is derived mainly from terrestrial sources (Cole et al., 2007), but as it moves from terrestrial environment through the aquatic network, it is processed by sunlight and microbes, and its quantity and composition change (Creed et al., 2015). This processing has important implications for carbon cycling, including CO_2 emissions (Koprivnjak et al., 2010) and delivery of DOM to the oceans (Jones et al., 2016), water chemistry, including metal speciation, aquatic ecosystem functioning, and drinking water treatability, including formation of disinfection by-products (DBP) (e.g., Oleinikova et al., 2017; Parsons et al., 2004; Porcal & Kopáček, 2018; Waite & Morel, 1984; Wilske et al., 2021). While aquatic processes, including photo- and biodegradation, flocculation and sedimentation, and primary production of DOM, contribute to spatial and temporal variations in the concentrations and composition of DOM, the importance of these processes is still poorly understood. Assessing the role of photo- and biodegradation in transforming aquatic DOM is key for understanding the effects of climate change and land disturbance on DOM, and how these processes affect drinking water treatability.

Studies of stream DOM degradation have been conducted in different boreal regions (e.g., Köhler et al., 2002; Raudina et al., 2022; Soares et al., 2019). However, findings from other regions may not apply to the Boreal Plains region due to its sub-humid climate, flat to undulating topography and thick overburden, the interactions of which produce large seasonal and interannual variability in hydrological connectivity and runoff generation. Peatlands that often comprise >50% of the landscape are the main sources of dark-colored high-DOC water to slow-moving, meandering, often beaver-impounded streams (Thompson et al., 2015). However, variations in surficial geology and landcover and the presence of lakes, coupled with seasonal changes in hydrology, create some heterogeneity in stream DOM concentrations and composition. It is not clear how important the spatial and temporal differences are for the degradability of stream DOM in this landscape.

Both UV-induced photochemical transformation of DOM and heterotrophic bacterial respiration are important pathways for DOM removal and alteration. Photodegradation can occur via complete photomineralization, partial photo-oxidation, photostimulated bacterial respiration and photoflocculation; the relative importance of each pathway will vary depending on DOM composition and the history of light exposure (Cory et al., 2014; Hu et al., 2022). High rates of photomineralization have been seen in shallow water bodies with high DOC concentrations (Vachon et al., 2017), and in small unshaded streams with limited prior exposure to sunlight (Cory et al., 2014). In contrast, forested headwater streams with short water residence times may act as a “passive pipe”, with no in-stream processing of DOM (Kothawala et al., 2015). The role and relative importance of photodegradation versus biodegradation in the boreal catchments remains unclear.

Photo- and biodegradation preferentially affect different DOM moieties (Benner and Kaizer, 2011), and are not independent of each other (Amado et al., 2015). Photodegradation mainly removes chromophoric DOM, such as lignin, enriches ^{13}C, reduces the number and structural diversity and the average molecular weight of organic compounds (Lou and Xie, 2006; Stubbins et al., 2010). Biodegradation, on the other hand, preferentially removes low-molecular weight compounds, including carbohydrates, carboxylic and amino acids (Berggren et al., 2010). Although autochthonous DOM is often seen as more bioavailable than allochthonous DOM, humic DOM, which is sometimes described as biologically refractory, can also support high levels of bacterial respiration (Guillemette et al., 2013; Volk et al., 1997). The effect of photodegradation on bioavailability is often positive for terrigenous DOM (Ward et al., 2017), and minimal or even negative for autochthonous DOM (Sulzberger and Durisch-Kaiser, 2009). The complex interactions, as well as spatial and temporal variability in DOM composition and concentrations typically seen across the Boreal Plains catchments, make it difficult to predict photo- and biodegradability of DOM in aquatic ecosystems.

The degradability of aquatic DOM, however, cannot be explained solely based on DOM composition, and environmental controls, such as catchment characteristics (Berggren & del Giorgio, 2015; Berggren et al., 2007; Guillemette and del Giorgio, 2011), water residence time (Soares et al., 2019) and physical environment, need to be considered. For example, wetland DOM is generally considered recalcitrant and contributes little to aquatic metabolism (Fellman et al., 2008), although in some wetland-dominated streams DOM can be highly labile (Fellman et al., 2009). At the same time, colored wetland DOM is photoreactive (Olefeldt et al., 2013; Pickard et al., 2017). Degradability of DOM decreases during water transit (Marín-Spiotta et al., 2014; Catalán et al., 2016), although photodegradation of recalcitrant DOM increases biodegradability

with longer water residence time (Soares et al., 2019). Biodegradation is influenced by water temperature and nutrients (Catalán et al., 2021), while photodegradation will vary based on salinity (Minor et al., 2006), pH (Molot et al., 2005), iron content (Gu et al., 2017; Bowen et al., 2020), wavelength of solar radiation (Molot and Dillon, 1997), and temperature (Porcal et al., 2015). Degradability can vary seasonally (Osburn et al., 2009; Groeneveld et al., 2016) and during storm events (Demars, 2018; Pickard et al., 2017), although no seasonal shift in biodegradability was found in small Arctic streams (Vonk et al., 2015). The importance of environmental controls on DOM degradability suggests that findings from different regions may not always be transferrable to other physiogeographic regions.

The goal of this study was to understand how the photo- and biodegradability of stream DOM varied among the streams in the Boreal Plains. In particular, we wanted to see whether DOM from certain catchments (different landcover or surficial geology) was preferentially degraded as it moved down the stream network, and how water residence time and seasonality (changes in runoff and temperature) affected DOM degradability. We also wanted to compare the relative importance of photo- and biodegradation and to assess their spatial and seasonal trends. Given that the Boreal Plains is a wetland-dominated region, we hypothesized that biodegradability of DOM would be relatively low and photodegradability high, and would be related to wetland cover in stream catchments. Because there was a strong seasonal trend in DOM concentrations and composition across the Boreal Plains streams, we also hypothesized that there should be a similar seasonal shift in degradability, from more biolabile DOM in the spring to less biolabile later in the season, consistent with increasing aromaticity. We were also interested in exploring DOM degradability along the stream network by comparing streams of different orders, and the effect of

water residence time. Finally, we wanted to assess the importance of photodegradation in determining DBP formation potential.

4.2. Methods

4.2.1. Study site and stream sampling

The study was conducted at the Utikuma Region Study Area (URSA), a research site north of Slave Lake, Alberta, in the Peace River watershed, within the low-relief Boreal Plains ecozone. To assess seasonal and spatial changes in DOM photo- and biolability, we focused on five streams with catchments that represent different landscape and surficial geology types and distinct water chemistries (Table 4-1). The streams include four small, unnamed streams (S2, S4, S8 and S15; Figure 4-1), draining mostly forested catchments that range in size from 3.5 km^2 (S2) to 90 km^2 (S4), and Redearth Creek (REC) that drains a larger catchment (585 km^2). REC is a source of drinking water for the community of Red Earth Creek. Therefore, we also sampled a water storage reservoir (RES) in Red Earth Creek, which consists of two cells that are refilled during high flows, to better understand the transformation of DOM during storage. In addition, we sampled the Utikuma River (UR) downstream of the large Utikuma Lake to compare the effect of long residence time on DOM composition with the results of the laboratory experiments (samples from UR were not incubated).

We used publicly available discharge data for the Water Survey of Canada hydrometric station Redearth Creek at Red Earth Creek (ECCC, 2023b) to determine flow conditions (low to high) in all streams. Water temperature, pH and specific conductance were measured in the field or upon return to the lab using a combination of the following handheld instruments: Hanna HI98129 Combo pH/EC/TDS tester (Hanna Instruments Inc., Romania), Ultrapen™ PT1 and PT2

conductivity, pH and temperature pens (Myron L® Company, Carlsbad, CA, USA), ProfiLine pH 3110 meter with SenTix® 41 pH sensor (WTW, Weilheim, Germany).

Small catchment areas were delineated in ArcGIS for Desktop version 10.8.1 (Esri) using available satellite imagery and digital elevation models (DEM). Large catchment boundaries (REC and UR) were available from ECCC (2023c). Because the regional topography is generally flat, and the surface and subsurface watershed boundaries may differ greatly, we expect some uncertainty in our catchment delineations (e.g., ±50% for smaller catchments). Proportions of different surficial geology and landscape types (including wetlands and lakes) and other catchment properties (elevation, slope, stream order) were estimated for each catchment using publicly available datasets (Table 4-1).

Water samples for the laboratory incubations were collected on different dates throughout the open-water season and once during the ice-covered season. The frequency and timing of sampling varied among the streams, but we were able to sample different seasons and hydrologic conditions. Most water samples were collected in 2020, with a few samples in 2019, 2021 and 2022. Samples were collected in 0.5-L or 1-L amber glass bottles. All glassware for this study was acid-washed using dilute hydrochloric acid (8-10% HCl) for a minimum of 24 hours and thoroughly rinsed with ASTM Type I (MilliQ®) water. Samples for the experiments were filtered to 0.45 µm using the Whatman PES syringe filters; frequently, samples were pre-filtered using the Whatman 0.7 µm GF/F filters. Filtration took place in the field whenever possible, or upon return to the laboratory on the same or the following day.

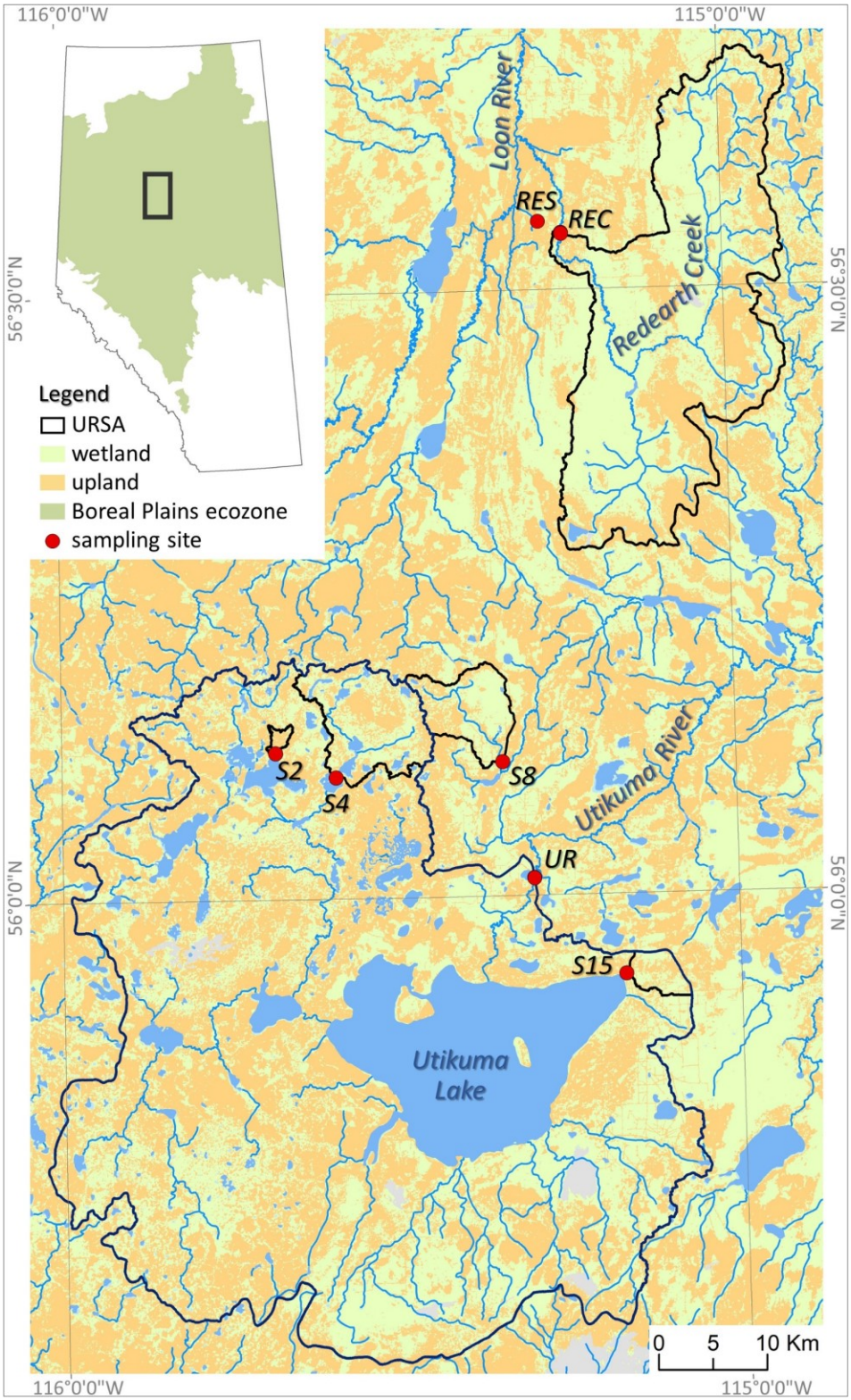

Figure 4-1. Location of the Utikuma Region Study Area (URSA) in northern Alberta, stream catchments and water sampling locations. The UR catchment (dark blue outline) includes S2, S4 and S15 catchments. Wetlands and uplands classification is based on the Ducks Unlimited Canada (2011) dataset summarized by Devito et al. (2017).

Table 4-1. Study catchment characteristics

Site ID	Stream description	Site coordinates		Catchment area (km^2)	Strahler order[1]	Elevation[2] (m)	Slope[2] (°)	Surficial Geology[3] (%)			% lakes[1]	% wetland[4,5]	2011 burn[6], %
		Latitude (° N)	Longitude (° W)					Coarse outwash	Hummocky moraine	Clay plain			
S2	tributary to Mink Lake	56.121	115.683	3.5	1	677	1.02	87	13	0	0	19.6	95.2
S4	Twin Lake outflow, tributary to Mink River	56.101	115.594	91.4	2	681	1.30	53	30	17	8.95	50.4	64.6
S8	tributary to Artisinn Lake	56.111	115.346	54.2	3	673	1.17	8	66	27	1.81	62.1	91.9
S15	tributary to Utikuma Lake	55.934	115.170	17.2	1	658	0.37	22	1	78	0.12	58.6	53.3
REC	Redearth Creek, tributary to Loon River	56.547	115.240	585	4	615	0.80	15	29	56	0.80	65.5	0.4
UR	Utikuma River downstream of Utikuma Lake	56.015	115.303	2587	6	676	0.85	30	47	23	16.97	39.2	8.0
RES	water storage reservoir in Red Earth Creek	56.557	115.280	–	–	–	–	–	–	–	–	–	–

Sources: [1]AEP (2022); [2]AEP (2017); [3]AER (2016a,b; 2008) and Devito et al. (2005, 2017); [4]Ducks Unlimited Canada (2011); [5]Devito et al. (2017); [6]Government of Alberta (2022)

4.2.2. Photodegradation incubations

We conducted laboratory experiments to assess the rates of DOM photochemical transformation and CO_2 production. Water samples were exposed to artificial solar light in a SunTest XLS+ II solar simulator equipped with a Xenon lamp and a daylight filter (300-800 nm), and a SunFlood flooding system (Atlas Material Testing Technology LLC, Linsengericht, Germany). The solar simulator irradiance was set to the maximum of 65 W m^{-2} for the 300-400 nm range (equivalent to 765 W m^{-2} for 300-800 nm), with the average total energy of about 5,615 kJ m^{-2} d^{-1}.

Water samples were irradiated in ~60-mL glass vials with a quartz glass top, designed following Koehler et al. (2014). Each vial was filled with sample water with no headspace. The sides of the vials were covered using "jackets" made of black duct tape to prevent the light from entering laterally. The quartz glass top piece was glued on with silicone glue. To prevent our photodegradation vials from breaking from water expansion as the temperature in the solar simulator increased, we poked one of the cap septa in each vial with a needle following Koehler et al. (2014).

Each sample was irradiated for 1 and 3 days (24 and 72 hours), except the October 2019 and April and May 2020 samples that were irradiated for 0.5 and 1 days, and several samples from July and October 2020 that were irradiated for 3 days only. Dark controls were used in each incubation to account for changes in DOM due to bacterial respiration. Dark control samples were irradiated in similar glass vials (no quartz top) wrapped in aluminum foil. During the experiment, the vials sat half-submerged in a water bath connected to an Isotemp® recirculating chiller (Fisher Scientific Inc., Pittsburg, PA, USA) to keep the temperature of irradiated samples at approximately 20°C (dark controls wrapped in foil remained a couple degrees cooler).

To compare sunlight in the field to the solar simulator, we measured UV-A (320-400 nm) and UV-B (280-320 nm) irradiance at URSA several times during the 2020 field season using a Solar Light model PMA2100 radiometer with NIST-traceable sensors PMA2110 and PMA2106 (Solar Light Company Inc., Glenside, PA, USA). The radiometer was set-up on a flat surface in an open area to log irradiance at regular intervals (e.g., 10 min) throughout the day, typically on sunny days. Similarly, irradiance was measured inside the solar simulator.

Before and after the experiments we measured DOC and dissolved inorganic carbon (DIC) concentrations (denoted with square brackets), as well as absorbance and fluorescence spectra. [DOC], [DIC] and absorbance measurements were done in duplicates or triplicates, where possible. We calculated absolute and relative (i.e. percent) changes (denoted with Δ) in parameters; negative values indicate a decrease/loss and positive an increase/gain. Relative changes were estimated as $100\% \cdot (C_x - C_0) / C_0$, where C_x is the concentration for incubation duration x, C_0 is initial concentration. To characterize initial (day 0) concentrations, a subsample was collected immediately prior to incubation. After the incubation (0.5/1/3 days), several vials with irradiated samples (and dark controls) were removed from the solar simulator, samples were re-filtered (0.45 μm) and transferred to 60-mL amber glass bottles. Samples for [DIC] analysis were transferred unfiltered from irradiated and dark control vials to 12-mL clear glass vials sealed with butyl rubber septa caps. The vials were filled without headspace by filling a syringe and then filling vials by allowing for some overflow to remove water that was in contact with air.

4.2.3. Disinfection By-Product Formation Potential

Six water samples from S2, S8 and REC collected in July and October 2020 were assessed for DBP-FP, including four trihalomethanes (THMs: TCM, BDCM, DBCM, TBM) and five haloacetic acids (HAAs: MCAA, DCAA, TCAA, MBAA, DBAA). Samples before and after the

3-day irradiation were analyzed for DBP-FP to determine how a change in DOM composition and concentration affects DBP-FP. To obtain sufficient sample volume for the analysis, water samples were irradiated in UV-transparent Whirl-Pak® bags, as well as the quartz vials. For consistency, water samples for DBP-FP analysis before and after the experiment were filtered. Samples from RES and UR collected in September 2019 and August 2020 were also analyzed for DBP-FP. These samples, however, were not filtered. Samples for DBP-FP analysis were collected in non-acid-washed 1-L HDPE or LDPE bottles. The DBP-FP analysis was conducted at the University of Waterloo WaterSTP Laboratory and is described in detail in Bourgeois (2021).

4.2.4. Biodegradation incubations

Biodegradability of DOM was assessed through dark incubation experiments, and generally followed the protocol in Vonk et al. (2015b). To assess DOM lability in our streams over different seasons, water samples were collected between late May 2020 and late July 2022 from the same five streams. However, the incubations were not necessarily conducted at the same time as photodegradation incubations. The samples were incubated in triplicates at 20°C in acid-washed and combusted (at 550°C for 6 hours) 60-mL amber glass bottles. Bacterial inoculum (1.2 μm filtrate of the same stream water, 1% by volume) was added to filtered (0.45 μm) stream samples at the start of incubations. Samples were shaken typically daily, or as often as possible, and caps were not tightened to prevent anaerobic conditions. Measurements of DOC concentration, absorbance and fluorescence spectra were performed at 0, 10, 28 and 60 days. Prior to measurements, MilliQ® water was added to samples to account for water loss due to evaporation and shaking based on weights before and after the incubation, and samples were re-filtered (0.45 μm). For consistency with the photodegradation results, we report DOC loss (%) for each

experiment duration (0, 10, 28 and 60 days) as negative values, which is the opposite of BDOC as per Vonk et al. (2015a).

4.2.5. Laboratory analyses

Concentrations of DOC and total dissolved nitrogen (TDN) were measured on the Shimadzu TOC-L_{CHP} Analyzer (Shimadzu Corporation, Jiangsu, China) at the NRAL in the Department of Renewable Resources. Detection limits for DOC and TDN analysis were 1 and 0.1 mg L^{-1}, respectively. DIC concentration was measured on the Apollo SciTech model AS-C3 DIC analyzer (Apollo SciTech LLC, Newark, DE, USA) connected to a LI-7000 infrared CO_2/H_2O detector (LI-COR Inc., Lincoln, NE, USA). Daily calibration and instrument drift checks were done with a Certified Reference Solution from the Scripps Institution of Oceanography that was opened on the day or within a couple of days prior to analysis.

UV-vis absorbance spectra were measured on the Shimadzu UV-1280 spectrophotometer (Shimadzu Corporation, Kyoto, Japan). From the absorbance spectra we determined the absorbance at 254 nm (A_{254}; Dobbs et al., 1972) and specific UV absorbance at 254 nm (SUVA; Weishaar et al., 2003), the ratio of absorbance values at 250 and 365 nm (E2:E3; de Haan & de Boer, 1987), the spectral slope between 275 and 295 nm ($S_{275\text{-}295}$) calculated using an exponential model, and the ratio of slopes $S_{275\text{-}295}$ and $S_{350\text{-}400}$ (S_R; Helms et al., 2008).

Fluorescence spectra were measured using a HORIBA Scientific Aqualog® fluorometer (Horiba Scientific, Edison, New Jersey, USA). Due to substantial variations in DOM concentrations and absorbance among the streams, the integration times were adjusted between 0.5 and 2 s, and samples with high absorbance were diluted with MilliQ® water using a maximum dilution of 2x (Kothawala et al. 2013). The water Raman signal-to-noise and emission calibration validation scans were performed upon every run. From the fluorescence excitation-emission

matrix (EEM), we estimated three common indices: fluorescence index (FI; Maie et al. 2006), biological index (BIX; Huguet et al., 2009), and humification index (HIX; Ohno, 2002). The FI is a ratio of fluorescence intensities at 470 and 520 nm, obtained at excitation of 370 nm. BIX is a proxy of the recent autochthonous contribution of DOM and is calculated as the ratio between emission at 380 nm (β peak representing recently derived DOM), and the emission maxima between 420 and 435 nm (α peak representing highly decomposed DOM), at an excitation of 310 nm. HIX is a measure of the degree of humification (lower H:C in humified organic matter), and is the ratio of fluorescence intensity at 435-480 nm and the total of fluorescence intensities at 300-345 nm and 435-480 nm, at excitation 254 nm. A parallel factor analysis (PARAFAC) and index calculation were performed in MATLAB® R2021b (The Mathworks, Inc.) using drEEM-0.6.3 toolbox (Murphy et al., 2013). Sample EEMs were corrected for the inner-filter effect and MilliQ® blanks, and Raman normalized. A PARAFAC model was developed using a normalized dataset that included 296 samples after the noisy parts of EEMs and three outliers were removed. The 5-component model was validated using a split-half analysis. A description of validated PARAFAC components is provided in Table 4-2.

Table 4-2. Description of validated PARAFAC components

PARAFAC component	Excitation maximum (nm)	Emission maximum (nm)	Probable source and/or reactivity	Select studies in OpenFluor with spectrally similar components*
C1	<250, 335	440	terrestrial, humic-like; photo-reactive	Eder et al., 2022 (C2); Murphy et al., 2014 (C1); Wauthy et al., 2018 (C1); Osburn et al., 2018 (C1)
C2	255, 360	507	humic-like, photodegradation product	Eder et al., 2022 (C1); Murphy et al., 2014 (C2); Wauthy et al., 2018 (C2); Osburn et al., 2015 (C1); 2018 (C3); Wünsch et al. 2017 (C6)
C3	<250, 310	391	microbial humic-like, likely fresh & labile	Eder et al., 2022 (C5); Murphy et al., 2014 (C4); Osburn et al., 2011 (C2); 2015 (C8), 2018 (C2); Wauthy et al., 2018 (C4)
C4	<250, 305	414	humic-like, terrestrial, photo-recalcitrant	Osburn et al., 2015 (C3); Shutova et al., 2014 (C3); Eder et al., 2022 (C3); Shutova et al., 2014 (C2)

PARAFAC component	Excitation maximum (nm)	Emission maximum (nm)	Probable source and/or reactivity	Select studies in OpenFluor with spectrally similar components*
C5	280	332	protein-like	Murphy et al., 2014 (C5); Shutova et al., 2014 (C4); Wünsch et al., 2017 (C1)

*Tucker congruence coefficient (TCC) >0.95; grey = TCC >0.9 (moderate congruence)

4.2.6. Data analysis

All statistical analyses were performed in RStudio (RStudio, PBC) with R version 4.2.1. Data were processed and summarized using the R packages *dplyr*, *tidyr*, *factoextra* and *tibble* (Kassambara & Mundt, 2020; Müller & Wickham, 2020; Wickham & Girlich, 2022; Wickham et al., 2020) and illustrated with the *ggplot2* package (Wickham, 2016). We used `prcomp` function in *stats* package (R Core Team, 2022) to conduct a principal component analysis (PCA) to assess changes in DOM composition during photo- and biodegradation, and `rda` function in *vegan* package (Oksanen et al., 2019) to conduct redundancy analysis (RDA) to assess how environmental and catchment characteristics relate to changes in [DOC], [DIC], A_{254} and SUVA. Data for the PCA were transformed using the `bestNormalize` function to reduce the nonlinearity (Peterson, 2021). In the RDA, runoff and catchment area were log-transformed, and all factor variables were scaled and centered.

To evaluate the importance of environmental characteristics on changes in DOM during experiments, we conducted linear mixed effects modeling (LMEM) using *lme4* and *lmerTest* packages (Bates et al., 2015; Kuznetsova et al., 2017). *Performance* package (Lüdecke et al., 2021) was used to obtain conditional (model goodness-of-fit) and marginal (goodness-of-fit of predictors, or fixed effects) R^2 and Akaike information criterion (AIC) and to assess model assumptions. Potential interactions between factor variables were not assessed. Other limitations of applying LMEM in our study included a relatively small dataset and few levels of random effect (2 and 3 durations for photo- and biodegradation, 5 sites).

4.3. Results

Detailed water chemistry results for all streams are presented in Chapter 3. Briefly, there were differences in the concentrations of major ions and nutrients at the five streams. Highest [DOC] and DOM aromaticity was recorded in S15, S8 and REC. Groundwater and lake influence in S2 and S4, respectively, resulted in lower [DOC] and SUVA.

4.3.1. Photodegradation

Field-measured UV-A and UV-B showed that the solar simulator irradiance was comparable to the highest light intensity during a sunny day. Maximum UV irradiance was observed in June: UV-A reached nearly 50 W m^{-2} and UV-B 1.6 W m^{-2} (Figure C3). Solar simulator values generally varied around 55-60 W m^{-2} for UV-A and 1.2-1.5 W m^{-2} for UV-B. Thus, one day of irradiation in the solar simulator would roughly be equivalent to 3 sunny cloudless days in mid-June and about 5-6 days in September.

In total, we conducted five 0.5-day incubations, 36 1-day incubations and 30 3-day incubations. A summary of the dark control sample checks is provided in Table C1. Dark control incubations showed only minor changes in A_{254}, [DOC] and [DIC] relative to the initial (before incubation) samples (Table C1). The changes usually remained within ±1% and always within ±10%, which is similar to the measurement error. There was no consistent pattern in change (i.e. both positive and negative changes observed), except A_{254} (mostly a decrease observed) in dark controls, and therefore, no correction of the experiment results was done.

During the photodegradation experiment, we saw decreases in A_{254} (on average, 9.2% and 23.6% after 1-day and 3-day experiments, respectively) and [DOC] (3.3% and 7.5%) and an increase in DIC (1.3 and 2.5 mg L^{-1}). The change between 1-day and 3-day values was mostly linear. The changes varied among the streams and over time (Figure 4-2). The smallest 3-day DIC

production (mg L^{-1}) and DOC loss (%) were seen at S4. DIC production was generally lower in the winter and fall and higher in the summer. There was no clear seasonal pattern in DOC loss (%). Based on change in A_{254} (%), relatively more colored DOM (%) was lost in the winter and spring. Change in SUVA also seemed to be greater later in the season. Visually, there was no clear relationship between changes in A_{254}, DOC or DIC and stream discharge or specific conductivity, which we used as an indicator of groundwater contribution (Figure 4-2).

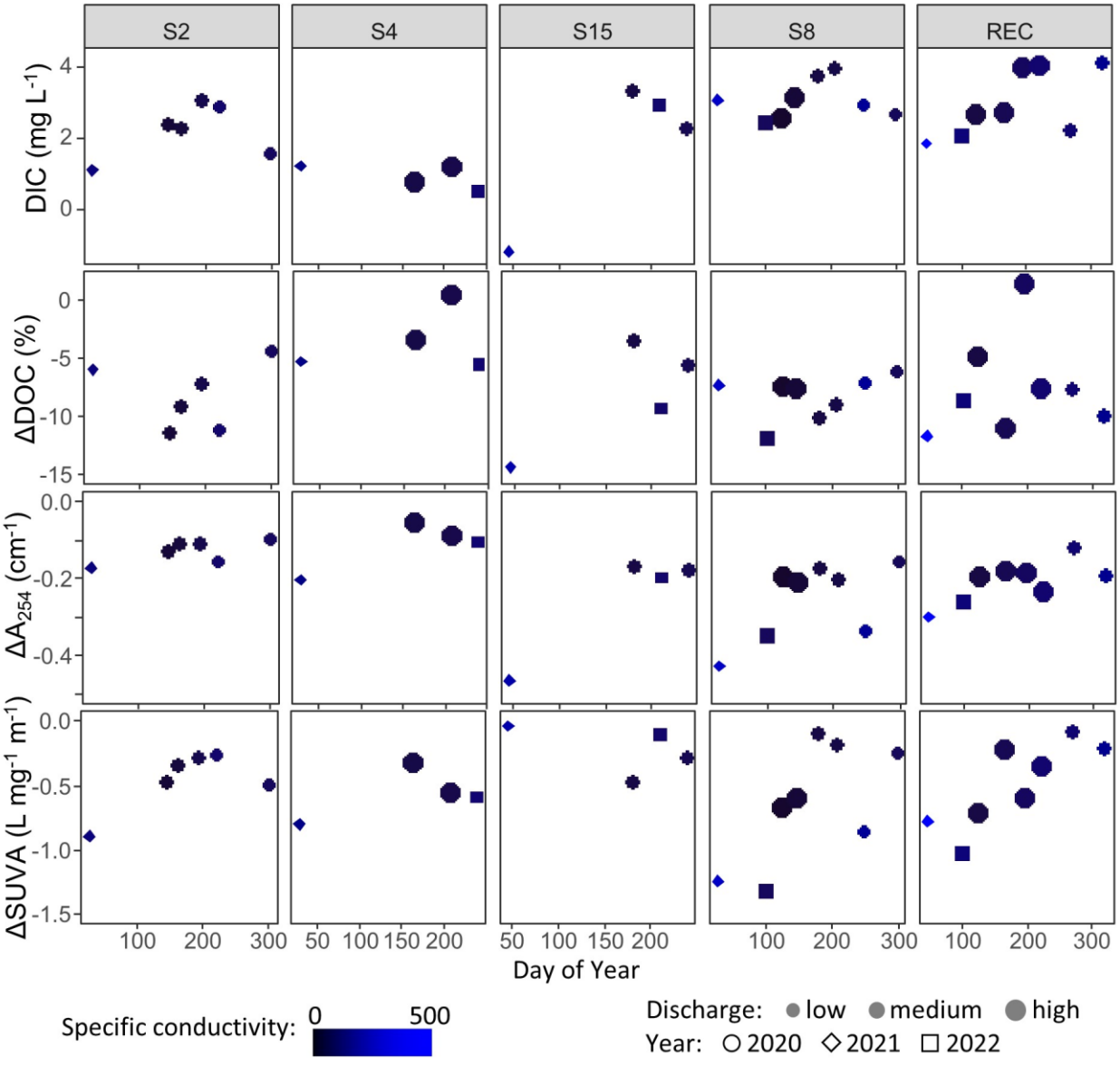

Figure 4-2. Changes in DIC, DOC, A_{254} and SUVA after 3-day photodegradation incubations.

The relationship between ΔDIC and ΔDOC was weak (Figure 4-3a). While the relationship between ΔDIC and ΔA_{254} was also weak overall, summer/fall and winter/spring samples had distinct trends, with less colored DOM converted to DIC for the winter/spring samples (greater A_{254} loss to produce the same [DIC]; Figure 4-3b).

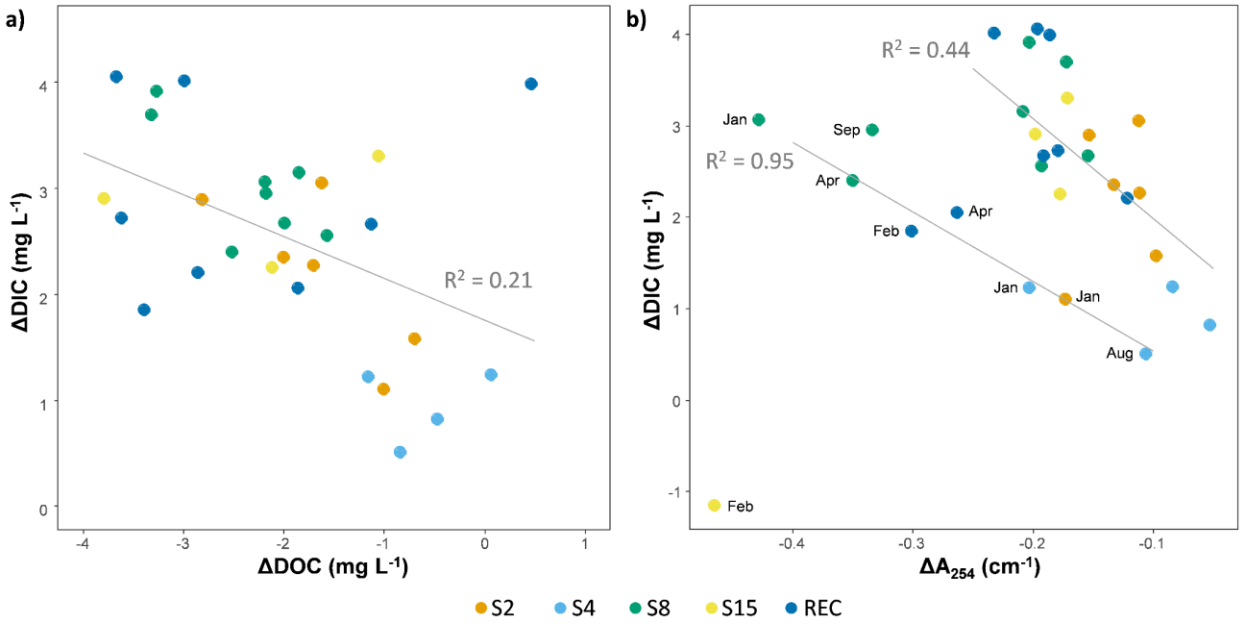

Figure 4-3. Absolute changes in (a) [DOC] and [DIC] (one outlier – S15 from February 2021 – not shown and not included in regression) and (b) A_{254} and [DIC] during 3-day photodegradation incubations. The regression lines in (b) are based on six samples from winter and spring (January, February and April), and the rest of the samples (excluding the S15 outlier).

Fluorescence intensity decreased for PARAFAC components C1, C2 and C3, increased or remained unchanged for C4, and typically slightly decreased for C5 (Figure C4). Most of C1, C2 and C3 was lost after 1 day of irradiation, with a total loss of up to 80% after 3 days. Proportions of components C1, C2 and C3 decreased, except S4, where proportion of C2 slightly increased or didn't change. Proportions of components C4 and C5 increased (Figure C5).

The results of LMEM analysis of photodegradation data show several controls on changes in A_{254}, DOC and DIC (Table 4-3 and C2). Using data from all durations (random effect), LMEM suggest that DOC loss (%) is to some degree explained by the presence of lakes, pH and catchment

area, with R^2 of ~0.5. When using A_{254} loss (%), R^2 increases to over 0.6, and temperature and SC were statistically significant predictors. For DIC gain (%), runoff, temperature, pH/lakes and wetlands, $SUVA_0$ explain similar proportion of the data. For the absolute change in SUVA, temperature, SC, lakes and $SUVA_0$ produce an R^2 of up to 0.6. The relationship between DOM parameters and factor variables was positive for temperature, negative SC and varied for other variables (Table 4-3).

To explain changes in DOC, DIC, A_{254} and SUVA after 3-day incubations at all sites (site as random effect), we only used five variables (water temperature, runoff, SC, pH and initial SUVA) that varied for each incubation. The best model for ΔDOC (%) used SC and runoff but had the lowest R^2 (0.22). A higher R^2 (0.41) for ΔA_{254} (%) was achieved using all variables. For ΔDIC (%), runoff, temperature and pH resulted in R^2 of about 0.84. Absolute change in SUVA had R^2 of 0.34 with water temperature being the only statistically significant predictor. Absolute change in A_{254} had SC as the only statistically significant predictor, with R^2 twice as high. The relationship between DOM and factor variables was positive for temperature and runoff, and negative for SC and pH (Table 4-3).

Table 4-3. Select LME models for predicting absolute and relative changes in DOC, DIC, A_{254} and SUVA during photodegradation and biodegradation incubations.

Dependent variable	Factor variables tested in model	Random effect & its significance	Highest R^2 achieved	Statistically significant variables (and correlation)
Photodegradation: all durations		1 | Duration		
ΔDOC%	runoff, water temperature, SC, pH, $SUVA_0$, wetlands, lakes, area	***	0.499	lakes (+), pH (-), area (+)
ΔA_{254}%		***	0.684	temperature (+), SC (-)
ΔDIC%		**	0.660	runoff (+), pH (-), $SUVA_0$ (+), wetlands (+), lakes (-), temperature (+)
ΔSUVA		***	0.605	temperature (+), SC (-), $SUVA_0$ (-), lakes (-)
Photodegradation: duration = 3 days		1 | Site		
ΔDOC%	runoff, water temperature, SC, pH, $SUVA_0$		0.225	
ΔA_{254}%			0.407	temperature (+)
ΔA_{254}		***	0.695	SC (-)
ΔSUVA			0.346	temperature (+)

Dependent variable	Factor variables tested in model	Random effect & its significance	Highest R^2 achieved	Statistically significant variables (and correlation)
ΔDIC%		***	0.838	temperature (+), pH (-), runoff (+)
Biodegradation: all durations		1 | Duration		
ΔDOC%	runoff, SC, pH, water temperature, wetlands, lakes, area, $SUVA_0$, C/N_0	***	0.580	SC (-), area (+)
ΔA_{254}%		***	0.773	temperature (-), SC (-), lakes (-)
Biodegradation: duration = 60 days		1 | Site		
ΔDOC%	runoff, water temperature, SC, pH, $SUVA_0$, C/N_0		0.317	
ΔA_{254}%		*	0.676	SC (-)
ΔA_{254}			0.747	$SUVA_0$ (-) SC (-), temperature (-)
ΔSUVA			0.406	temperature (-), SC (-)

Notes:
Significance codes: *** $p<0.001$; ** $p<0.01$; * $p<0.05$
Δ – change in parameter during incubation
$SUVA_0$ – initial SUVA; C/N_0 – initial C/N

4.3.2. Biodegradation

We conducted a total of 30 biodegradation incubations between May 2020 and October 2022, including five for S2 and S15, six for S4 and S8 and eight for REC. After 60 days of incubation, we saw greater absolute loss in DOC (and A_{254}) at S15, S8 and REC (1.7-6.1 ppm, except S15 in winter) and smaller at S2 and S4 (up to 3 ppm). DOC loss (%), or BDOC, varied generally within similar range at all sites. On average, BDOC comprised 4.4% after 10 days, 8.8% after 28 days and 13.3% after 60 days of incubation. The 60-day BDOC varied between about 6 and 35%. Temporally, greater DOC loss (%) was seen in winter samples (10-16% and >20 at S15), and smaller in the summer (Figure 4-4). SUVA slightly increased or remained the same during incubation at S2, and on several occasions at other streams, especially in the fall. Small decreases in SUVA were seen at some streams in the summer and winter.

At 28 days, most samples lost more than a half of the DOC lost after 60 days of incubation (on average 67%); absorbance losses were similar (14 samples lost >50% A_{254} lost at 60 days). However, at 10 days, A_{254} losses were small (on average 12% of A_{254} lost after 60 days); A_{254}

slightly increased in 5 samples after 10 days and 2 samples after 28 days, most of them winter or spring samples.

There was no clear relationships with stream discharge or specific conductivity. Only at REC, BDOC was smallest in samples with high SC (405 μS cm^{-1} in late August 2022). In the winter, when SC was the highest at all streams, BDOC was also elevated.

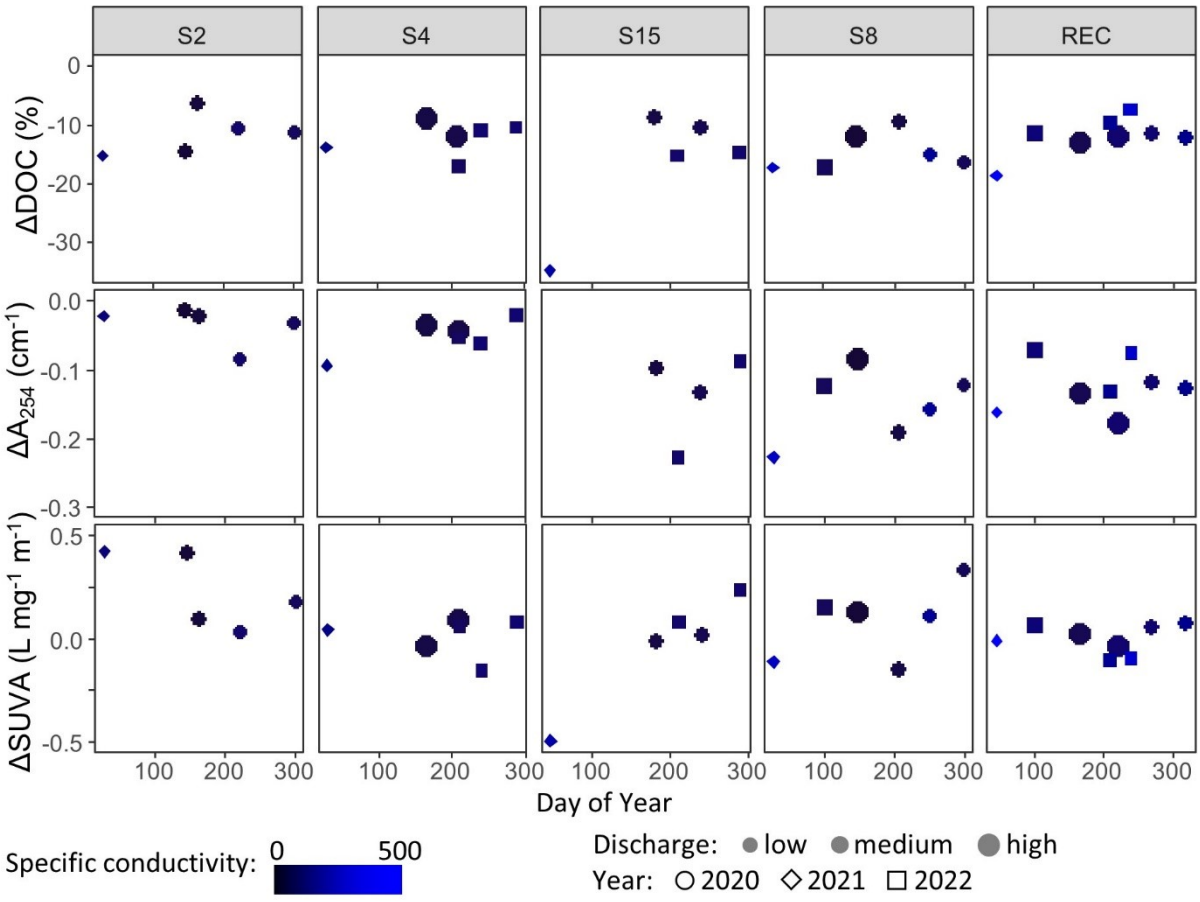

Figure 4-4. Relative change in [DOC] (BDOC) and absolute changes in absorbance and SUVA after 60-day biodegradation incubations. An outlier removed in ΔA_{254} plot for S15 (winter sample with A_{254} loss of 1.23 cm^{-1}).

Fluorescence intensity increased for PARAFAC components C1, C2 and C3 after 10 days of incubations, and after that slightly degreased or remained unchanged after 28 and 60 days, except S4, where a progressive increase occurred. There was minimal change in C4 and C5 at S4

during incubations. At other streams, patterns varied (Figure C6). Proportions of PARAFAC components changed little (Figure C7). Overall, proportions of C1, C2 and C3 slightly increased, and proportions of C4 and C5 slightly decreased.

The results of LMEM of biodegradation data are summarized in Table 4-3 and C3. Using data from all durations (random effect), LMEM suggests that ΔDOC (%) can be explained to some degree by SC, catchment area and water temperature, with R^2 of 0.58. When using ΔA_{254} (%), temperature, SC, and proportions of lakes, R^2 increased to over 0.7. The relationship between DOM parameters and factor variables was positive for catchment area, and negative for all other variables (Table 4-3).

To explain changes in [DOC], A_{254}, and SUVA after 60-day incubations at all sites (random effect), we only used five variables that varied for each incubation. The best model for ΔDOC (%) had lower R^2 (0.58) than for ΔA_{254} (0.77). Water temperature, SC and $SUVA_0$ were statistically significant predictors, all negatively correlated with the DOM parameters (Table 4-3).

There is large variation in DOM composition among the streams and over time, and also some overlap, as shown by the PCA (Figure 4-5a). The composition of DOM in UR, RES and lakes is more distinct. In the PCA, the first two principal components explained 86% of variance in DOM data. RES, UR, several lakes and to some extent S4 samples had low scores on PC1, with higher loadings on S_R, $S_{275-295}$, E2:E3 and PARAFAC component C5. UR had higher scores on PC2 with greater BIX loadings, while several lakes exhibited lower PC2 scores with greater PARAFAC component C4 and SUVA loadings. When comparing the impact of photo- and biodegradation on DOM composition, there was a greater change during photodegradation, with the irradiated samples plotting farther from the original non-degraded samples compared to the biodegraded samples (Figure 3-4b,c). The photodegraded samples plotted closer to RES and some

lake samples, along S_R and E2:E3, and PARAFAC components C4 and C5. The biodegraded samples had a small shift toward higher FI and PARAFAC components C3 and C1, as well as BIX for lake-dominated S4.

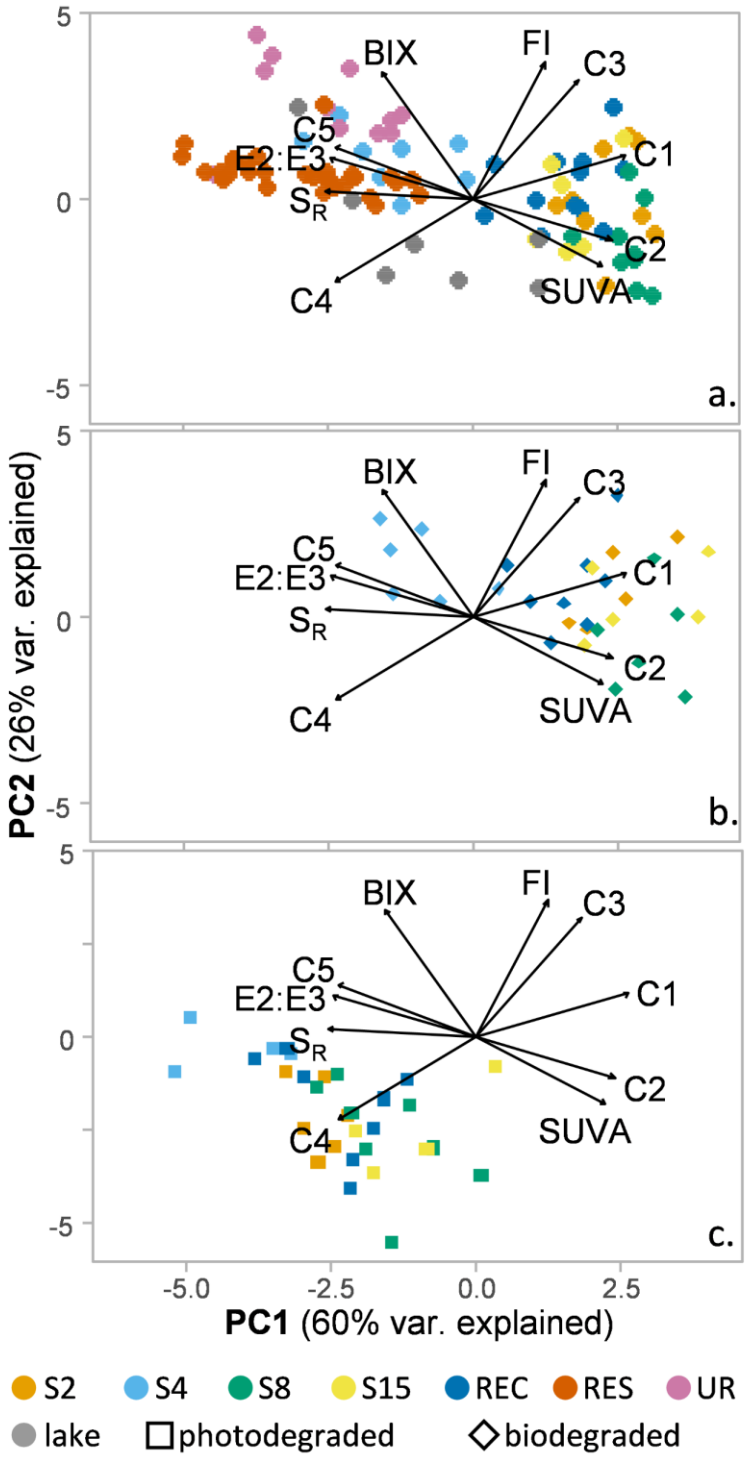

Figure 4-5. PCA using stream, lake and reservoir samples (a), biodegraded samples (b) and photodegraded samples (c). Only the longest experiment durations are included (60-day for biodegradation, and 3-day for photodegradation). Variables HIX and $S_{275-295}$ are excluded due to strong correlations with C2 and E2:E3, respectively. The scale of variable loadings (arrows) is increased for clarity.

4.3.3. Disinfection by-product formation potential

While photodegradation led to a loss of aromatic DOM (A_{254}), there was no consistent change in the DBP-FP before and after photodegradation, when comparing two summer and fall samples from S2, S8 and REC (Figure 4-6 and C9). For example, TCAA seemed to drop, while MCAA seemed to increase for most samples after photodegradation. TBM, DBCM, MBAA remained below the detection limits before and after the incubation (Figure C9). HAAs-FP was similar (S2) or lower (REC, S8) after the experiment. THMs-FP change was more variable, with no change (REC in fall), small increases (S8 in summer and S2 in fall) or decreases. A_{254} was slightly higher in the summer than in the fall, but THMs-FP were higher in the summer at S2 and S8. In comparison with UR and RES samples, which were characterized by lower A_{254}, stream DBPs-FP was lower (REC in fall for THMs), similar (S2 in summer and fall for THMs, and in fall for HAAs) or greater.

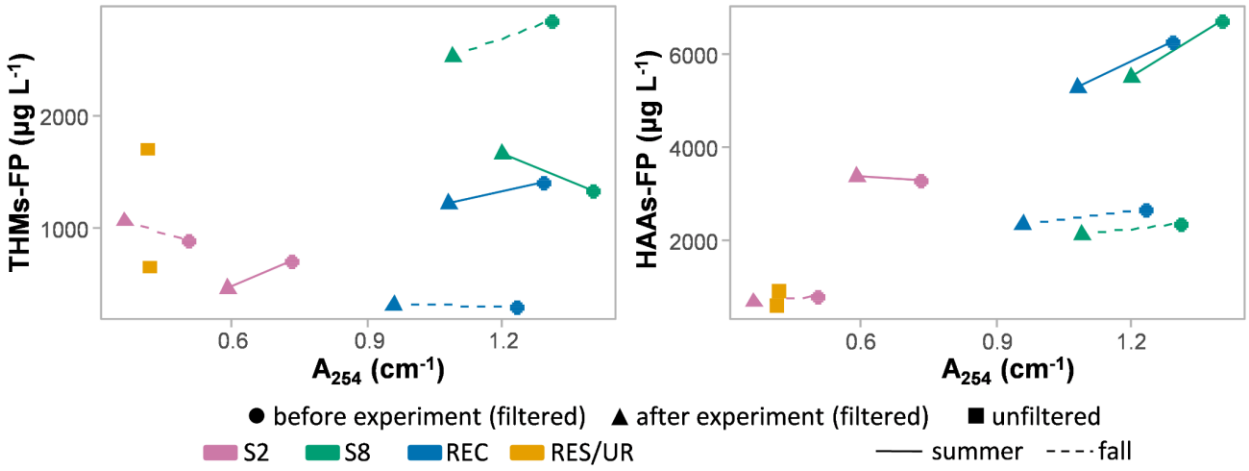

Figure 4-6. Changes in formation potentials of THMs and HAAs after 3-day irradiation for three streams (S2, S8 and REC) in the summer and fall 2020, and summer formation potentials in RES and UR.

4.4. Discussion

4.4.1. Changes in DOM as a result of photodegradation and biodegradation

Our data showed small DOC losses over time during both the 3-day photodegradation incubations and the 60-day biodegradation incubations. BDOC of 4.4% (on average) after 10 days of dark incubations was less than the average loss of DOC (7.5%) achieved after 3 days of photodegradation incubations (which are equivalent to under a week of full sun conditions in June-July). Photodegradation also resulted in more pronounced compositional changes in DOM, including lower SUVA and HIX, and higher $S_{275-295}$, S_R and E3:E3. While it is difficult to directly compare the importance of photo- and biodegradation because of different incubation durations, our data suggest that photodegradation has potentially a stronger effect on [DOC] than biodegradation in our streams. This can be seen in Figure 4-5, where photodegraded samples trend toward RES and lakes. Our results support previous findings of low influence of biodegradation on [DOC] and DOM composition in the boreal streams with short water residence time (Kothawala et al., 2015).

The relative importance of these two processes in the Boreal Plains streams may vary temporally and spatially as DOM composition and environmental conditions change (Casas-Ruiz et al. 2017). In particular, we saw differences in DIC production in winter/spring vs. summer/fall samples. This shows that DOM composition influences DIC production during photodegradation, with less DIC photoproduced for the same amount of photobleaching (i.e. A_{254} loss). We also saw slightly higher biodegradation rates early in the season (late spring and early summer), which is similar to other studies (e.g., Fellman et al., 2009; Raudina et al., 2022).

There were no clear differences in the influence of photodegradation and biodegradation on DOM as we moved downstream. In particular, the results for REC were similar to those for smaller

streams S8 and S15 (order of magnitude difference in catchment sizes). While the smallest stream S2 had lower [DOC] and aromaticity due to greater groundwater contribution, relative changes in DOM concentrations and composition during the incubations were similar to those at S8, S15 and REC.

Stream DOM composition after photodegradation converged toward DOM composition observed in lakes and RES. The shift in DOM composition suggests that photodegradation plays a big role in DOM transformation in the drinking water reservoir as well as lakes in the Boreal Plains. It is important to note that changes in DOM as a result of photodegradation (reduction in aromaticity, molecular weight, etc.) would be similar to changes due to autochthonous production (Liu et al., 2020); therefore, we cannot confidently attribute the difference in lake and reservoir DOM composition relative to streams solely to the effect of photodegradation. Interestingly, most lakes were not similar to UR. Distinct DOM composition with higher BIX and FI in UR suggests that autochthonous DOM production and possibly microbial degradation in Utikuma Lake likely have a strong influence on DOM in UR.

Streams in this region may have variable channel morphology, with depths ranging from centimeters (upland areas) to over a meter (deeply incised channels in wetlands). But in colored streams and lakes, the rate of photodegradation will rapidly decrease with depth according to the Beer-Lambert law, and may be negligible at a depth of several cm. Thus, photodegradation is likely limited to the surface layer. The rate of biodegradation, however, is not expected to vary much in the water column. Additionally, although our streams may be unshaded as they flow though wetlands, lakes and beaver ponds, large stretches of the streams are often shaded by trees, which also limits photodegradation. Most of the DOM processing likely occurs in numerous lakes and beaver ponds; at lake-dominated S4, absorbance is reduced by half compared to other streams.

Increased water residence time makes lakes hotspots for DOM degradation (Palmer et al., 2016). Because most streams at some point pass through lakes in this landscape (e.g., S2, S4 and S15 eventually drain into Utikuma Lake), lakes have a major impact on the DOM composition leaving the Boreal Plains watersheds and moving downstream. This is consistent with previous finding that DOM degradation in streams is controlled by water residence time (Catalán et al., 2016).

We found that RES, which is annually refilled with water from REC, was very different from REC in terms of DOM concentrations and composition. All RES samples plotted along the S_R and E2:E3 gradient, suggesting different degrees of sunlight exposure, and little autochthonous productivity compared to UR. Thus, raw drinking water from RES does not represent stream water in terms of drinking water treatability after extended residence time. This has implications for drinking water treatability, including coagulation, which preferentially removes DOM characterized by high SUVA and molecular weight, and DBP-FP (Marais et al., 2019).

Based on the results of LMEM, we could not identify one good predictor of variations in changes in DOM as a result of photo- and biodegradation. It seems that water temperature, runoff, SC, and in some cases the presence of lakes (and pH), the proportion of wetlands (and $SUVA_0$) and catchment area explained some variations in the data. The R^2 of the LMEM was low for [DOC] and SUVA, which is calculated using [DOC], likely due to the uncertainty of [DOC] analysis, and higher for A_{254} and [DIC]. Our incubations were conducted at a temperature of about 18-20°C, which is within the range observed in the streams in the summer. However, the actual water temperature varied greatly over seasons, and temperature is an important control on biodegradation (Berggren et al., 2022). Water temperature used as a factor in our RDA (Figure C8) and LMEM is indicative of the amount of processing that has occurred prior to sampling, thus reflecting seasonal variations in stream DOM composition. But overall, with the exception of the winter samples,

seasonal patterns in the data were not obvious, which is similar to other studies (Vonk et al., 2015a). The effect of runoff and SC may be indicative of groundwater contribution to the streams, which increases during dry periods (i.e. low runoff and elevated SC) and results in the delivery of low-aromaticity DOM and reduced [DOC]. Wetlands, on the other hand, contribute large quantities of high-aromaticity DOM. Although there is evidence that wetland-dominated streams have more biolabile DOM than forest-dominated streams (Berggren & del Giorgio, 2015), we did not see much of a difference between the forest-dominated S2 and the rest of the streams. Catchment area may have appeared in the model due to the fact that the smallest stream (S2) had fewer wetlands than other streams and is groundwater-influenced. Overall, the LMEM results confirm the importance of lakes discussed above, and suggest the effects of temperature, runoff and sources of DOM to streams (e.g., high-aromaticity wetland DOM vs. low-aromaticity groundwater DOM) on DOM degradation rates.

4.4.2. Uncertainties and limitations

There were several potential sources of uncertainty in our study. We found that the analytical error for [DOC] measurement was about ±3 ppm between different batches of samples. The average DOC change during experiments (1-3 mg L^{-1}) was often less than the instrument precision and, therefore, should be used with caution. In particular, we have less confidence in some biodegradation [DOC] results when samples from 0- and 10-day incubations were analyzed separately from the 28- and 60-day incubations. However, we have good confidence in A_{254} and [DIC] results (Figure 4-3).

Another potential source of uncertainty for the photodegradation experiments was instrument drift. We noticed that the solar simulator irradiance was fluctuating around the mean.

Xenon lamp was replaced and the instrument recalibrated in October 2020, but the fluctuation remained.

During and sometimes before the photodegradation incubations, we had air bubbles forming in the vials (including dark controls). To reduce water saturation with air, we warmed the sample water prior to the incubations and shook the samples, which largely helped with the problem. We still had some bubbles present at the end of experiments, which may have affected [DIC]. Additionally, when sampling for [DIC], we transferred water from a photodegradation vial to a syringe and then to a DIC vial, and some of the sample was in contact with air during the transfer, which may have potentially resulted in some loss of DIC. Although we believe that our interpretation of [DIC] results was not affected.

Our photo- and biodegradation results do not account for the changes in environmental conditions (e.g., temperature, flow and the amount of sunlight). Water chemistry, including pH and metals, may also affect the rate of photodegradation (Gu et al., 2017). Although streams had variable water chemistry, we did not correct our data.

4.4.3. Disinfection by-product formation potential

A_{254}, SUVA and HMW fraction have been used as indicators of DBP-FP (Marais et al., 2019). However, the relationships between DBP-FP and DOM indexes are not universal. While photodegradation reduced [DOC] and DOM aromaticity in our study, there was no strong, consistent influence of photodegradation on DBP-FP, with possibly a few exceptions (TCAA and MCAA). It is important to note that the quality control analysis shows an error of 5-20% for both THMs-FP and HAAs-FP (Amiri, *pers.comm.*), thus most changes in DBP-FP are within the error and have low confidence. Also, as DOM is removed prior to disinfection during water treatment, the results in our study are not representative of the actual DBP formation. While the reduction in

TCAA-FP was proportional to the loss of A_{254}, other DBP-FPs were not affected similarly, suggesting that they may be less sensitive to photodegradation. This confirms that A_{254} cannot be used as a universal predictor of DBP-FPs, as some shifts in DOM composition are not reflected by A_{254}, and other factors likely also play a role.

4.5. Conclusion

The effects of photodegradation and biodegradation on boreal stream DOM concentrations and composition were examined using laboratory incubations. Using samples from five streams located in the Boreal Plains, we assessed relative importance of these processes, seasonal and spatial variations, environmental controls, and the effect of photodegradation on DBP-FP. We found that decreases in [DOC] were small, but large changes in DOM composition occurred during photodegradation incubations, and the DOM composition of irradiated samples resembled that of lakes. Our findings emphasize the importance of lakes in the Boreal Plains, where many streams are fed by or flow through lakes, and also suggest that other environmental controls, like runoff, SC (as a proxy for water source), wetlands and temperature, may influence the rates of photo- and biodegradation. Our findings, including the role of lakes and seasonal patterns in photo- and biodegradation are similar to studies conducted in other forested regions. Despite large changes in DOM composition during photodegradation incubations, changes in DBP-FP were not consistent among the streams, incubations and individual DBPs. While both photodegradation and microbial degradation transform DOM as it moves downstream, the effect of photodegradation seems more pronounced, but it is clear that both processes are important in reducing [DOC] and changing DOM composition.

5. Synthesis and Conclusions

In my three studies (Chapters 2-4), I examined variations in DOM concentration and composition in Canadian streams and assessed environmental controls on DOM at the national and regional scales. While Chapter 3 focused on the Boreal Plains ecozone and the controls that operate at this scale, Chapter 2 allowed me to assess stream DOM in this region relative to other forested regions of Canada. Chapter 4 deepened my understanding of the fate of DOM as it moves through the stream network in the Boreal Plains.

5.1. Environmental controls on DOM across scales

In Chapters 2 and 3, I observed large variability in stream DOM concentration and composition over space and time. These variations were driven by a range of environmental controls, some of which were similar at both scales (sub-continental and regional), including wetlands, lakes and temperature, while others differed (e.g., surficial geology was important at the regional scale). We saw the same terrestrial controls on stream DOM operating across different Canadian ecozones. In particular, catchments with larger proportions of wetlands were characterized by greater DOC concentrations and aromaticity. In the Boreal Plains, where organic soils are widespread and commonly cover most of the catchment, the relationship between the proportion of wetlands and DOC concentration was noisy. The effect of lakes was typically similar in Chapters 2 and 3, and expressed in lower SUVA and HIX, and higher S_R, E2:E3, and PARAFAC component C5. The effect of lakes was seen in streams with some of the lowest DOC concentrations (Pacific Maritime ecozone) as well as high-DOC streams (Boreal Plains ecozone). The effects on DOM concentration and composition I observed are similar to observations from other forested regions. However, my results show that although most controls on DOC

concentration and composition can be seen across different physiogeographic regions, some controls may be missed when looking at very large scales.

The results from Chapter 3 highlight the importance of hydrologic connectivity for stream discharge and DOC export in the Boreal Plains ecozone. Differences in surficial geology produce differences in hydrologic connectivity of individual streams to surface and subsurface flowpaths, which has implications for stream flow and water chemistry, and DOM in particular. The differences in hydrologic connectivity were expressed primarily as lower DOC concentrations at two streams with coarse-textures surficial geology (S2 and S4), and artesian groundwater-dominated stream (S11), as well as at larger (585 km^2) stream (REC), where relative groundwater contribution increased during low-flow periods.

In addition to terrestrial controls on DOM, we also explored temporal changes in DOM and their main drivers – temperature and stream discharge. In Chapter 2, I was not able to assess the effect of hydrology on DOM at the national scale due to the limited number of samples, but mean annual air temperature was an important predictor of DOM composition. At a sub-continental scale (Chapter 2), cooler mean annual air temperature was associated with greater aromaticity of DOM, as it was associated with the differences in soils (podzolic soils in BS, PM2 vs. organic soils in northern sites like BP, TP and PM1).

Chapter 3 results were similar to other studies examining the importance of discharge and temperature, which act independently of each other, and thus result in different trends. Frequently, DOM monitoring programs are designed to target either hydrologic events or seasonal trends. Thus, it is easy to miss short-term event changes or longer-term patterns in concentration and composition of stream DOM. My results show the presence of both seasonal and event patterns in DOM in streams of the Boreal Plains, and highlight the importance of careful monitoring program

design and data interpretation. My rain event sampling was limited to the summer months and included only two streams with distinct catchment characteristics. I was not able to collect high-frequency samples during snowmelt and rain events early and later in the season, or to sample larger streams. I also collected limited winter DOM data. Further monitoring of the Boreal Plains streams during events would help us better constrain intra-annual variations in DOM composition, and get better estimates of annual export of DOM from these catchments.

I used five different analytical techniques in Chapter 2, some of which are very costly and sophisticated. Absorbance and fluorescence spectroscopy provided enough insight into the composition of DOM to differentiate sites across Canada and individual streams within those sites. This was one of the reasons why only these two techniques were used in Chapter 3. Absorbance indices alone (SUVA, S_R, E2:E3 etc.) did not seem sufficient for describing all dimensions of variation in DOM in my studies. Even without conducting a complex and time-consuming PARAFAC analysis, fluorescence indices are relatively easy to estimate, and can provide useful insight into the compositional differences in stream DOM. I found the results from both optical techniques complementary, and believe that an aquatic DOM monitoring program would benefit from the use of both techniques.

My URSA study (Chapter 3) observed several patterns in DOC concentration and composition for catchments with different characteristics, some of which have not been described in this region previously, in particular the relationship with discharge. But our conclusions are based on limited data (e.g., only two streams with high-frequency/daily data, and only summer rain events). Future studies of DOM in the Boreal Plains ecozone could focus on storm events and snowmelt to confirm that dilution and flushing are ubiquitously present in wetland-dominated and forest-dominated streams, respectively, and to determine to what extent this effect can be seen

larger rivers. It would also useful to check whether this pattern is seen during hydrologic events in the spring and fall, including snowmelt, and during extreme floods and droughts, and to quantify the effect of dilution/flushing on annual DOC export. Continued monitoring of the Boreal Plains streams would help us better constrain the range of variability in DOC export, and building a long-term dataset is required to track the effects of climate change on stream DOM. Further, these results can be useful for carbon cycling models to improve our estimates of carbon fluxes in the Boreal Plains ecozone.

Overall, my studies contributed to a better understanding of the similarities and differences in stream DOM variability and controls between the Boreal Plains and other forested regions. For example, I measured high concentrations of DOM, but lower aromaticity than in some other regions with relatively high or lower DOM concentrations (Scandinavian Shield, Atlantic and Pacific Maritimes, Boreal Shield). Other compositional differences included higher O/C and PARAFAC component C2 content in the Boreal Plains streams. Further studies can investigate the importance of these differences for aquatic ecosystems, DOM degradability and drinking water treatability. I did not observe the same magnitude of DOM dilution or flushing during rain events as seen in the studies from the Boreal Shield or Scandinavian Shield, and I found a clear increasing seasonal trend. Together, my results show that although most controls and processes are the same across different forested regions, their importance is sometimes different, which may have implications for how we design monitoring program, model water quality, and possibly treat our drinking water in the Boreal Plains ecozone.

5.2. Aquatic processes

My final study (Chapter 4) examined the importance of aquatic processes on DOM concentration and composition. The results of my incubations suggest that photodegradation is

relatively more important than biodegradation, although the result of incubations are not directly transferrable to field conditions, as these processes occur concurrently and act synergistically in surface waters, and I did not account for seasonal variations in field conditions. However, my results (greater role of photodegradation, a lack of seasonal pattern) are consistent with previous findings from URSA and other boreal regions. Future studies of bio- and photodegradation in the Boreal Plains streams should attempt to study these processes together, as they are inherently linked, using either field or laboratory experiments, and to quantify the loss of DOC along the stream network under a range of scenarios. In addition, estimating the apparent quantum yield of DOC photoproduction would allow for direct comparison of my results with those from other boreal regions.

In all three studies, I observed a strong influence of lakes on DOM composition. Small streams in the boreal regions are often shaded by trees in riparian areas, which limits DOM turnover (Kothawala et al., 2015). But the abundance of lakes and beaver activity in the Boreal Plains creates large open areas and increases water residence time, thus providing opportunity for DOM photodegradation. Due to variations in lake size and morphometry, geologic setting, residence time, hydrologic connectivity with wetlands, and the resulting differences in the rates of photodegradation and autochthonous production of DOM, there is substantial spatial and inter-annual variability in lake DOM in the Boreal Plains ecozone. Lakes at URSA accounted on average for a net loss of 17% for DOC concentration and 39% for A_{254} (Pugh et al., 2021), which aligns with our observations of reduced DOC concentration and A_{254} in lake-dominated streams and changes in DOM during photodegradation incubations. The large variability in lake properties and lake DOM concentration and composition also suggests that the impact of lakes on DOM exported

downstream will vary across catchments, which will have implications for aquatic functions, DOM turnover and drinking water treatability.

The results of this study are important to better understand drinking water treatability in the region. In the Boreal Plains ecozone, small communities usually rely on surface waters for drinking water supply, and use water reservoirs for water storage, as water availability in this region is highly variable and hard to predict. I saw changes in disinfection by-product formation potential (DBP-FP) in photodegraded samples, but was not able to identify clear patterns. My results (Chapter 4) show that the influence of photodegradation may vary by DBP, as DBP-FP is not strongly correlated with DOC concentration, A_{254} or SUVA. I also found that long-term (i.e., months) water storage in a drinking water reservoir alters DOM concentration and composition relative to the water source (REC) to the point that it likely does not matter when water is withdrawn. Although DOM concentrations in the streams doubled throughout the summer, degradability of DOM did not have a seasonal pattern, which may be a result of other environmental factors (e.g., temperature and sunlight) impacting the composition of DOM delivered to streams and aquatic processing of DOM in stream water.

5.3. Climate change and disturbance

My three studies demonstrated the relationships between stream DOM and climatic parameters, including temperature, precipitation and discharge. For example, in Chapter 3, intra-annual variability in precipitation resulted in large differences in runoff and hence DOM export. There was also large inter-annual variability in precipitation, which led to differences in annual export. Climate change is already affecting climatic parameters (e.g., rising temperature, changes in precipitation amounts and seasonal patterns). While we have varying confidence in climate projections for the magnitude of change in different parameters (Bush & Lemmen, 2019), we can

be certain that these changes have the potential to affect water availability and chemistry in Canada's surface water, and will likely lead to changes in stream DOM.

Northern latitudes are projected to experience an increase in mean annual air temperature greater than the global mean, with the largest increase in the winter (Bush & Lemmen, 2019). There is evidence that warmer and shorter winters, and early disappearance of seasonal frost in the boreal regions may lead to higher DOC export in the winter months (Laudon et al., 2013) and reduced DOC concentrations in streams in the spring and summer (Haei et al., 2010).

Across Canada, trends in streamflow based on historical data have not been spatially consistent. Streamflow is projected to decrease in the southern watersheds of interior Canada and increase in northern watersheds (Bush & Lemmen, 2019). Streamflow projections for large rivers in most of Western Canada indicate a shift in timing of snowmelt, higher winter flows, lower summer flows and an overall increase in annual runoff (Poitras et al., 2011).

As climate alters water residence time in lakes and streams, Catalán et al. (2016) predicted a change in DOM degradation up to 10%. The relationship between stream DOM and mean annual temperature (Chapter 2) or water temperature (Chapter 3) suggests that climate warming may accelerate the processing of organic material in soils, leading to higher stream DOC concentration, A_{254}, SUVA and lower DOM oxygenation. Alternatively, higher microbial respiration in soils under warmer climate may lead to decreased delivery of DOM to streams.

Climate change may also affect the distribution of wetlands and lakes. Pugh (2021) found that lakes in different geologic settings in the Boreal Plains had different resistance to dry periods. Lakes in the coarse outwash region were most resistant to drought due to their connectivity to regional groundwater systems (Devito et al., 2017; Hokanson et al., 2019). Lakes in the clay plain areas (fine-grained deposits) were also resistant, which was likely due to the slow release of water

by wetlands, while smaller lakes in the hummocky moraine areas were less resistant, due to fewer connected wetlands. However, smaller, isolated lakes with shallow depths and limited wetland connectivity, and lakes in the clay plain areas with large wetland connectivity were both susceptible to terrestrialization (Pugh, 2021), which over the long term may reduce DOM turnover in lakes and increase DOM export (especially export of colored DOM) downstream, given that most lakes act as DOM sinks in this region. In cases where lakes have significant autochthonous production, DOM export is expected to decrease. Because water loss to evapotranspiration is reduced in wetlands, they are also resistant to droughts in this landscape (Kettridge & Waddington, 2014). It is, however, unclear how wetlands and lakes in other regions will be affected.

During the monitoring program, I observed some small streams going dry during prolonged dry periods. These no-flow periods may become longer and more widespread. I noticed a switch in water chemistry (including DOM concentration and composition) in REC, indicating reduced wetland contribution and relatively higher groundwater contribution to the stream under extended dry conditions. Thus, droughts will also have an effect on DOM export and DOM composition.

I did not see a clear relationship between stream DOM and proportion of disturbed catchment area, where disturbances included areas harvested or burned in the past 30 years (Chapter 2), or areas burned in 2011 (Chapter 3). In Chapter 2, due to the study design limitation, it was not possible for me to assess the effects on stream DOM from disturbances of the same type and age across different ecozones. While studies of the effects of disturbance on water fluxes and select water quality parameters (e.g., nutrients and suspended sediment) have been conducted in different regions across Canada, there has been no synthesis of the findings, and the monitoring programs differed. Very few studies looked at the effects on DOM. Thus, we still have limited knowledge of the impact of forest harvesting and wildfires on DOM in many regions, and whether this

knowledge is transferrable from one region to another. Therefore, future research should use a common monitoring approach.

Wildfires are common in the Boreal Plains ecozone (Beverly & McLoughlin, 2019). Under climate warming and intensified human activities, their frequency and magnitude are expected to increase (Ireson et al., 2015). Prescribed burns and commercial thinning can be used to reduce the risk of wildfires in the Boreal Plains (Beverly et al., 2009; Pinno et al., 2021). Aspen harvest affects different components of water balance (e.g., Carrera-Hernandez et al., 2011; Donnelly et al., 2016; Petrone et al. 2015), but it is less clear what impact forest management may have on soil carbon inputs and water quality (Hillman et al., 1997). Wildfires and prescribed burns have limited effect on DOM in wetland shallow groundwater (Olefeldt et al., 2013; Orlova et al., 2021) and large rivers, yet were seen to affect drinking water treatment (Emmerton et al., 2020). The lack of relationship between the burned area and stream DOM in Chapter 3 aligns with the previous findings, but does not imply the absence of effect of disturbance on stream DOM.

In this low-relief landscape with large storage potential and variable hydrogeologic settings, groundwater connectivity and precipitation pattern control burn severity (Hokanson et al., 2016), time lag and magnitude of hydrologic response to disturbance (Donnelly et al., 2016; Emmerton et al., 2020). Thus, to further our understanding of wildfires and harvesting on stream DOM in the Boreal Plains ecozone, future studies should be initiated soon after the occurrence of disturbance, and need to focus on storm events and include the analysis of particulates (to measure the export of ash). However, I expect the effect to be generally short-lived (due to fast aspen regeneration), and to be noticeable only for large-scale disturbance and during storm events.

To conclude, my three studies described variability in stream DOM at the national and regional scales, and uncovered the main environmental controls on the concentration and

composition of DOM. The presence of lakes and wetlands, temperature, hydrologic connectivity to surface and subsurface flowpaths and discharge play a role in controlling stream DOM at different scales, but their relative importance varies. As multiple environmental controls contribute to stream DOM concentrations and composition, and these controls may be affected differently by the changes in temperature and precipitation, wildfires or forest harvesting, it is hard to accurately predict shifts in stream DOM under climate change or land disturbance. My studies provided an important insight into how DOM concentrations and composition may be affected, and how monitoring programs should be designed to better capture variability in the concentrations and composition of stream DOM.

References

AEP (Alberta Environment and Parks) (2017). Alberta Provincial Digital Elevation Model – Alberta Provincial 25 Metre Hillshade [digital data]. https://open.alberta.ca/opendata/gda-c16469a2-5541-455c-bba0-63a24c0ff08a

AEP (2022). Fisheries and Wildlife Management Information System – Access FWMIS data [Online mapping tool]. https://www.alberta.ca/access-fwmis-data.aspx

AER (Alberta Energy Regulator) (2016a). Surficial Geology of the Utikuma Area (NTS 83O/NW) (GIS data, polygon features) [Shapefile]. https://open.alberta.ca/opendata/gda-dig_2004_0003

AER (2016b). Surficial Geology of the Peerless Lake Area, Alberta (NTS 84B) (GIS data, polygon features) [Shapefile]. https://open.alberta.ca/opendata/gda-dig_2005_0012

AER (2008). Surficial Geology of the McLennan Area (NTS 83N/NE) (GIS data, polygon features) [Shapefile]. https://open.alberta.ca/opendata/gda-dig_2008_0353

Aiken, G. R., Hsu-Kim, H., & Ryan, J. N. (2011). Influence of dissolved organic matter on the environmental fate of metals, nanoparticles, and colloids. *Environmental Science & Technology*, *45*(8), 3196–3201. https://doi.org/10.1021/es103992s

Aiken, G. R., & Malcolm, R. L. (1987). Molecular weight of aquatic fulvic acids by vapor pressure osmometry. *Geochimica et Cosmochimica Acta, 51*(8). https://doi.org/10.1016/0016-7037(87)90267-5

Aitkenhead, J. A., & McDowell, W. H. (2000). Soil C:N ratio as a predictor of annual riverine DOC flux at local and global scales. *Global Biogeochemical Cycles*, *14*(1), 127–138. https://doi.org/10.1029/1999GB900083

Alberta Environment and Parks (2022). Fisheries and Wildlife Management Information System – Access FWMIS data [Online mapping tool]. https://www.alberta.ca/access-fwmis-data.aspx

Amado, A. M., Cotner, J. B., Cory, R. M., Edhlund, B. L., & McNeill, K. (2015). Disentangling the interactions between photochemical and bacterial degradation of dissolved organic matter: Amino acids play a central role. *Microbial Ecology*, *69*(3), 554–566. https://doi.org/10.1007/s00248-014-0512-4

Ågren, A., Buffam, I., Berggren, M., Bishop, K., Jansson, M., & Laudon, H. (2008). Dissolved organic carbon characteristics in boreal streams in a forest-wetland gradient during the transition between winter and summer. *Journal of Geophysical Research: Biogeosciences*, *113*(3). https://doi.org/10.1029/2007JG000674

Aulenbach, B. T., Burns, D. A., Shanley, J. B., Yanai, R. D., Bae, K., Wild, A. D., Yang, Y., & Yi, D. (2016). Approaches to stream solute load estimation for solutes with varying dynamics from five diverse small watersheds. *Ecosphere*, *7*(6), e01298. https://doi.org/10.1002/ecs2.1298

Aukes, P. J. K., Schiff, S. L., Venkiteswaran, J. J., Elgood, R. J., & Spoelstra, J. (2021). Size-based characterization of freshwater dissolved organic matter finds similarities within a

waterbody type across different Canadian ecozones. *Limnology and Oceanography Letters*, *6*(2), 85–95. https://doi.org/10.1002/lol2.10180

Bakdash, J. Z., & Marusich, L. R. (2017). Repeated Measures Correlation. *Frontiers in Psychology*, *8*. https://www.frontiersin.org/articles/10.3389/fpsyg.2017.00456

Baker, A. (2003). Land use and water quality. *Hydrological Processes*, *17*(12), 2499–2501. https://doi.org/10.1002/hyp.5140

Baldwin, K., Allen, L., Basquill, S., Chapman, K., Downing, D., Flynn, N., et al. (2019). Vegetation zones of Canada: A biogeoclimatic perspective [Map, scale 1:5,000,000]. Natural Resources Canada, Canadian Forest Service. Great Lake Forestry Center, Sault Ste. Marie, ON. https://open.canada.ca/data/en/dataset/22b0166b-9db3-46b7-9baf-6584a3acc7b1

Bates, D., Mächler, M., Bolker, B. M., & Walker, S. C. (2015). Fitting linear mixed-effects models using lme4. *Journal of Statistical Software*, *67*(1). https://doi.org/10.18637/jss.v067.i01

Battin, T. J., Kaplan, L. A., Findlay, S., Hopkinson, C. S., Marti, E., Packman, A. I., Newbold, J. D., & Sabater, F. (2008). Biophysical controls on organic carbon fluxes in fluvial networks. *Nature Geoscience*, *1*(2), 95–100. https://doi.org/10.1038/ngeo101

Bauer, J. E., Cai, W. J., Raymond, P. A., Bianchi, T. S., Hopkinson, C. S., & Regnier, P. A. G. (2013). The changing carbon cycle of the coastal ocean. In *Nature* (Vol. 504, Issue 7478). https://doi.org/10.1038/nature12857

Benner, R., & Kaiser, K. (2011). Biological and photochemical transformations of amino acids and lignin phenols in riverine dissolved organic matter. *Biogeochemistry*, *102*(1). https://doi.org/10.1007/s10533-010-9435-4

Berggren, M., & del Giorgio, P. A. (2015). Distinct patterns of microbial metabolism associated to riverine dissolved organic carbon of different source and quality. *Journal of Geophysical Research-Biogeosciences*, *120*(6), 989–999. https://doi.org/10.1002/2015JG002963

Berggren, M., Guillemette, F., Bieroza, M., Buffam, I., Deininger, A., Hawkes, J. A., Kothawala, D. N., LaBrie, R., Lapierre, J. F., Murphy, K. R., Al-Kharusi, E. S., Rulli, M. P. D., Hensgens, G., Younes, H., & Wünsch, U. J. (2022). Unified understanding of intrinsic and extrinsic controls of dissolved organic carbon reactivity in aquatic ecosystems. *Ecology*, *103*(9). https://doi.org/10.1002/ecy.3763

Berggren, M., Klaus, M., Panneer Selvam, B., Ström, L., Laudon, H., Jansson, M., & Karlsson, J. (2018). Quality transformation of dissolved organic carbon during water transit through lakes: Contrasting controls by photochemical and biological processes. *Biogeosciences*, *15*(2). https://doi.org/10.5194/bg-15-457-2018

Berggren, M., Laudon, H., Haei, M., Ström, L., & Jansson, M. (2010). Efficient aquatic bacterial metabolism of dissolved low-molecular-weight compounds from terrestrial sources. *ISME Journal*, *4*(3). https://doi.org/10.1038/ismej.2009.120

Bertilsson, S., & Tranvik, L. J. (2000). Photochemical transformation of dissolved organic matter in lakes. *Limnology and Oceanography*, *45*(4). https://doi.org/10.4319/lo.2000.45.4.0753

Beverly, J. L., Herd, E. P. K., & Conner, J. C. R. (2009). Modeling fire susceptibility in west central Alberta, Canada. *Forest Ecology and Management*, *258*(7). https://doi.org/10.1016/j.foreco.2009.06.052

Beverly, J. L., & McLoughlin, N. (2019). Burn probability simulation and subsequent wildland fire activity in Alberta, Canada – Implications for risk assessment and strategic planning. *Forest Ecology and Management*, *451*. https://doi.org/10.1016/j.foreco.2019.117490

Bourgeois, A. K. (2021). Assessing spatial and temporal variation in source water quality and drinking water treatability across a gradient of forest harvest on Vancouver Island, BC (Master's thesis). Retrieved from ERA: Education & Research Archive Theses & Dissertations (https://guides.library.ualberta.ca/theses-dissertations). Edmonton, AB: University of Alberta.

Bowen, J. C., Ward, C. P., Kling, G. W., & Cory, R. M. (2020). Arctic amplification of global warming strengthened by sunlight oxidation of permafrost carbon to CO2. *Geophysical Research Letters*, *47*(12), e2020GL087085. https://doi.org/10.1029/2020GL087085

Brandt, J. P., Flannigan, M. D., Maynard, D. G., Thompson, I. D., & Volney, W. J. A. (2013). An introduction to Canada's boreal zone: Ecosystem processes, health, sustainability, and environmental issues. *Environmental Reviews*, *21*(4), 207–226. https://doi.org/10.1139/er-2013-0040

Burd, K., Tank, S. E., Dion, N., Quinton, W. L., Spence, C., Tanentzap, A. J., & Olefeldt, D. (2018). Seasonal shifts in export of DOC and nutrients from burned and unburned peatland-rich catchments, Northwest Territories, Canada. *Hydrology and Earth System Sciences*, *22*(8), 4455–4472. https://doi.org/10.5194/hess-22-4455-2018

Bush, E., & Lemmen, D. S. (2019). Canada's Changing Climate Report. Government of Canada. Ottawa, ON. 444 p. https://changingclimate.ca/CCCR2019/

Buttle, J. M., Beall, F. D., Webster, K. L., Hazlett, P. W., Creed, I. F., Semkin, R. G., & Jeffries, D. S. (2018). Hydrologic response to and recovery from differing silvicultural systems in a deciduous forest landscape with seasonal snow cover. *Journal of Hydrology*, *557*, 805–825. https://doi.org/10.1016/j.jhydrol.2018.01.006

Buttle, J. M., Webster, K. L., Hazlett, P. W., & Jeffries, D. S. (2019). Quickflow response to forest harvesting and recovery in a northern hardwood forest landscape. *Hydrological Processes*, *33*(1), 47–65. https://doi.org/10.1002/hyp.13310

Carignan, R., D'Arcy, P., & Lamontagne, S. (2000). Comparative impacts of fire and forest harvesting on water quality in Boreal Shield lakes. *Canadian Journal of Fisheries and Aquatic Sciences*, *57*, 105–117. https://doi.org/10.1139/f00-125

Carrera-Hernández, J. J., Mendoza, C. A., Devito, K. J., Petrone, R. M., & Smerdon, B. D. (2011). Effects of aspen harvesting on groundwater recharge and water table dynamics in a subhumid climate. *Water Resources Research*, *47*(5). https://doi.org/10.1029/2010WR009684

Cartwright, I., Morgenstern, U., & Hofmann, H. (2020). Concentration versus streamflow trends of major ions and tritium in headwater streams as indicators of changing water stores. *Hydrological Processes*, *34*(2). https://doi.org/10.1002/hyp.13600

Casas-Ruiz, J. P., Catalán, N., Gómez-Gener, L., von Schiller, D., Obrador, B., Kothawala, D. N., López, P., Sabater, S., & Marcé, R. (2017). A tale of pipes and reactors: Controls on the in-stream dynamics of dissolved organic matter in rivers. *Limnology and Oceanography*, *62*. https://doi.org/10.1002/lno.10471

Catalán, N., Marcé, R., Kothawala, D. N., & Tranvik, L. J. (2016). Organic carbon decomposition rates controlled by water retention time across inland waters. *Nature Geoscience*, *9*(7), 501–504. https://doi.org/10.1038/ngeo2720

Catalán, N., Pastor, A., Borrego, C. M., Casas-Ruiz, J., Hawkes, J. A., Gutiérrez, C., von Schiller, D., & Marcé, R. (2021). The relevance of environment vs. composition on dissolved organic matter degradation in freshwaters. *Limnology and Oceanography*, *66*(2), 306–320. https://doi.org/10.1002/lno.11606

Ceroici, W. J. (1979). Hydrogeology of the Peerless Lake area, Alberta. Earth Sciences Report 79-5. Alberta Research Council. https://ags.aer.ca/publication/esr-1979-05

Chen, W., & Yu, H.-Q. (2021). Advances in the characterization and monitoring of natural organic matter using spectroscopic approaches. *Water Research*, *190*, 116759. https://doi.org/10.1016/j.watres.2020.116759

Chin, Y. P., Alken, G., & O'Loughlin, E. (1994). Molecular weight, polydispersity, and spectroscopic properties of aquatic humic substances. *Environmental Science and Technology*, *28*(11), 1853–1858. https://doi.org/10.1021/es00060a015

Coble, P. G. (1996). Characterization of marine and terrestrial DOM in seawater using excitation emission matrix spectroscopy. *Marine Chemistry*, *51*(4), 325–346. https://doi.org/10.1016/0304-4203(95)00062-3

Cole, J. J., Prairie, Y. T., Caraco, N. F., McDowell, W. H., Tranvik, L. J., Striegl, R. G., Duarte, C. M., Kortelainen, P., Downing, J. A., Middelburg, J. J., & Melack, J. (2007). Plumbing the global carbon cycle: Integrating inland waters into the terrestrial carbon budget. *Ecosystems*, *10*(1), 171–184. https://doi.org/10.1007/s10021-006-9013-8

Cory, R. M., Ward, C. P., Crump, B. C., & Kling, G. W. (2014). Sunlight controls water column processing of carbon in arctic fresh waters. *Science*, *345*(6199), 925–928. https://doi.org/10.1126/science.1253119

Creed, I. F., Beall, F. D., Clair, T. A., Dillon, P. J., & Hesslein, R. H. (2008). Predicting export of dissolved organic carbon from forested catchments in glaciated landscapes with shallow soils. *Global Biogeochemical Cycles*, *22*(4). https://doi.org/10.1029/2008GB003294

Creed, I. F., McKnight, D. M., Pellerin, B. A., Green, M. B., Bergamaschi, B. A., Aiken, G. R., Burns, D. A., Findlay, S. E. G., Shanley, J. B., Striegl, R. G., Aulenbach, B. T., Clow, D. W., Laudon, H., McGlynn, B. L., McGuire, K. J., Smith, R. A., & Stackpoole, S. M. (2015). The river as a chemostat: fresh perspectives on dissolved organic matter flowing down the river continuum. *Canadian Journal of Fisheries and Aquatic Sciences*, *72*(8), 1272–1285. https://doi.org/10.1139/cjfas-2014-0400

Cuss, C. W., Glover, C. N., Javed, M. B., Nagel, A., & Shotyk, W. (2020). Geochemical and biological controls on the ecological relevance of total, dissolved, and colloidal forms of trace elements in large boreal rivers: Review and case studies. Environmental Reviews, *28*(2), 138–163. https://doi.org/10.1139/er-2019-0014

Cuss, C. W., Grant-Weaver, I., & Shotyk, W. (2017). AF4-ICPMS with the 300 Da membrane to resolve metal-bearing "colloids" < 1 kDa: Optimization, fractogram deconvolution, and advanced quality control. *Analytical Chemistry*, *89*(15), 8027−8035. https://doi.org/10.1021/acs.analchem.7b01427

Cuss, C. W., & Guéguen, C. (2015). Relationships between molecular weight and fluorescence properties for size-fractionated dissolved organic matter from fresh and aged sources. *Water Research*, *68*, 487–497. https://doi.org/10.1016/j.watres.2014.10.013

D'Amore, D. V., Edwards, R. T., Herendeen, P. A., Hood, E., & Fellman, J. B. (2015). Dissolved organic carbon fluxes from hydropedologic units in Alaskan coastal temperate rainforest watersheds. *Soil Science Society of America Journal*, *79*(2), 378–388. https://doi.org/10.2136/sssaj2014.09.0380

Davidson, E. A., & Janssens, I. A. (2006). Temperature sensitivity of soil carbon decomposition and feedbacks to climate change. *Nature*, *440*(7081). https://doi.org/10.1038/nature04514

De Haan, H., & De Boer, T. (1987). Applicability of light absorbance and fluorescence as measures of concentration and molecular size of dissolved organic carbon in humic Lake Tjeukemeer. *Water Research*, *21*(6), 731–734. https://doi.org/10.1016/0043-1354(87)90086-8

De Melo, M. L., Teodoru, C. R., & del Giorgio, P. A. (2023). Catchment-scale carbon fluxes and processes in major rivers of northern Québec, Canada. *Science of the Total Environment*, *873*. https://doi.org/10.1016/j.scitotenv.2023.162308

Demars, B. O. L. (2019). Hydrological pulses and burning of dissolved organic carbon by stream respiration. *Limnology and Oceanography*, *64*(1), 406–421. https://doi.org/10.1002/lno.11048

Devito, K. J., Hokanson, K. J., Moore, P. A., Kettridge, N., Anderson, A. E., Chasmer, L., Hopkinson, C., Lukenbach, M. C., Mendoza, C. A., Morissette, J., Peters, D. L., Petrone, R. M., Silins, U., Smerdon, B., & Waddington, J. M. (2017). Landscape controls on long-term runoff in subhumid heterogeneous Boreal Plains catchments. *Hydrological Processes*, *31*(15), 2737–2751. https://doi.org/10.1002/hyp.11213

Devito, K. J., Mendoza, C., Petrone, R. M., Kettridge, N., & Waddington, J. M. (2016). Utikuma Region Study Area (URSA) – Part 1: Hydrogeological and ecohydrological studies (HEAD). *Forestry Chronicle*, *92*(1), 57–61. https://doi.org/10.5558/tfc2016-017

Devito, K. J., Mendoza, C., & Qualizza, C. (2012). Conceptualizing water movement in the Boreal Plains. Implications for watershed reconstruction. Synthesis report prepared for the Canadian Oil Sands Network for Research and Development, Environmental and Reclamation Research Group. 164 p.

Devito, K. J., O'Sullivan, A. M., Peters, D. L., Hokanson, K. J., Kettridge, N., & Mendoza, C. A. (2023). Runoff threshold responses in continental boreal catchments: Nexus of subhumid climate, low-relief, surficial geology, and land cover. *Water Resources Research, 59*(11), e2023WR034752. https://doi.org/10.1029/2023WR034752

Dittmar, T., Koch, B., Hertkorn, N., & Kattner, G. (2008). A simple and efficient method for the solid-phase extraction of dissolved organic matter (SPE-DOM) from seawater. *Limnology and Oceanography: Methods*, *6*, 230–235. https://doi.org/10.4319/lom.2008.6.230

Dobbs, R. A., Wise, R. H., & Dean, R. B. (1972). The use of ultra-violet absorbance for monitoring the total organic carbon content of water and wastewater. *Water Research*, *6*(10), 1173–1180. https://doi.org/10.1016/0043-1354(72)90017-6

Donnelly, M., Devito, K. J., Mendoza, C., Petrone, R., & Spafford, M. (2016). Al-Pac Catchment Experiment (ACE). *The Forestry Chronicle*, *92*(1), 23–26. https://doi.org/10.5558/tfc2016-007

Ducks Unlimited Canada (2011). Enhanced wetland classification: inferred products user guide version 1.0 [Dataset]. https://www.ducks.ca/resources/industry/enhanced-wetland-classification-inferred-products-user-guide/

ECCC (Environment and Climate Change Canada; 2023a). Historical climate data. Accessed Apr 19, 2023. https://climate.weather.gc.ca/index_e.html

ECCC (2023b). Historical hydrometric data. Accessed Apr 19, 2023. https://climate.weather.gc.ca/historical_data/search_historic_data_e.html

ECCC (2023c). National hydrometric network basin polygons. Accessed Dec 28, 2023. https://open.canada.ca/data/en/dataset/0c121878-ac23-46f5-95df-eb9960753375

Eckhardt, B. W., & Moore, T. R. (1990). Controls on dissolved organic carbon concentrations in streams, southern Quebec. *Canadian Journal of Fisheries and Aquatic Sciences*, *47*(8). https://doi.org/10.1139/f90-173

Ecological Stratification Working Group (1996). A national ecological framework for Canada. Report and national map at 1:7,500,000 scale. Agriculture and Agri-Food Canada, Research Branch, Centre for Land and Biological Resources Research, and Environment Canada, State of the Environment Directorate, Ecozone Analysis Branch, Ottawa/Hull, ON. https://sis.agr.gc.ca/cansis/publications/manuals/1996/index.html

Eder, A., Weigelhofer, G., Pucher, M., Tiefenbacher, A., Strauss, P., Brandl, M., & Blöschl, G. (2022). Pathways and composition of dissolved organic carbon in a small agricultural catchment during base flow conditions. *Ecohydrology and Hydrobiology*, *22*(1). https://doi.org/10.1016/j.ecohyd.2021.07.012

Eimers, M. C., Buttle, J., & Watmough, S. A. (2008). Influence of seasonal changes in runoff and extreme events on dissolved organic carbon trends in wetland- and upland-draining streams. *Canadian Journal of Fisheries and Aquatic Sciences*, *65*(5), 796–808. https://doi.org/10.1139/f07-194

Emelko, M. B., Silins, U., Bladon, K. D., & Stone, M. (2011). Implications of land disturbance on drinking water treatability in a changing climate: Demonstrating the need for "source water supply and protection" strategies. *Water Research*, *45*(2), 461–472. https://doi.org/10.1016/j.watres.2010.08.051

Emelko, M. B., Stone, M., Silins, U., Allin, D., Collins, A. L., Williams, C. H. S., Martens, A. M., & Bladon, K. D. (2016). Sediment-phosphorus dynamics can shift aquatic ecology and cause downstream legacy effects after wildfire in large river systems. *Global Change Biology*, *22*(3), 1168-1184. https://doi.org/10.1111/gcb.13073

Emmerton, C. A., Cooke, C. A., Hustins, S., Silins, U., Emelko, M. B., Lewis, T., et al. (2020). Severe western Canadian wildfire affects water quality even at large basin scales. *Water Research*, *183*, 116071. https://doi.org/10.1016/j.watres.2020.116071

Erlandsson, M., Buffam, I., Folster, J., Laudon, H., Temnerud, J., Weyhenmeyer, G. A., & Bishop, K. (2008). Thirty-five years of synchrony in the organic matter concentrations of Swedish rivers explained by variation in flow and sulphate. *Global Change Biology*, *14*(5), 1191–1198. https://doi.org/10.1111/j.1365-2486.2008.01551.x

Evans, C. D., Futter, M. N., Moldan, F., Valinia, S., Frogbrook, Z., & Kothawala, D. N. (2017). Variability in organic carbon reactivity across lake residence time and trophic gradients. *Nature Geoscience*, *10*(11), 832–835. https://doi.org/10.1038/ngeo3051

Fellman, J. B., D'Amore, D. v., Hood, E., & Boone, R. D. (2008). Fluorescence characteristics and biodegradability of dissolved organic matter in forest and wetland soils from coastal temperate watersheds in southeast Alaska. *Biogeochemistry*, *88*(2). https://doi.org/10.1007/s10533-008-9203-x

Fellman, J. B., Hood, E., Behnke, M. I., Welker, J. M., & Spencer, R. G. M. (2020). Stormflows drive stream carbon concentration, speciation, and dissolved organic matter composition in coastal temperate rainforest watersheds. *Journal of Geophysical Research: Biogeosciences*, *125*(9), e2020JG005804. https://doi.org/10.1029/2020JG005804

Fellman, J. B., Hood, E., D'Amore, D. v, Edwards, R. T., & White, D. (2009). Seasonal changes in the chemical quality and biodegradability of dissolved organic matter exported from soils to streams in coastal temperate rainforest watersheds. *Biogeochemistry*, *95*(2), 277–293. https://doi.org/10.1007/s10533-009-9336-6

Freeman, C., Evans, C. D., Monteith, D. T., Reynolds, B., & Fenner, N. (2001). Export of organic carbon from peat soils. *Nature*, *412*(6849). https://doi.org/10.1038/35090628

Freeman, C., Ostle, N., & Kang, H. (2001). An enzymic "latch" on a global carbon store. Nature, *409*(6817). https://doi.org/10.1038/35051650

Frey, K. E., & Smith, L. C. (2005). Amplified carbon release from vast West Siberian peatlands by 2100. *Geophysical Research Letters*, *32*(9), L09401. https://doi.org/10.1029/2004GL022025

Frey, R. (2023). Consequences of peatland disturbance for dissolved organic matter and nutrient transport and fate in northern catchments (PhD thesis). Retrieved from ERA: Education & Research Archive Theses & Dissertations (https://guides.library.ualberta.ca/theses-dissertations). Edmonton, AB: University of Alberta.

Frost, P. C., Larson, J. H., Johnston, C. A., Young, K. C., Maurice, P. A., Lamberti, G. A., & Bridgham, S. D. (2006). Landscape predictors of stream dissolved organic matter concentration and physicochemistry in a Lake Superior river watershed. *Aquatic Sciences*, *68*(1), 40–51. https://doi.org/10.1007/s00027-005-0802-5

Gorham, E., Underwood, J. K., Janssens, J. A., Freedman, B., Maass, W., Waller, D. H., & Ogden, J. G. (1998). The chemistry of streams in southwestern and central Nova Scotia, with particular reference to catchment vegetation and the influence of dissolved organic carbon primarily from wetlands. *Wetlands*, *18*(1), 115–132. https://doi.org/10.1007/BF03161449

Government of Alberta (2022). Spatial wildfire data. Historical wildfire perimeter data: 1931–2021 [Shapefile]. https://wildfire.alberta.ca/resources/historical-data/spatial-wildfire-data.aspx

Government of Alberta (2023). Current and Historical Alberta Weather Station Data Viewer. Data provided by Agriculture and Irrigation, Alberta Climate Information Service (ACIS). Accessed Apr 19, 2023. https://agriculture.alberta.ca/acis/weather-data-viewer.jsp

Government of Alberta (2022). Wildfire maps and data. Historical Wildfire Perimeter Data: 1931–2022 [Shapefile]. Accessed on April 24, 2023. https://www.alberta.ca/wildfire-maps-and-data.aspx

Government of British Columbia (2021). iMapBC [Online mapping tool]. https://www2.gov.bc.ca/gov/content/data/geographic-data-services/web-based-mapping/imapbc

Groeneveld, M., Catalán, N., Einarsdottir, K., Bravo, A. G., & Kothawala, D. N. (2022). The influence of pH on dissolved organic matter fluorescence in inland waters. *Analytical Methods*, *14*(13). https://doi.org/10.1039/d1ay01702k

Groeneveld, M., Tranvik, L., Natchimuthu, S., & Koehler, B. (2016). Photochemical mineralisation in a boreal brown water lake: considerable temporal variability and minor contribution to carbon dioxide production. *Biogeosciences*, *13*(13), 3931–3943. https://doi.org/10.5194/bg-13-3931-2016

Gruber, S. (2012). Derivation and analysis of a high-resolution estimate of global permafrost zonation. *Cryosphere*, *6*(1), 221–233. https://doi.org/10.5194/tc-6-221-2012

Gu, Y., Lensu, A., Peramaki, S., Ojala, A., & Vahatalo, A. v. (2017). Iron and pH Regulating the Photochemical Mineralization of Dissolved Organic Carbon. *Acs Omega*, *2*(5), 1905–1914. https://doi.org/10.1021/acsomega.7b00453

Guéguen, C., & Cuss, C. W. (2011). Characterization of aquatic dissolved organic matter by asymmetrical flow field-flow fractionation coupled to UV-visible diode array and excitation emission matrix fluorescence. *Journal of Chromatography A*, *1218*(27), 4188–4198. https://doi.org/10.1016/j.chroma.2010.12.038

Guéguen, C., Cuss, C. W., Cassels, C. J., & Carmack, E. C. (2014). Absorption and fluorescence of dissolved organic matter in the waters of the Canadian Arctic Archipelago, Baffin Bay, and the Labrador Sea. *Journal of Geophysical Research: Oceans*, *119*(3), 2034–2047. https://doi.org/10.1002/2013JC009173

Guillemette, F., & del Giorgio, P. A. (2011). Reconstructing the various facets of dissolved organic carbon bioavailability in freshwater ecosystems. *Limnology and Oceanography*, *56*(2). https://doi.org/10.4319/lo.2011.56.2.0734

Guillemette, F., McCallister, S. L., & del Giorgio, P. A. (2013). Differentiating the degradation dynamics of algal and terrestrial carbon within complex natural dissolved organic carbon in temperate lakes. *Journal of Geophysical Research: Biogeosciences*, *118*(3). https://doi.org/10.1002/jgrg.20077

Haei, M., Öquist, M. G., Buffam, I., Ågren, A., Blomkvist, P., Bishop, K., Löfvenius, M. O., & Laudon, H. (2010). Cold winter soils enhance dissolved organic carbon concentrations in

soil and stream water. *Geophysical Research Letters*, *37*(8). https://doi.org/10.1029/2010GL042821

Hansen, A. M., Kraus, T. E. C., Pellerin, B. A., Fleck, J. A., Downing, B. D., & Bergamaschi, B. A. (2016). Optical properties of dissolved organic matter (DOM): Effects of biological and photolytic degradation. *Limnology and Oceanography*, *61*(3), 1015–1032. https://doi.org/10.1002/lno.10270

Harms, T. K., Edmonds, J. W., Genet, H., Creed, I. F., Aldred, D., Balser, A., and Jones, J. B. (2016), Catchment influence on nitrate and dissolved organic matter in Alaskan streams across a latitudinal gradient, *Journal of Geophysical Research: Biogeosciences*, 121, 350–369, https://doi.org/10.1002/2015JG003201

Harjung, A., Ejarque, E., Battin, T., Butturini, A., Sabater, F., Stadler, M., & Schelker, J. (2019). Experimental evidence reveals impact of drought periods on dissolved organic matter quality and ecosystem metabolism in subalpine streams. *Limnology and Oceanography*, *64*(1), 46–60. https://doi.org/10.1002/lno.11018

Hawkes, J. A., Radoman, N., Bergquist, J., Wallin, M. B., Tranvik, L. J., & Löfgren, S. (2018). Regional diversity of complex dissolved organic matter across forested hemiboreal headwater streams. *Scientific Reports*, *8*, 16060. https://doi.org/10.1038/s41598-018-34272-3

Helms, J. R., Mao, J., Stubbins, A., Schmidt-Rohr, K., Spencer, R. G. M., Hernes, P. J., & Mopper, K. (2014). Loss of optical and molecular indicators of terrigenous dissolved organic matter during long-term photobleaching. *Aquatic Sciences*, *76*(3), 353–373. https://doi.org/10.1007/s00027-014-0340-0

Helms, J. R., Stubbins, A., Ritchie, J. D., Minor, E. C., Kieber, D. J., & Mopper, K. (2008). Absorption spectral slopes and slope ratios as indicators of molecular weight, source, and photobleaching of chromophoric dissolved organic matter. *Limnology and Oceanography*, *53*(3), 955–969. https://doi.org/10.4319/lo.2008.53.3.0955

Helsel, D. R. (2006). Fabricating data: How substituting values for nondetects can ruin results, and what can be done about it. *Chemosphere*, *65*(11), 2434–2439. https://doi.org/10.1016/j.chemosphere.2006.04.051

Hillman, G. R., Feng, J. C., & Feng, C. C. (1997). *Effects of watershed characteristics and disturbances on the water quality of two boreal streams*. Natural Resources Canada, Canadian Forest Service, Northern Forestry Centre, Edmonton, Alberta. Canada-Alberta Partnership Agreement in Forestry Report. 67 p. https://cfs.nrcan.gc.ca/publications?id=18866

Hinton, M. J., Schiff, S. L., & English, M. C. (1997). The significance of storms for the concentration and export of dissolved organic carbon from two Precambrian Shield catchments. *Biogeochemistry*, *36*(1), 67–88. https://doi.org/10.1023/A:1005779711821

Hinton, M. J., Schiff, S. L., & English, M. C. (1998). Sources and flowpaths of dissolved organic carbon during storms in two forested watersheds of the Precambrian Shield. *Biogeochemistry*, *41*(2), 175–197. https://doi.org/10.1023/A:1005903428956

Hogg, E. H. (1997). Temporal scaling of moisture and the forest-grassland boundary in western Canada. *Agricultural and Forest Meteorology*, *84*(1–2), 115–122. https://doi.org/10.1016/S0168-1923(96)02380-5

Hokanson, K. J., Lukenbach, M. C., Devito, K. J., Kettridge, N., Petrone, R. M., & Waddington, J. M. (2016). Groundwater connectivity controls peat burn severity in the boreal plains. *Ecohydrology*, *9*(4), 574–584. https://doi.org/10.1002/eco.1657

Hokanson, K. J., Mendoza, C. A., & Devito, K. J. (2019). Interactions between regional climate, surficial geology, and topography: Characterizing shallow groundwater systems in subhumid, low-relief landscapes. *Water Resources Research*, *55*(1), 284–297. https://doi.org/10.1029/2018WR023934

Hokanson, K. J., Rostron, B. J., Devito, K. J., Hopkinson, C., & Mendoza, C. A. (2022). Landscape controls of surface-water/groundwater interactions on shallow outwash lakes: how the long-term groundwater signal overrides interannual variability due to evaporative effects. *Hydrogeology Journal*, *30*(1). https://doi.org/10.1007/s10040-021-02422-z

Hu, B., Wang, P., Wang, C., & Bao, T. (2022). Photogeochemistry of particulate organic matter in aquatic systems: A review. *Science of The Total Environment, 806*, 150467. https://doi.org/10.1016/j.scitotenv.2021.150467

Huber, S. A., & Frimmel, F. H. (1991). Flow injection analysis of organic and inorganic carbon in the low-ppb range. *Analytical Chemistry*, *63*(19), 2122–2130. https://doi.org/10.1021/ac00019a011

Huber, S. A., Balz, A., Abert, M., & Pronk, W. (2011). Characterisation of aquatic humic and non-humic matter with size-exclusion chromatography – organic carbon detection – organic nitrogen detection (LC-OCD-OND). *Water Research*, *45*(2), 879–885. https://doi.org/10.1016/j.watres.2010.09.023

Huguet, A., Vacher, L., Relexans, S., Saubusse, S., Froidefond, J. M., & Parlanti, E. (2009). Properties of fluorescent dissolved organic matter in the Gironde Estuary. *Organic Geochemistry, 40*(6). https://doi.org/10.1016/j.orggeochem.2009.03.002

Huntington, T. G., Richardson, A. D., McGuire, K. J., & Hayhoe, K. (2009). Climate and hydrological changes in the northeastern United States: Recent trends and implications for forested and aquatic ecosystems. *Canadian Journal of Forest Research*, *39*(2), 199–212. https://doi.org/10.1139/X08-116

Hutchins, R. H. S., Aukes, P., Schiff, S. L., Dittmar, T., Prairie, Y. T., & del Giorgio, P. A. (2017). The optical, chemical, and molecular dissolved organic matter succession along a boreal soil-stream-river continuum. *Journal of Geophysical Research: Biogeosciences*, *122*(11), 2892–2908. https://doi.org/10.1002/2017JG004094

Ireson, A. M., Barr, A. G., Johnstone, J. F., Mamet, S. D., van der Kamp, G., Whitfield, C. J., Michel, N. L., North, R. L., Westbrook, C. J., Debeer, C., Chun, K. P., Nazemi, A., & Sagin, J. (2015). The changing water cycle: the Boreal Plains ecozone of Western Canada. *Wiley Interdisciplinary Reviews: Water*, *2*(5). https://doi.org/10.1002/WAT2.1098

Jackson, C., & Blecic, B. (1996). Water allocation plan – Sooke. https://www2.gov.bc.ca/gov/content/environment/air-land-water/water/water-planning-strategies/water-allocation-plans

Jaffé, R., McKnight, D., Maie, N., Cory, R., McDowell, W. H., & Campbell, J. L. (2008). Spatial and temporal variations in DOM composition in ecosystems: The importance of long-term monitoring of optical properties. *Journal of Geophysical Research: Biogeosciences*, *113*, G04032. https://doi.org/10.1029/2008JG000683

Jaffé, R., Yamashita, Y., Maie, N., Cooper, W. T., Dittmar, T., Dodds, W. K., et al. (2012). Dissolved organic matter in headwater streams: Compositional variability across climatic regions of North America. *Geochimica et Cosmochimica Acta*, *94*, 95–108. https://doi.org/10.1016/j.gca.2012.06.031

Jankowski, K. J., & Schindler, D. E. (2019). Watershed geomorphology modifies the sensitivity of aquatic ecosystem metabolism to temperature. *Scientific Reports*, *9*(1). https://doi.org/10.1038/s41598-019-53703-3

Jeffries, D. S., Kelso, J. R. M., & Morrison, I. K. (1988). Physical, chemical, and biological characteristics of the Turkey Lakes Watershed, central Ontario, Canada. *Canadian Journal of Fisheries and Aquatic Sciences*, *45*(S1), s3–s13. https://doi.org/10.1139/f88-262

Jones, T. G., Evans, C. D., Jones, D. L., Hill, P. W., & Freeman, C. (2016). Transformations in DOC along a source to sea continuum; impacts of photo-degradation, biological processes and mixing. *Aquatic Sciences*, *78*(3), 433–446. https://doi.org/10.1007/s00027-015-0461-0

Jutras, M. F., Nasr, M., Castonguay, M., Pit, C., Pomeroy, J. H., Smith, T. P., et al. (2011). Dissolved organic carbon concentrations and fluxes in forest catchments and streams: DOC-3 model. *Ecological Modelling*, *222*(14), 2291–2313. https://doi.org/10.1016/j.ecolmodel.2011.03.035

Kalbitz, K., Solinger, S., Park, J. H., Michalzik, B., & Matzner, E. (2000). Controls on the dynamics of dissolved organic matter in soils: A review. *Soil Science*, *165*(4), 277–304. https://doi.org/10.1097/00010694-200004000-00001

Kassambara, A., & Mundt, F. (2020). factoextra: Extract and visualize the results of multivariate data analyses. R package version 1.0.7.999. http://www.sthda.com/english/rpkgs/factoextra

Kasurinen, V., Alfredsen, K., Ojala, A., Pumpanen, J., Weyhenmeyer, G. A., Futter, M. N., Laudon, H., & Berninger, F. (2016). Modeling nonlinear responses of DOC transport in boreal catchments in Sweden. *Water Resources Research*, *52*(7), 4970–4989. https://doi.org/10.1002/2015WR018343

Kellerman, A. M., Dittmar, T., Kothawala, D. N., & Tranvik, L. J. (2014). Chemodiversity of dissolved organic matter in lakes driven by climate and hydrology. *Nature Communications*, *5*(1), 3804. https://doi.org/10.1038/ncomms4804

Kettridge, N., & Waddington, J. M. (2014). Towards quantifying the negative feedback regulation of peatland evaporation to drought. *Hydrological Processes*, *28*(11). https://doi.org/10.1002/hyp.9898

Kleber, M. (2010). What is recalcitrant soil organic matter? *Environmental Chemistry*, *7*(4). https://doi.org/10.1071/EN10006

Kleber, M., Eusterhues, K., Keiluweit, M., Mikutta, C., Mikutta, R., & Nico, P. S. (2015). Chapter One – Mineral-organic associations: Formation, properties, and relevance in soil

environments. In D. L. Sparks (Ed.), *Advances in Agronomy* (Vol. 130, pp. 1–140). Academic Press. https://doi.org/10.1016/bs.agron.2014.10.005

Koch, B. P., & Dittmar, T. (2006). From mass to structure: An aromaticity index for high-resolution mass data of natural organic matter. *Rapid Communications in Mass Spectrometry*, *20*(5), 926–932. https://doi.org/10.1002/rcm.2386

Köhler, S., Buffam, I., Jonsson, A., & Bishop, K. (2002). Photochemical and microbial processing of stream and soilwater dissolved organic matter in a boreal forested catchment in northern Sweden. *Aquatic Sciences*, *64*(3), 269–281. https://doi.org/10.1007/s00027-002-8071-z

Köhler, S.J., Buffam, I., Seibert, J., Bishop, K. H., Laudon, H. (2009). Dynamics of stream water TOC concentrations in a boreal headwater catchment: Controlling factors and implications for climate scenarios. *Journal of Hydrology*, *373*(1–2), 44-56. https://doi.org/10.1016/j.jhydrol.2009.04.012.

Köhler, S. J., Kothawala, D., Futter, M. N., Liungman, O., & Tranvik, L. (2013). In-lake processes offset increased terrestrial inputs of dissolved organic carbon and color to lakes. *PLoS ONE*, *8*(8). https://doi.org/10.1371/journal.pone.0070598

Köhler, S. J., Lidman, F., & Laudon, H. (2014). Landscape types and pH control organic matter mediated mobilization of Al, Fe, U and La in boreal catchments. *Geochimica et Cosmochimica Acta*, 135, 190–202. https://doi.org/10.1016/j.gca.2014.03.033

Koprivnjak, J. F., Dillon, P. J., & Molot, L. A. (2010). Importance of CO_2 evasion from small boreal streams. *Global Biogeochemical Cycles*, *24*(4). https://doi.org/10.1029/2009GB003723

Kothawala, D. N., Ji, X., Laudon, H., Ågren, A. M., Futter, M. N., Köhler, S. J., & Tranvik, L. J. (2015). The relative influence of land cover, hydrology, and in-stream processing on the composition of dissolved organic matter in boreal streams. *Journal of Geophysical Research-Biogeosciences*, *120*(8), 1491–1505. https://doi.org/10.1002/2015JG002946

Kothawala, D. N., Murphy, K. R., Stedmon, C. A., Weyhenmeyer, G. A., & Tranvik, L. J. (2013). Inner filter correction of dissolved organic matter fluorescence. *Limnology and Oceanography: Methods*, *11*(12), 616–630. https://doi.org/10.4319/lom.2013.11.616

Kothawala, D. N., Stedmon, C. A., Müller, R. A., Weyhenmeyer, G. A., Köhler, S. J., & Tranvik, L. J. (2014). Controls of dissolved organic matter quality: evidence from a large-scale boreal lake survey. *Global Change Biology*, *20*(4), 1101–1114. https://doi.org/10.1111/gcb.12488

Kurek, M. R., Garcia-Tigreros, F., Wickland, K. P., Frey, K. E., Dornblaser, M. M., Striegl, R. G., et al. (2023). Hydrologic and landscape controls on dissolved organic matter composition across western North American Arctic lakes. *Global Biogeochemical Cycles*, *37*(1), e2022GB007495. https://doi.org/10.1029/2022GB007495

Kurz, W. A., Shaw, C. H., Boisvenue, C., Stinson, G., Metsaranta, J., Leckie, D., Dyk, A., Smyth, C., & Neilson, E. T. (2013). Carbon in Canada's boreal forest - A synthesis. *Environmental Reviews*, *21*(4), 260–292. https://doi.org/10.1139/er-2013-0041

Kuznetsova, A., Brockhoff, P. B., & Christensen, R. H. B. (2017). lmerTest Package: Tests in Linear Mixed Effects Models. *Journal of Statistical Software*, *82*(13). https://doi.org/10.18637/JSS.V082.I13

Lapierre, J. F., & del Giorgio, P. A. (2014). Partial coupling and differential regulation of biologically and photochemically labile dissolved organic carbon across boreal aquatic networks. *Biogeosciences*, *11*(20), 5969–5985. https://doi.org/10.5194/bg-11-5969-2014

Larsen, I. J., MacDonald, L. H., Brown, E., Rough, D., Welsh, M. J., Pietraszek, J. H., et al. (2009). Causes of post-fire runoff and erosion: Water repellency, cover, or soil sealing? *Soil Science Society of America Journal*, *73*(4), 1393–1407. https://doi.org/10.2136/sssaj2007.0432

Larson, J. H., Frost, P. C., Zheng, Z., Johnston, C. A., Bridgham, S. D., Lodge, D. M., & Lamberti, G. A. (2007). Effects of upstream lakes on dissolved organic matter in streams. *Limnology and Oceanography*, *52*(1), 60–69. https://doi.org/10.4319/lo.2007.52.1.0060

Laudon, H., Berggren, M., Ågren, A., Buffam, I., Bishop, K., Grabs, T., Jansson, M., & Köhler, S. (2011). Patterns and dynamics of dissolved organic carbon (DOC) in boreal streams: The role of processes, connectivity, and scaling. *Ecosystems*, *14*(6), 880–893. https://doi.org/10.1007/s10021-011-9452-8

Laudon, H., Hasselquist, E. M., Peichl, M., Lindgren, K., Sponseller, R., Lidman, F., Kuglerová, L., Hasselquist, N. J., Bishop, K., Nilsson, M. B., & Ågren, A. M. (2021). Northern landscapes in transition: Evidence, approach and ways forward using the Krycklan Catchment Study. *Hydrological Processes*, *35*(4). https://doi.org/10.1002/hyp.14170

Laudon, H., Hedtjarn, J., Schelker, J., Bishop, K., Sorensen, R., & Agren, A. (2009). Response of dissolved organic carbon following forest harvesting in a boreal forest. *Ambio*, *38*(7), 381–386. https://doi.org/10.1579/0044-7447-38.7.381

Laudon, H., Köhler, S., & Buffam, I. (2004). Seasonal TOC export from seven boreal catchments in northern Sweden. *Aquatic Sciences*, *66*(2). https://doi.org/10.1007/s00027-004-0700-2

Laudon, H., Tetzlaff, D., Soulsby, C., Carey, S., Seibert, J., Buttle, J., Shanley, J., Mcdonnell, J. J., & Mcguire, K. (2013). Change in winter climate will affect dissolved organic carbon and water fluxes in mid-to-high latitude catchments. *Hydrological Processes*, *27*(5). https://doi.org/10.1002/hyp.9686

Lavonen, E. E., Kothawala, D. N., Tranvik, L. J., Gonsior, M., Schmitt-Kopplin, P., & Köhler, S. J. (2015). Tracking changes in the optical properties and molecular composition of dissolved organic matter during drinking water production. *Water Research*, *85*, 286–294. https://doi.org/10.1016/j.watres.2015.08.024

Lead, J. R., & Wilkinson, K. J. (2006). Aquatic colloids and nanoparticles: Current knowledge and future trends. *Environmental Chemistry*, *3*(3). https://doi.org/10.1071/EN06025

Liaw, A., & Wiener, M. (2002). Classification and regression by randomForest. *R News*, 2(3). https://journal.r-project.org/articles/RN-2002-022/

Liu, S., He, Z., Tang, Z., Liu, L., Hou, J., Li, T., Zhang, Y., Shi, Q., Giesy, J. P., & Wu, F. (2020). Linking the molecular composition of autochthonous dissolved organic matter to source identification for freshwater lake ecosystems by combination of optical spectroscopy and

FT-ICR-MS analysis. Science of the Total Environment, 703. https://doi.org/10.1016/j.scitotenv.2019.134764

Lou, T., & Xie, H. (2006). Photochemical alteration of the molecular weight of dissolved organic matter. *Chemosphere*, *65*(11), 2333–2342. https://doi.org/10.1016/j.chemosphere.2006.05.001

Lüdecke, D., Ben-Shachar, M., Patil, I., Waggoner, P., & Makowski, D. (2021). performance: An R Package for Assessment, Comparison and Testing of Statistical Models. *Journal of Open Source Software*, *6*(60). https://doi.org/10.21105/joss.03139

Maie, N., Parish, K. J., Watanabe, A., Knicker, H., Benner, R., Abe, T., Kaiser, K., Jaffé, R. (2006). Chemical characteristics of dissolved organic nitrogen in an oligotrophic subtropical coastal ecosystem. *Geochimica et Cosmochimica Acta*, *70*(17), 4491-4506. https://doi.org/10.1016/j.gca.2006.06.1554

Marais, S. S., Ncube, E. J., Msagati, T. A. M., Mamba, B. B., & Nkambule I., T. T. (2019). Assessment of trihalomethane (THM) precursors using specific ultraviolet absorbance (SUVA) and molecular size distribution (MSD). *Journal of Water Process Engineering*, *27*, 143–151. https://doi.org/10.1016/j.jwpe.2018.11.019

Marshall, I. B., Schut, P. H., & Ballard, M. (1999). A national ecological framework for Canada: Attribute data. Agriculture and Agri-Food Canada, Research Branch, Centre for Land and Biological Resources Research, and Environment Canada, State of the Environment Directorate, Ecozone Analysis Branch, Ottawa/Hull. https://sis.agr.gc.ca/cansis/nsdb/ecostrat/1999report/index.html

Marín-Spiotta, E., Gruley, K. E., Crawford, J., Atkinson, E. E., Miesel, J. R., Greene, S., Cardona-Correa, C., & Spencer, R. G. M. (2014). Paradigm shifts in soil organic matter research affect interpretations of aquatic carbon cycling: Transcending disciplinary and ecosystem boundaries. *Biogeochemistry*, *117*(2), 279–297. https://doi.org/10.1007/s10533-013-9949-7

Matilainen, A., Vepsalainen, M., & Sillanpaa, M. (2010). Natural organic matter removal by coagulation during drinking water treatment: A review. *Advances in Colloid and Interface Science*, *159*(2), 189–197. https://doi.org/10.1016/j.cis.2010.06.007

McDonough, L. K., Andersen, M. S., Behnke, M. I., Rutlidge, H., Oudone, P., Meredith, K., O'Carroll, D. M., Santos, I. R., Marjo, C. E., Spencer, R. G. M., McKenna, A. M., & Baker, A. (2022). A new conceptual framework for the transformation of groundwater dissolved organic matter. *Nature Communications*, *13*(1), 2153. https://doi.org/10.1038/s41467-022-29711-9

McGivern, B. B., Tfaily, M. M., Borton, M. A., Kosina, S. M., Daly, R. A., Nicora, C. D., et al. (2021). Decrypting bacterial polyphenol metabolism in an anoxic wetland soil. *Nature Communications*, *12*(1), 2466. https://doi.org/10.1038/s41467-021-22765-1

McSorley, H. J. (2020). Spatial and temporal variation in natural organic matter quantity and quality across a second growth forested drinking water supply area on Vancouver Island, BC (Master's thesis). Retrieved from UBC Theses and Dissertations (https://open.library.ubc.ca/cIRcle/collections/ubctheses). Vancouver, BC: University of British Columbia.

Merder, J., Freund, J. A., Feudel, U., Hansen, C. T., Hawkes, J. A., Jacob, B., et al. (2020). ICBM-OCEAN: Processing ultrahigh-resolution mass spectrometry data of complex molecular mixtures. *Analytical Chemistry*, *92*(10), 6832–6838. https://doi.org/10.1021/acs.analchem.9b05659

Minor, E. C., Pothen, J., Dalzell, B. J., Abdulla, H., & Mopper, K. (2006). Effects of salinity changes on the photodegradation and ultraviolet-visible absorbance of terrestrial dissolved organic matter. *Limnology and Oceanography*, *51*(5), 2181–2186. https://doi.org/10.4319/lo.2006.51.5.2181

Mistick, E., & Johnson, M. S. (2020). High-frequency analysis of dissolved organic carbon storm responses in headwater streams of contrasting forest harvest history. *Journal of Hydrology*, 590. https://doi.org/10.1016/j.jhydrol.2020.125371

Molot, L. A., & Dillon, P. J. (1997). Photolytic regulation of dissolved organic carbon in northern lakes. *Global Biogeochemical Cycles*, *11*(3), 357–365. https://doi.org/10.1029/97GB01198

Molot, L. A., Hudson, J. J., Dillon, P. J., & Miller, S. A. (2005). Effect of pH on photo-oxidation of dissolved organic carbon by hydroxyl radicals in a coloured, softwater stream. *Aquatic Sciences*, *67*(2), 189–195. https://doi.org/10.1007/s00027-005-0754-9

Moody, C. S., Worrall, F., Evans, C. D., & Jones, T. G. (2013). The rate of loss of dissolved organic carbon (DOC) through a catchment. *Journal of Hydrology*, *492*, 139–150. https://doi.org/10.1016/j.jhydrol.2013.03.016

Moore, T. R. (2003). Dissolved organic carbon in a northern boreal landscape. *Global Biogeochemical Cycles*, *17*(4). https://doi.org/10.1029/2003gb002050

Moore, R., & Wondzell, S. M. (2005). Physical hydrology and the effects of forest harvesting in the Pacific Northwest: A review. *Journal of the American Water Resources Association*, *41*(4), 763–784. https://doi.org/10.1111/j.1752-1688.2005.tb03770.x

Mulholland, P. J., & Kuenzler, E. J. (1979). Organic carbon export from upland and forested wetland watersheds1. *Limnology and Oceanography*, *24*(5), 960–966. https://doi.org/10.4319/lo.1979.24.5.0960

Müller, K., & Wickham, H. (2020). tibble: Simple data frames. R package version 3.0.1. https://CRAN.R-project.org/package=tibble

Murphy, K. R., Bro, R., & Stedmon, C. A. (2014). Chemometric Analysis of Organic Matter Fluorescence. In P. Coble, J. Lead, A. Baker, D. Reynolds, & R. G. M. Spencer (Eds.), *Aquatic Organic Matter Fluorescence*. Cambridge University Press. https://doi.org/10.1017/cbo9781139045452.016

Murphy, K. R., Stedmon, C. A., Graeber, D., & Bro, R. (2013). Fluorescence spectroscopy and multi-way techniques. PARAFAC. *Analytical Methods*, *5*(23), 6557–6566. https://doi.org/10.1039/c3ay41160e

Murphy, K. R., Stedmon, C. A., Wenig, P., & Bro, R. (2014). OpenFluor—An online spectral library of auto-fluorescence by organic compounds in the environment. *Analytical Methods*, *6*(3), 658–661. https://doi.org/10.1039/c3ay41935e

Natural Regions Committee (2006). Natural regions and subregions of Alberta. Compiled by D. J. Downing and W. W. Pettapiece. Government of Alberta. Pub. No. T/852. https://open.alberta.ca/publications/0778545725

Natural Resources Canada (2020). *The state of Canada's forests. Annual report 2020*. Natural Resources Canada, Canadian Forest Service, Ottawa. 88 p. https://cfs.nrcan.gc.ca/publications?id=40219

Natural Resources Canada (2021). Canadian Wildland Fire Information System. National Fire Database fire polygon data [Shapefile]. https://cwfis.cfs.nrcan.gc.ca/datamart

Nova Scotia Natural Resources and Renewables (2021). Provincial Landscape Viewer [Online mapping tool]. https://novascotia.ca/natr/landscape/

Ohno, T. (2002). Fluorescence inner-filtering correction for determining the humification index of dissolved organic matter. *Environmental Science & Technology*, *36*(4), 742–746. https://doi.org/10.1021/es0155276

Oksanen, J., Simpson, G., Blanchet, F.G., Kindt, R., Legendre, P., Minchin, P., O'Hara, R., Solymos, P., Stevens, M., Szoecs, E., Wagner, H., Barbour, M., Bedward, M., Bolker, B., Borcard, D., Carvalho, G., Chirico, M., De Caceres, M., Durand, S., Evangelista, H., FitzJohn, R., Friendly, M., Furneaux, B., Hannigan, G., Hill, M., Lahti, L., McGlinn, D., Ouellette, M., Ribeiro Cunha, E., Smith, T., Stier, A., Ter Braak, C., Weedon, J. (2022). vegan: Community ecology package. R package version 2.6-2, https://CRAN.R-project.org/package=vegan.

Olefeldt, D., Devito, K. J., & Turetsky, M. R. (2013a). Sources and fate of terrestrial dissolved organic carbon in lakes of a Boreal Plains region recently affected by wildfire. *Biogeosciences*, *10*(10), 6247–6265. https://doi.org/10.5194/bg-10-6247-2013

Olefeldt, D., Persson, A., & Turetsky, M. R. (2014). Influence of the permafrost boundary on dissolved organic matter characteristics in rivers within the Boreal and Taiga plains of western Canada. *Environmental Research Letters*, *9*(3). https://doi.org/10.1088/1748-9326/9/3/035005

Olefeldt, D., Roulet, N., Giesler, R., & Persson, A. (2013b). Total waterborne carbon export and DOC composition from ten nested subarctic peatland catchments—importance of peatland cover, groundwater influence, and inter-annual variability of precipitation patterns. *Hydrological Processes*, *27*(16), 2280-2294. https://doi.org/10.1002/hyp.9358

Olefeldt, D., Turetsky, M. R., & Blodau, C. (2013c). Altered composition and microbial versus UV-mediated degradation of dissolved organic matter in boreal soils following wildfire. *Ecosystems*, *16*(8), 1396–1412. https://doi.org/10.1007/s10021-013-9691-y

Oleinikova, O. v, Drozdova, O. Y., Lapitskiy, S. A., Demin, V. v, Bychkov, A. Y., & Pokrovsky, O. S. (2017). Dissolved organic matter degradation by sunlight coagulates organo-mineral colloids and produces low-molecular weight fraction of metals in boreal humic waters. *Geochimica et Cosmochimica Acta*, *211*, 97–114. https://doi.org/10.1016/j.gca.2017.05.023

Oliver, A. A., Tank, S. E., Giesbrecht, I., Korver, M. C., Floyd, W. C., Sanborn, P., Bulmer, C., & Lertzman, K. P. (2017). A global hotspot for dissolved organic carbon in hypermaritime

watersheds of coastal British Columbia. *Biogeosciences*, *14*(15), 3743–3762. https://doi.org/10.5194/bg-14-3743-2017

Orlova, J., Olefeldt, D., Yasinski, J. H., & Anderson, A. E. (2020). Effects of prescribed burn on nutrient and dissolved organic matter characteristics in peatland shallow groundwater. *Fire*, *3*(3). https://doi.org/10.3390/fire3030053

Osburn, C. L., Mikan, M. P., Etheridge, J. R., Burchell, M. R., & Birgand, F. (2015). Seasonal variation in the quality of dissolved and particulate organic matter exchanged between a salt marsh and its adjacent estuary. *Journal of Geophysical Research: Biogeosciences*, *120*(7), 1430–1449. https://doi.org/10.1002/2014JG002897

Osburn, C. L., Oviedo-Vargas, D., Barnett, E., Dierick, D., Oberbauer, S. F., & Genereux, D. P. (2018). Regional groundwater and storms are hydrologic controls on the quality and export of dissolved organic matter in two tropical rainforest streams, Costa Rica. *Journal of Geophysical Research: Biogeosciences*, *123*(3), 850–866. https://doi.org/10.1002/2017JG003960

Osburn, C. L., Retamal, L., & Vincent, W. F. (2009). Photoreactivity of chromophoric dissolved organic matter transported by the Mackenzie River to the Beaufort Sea. In *Marine Chemistry* (Vol. 115, Issue 1, pp. 10–20). https://doi.org/10.1016/j.marchem.2009.05.003

Osburn, C. L., Wigdahl, C. R., Fritz, S. C., & Saros, J. E. (2011). Dissolved organic matter composition and photoreactivity in prairie lakes of the U.S. Great Plains. *Limnology and Oceanography*, *56*(6), 2371–2390. https://doi.org/10.4319/lo.2011.56.6.2371

Oswald, C. J., & Branfireun, B. A. (2014). Antecedent moisture conditions control mercury and dissolved organic carbon concentration dynamics in a boreal headwater catchment. *Water Resources Research, 50*(8). https://doi.org/10.1002/2013WR014736

Palmer, S. M., Evans, C. D., Chapman, P. J., Burden, A., Jones, T. G., Allott, T. E. H., Evans, M. G., Moody, C. S., Worrall, F., & Holden, J. (2016). Sporadic hotspots for physico-chemical retention of aquatic organic carbon: from peatland headwater source to sea. *Aquatic Sciences*, *78*(3), 491–504. https://doi.org/10.1007/s00027-015-0448-x

Parsons, S. A., Jefferson, B., Goslan, E. H., Jarvis, P. R., & Fearing, D. A. (2004). Natural organic matter - the relationship between character and treatability. *4th World Water Congress: Innovation in Drinking Water Treatment*, *4*(5–6), 43–48. https://doi.org/10.2166/ws.2004.0091

Peterson, R. A. (2021). Finding optimal normalizing transformations via bestNormalize. *The R Journal*, *13*(1). https://doi.org/10.32614/rj-2021-041

Peterson, B. G., & Carl, P. (2020). PerformanceAnalytics: Econometric tools for performance and risk analysis. R package version 2.0.4. https://CRAN.R-project.org/package=PerformanceAnalytics

Petrone, R., Devito, K. J., & Mendoza, C. (2016). Utikuma Region Study Area (URSA) - Part 2: Aspen harvest and recovery study. *Forestry Chronicle*, *92*(1), 62–65. https://doi.org/10.5558/tfc2016-018

Pickard, A. E., Heal, K. v, McLeod, A. R., & Dinsmore, K. J. (2017). Temporal changes in photoreactivity of dissolved organic carbon and implications for aquatic carbon fluxes

from peatlands. *Biogeosciences*, *14*(7), 1793–1809. https://doi.org/10.5194/bg-14-1793-2017

Pietikäinen, J., Pettersson, M., & Bååth, E. (2005). Comparison of temperature effects on soil respiration and bacterial and fungal growth rates. *FEMS Microbiology Ecology*, *52*(1), 49–58. https://doi.org/10.1016/j.femsec.2004.10.002

Pinno, B. D., Hossain, K. L., Gooding, T., & Lieffers, V. J. (2021). Opportunities and challenges for intensive silviculture in Alberta, Canada. *Forests*, *12*(6). https://doi.org/10.3390/f12060791

Pinsonneault, A. J., Moore, T. R., & Roulet, N. T. (2016). Temperature the dominant control on the enzyme-latch across a range of temperate peatland types. *Soil Biology and Biochemistry*, *97*. https://doi.org/10.1016/j.soilbio.2016.03.006

Poitras, V., Sushama, L., Seglenieks, F., Khaliq, M. N., & Soulis, E. (2011). Projected changes to streamflow characteristics over western Canada as simulated by the Canadian RCM. *Journal of Hydrometeorology*, *12*(6). https://doi.org/10.1175/JHM-D-10-05002.1

Porcal, P., Dillon, P. J., & Molot, L. A. (2015). Temperature dependence of photodegradation of dissolved organic matter to dissolved inorganic carbon and particulate organic carbon. *Plos One*, *10*(6), e0128884. https://doi.org/10.1371/journal.pone.0128884

Porcal, P., & Kopáček, J. (2018). Photochemical degradation of dissolved organic matter reduces the availability of phosphorus for aquatic primary producers. *Chemosphere*, *193*, 1018–1026. https://doi.org/10.1016/j.chemosphere.2017.11.140

Poulin, B. A., Ryan, J. N., & Aiken, G. R. (2014). Effects of iron on optical properties of dissolved organic matter. *Environmental Science & Technology*, *48*(17), 10098–10106. https://doi.org/10.1021/es502670r

Prairie, Y. T. (2008). Carbocentric limnology: looking back, looking forward. *Canadian Journal of Fisheries and Aquatic Sciences*, *65*(3), 543–548. https://doi.org/10.1139/f08-011

Price, D. T., Alfaro, R. I., Brown, K. J., Flannigan, M. D., Fleming, R. A., Hogg, E. H., Girardin, M. P., Lakusta, T., Johnston, M., McKenney, D. W., Pedlar, J. H., Stratton, T., Sturrock, R. N., Thompson, I. D., Trofymow, J. A., & Venier, L. A. (2013). Anticipating the consequences of climate change for Canada's boreal forest ecosystems. *Environmental Reviews*, *21*(4), 322–365. https://doi.org/10.1139/er-2013-0042

Pugh, E. A., Olefeldt, D., Leader, S. N., Hokanson, K. J., & Devito, K. J. (2021). Characteristics of dissolved organic carbon in boreal lakes: High spatial and inter-annual variability controlled by landscape attributes and wet-dry periods. *Water Resources Research*, *57*(11). https://doi.org/10.1029/2021WR030021

Quinton, W. L., Hayashi, M., & Pietroniro, A. (2003). Connectivity and storage functions of channel fens and flat bogs in northern basins. *Hydrological Processes*, *17*(18), 3665–3684. https://doi.org/10.1002/hyp.1369

Quinton, W., Berg, A., Braverman, M., Carpino, O., Chasmer, L., Connon, R., Craig, J., Devoie, E., Hayashi, M., Haynes, K., Olefeldt, D., Pietroniro, A., Rezanezhad, F., Schincariol, R., & Sonnentag, O. (2019). A synthesis of three decades of hydrological research at Scotty

Creek, NWT, Canada. *Hydrology and Earth System Sciences*, *23*(4). https://doi.org/10.5194/hess-23-2015-2019

R Core Team (2022). R: A language and environment for statistical computing. R Foundation for Statistical Computing, Vienna, Austria. https://www.R-project.org/.

RStudio Team (2020). RStudio: Integrated Development for R [Software]. RStudio, Inc., Boston, MA. http://www.rstudio.com/

Raudina, T. v., Smirnov, S. v., Lushchaeva, I. v., Istigechev, G. I., Kulizhskiy, S. P., Golovatskaya, E. A., Shirokova, L. S., & Pokrovsky, O. S. (2022). Seasonal and Spatial Variations of Dissolved Organic Matter Biodegradation along the Aquatic Continuum in the Southern Taiga Bog Complex, Western Siberia. *Water*, *14*(23). https://doi.org/10.3390/w14233969

Raymond, P. A., Hartmann, J., Lauerwald, R., Sobek, S., McDonald, C., Hoover, M., Butman, D., Striegl, R., Mayorga, E., Humborg, C., Kortelainen, P., Dürr, H., Meybeck, M., Ciais, P., & Guth, P. (2013). Global carbon dioxide emissions from inland waters. *Nature*, *503*(7476). https://doi.org/10.1038/nature12760

Raymond, P. A., & Saiers, J. E. (2010). Event controlled DOC export from forested watersheds. *Biogeochemistry*, *100*(1). https://doi.org/10.1007/s10533-010-9416-7

Redden, D., Trueman, B. F., Dunnington, D. W., Anderson, L. E., & Gagnon, G. A. (2021). Chemical recovery and browning of Nova Scotia surface waters in response to declining acid deposition. *Environmental Science: Processes and Impacts*, *23*(3), 446–456. https://doi.org/10.1039/d0em00425a

Reitsema, R. E., Meire, P., & Schoelynck, J. (2018). The future of freshwater macrophytes in a changing world: Dissolved organic carbon quantity and quality and its interactions with macrophytes. *Frontiers in Plant Science*, *9*, 629. https://doi.org/10.3389/fpls.2018.00629

Rhoades, C. C., Nunes, J. P., Silins, U., & Doerr, S. H. (2019). The influence of wildfire on water quality and watershed processes: New insights and remaining challenges. *International Journal of Wildland Fire*, 28(10), 721–725. https://doi.org/10.1071/WFv28n10_FO

Riddell, A., & Bryden, G. (1996). Water allocation plan – Courtenay River. https://www2.gov.bc.ca/gov/content/environment/air-land-water/water/water-planning-strategies/water-allocation-plans

Rivera Vasconcelos, F., Diehl, S., Rodríguez, P., Karlsson, J., & Byström, P. (2018). Effects of Terrestrial Organic Matter on Aquatic Primary Production as Mediated by Pelagic–Benthic Resource Fluxes. *Ecosystems*, *21*(6), 1255–1268. https://doi.org/10.1007/s10021-017-0217-x

Römkens, P. F. A. M., & Dolfing, J. (1998). Effect of Ca on the solubility and molecular size distribution of DOC and Cu binding in soil solution samples. *Environmental Science and Technology, 32*(3). https://doi.org/10.1021/es970437f

Sachse, A., Henrion, R., Gelbrecht, J., & Steinberg, C. E. W. (2005). Classification of dissolved organic carbon (DOC) in river systems: Influence of catchment characteristics and autochthonous processes. *Organic Geochemistry*, *36*(6), 923–935. https://doi.org/10.1016/j.orggeochem.2004.12.008

Sanders, R. W., Cooke, S. L., Fischer, J. M., Fey, S. B., Heinze, A. W., Jeffrey, W. H., Macaluso, A. L., Moeller, R. E., Morris, D. P., Neale, P. J., Olson, M. H., Pakulski, J. D., Porter, J. A., Schoener, D. M., & Williamson, C. E. (2015). Shifts in microbial food web structure and productivity after additions of naturally occurring dissolved organic matter: Results from large-scale lacustrine mesocosms. *Limnology and Oceanography*, *60*(6), 2130–2144. https://doi.org/10.1002/lno.10159

Schindler, D. W., & Donahue, W. F. (2006). An impending water crisis in Canada's western prairie provinces. *Proceedings of the National Academy of Sciences of the United States of America*, *103*(19). https://doi.org/10.1073/pnas.0601568103

Schneider, R. R., Devito, K., Kettridge, N., & Bayne, E. (2016). Moving beyond bioclimatic envelope models: integrating upland forest and peatland processes to predict ecosystem transitions under climate change in the western Canadian boreal plain. *Ecohydrology*, *9*(6), 899–908. https://doi.org/10.1002/eco.1707

Shakesby, R. A., & Doerr, S. H. (2006). Wildfire as a hydrological and geomorphological agent. *Earth-Science Reviews*, *74*(3–4), 269–307. https://doi.org/10.1016/j.earscirev.2005.10.006

Shutova, Y., Baker, A., Bridgeman, J., & Henderson, R. K. (2014). Spectroscopic characterisation of dissolved organic matter changes in drinking water treatment: From PARAFAC analysis to online monitoring wavelengths. *Water Research*, *54*. https://doi.org/10.1016/j.watres.2014.01.053

Silins, U., Anderson, A., Bladon, K. D., Emelko, M. B., Stone, M., Spencer, S. A., Williams, C. H., Wagner, M. J., Martens, A. M., & Hawthorn, K. (2016). Southern Rockies Watershed Project. *The Forestry Chronicle*, *92*(01), 39–42. https://doi.org/10.5558/tfc2016-012

Sillanpää, M. (2015). Chapter 1 – General introduction. In M. Sillanpää (Ed.), *Natural Organic Matter in Water*, 1–15. Butterworth-Heinemann. https://doi.org/10.1016/B978-0-12-801503-2.00001-X

Smerdon, B. D., Devito, K. J., & Mendoza, C. A. (2005). Interaction of groundwater and shallow lakes on outwash sediments in the sub-humid Boreal Plains of Canada. *Journal of Hydrology*, *314*(1–4). https://doi.org/10.1016/j.jhydrol.2005.04.001

Soares, A. R. A., Lapierre, J.-F., Selvam, B. P., Lindström, G., & Berggren, M. (2019). Controls on Dissolved Organic Carbon Bioreactivity in River Systems. *Scientific Reports*, *9*(1), 14897. https://doi.org/10.1038/s41598-019-50552-y

Spencer, S. A., Silins, U., & Anderson, A. E. (2019). Precipitation-runoff and storage dynamics in watersheds underlain by till and permeable bedrock in Alberta's Rocky Mountains. *Water Resources Research*, *55*(12), 10,690–10,706. https://doi.org/10.1029/2019WR025313

Squires, A. J., Westbrook, C. J., & Dubé, M. G. (2010). An approach for assessing cumulative effects in a model river, the Athabasca River basin. *Integrated Environmental Assessment and Management, 6*(1), 119–134. https://doi.org/10.1897/IEAM_2008-081.1

St. Amour, N. A., Gibson, J. J., Edwards, T. W. D., Prowse, T. D., & Pietroniro, A. (2005). Isotopic time-series partitioning of streamflow components in wetland-dominated catchments, lower Liard River basin, Northwest Territories, Canada. *Hydrological Processes*, *19*(17), 3357–3381. https://doi.org/10.1002/hyp.5975

Stenson, A. C., Landing, W. M., Marshall, A. G., & Cooper, W. T. (2002). Ionization and fragmentation of humic substances in electrospray ionization Fourier transform-ion cyclotron resonance mass spectrometry. *Analytical Chemistry*, *74*(17), 4397−4409. https://doi.org/10.1021/ac020019f

Stralberg, D., Arseneault, D., Baltzer, J. L., Barber, Q. E., Bayne, E. M., Boulanger, Y., Brown, C. D., Cooke, H. A., Devito, K., Edwards, J., Estevo, C. A., Flynn, N., Frelich, L. E., Hogg, E. H., Johnston, M., Logan, T., Matsuoka, S. M., Moore, P., Morelli, T. L., Morissette, J. L., Nelson, E. A., Nenzén, H., Nielsen, S. E., Parisien, M.-A., Pedlar, J. H., Price, D. T., Schmiegelow, F. K. A., Slattery, S. M., Sonnentag, O., Thompson, D. K., Whitman, E. (2020). Climate-change refugia in boreal North America: what, where, and for how long? *Frontiers in Ecology and the Environment, 18*(5). https://doi.org/10.1002/fee.2188

Strohmeier, S., Knorr, K. H., Reichert, M., Frei, S., Fleckenstein, J. H., Peiffer, S., & Matzner, E. (2013). Concentrations and fluxes of dissolved organic carbon in runoff from a forested catchment: Insights from high frequency measurements. *Biogeosciences*, *10*(2). https://doi.org/10.5194/bg-10-905-2013

Stubbins, A., Lapierre, J. F., Berggren, M., Prairie, Y. T., Dittmar, T., & del Giorgio, P. A. (2014). What's in an EEM? Molecular signatures associated with dissolved organic fluorescence in boreal Canada. *Environmental Science and Technology*, *48*(18), 10598−10606. https://doi.org/10.1021/es502086e

Stubbins, A., Spencer, R. G. M., Chen, H., Hatcher, P. G., Mopper, K., Hernes, P. J., Mwamba, V. L., Mangangu, A. M., Wabakanghanzi, J. N., & Six, J. (2010). Illuminated darkness: Molecular signatures of Congo River dissolved organic matter and its photochemical alteration as revealed by ultrahigh precision mass spectrometry. *Limnology and Oceanography*, *55*(4), 1467–1477. https://doi.org/10.4319/lo.2010.55.4.1467

Sulzberger, B., & Durisch-Kaiser, E. (2009). Chemical characterization of dissolved organic matter (DOM): A prerequisite for understanding UV-induced changes of DOM absorption properties and bioavailability. *Aquatic Sciences*, *71*(2), 104–126. https://doi.org/10.1007/s00027-008-8082-5

Tank, J. L., Rosi-Marshall, E. J., Griffiths, N. A., Entrekin, S. A., & Stephen, M. L. (2010). A review of allochthonous organic matter dynamics and metabolism in streams. *Journal of the North American Benthological Society*, *29*(1), 118–146. https://doi.org/10.1899/08-170.1

Tank, S. E., Fellman, J. B., Hood, E., & Kritzberg, E. S. (2018). Beyond respiration: Controls on lateral carbon fluxes across the terrestrial-aquatic interface. *Limnology and Oceanography Letters*, *3*(3). https://doi.org/10.1002/lol2.10065

Thompson, C., Mendoza, C. A., Devito, K. J., & Petrone, R. M. (2015). Climatic controls on groundwater–surface water interactions within the Boreal Plains of Alberta: Field observations and numerical simulations. *Journal of Hydrology*, *527*, 734–746. https://doi.org/10.1016/j.jhydrol.2015.05.027

Thorp, J. H., & Delong, M. D. (2002). Dominance of autochthonous autotrophic carbon in food webs of heterotrophic rivers. In *Oikos* (Vol. 96, Issue 3). https://doi.org/10.1034/j.1600-0706.2002.960315.x

Tiwari, T., Sponseller, R. A., & Laudon, H. (2022). The emerging role of drought as a regulator of dissolved organic carbon in boreal landscapes. *Nature Communications*, *13*(1). https://doi.org/10.1038/s41467-022-32839-3

Tranvik, L. J., Downing, J. A., Cotner, J. B., Loiselle, S. A., Striegl, R. G., Ballatore, T. J., Dillon, P., Finlay, K., Fortino, K., Knoll, L. B., Kortelainen, P. L., Kutser, T., Larsen, S., Laurion, I., Leech, D. M., McCallister, S. L., McKnight, D. M., Melack, J. M., Overholt, E., Porter, J. A., Prairie, Y., Renwick, W. H., Roland, F., Sherman, B. S., Schindler, D. W., Sobek, S., Tremblay, A., Vanni, M. J., Verschoor, A. M., von Wachenfeldt, E., and Weyhenmeyer, G. A. (2009). Lakes and reservoirs as regulators of carbon cycling and climate. *Limnology and Oceanography*, *54*(6), 2298–2314. https://doi.org/10.4319/lo.2009.54.6_part_2.2298

Thevenot, M., Dignac, M. F., & Rumpel, C. (2010). Fate of lignins in soils: A review. *Soil Biology & Biochemistry*, *42*(8), 1200–1211. https://doi.org/10.1016/j.soilbio.2010.03.017

Thieme, L., Graeber, D., Hofmann, D., Bischoff, S., Schwarz, M. T., Steffen, B., Meyer, U. N., Kaupenjohann, M., Wilcke, W., Michalzik, B., & Siemens, J. (2019). Dissolved organic matter characteristics of deciduous and coniferous forests with variable management: Different at the source, aligned in the soil. *Biogeosciences*, *16*(7), 1411–1432. https://doi.org/10.5194/bg-16-1411-2019

Vachon, D., Solomon, C. T., & del Giorgio, P. A. (2017). Reconstructing the seasonal dynamics and relative contribution of the major processes sustaining CO2 emissions in northern lakes. *Limnology and Oceanography*, *62*(2), 706–722. https://doi.org/10.1002/lno.10454

Vähätalo, A. V., & Wetzel, R. G. (2004). Photochemical and microbial decomposition of chromophoric dissolved organic matter during long (months–years) exposures. *Marine Chemistry*, *89*(1–4), 313–326. https://doi.org/10.1016/j.marchem.2004.03.010

Van Leeuwen, H. P., & Buffle, J. (2009). Chemodynamics of aquatic metal complexes: From small ligands to colloids. *Environmental Science & Technology*, *43*(19), 7175–7183. https://doi.org/10.1021/es900894h

Verbeke, B. A., Lamit, L. J., Lilleskov, E. A., Hodgkins, S. B., Basiliko, N., Kane, E. S., et al. (2022). Latitude, Elevation, and Mean Annual Temperature Predict Peat Organic Matter Chemistry at a Global Scale. *Global Biogeochemical Cycles*, *36*(2), e2021GB007057. https://doi.org/10.1029/2021GB007057

Volk, C. J., Volk, C. B., & Kaplan, L. A. (1997). Chemical composition of biodegradable dissolved organic matter in streamwater. *Limnology and Oceanography*, *42*(1), 39–44. https://doi.org/10.4319/lo.1997.42.1.0039

Von Wachenfeldt, E., & Tranvik, L. J. (2008). Sedimentation in boreal lakes – The role of flocculation of allochthonous dissolved organic matter in the water column. *Ecosystems*, *11*(5), 803–814. https://doi.org/10.1007/s10021-008-9162-z

Vonk, J. E., Tank, S. E., Mann, P. J., Spencer, R. G. M., Treat, C. C., Striegl, R. G., Abbott, B. W., & Wickland, K. P. (2015a). Biodegradability of dissolved organic carbon in permafrost soils and aquatic systems: a meta-analysis. *Biogeosciences*, *12*(23), 6915–6930. https://doi.org/10.5194/bg-12-6915-2015

Vonk, J. E., Tank, S. E., Mann, P. J., Spencer, R. G. M., Treat, C. C., Striegl, R. G., Abbott, B. W., & Wickland, K. P. (2015b). Supplement of Biodegradability of dissolved organic carbon in permafrost soils and waterways: a meta-analysis. *Biogeosciences*, *12*(11).

Waite, T. D., & Morel, F. M. M. (1984). Photoreductive dissolution of colloidal iron oxides in natural waters. *Environmental Science & Technology*, *18*(11), 860–868. https://doi.org/10.1021/es00129a010

Wallin, M. B., Grabs, T., Buffam, I., Laudon, H., Ågren, A., Öquist, M. G., & Bishop, K. (2013). Evasion of CO_2 from streams – The dominant component of the carbon export through the aquatic conduit in a boreal landscape. *Global Change Biology*, *19*(3). https://doi.org/10.1111/gcb.12083

Wallin, M. B., Weyhenmeyer, G. A., Bastviken, D., Chmiel, H. E., Peter, S., Sobek, S., & Klemedtsson, L. (2015). Temporal control on concentration, character, and export of dissolved organic carbon in two hemiboreal headwater streams draining contrasting catchments. *Journal of Geophysical Research-Biogeosciences*, *120*(5), 832–846. https://doi.org/10.1002/2014JG002814

Ward, N. D., Bianchi, T. S., Medeiros, P. M., Seidel, M., Richey, J. E., Keil, R. G., & Sawakuchi, H. O. (2017). Where carbon goes when water flows: Carbon cycling across the aquatic continuum. *Frontiers in Marine Science, 4*. https://doi.org/10.3389/fmars.2017.00007

Ward, C. P., Nalven, S. G., Crump, B. C., Kling, G. W., & Cory, R. M. (2017). Photochemical alteration of organic carbon draining permafrost soils shifts microbial metabolic pathways and stimulates respiration. *Nature Communications*, *8*(1), 772. https://doi.org/10.1038/s41467-017-00759-2

Wauthy, M., Rautio, M., Christoffersen, K. S., Forsström, L., Laurion, I., Mariash, H. L., Peura, S., & Vincent, W. F. (2018). Increasing dominance of terrigenous organic matter in circumpolar freshwaters due to permafrost thaw. *Limnology and Oceanography Letters*, *3*(3), 186–198. https://doi.org/10.1002/lol2.10063

Webster, K. L., Leach, J. A., Hazlett, P. W., Fleming, R. L., Emilson, E. J. S., Houle, D., Chan, K., Norouzian, F., Cole, A., O'Brien, J., Smokorowski, K., Nelson, S., & Yanni, S. (2021a). Turkey Lakes Watershed, Ontario, Canada: 40 years of interdisciplinary whole-ecosystem research. *Hydrological Processes*, *35*(4), e14109. https://doi.org/10.1002/hyp.14109

Webster, K. L., Leach, J. A., Houle, D., Hazlett, P. W., & Emilson, E. J. S. (2021b). Acidification recovery in a changing climate: Observations from thirty-five years of stream chemistry monitoring in forested headwater catchments at the Turkey Lakes watershed, Ontario. *Hydrological Processes*, *35*(9), e14346. https://doi.org/10.1002/hyp.14346

Webster, K. L., Leach, J. A., Hazlett, P. W., Buttle, J. M., Emilson, E. J. S., & Creed, I. F. (2022). Long-term stream chemistry response to harvesting in a northern hardwood forest watershed experiencing environmental change. *Forest Ecology and Management*, *519*, 120345. https://doi.org/10.1016/j.foreco.2022.120345

Wei, T., & Simko, V. (2017). R package "corrplot": Visualization of a correlation matrix. R package version 0.92. https://github.com/taiyun/corrplot

Weishaar, J. L., Aiken, G. R., Bergamaschi, B. A., Fram, M. S., Fujii, R., & Mopper, K. (2003). Evaluation of specific ultraviolet absorbance as an indicator of the chemical composition

and reactivity of dissolved organic carbon. *Environmental Science & Technology*, *37*(20), 4702–4708. https://doi.org/10.1021/es030360x

Wetzel, R. G. (1995). Death, detritus, and energy-flow in aquatic ecosystems. *Freshwater Biology*, *33*(1), 83–89. https://doi.org/10.1111/j.1365-2427.1995.tb00388.x

Wickham, H. (2011). The split-apply-combine strategy for data analysis. *Journal of Statistical Software*, *40*(1), 1–29. https://doi.org/10.18637/jss.v040.i01

Wickham, H. (2016). ggplot2: Elegant graphics for data analysis. Springer-Verlag New York, NY. https://doi.org/10.1007/978-3-319-24277-4

Wickham, H., François, R., Henry, L., & Müller, K. (2020). dplyr: A grammar of data manipulation. R package version 0.8.5. https://CRAN.R-project.org/package=dplyr

Wickham, H., & Girlich, M. (2022). tidyr: Tidy messy data. R package version 1.2.1, https://CRAN.R-project.org/package=tidyr

Williams, C. H. S., Silins, U., Spencer, S. A., Wagner, M. J., Stone, M., & Emelko, M. B. (2019). Net precipitation in burned and unburned subalpine forest stands after wildfire in the northern Rocky Mountains. *International Journal of Wildland Fire, 28*(10). https://doi.org/10.1071/WF18181

Williamson, C. E., Stemberger, R. S., Morris, D. P., Frost, T. M., & Paulsen, S. G. (1996). Ultraviolet radiation in North American lakes: Attenuation estimates from DOC measurements and implications for plankton communities. *Limnology and Oceanography*, *41*(5), 1024–1034. https://doi.org/10.4319/lo.1996.41.5.1024

Wilske, C., Herzsprung, P., Lechtenfeld, O. J., Kamjunke, N., Einax, J. W., & Tümpling, W. von. (2021). New insights into the seasonal variation of DOM quality of a humic-rich drinking-water reservoir—coupling 2d-fluorescence and FTICR MS measurements. *Water (Switzerland)*, *13*(12). https://doi.org/10.3390/w13121703

Winterdahl, M., Erlandsson, M., Futter, M. N., Weyhenmeyer, G. A., & Bishop, K. (2014). Intra-annual variability of organic carbon concentrations in running waters: Drivers along a climatic gradient. *Global Biogeochemical Cycles*, *28*(4), 451–464. https://doi.org/10.1002/2013GB004770

Worrall, F., Davies, H., Bhogal, A., Lilly, A., Evans, M., Turner, K., Burt, T., Barraclough, D., Smith, P., Merrington, G. (2012). The flux of DOC from the UK – Predicting the role of soils, land use and net watershed losses. Journal of Hydrology, 448–449, 149-160. https://doi.org/10.1016/j.jhydrol.2012.04.053.

Wünsch, U. J., Murphy, K. R., & Stedmon, C. A. (2017). The one-sample PARAFAC approach reveals molecular size distributions of fluorescent components in dissolved organic matter. *Environmental Science and Technology*, *51*(20). https://doi.org/10.1021/acs.est.7b03260

Yamashita, Y., Kloeppel, B. D., Knoepp, J., Zausen, G. L., & Jaffé, R. (2011). Effects of watershed history on dissolved organic matter characteristics in headwater streams. *Ecosystems*, *14*(7), 1110–1122. https://doi.org/10.1007/s10021-011-9469-z

Zsolnay, A. (2003). Dissolved organic matter: artefacts, definitions, and functions. *Geoderma*, *113*(3–4), 187–209. https://doi.org/10.1016/S0016-7061(02)00361-0

Appendices

Appendix A. Supporting information for Chapter 2

Supporting information in this appendix includes characterization of research sites and streams (Tables A1, A2 and A5), and time of sampling (Figure A1). We also provide detailed results for the PCA analyses (Tables A6-A10, Figures A6-A8 and A10-A11), including plots for all significant principal components not included in the main manuscript, where applicable. Additionally, we include a list of DOM composition indices used in the analysis (Table A4), boxplots for several DOM indices (Figure A5), method detection limits (Table A3), and PARAFAC results (Figures A3-A4).

Table A1. Stream sampling locations and catchment characteristics.

Research site	Stream ID	Stream name & description	Latitude (°N)	Longitude (°W)	Strahler order	Catchment area (km^2)	Slope (°)	% wetland area	% open water	% disturbed area	Disturbance type & year
Pacific Maritime 1	1015	unnamed stream	51.691	-128.067	3	3.3	18.9	23.8	9.1	0	
	819	unnamed stream	51.657	-128.042	3	4.8	16.8	50.2	0.3	0	
	703	unnamed stream	51.648	-128.026	4	12.8	21.9	24.3	1.9	0	
Pacific Maritime 2	BOC	Boston Creek, Comox Lake tributary	49.636	-125.136	3	9.20	26.3	0	0.09	10.8	clearcut (1990-2018)
	MOC	Cruickshank River upstream of Eric Creek	49.650	-125.296	4	29.8	24.2	0.3	4.50	5.2	clearcut (2000-2018)
	PV2	Perseverance Creek	49.605	-125.043	3	6.93	11.4	0	2.30	54.2	clearcut (1990-2018)
	TO2	Toma Creek tributary	49.537	-125.154	2	3.61	24.7	0	0	32.7	clearcut (2000-2018)
	DCP	Deception Reservoir	48.514	-123.710	2	7.34	12.7	9.3	8.11	33.5	clearcut (1991-2010)
	JDG	Judge Creek	48.586	-123.674	2	8.33	9.2	1.1	0	4.2	clearcut (1991-2010)
	RTH	Rithet Creek	48.591	-123.725	3	11.1	12.3	0.5	0	1.9	clearcut (1991-2010)
	TUN	Leech River d/s of West Leech River	48.507	-123.768	5	94.6	11.8	1.1	0.78	9.1	clearcut (1991-2010)
Montane Cordillera	SWE	Star Creek (west subwatershed)	49.605	-114.568	2	4.63	30.4	0	0	13.9	clearcut with retention (2015)
	SEA	Star Creek (east subwatershed)	49.605	-114.568	2	3.89	27.8	0	0	11.4	strip-shelterwood (2015)
	MCL	McLaren Creek (Star Creek tributary)	49.607	-114.563	2	0.95	14.2	0	0	54.5	partial-cut (2015)
	NYU	North York Creek	49.582	-114.546	3	6.14	31.1	0	0	0	
Boreal Plains	S2	Mink Lake #1 tributary, Mink River basin	56.121	-115.683	1	3.53	1.02	19.4	0	95.2	wildfire (2011)
	S4	Twin Lake outlet, Mink River basin	56.100	-115.593	2	91.4	1.30	45.0	8.95	64.6	wildfire (2011)
	S8	Artisinn Lake tributary, Utikuma River basin	56.111	-115.346	3	54.2	1.17	59.2	1.81	91.9	wildfire (2011)
	S15	Utikuma Lake tributary	55.934	-115.170	1	17.2	0.37	54.2	0.12	55.0	wildfire (2011)
	S16	Utikuma Lake tributary	55.914	-115.163	1	16.3	0.42	65.0	1.34	0.6	wildfire (2015)
	REC	Redearth Creek	56.547	-115.240	4	585.1	0.80	64.7	0.80	0.4	wildfire (2011)
	SMC	Smith Creek	63.174	-123.337	3	146	10.6	12.3	0.75	0	

Research site	Stream ID	Stream name & description	Latitude (°N)	Longitude (°W)	Strahler order	Catchment area (km^2)	Slope (°)	% wetland area	% open water	% disturbed area	Disturbance type & year
Taiga Plains	WS1	unnamed tributary to the Mackenzie River	63.090	-123.233	3	75.5	11.0	10.9	1.93	12.3	wildfire (2013)
	WS2	unnamed tributary to the Mackenzie River	63.112	-123.249	1	1.99	1.50	51.4	0.41	0	
	WS4	unnamed tributary to the Mackenzie River	63.143	-123.259	1	3.50	2.08	33.1	9.03	5	
	WS6	unnamed tributary to WS4	63.150	-123.270	1	0.14	0.53	80.5	0	0	
	WS11	unnamed tributary to Smith Creek	63.164	-123.253	2	6.54	1.01	56.7	1.86	0	
	SCC	Scotty Creek	61.416	-121.455	2	130	0.18	75.9	2.57	2.4	wildfire (2014)
	JMR	Jean Marie River	61.445	-121.238	4	1,260	0.19	65.7	1.40	6.4	wildfire (2011, 2013, 2014, 2016)
	SS4	Notawohka Creek	61.161	-119.936	3	330	0.66	69.9	5.78	94.3	wildfire (2013)
	SS5	unnamed tributary to Jean Marie River	61.224	-120.381	2	74.9	0.35	82.7	4.15	25	wildfire (2013)
	SS6	unnamed tributary to Jean Marie River	61.292	-120.624	1	60.3	1.35	51.1	0.06	0	
	SS7	unnamed tributary to Trout River	61.155	-119.896	1	1.00	0.81	71.0	0	60	wildfire (2013)
	LS1	unnamed tributary to Meander River, Hay River basin	59.030	-117.697	2	36.9	0.57	79.4	0.16	0	
	LS2	Mission Creek, Hay River basin	59.090	-117.694	3	173	0.41	84.9	0.02	0	
	LS3	Lutose Creek	59.406	-117.281	3	293	0.48	82.1	0.10	11.7	wildfire (2007, 2012, 2015)
	LS4	unnamed tributary to Steen River, Hay River basin	59.590	-117.203	3	8.92	0.38	85.8	0.03	88.5	wildfire (2003)
	LS5	unnamed tributary, Steen River basin, Hay River basin	59.593	-117.270	1	13.3	0.49	82.0	0	78.5	
	LS6	unnamed, Hay River basin	59.458	-117.215	2	17.0	0.56	78.7	0.02	65	wildfire (2000, 2007)
	LS8	unnamed tributary to Jackpot Creek, Hay River basin	59.859	-117.038	5	501	2.45	34.2	5.11	9.5	wildfire (2000, 2015)
Boreal Shield	C31	unnamed tributary to Norberg Creek	47.063	-84.429	1	0.046	14.6	2.9	0	100	clearcut (1997)
	C32	unnamed tributary to Norberg Creek	47.061	-84.426	1	0.067	17.5	1.0	0	0	
	C38	unnamed tributary to Norberg Creek	47.048	-84.408	1	0.085	13.5	20.5	0	0	

Research site	Stream ID	Stream name & description	Latitude (°N)	Longitude (°W)	Strahler order	Catchment area (km^2)	Slope (°)	% wetland area	% open water	% disturbed area	Disturbance type & year
	C46	unnamed tributary to Norberg Creek	47.063	-84.401	1	0.442	17.2	1.4	0	0	
	S3	Norberg Creek at the outlet of Little Turkey Lake	47.045	-84.410	2	5.08	10	12.5	10.5	0	
	S5	Norberg Creek below Turkey Lake, above Batchawana River	47.063	-84.431	3	10.5	15.3	10.9	10.1	7.2	clearcut, selection, shelterwood (1997)
Atlantic Maritime	S11	unnamed tributary to Pockwock Lake	44.833	-63.827	1	1.24	6.79	7.1	0	1.0	2019
	S21	Peggy Brook	44.816	-63.843	2	3.06	8.05	5.2	0.95	0	
	S31	Moose Cove tributary / Crane Nest Brook	44.807	-63.861	2	1.21	8.59	1.4	0.08	0	
	S41	unnamed tributary upstream of Long Ponds	44.810	-63.888	1	0.26	8.30	0	0	45.3	2020
	S42	unnamed tributary downstream of Long Ponds	44.801	-63.869	2	4.01	6.22	3.2	0.37	6.4	2020
	S51	Long Gullies Creek	44.831	-63.834	2	2.60	7.87	7.7	0	0.85	variable retention (2020)

Notes:

Catchment characteristics come from published data and regional maps, where available. In some cases, catchment characteristics were determined in ESRI ArcMAP. Although the methods for determining the characteristics for different research sites may be inconsistent, the data provide sufficient characterization and highlight the differences between the research sites and streams. The following data sources were used:

- Pacific Maritime 1: Oliver et al. (2017)
- Pacific Maritime 2: Government of British Columbia (2022);
- Montane Cordillera: Spencer et al. (2019), Alberta Environment and Parks (2022)
- Boreal Plains: Ducks Unlimited Canada (2011), Alberta Environment and Parks (2022), Government of Alberta (2022)
- Taiga Plains: Quinton et al. (2003); Natural Resources Canada (2022), Alberta Environment and Parks (2022);
- Boreal Shield: Creed et al. (2015), Jeffries et al. (1988), Buttle et al. (2018, 2019)
- Atlantic Maritime: Nova Scotia Natural Resources and Renewables (2021)

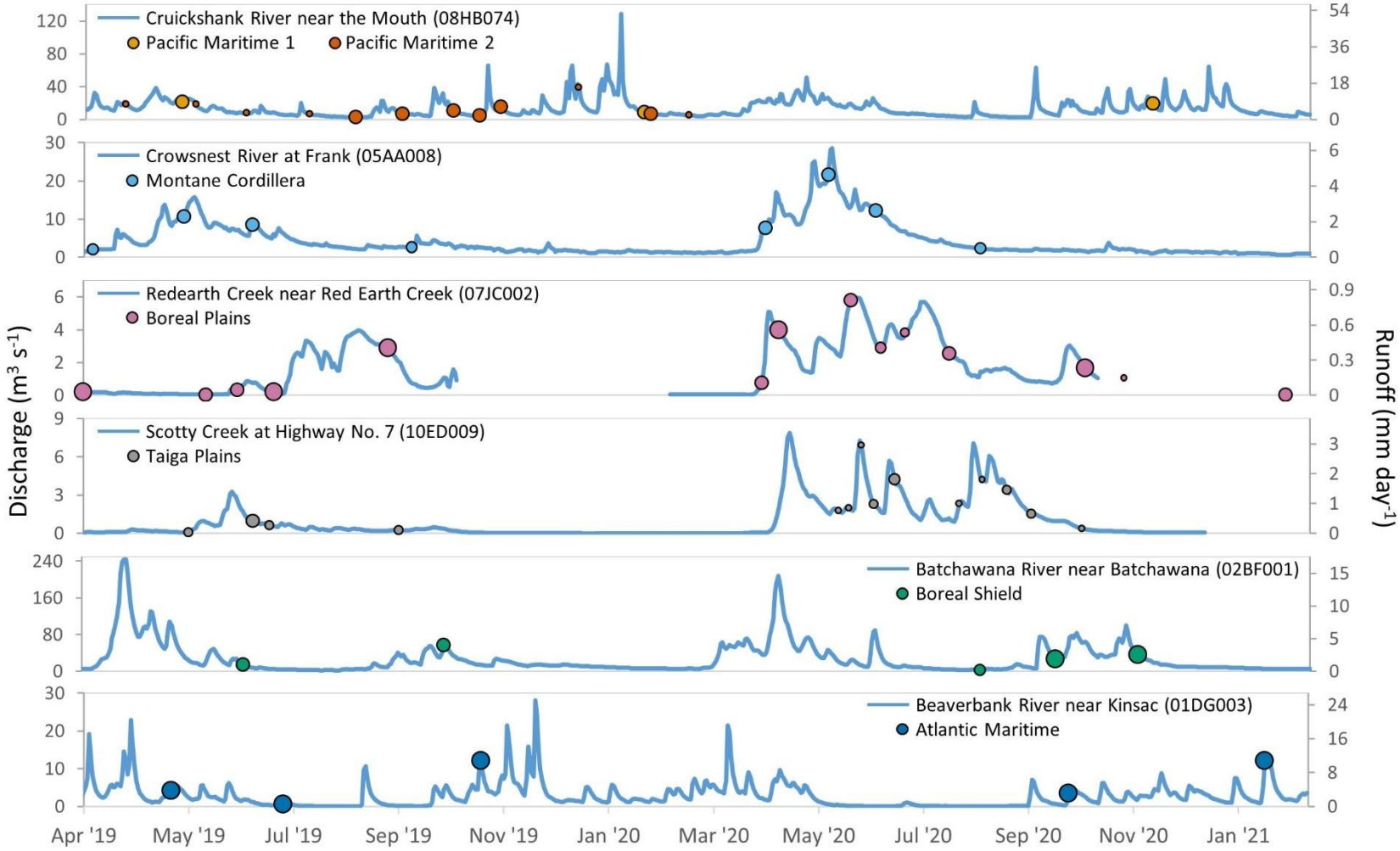

Figure A1. Stream sampling in 2019-2021 under high- and low-flow conditions at each research site. The size of circle is proportional to the number of streams sampled (1 to 6). The hydrographs are for the nearby Water Survey of Canada hydrometric station, and thus provide an approximation of flow conditions at the research site.

Table A2. Climatic, soil and forest characteristics of stream catchments based on ecodistrict data (Ecological Stratification Working Group, 1996).

Research site	Stream ID	Ecodistrict	MAT (°C)	MAP (mm)	CMI (mm)	Soil type[1] (%)					Forest type[2] (%)		
						Wetland	Podzol	Bruni-sol	Luvi-sol	Rock & regosol	Coni-ferous	Mixed	Broad-leaf
Pacific Maritime 1	1015	Hecate Lowland	8.0	2917	2459	64	36	0	0	0	99	1	0
	819	Hecate Lowland	8.0	2917	2459	64	36	0	0	0	99	1	0
	703	Hecate Lowland	8.0	2917	2459	64	36	0	0	0	99	1	0
Pacific Maritime 2	BOC	Leeward Island Mountains	9.0	2027	1400	2	87	2	0	9	79	19	0
	MOC	Leeward Island Mountains	9.0	2027	1400	2	87	2	0	9	79	19	0
	PV2	Leeward Island Mountains	9.0	2027	1400	2	87	2	0	9	79	19	0
	TO2	Leeward Island Mountains	9.0	2027	1400	2	87	2	0	9	79	19	0
	DCP	Leeward Island Mountains	9.0	2027	1400	2	87	2	0	9	79	19	0
	JDG	Nanaimo Lowland	9.5	1184	558	7	33	57	0	3	77	18	0
	RTH	Leeward Island Mountains	9.0	2027	1400	2	87	2	0	9	79	19	0
	TUN	Leeward Island Mountains, Windward Island Mountains	9.0	2220	1609	3	87	1.7	0	8.3	80.7	17.5	0
Montane Cordillera	SWE	Crowsnest Mountains	6.0	795	-7.5	0	26	23	30	16	18	43	20
	SEA	Crowsnest Mountains	6.0	795	-7.5	0	26	23	30	16	18	43	20
	MCL	Crowsnest Mountains	6.0	795	-7.5	0	26	23	30	16	18	43	20
	NYU	Crowsnest Mountains	6.0	795	-7.5	0	26	23	30	16	18	43	20
Boreal Plains	S2	Heart River Upland	1.2	469	-98	37	0	36	27	0	29	33	36
	S4	Heart River Upland	1.2	469	-98	37	0	36	27	0	29	33	36
	S8	Utikuma Plain, Heart River Upland	1.3	481	-86	48	0	23.5	28.5	0	37	33.5	28.5
	S15	Utikuma Plain	1.4	493	-73	59	0	11	30	0	45	34	21
	S16	Utikuma Plain	1.4	493	-73	59	0	11	30	0	45	34	21
	REC	Loon Lake Plain, Wabasca Plain, Peerless Upland	-0.2	411	-148	49	0.0	5.9	43	2.1	31.7	42.9	24.5
Taiga Plains	SMC	Wrigley, Ochre River, Tseepantee Lake	-4.9	337	-140	41.3	0.0	41.8	0	12.5	80.2	9.1	3.1
	WS1	Wrigley, Tseepantee Lake	-4.7	340	-138	51.3	0.0	32.0	0	16.7	79	7	2

Research site	Stream ID	Ecodistrict	MAT (°C)	MAP (mm)	CMI (mm)	Soil type[1] (%)					Forest type[2] (%)		
						Wetland	Podzol	Bruni-sol	Luvi-sol	Rock & regosol	Coni-ferous	Mixed	Broad-leaf
Taiga Plains	WS2	Wrigley	-4.8	337	-141	45	0	30	0	25	91	6	3
	WS4	Wrigley	-4.8	337	-141	45	0	30	0	25	91	6	3
	WS6	Wrigley	-4.8	337	-141	45	0	30	0	25	91	6	3
	WS11	Wrigley	-4.8	337	-141	45	0	30	0	25	91	6	3
	SCC	Fort Simpson	-3.8	361	-127	62	0	11	11	16	34	63	3
	JMR	Fort Simpson, Trout Lake North	-3.7	363	-126	64.3	0	9.9	11.4	14.4	32.5	64.5	3
	SS4	Yates River Plain, Fort Simpson	-3.6	333	-149	70.3	0	5.8	8.8	15.3	25.8	71.3	3
	SS5	Yates River Plain, Fort Simpson	-3.7	342	-142	67.5	0	7.5	9.5	15.5	28.5	68.5	3
	SS6	Fort Simpson	-3.8	361	-127	62	0	11	11	16	34	63	3
	SS7	Yates River Plain	-3.5	324	-156	73	0	4	8	15	23	74	3
	LS1	Hay River Plain	-1.2	411	-125	72	0	3	24	1	25	46	29
	LS2	Hay River Plain	-1.2	411	-125	72	0	3	24	1	25	46	29
	LS3	Hay River Plain	-1.2	411	-125	72	0	3	24	1	25	46	29
	LS4	Yates River Plain	-3.5	324	-156	73	0	4	8	15	23	74	3
	LS5	Yates River Plain	-3.5	324	-156	73	0	4	8	15	23	74	3
	LS6	Yates River Plain	-3.5	324	-156	73	0	4	8	15	23	74	3
	LS8	Yates River Plain, Hay River Plain, Cameron Slope, Cameron Hills Upland	-2.2	356	-134	68.3	0	7.1	21.2	3.4	17.3	71.3	11.4
Boreal Shield	C31	Montreal River	4.3	946	418	6	31	0	1	62	0	47	52
	C32	Montreal River	4.3	946	418	6	31	0	1	62	0	47	52
	C38	Montreal River	4.3	946	418	6	31	0	1	62	0	47	52
	C46	Montreal River	4.3	946	418	6	31	0	1	62	0	47	52
	S3	Montreal River	4.3	946	418	6	31	0	1	62	0	47	52
	S5	Montreal River	4.3	946	418	6	31	0	1	62	0	47	52
Atlantic Maritime	S11	Beaverbank	5.9	1465	906	16	83	0	0	1	44	39	12
	S21	South Mountain, Beaverbank	6.5	1350	752	20	79	0	0	1	48	36	15
	S31	South Mountain	6.5	1350	752	20	79	0	0	1	48	36	15

Research site	Stream ID	Ecodistrict	MAT (°C)	MAP (mm)	CMI (mm)	Soil type[1] (%)					Forest type[2] (%)		
						Wetland	Podzol	Bruni-sol	Luvi-sol	Rock & regosol	Coni-ferous	Mixed	Broad-leaf
Atlantic Maritime	S41	South Mountain	6.5	1350	752	20	79	0	0	1	48	36	15
	S42	South Mountain	6.5	1350	752	20	79	0	0	1	48	36	15
	S51	Beaverbank, South Mountain	5.9	1465	906	16	83	0	0	1	44	39	12

Notes:

Catchment climatic and landcover characteristics were estimated using ecodistrict data (Marshall et al., 1999). When a catchment spanned several ecodistricts, the characteristics were estimated as weighted averages, based on approximate proportions of the catchment in each ecodistrict.

MAT = mean annual temperature; MAP = mean annual precipitation; CMI = climate moisture index

[1]Wetland soils include folisols, humisols, mesisols, fibrisols, organic cryosolic, gleysolic and gleysolic turbic cryosolic soils. Podzols include ferro-humic and humo-ferric podzolic soils. Brunizols include eutric brunisolic and brunisolic turbic cryosolic. Luvisols include brunisolic gray luvisolic, gray luvisolic and dark gray luvisolic soils. The presence of other soil types was minimal and not considered.

[2]Mixed forests have canopy of 26-75% coniferous/broadleaf trees; broadleaf and coniferous forests have canopy >75% broadleaf and coniferous trees, respectively. Other landcover types (e.g., agricultural land and sparsely vegetated land) present in the ecodistricts were not considered. Only proportions of coniferous and broadleaf forests were included in random forest analysis.

Table A3. Typical method detection limits (DL) and the number of concentration values <DL.

Analyte	DL* (mg L^{-1})	Number (%) of values below DL	Number (%) of values replaced
NH_4-N	0.005	29 (13.7%)	1 (0.5%)
NO_2+NO_3-N	0.013	107 (50.5%)	32 (15.0%)
SRP	0.018	150 (70.8%)	0
Cl^-	0.3	35 (16.5%)	0
SO_4^{2-}	3	138 (65.1%)	60 (28.2%)
Ca	0.007	0	0
Na	0.002	0	0
Fe	0.001	7 (3.3%)	7 (3.3%)
Mn	0.001	27 (12.6%)	27 (12.6%)
DOC	1** / 0.05***	10** (4.7%) / 0***	0
TDN	0.1	13 (6.1%)	0

Notes:

Imputing a constant value for non-detects such as one half of the DL may lead to anomalous results in PCA due to its impact on summary statistics and variation within the dataset (Helsel, 2006). A cautious distribution-based imputation approach was used to minimize the risk of bias. Specifically, values below DL in PCA (Figure 2a) were imputed by drawing random values from a Gaussian distribution with a center and standard deviation of one fifth of the DL. Negative values were redrawn from the distribution, such that the center of the overall distribution was shifted back towards the DL. Values below DL that had been included in lab reports were used as reported.

* limit of detection is reported for Ca, Na, Fe, Mn, DOC and TDN, and limit of quantification for the rest of the analytes, ** combustion catalytic oxidation method, *** persulfate wet oxidation method

Table A4. DOM compositional indices used in the analysis and the corresponding analytical techniques.

Analytical technique	Abbreviation / notation used in this study	Description
UV-vis absorbance	A_{254}	absorbance at 254 nm
	SUVA	specific UV absorbance at 254 nm
	E2:E3	ratio of absorbance at 250 and 365 nm
	$S_{275\text{-}295}$	spectral slope between 275 and 295 nm
	S_R	ratio of slopes $S_{275–295}$ and $S_{350–400}$
Fluorescence	BIX	biological index
	HIX	humification index
	C1 to C5	PARAFAC fluorescent components
AF4	M_p	molecular mass
FT-ICR-MS	H/C	intensity-weighted average of hydrogen-to-carbon ratio, indicates hydrogen saturation
	O/C	intensity-weighted average of oxygen-to-carbon ratio, indicates oxygenation
	Aliphatic	aliphatic fraction
	Low-O Unsaturated	low-o unsaturated fraction
	High-O Unsaturated	high-o unsaturated fraction
	Aromatic	aromatic fraction
	Condensed Aromatic	condensed aromatic fraction
LC-OCD	BP	biopolymers
	HS	humic substances
	BB	building blocks
	LMWN	low molecular weight neutrals
	LMWA	low molecular weight acids

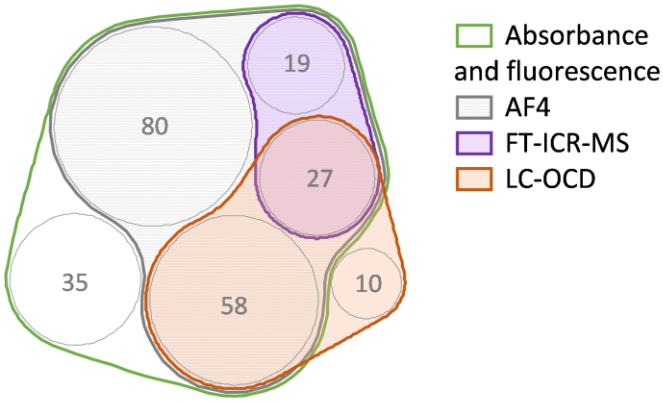

Figure A2. Venn diagram showing DOM composition data overlap (number of samples shown in grey) for different methods.

Table A5. Variability in DOC and TDN concentrations and DOM composition indices by research site (mean value ± standard deviation, and number of samples analyzed in parentheses).

Analyte	Pacific Maritime 1	Pacific Maritime 2	Montane Cordillera	Boreal Plains	Taiga Plains	Boreal Shield	Atlantic Maritime
Ca (mg L^{-1})	0.796 ± 0.378 (9)	7.01 ± 3.95 (30)	43.7 ± 10.0 (29)	31.8 ± 15.7 (61)	43.5 ± 21.3 (37)	5.60 ± 2.26 (23)	1.21 ± 0.53 (30)
Mg (mg L^{-1})	0.363 ± 0.091 (9)	1.18 ± 0.62 (30)	11..0 ± 3.1 (29)	6.34 ± 3.55 (61)	11.6 ± 7.6 (37)	0.486 ± 0.142 (23)	0.400 ± 0.117 (30)
Na (mg L^{-1})	2.46 ± 0.51 (9)	1.10 ± 0.64 (30)	1.53 ± 0.82 (29)	3.16 ± 3.01 (61)	12.5 ± 16.7 (37)	0.70 ± 0.14 (23)	2.58 ± 0.53 (30)
NO_2^-+NO_3^--N (µg L^{-1})	12.0 ± 13.7 (9)	27.8 ± 28.8 (30)	177.6 ± 44.2 (29)	34.0 ± 64.1 (61)	17.7 ± 25.0 (37)	121.5 ± 107.9 (23)	5.2 ± 2.9 (30)
NH_4-N (µg L^{-1})	10.1 ± 7.9 (9)	7.1 ± 6.8 (24)	13.3 ± 17.4 (29)	120.4 ± 190.6 (60)	24.1 ± 15.3 (37)	9.8 ± 9.3 (23)	21.3 ± 20.8 (30)
SRP (µg L^{-1})	3.6 ± 1.1 (9)	11.0 ± 14.6 (24)	8.4 ± 15.2 (29)	70.2 ± 70.8 (60)	26.3 ± 51.3 (37)	5.7 ± 7.6 (23)	6.4 ± 6.8 (30)
Cl^- (mg L^{-1})	5.3 ± 1.5 (9)	1.1 ± 1.1 (30)	0.3 ± 0.1 (29)	3.9 ± 5.6 (61)	14.5 ± 24.2 (37)	0.3 ± 0.2 (23)	4.7 ± 1.2 (30)
SO_4^{2-} (mg L^{-1})	0.5 ± 0.4 (9)	0.7 ± 0.3 (30)	8.9 ± 3.7 (29)	10.4 ± 18.1 (61)	24.1 ± 43.8 (37)	2.7 ± 2.3 (23)	1.0 ± 0.6 (30)
Fe (mg L^{-1})	0.208 ± 0.074 (9)	0.040 ± 0.041	0.010 ± 0.008 (29)	0.884 ± 0.803 (60)	0.215 ± 0.294 (37)	0.031 ± 0.034 (23)	0.303 ± 0.135 (30)
Mn (µg L^{-1})	4.4 ± 1.5 (9)	5.2 ± 9.8 (24)	1.3 ± 1.0 (29)	200 ± 221 (60)	31.5 ± 47.9 (37)	6.0 ± 13.0 (23)	34.3 ± 13.7 (30)
pH	5.20 ± 1.10 (9)	7.18 ± 0.42 (30)	8.15 ± 0.28 (37)	7.28 ± 0.51 (61)	7.65 ± 0.32 (37)	6.81 ± 0.29 (25)	4.17 ± 0.39 (30)
DOC (mg L^{-1})	7.8 ± 2.6 (9)	2.2 ± 1.2 (30)	1.32 ± 0.65 (29)	25.0 ± 7.9 (60)	20.3 ± 7.9 (37)	5.1 ± 4.4 (23)	17.6 ± 7.9 (30)
TDN (mg L^{-1})	0.183 ± 0.072 (9)	0.16 ± 0.13 (24)	0.29 ± 0.12 (29)	0.86 ± 0.30 (60)	0.68 ± 0.36 (37)	0.31 ± 0.10 (23)	0.33 ± 0.11 (30)
C/N	48 ± 27 (9)	24 ± 16 (24)	4.8 ± 2.0 (29)	30.6 ± 8.2 (61)	31.7 ± 6.7 (37)	16.6 ± 9.8 (23)	54 ± 12 (30)
A_{254} (cm^{-1})	0.38 ± 0.14 (9)	0.067 ± 0.052 (30)	0.027 ± 0.015 (29)	0.88 ± 0.37 (60)	0.71 ± 0.28 (37)	0.18 ± 0.21 (23)	0.75 ± 0.30 (30)
SUVA (L mg^{-1} m^{-1})	4.87 ± 0.62 (9)	2.95 ± 0.92 (30)	2.15 ± 0.64 (29)	3.46 ± 0.65 (61)	3.49 ± 0.32 (37)	3.04 ± 0.79 (23)	4.33 ± 0.44 (30)
$S_{275-295}$	0.013 ± 0.001 (9)	0.015 ± 0.001 (30)	0.017 ± 0.001 (29)	0.016 ± 0.002 (61)	0.016 ± 0.001 (37)	0.015 ± 0.002 (23)	0.013 ± 0.001 (30)
S_R	0.787 ± 0.039 (9)	0.86 ± 0.12 (30)	1.10 ± 0.32 (29)	0.86 ± 0.13 (61)	0.871 ± 0.058 (37)	0.87 ± 0.14 (23)	0.749 ± 0.018 (30)
E2:E3	4.49 ± 0.14 (9)	5.24 ± 0.60 (30)	6.3 ± 1.4 (29)	5.9 ± 1.0 (61)	5.90 ± 0.54 (37)	5.60 ± 0.82 (23)	4.70 ± 0.27 (30)
BIX	0.499 ± 0.018 (9)	0.584 ± 0.046 (30)	0.705 ± 0.021 (29)	0.603 ± 0.069 (61)	0.584 ± 0.035 (37)	0.623 ± 0.094 (23)	0.501 ± 0.030 (30)
HIX	0.925 ± 0.010 (9)	0.860 ± 0.053 (30)	0.877 ± 0.041 (29)	0.921 ± 0.032 (61)	0.936 ± 0.017 (37)	0.896 ± 0.064 (23)	0.920 ± 0.034 (30)
C1 (%)	45.0 ± 1.4 (9)	38.7 ± 3.4 (30)	33.0 ± 2.6 (29)	36.2 ± 5.0 (61)	37.6 ± 2.3 (37)	40.0 ± 7.2 (23)	46.3 ± 1.4 (30)
C2 (%)	17.3 ± 3.0 (9)	14.2 ± 3.3 (30)	19.2 ± 2.5 (29)	29.2 ± 4.3 (61)	27.9 ± 3.1 (37)	15.5 ± 6.2 (23)	13.9 ± 2.9 (30)
C3 (%)	16.04 ± 0.63 (9)	19.9 ± 3.0 (30)	22.6 ± 1.5 (29)	20.1 ± 2.1 (61)	19.0 ± 1.2 (37)	22.4 ± 3.7 (23)	16.6 ± 2.0 (30)
C4 (%)	16.3 ± 2.2 (9)	15.3 ± 2.8 (30)	14.73 ± 0.95 (29)	9.8 ± 2.3 (61)	12.3 ± 2.0 (37)	14.0 ± 4.2 (23)	18.1 ± 1.2 (30)
C5 (%)	5.3 ± 1.0 (9)	12.0 ± 6.4 (30)	10.5 ± 5.1 (29)	4.7 ± 3.3 (61)	3.2 ± 1.7 (37)	8.1 ± 6.5 (23)	5.1 ± 1.9 (30)
BP (%)	2.75 ± 0.84 (6)	3.4 ± 3.4 (12)	0.74 ± 0.48 (11)	3.4 ± 2.7 (26)	1.3 ± 1.5 (11)	4.2 ± 4.0 (11)	2.8 ± 1.4 (18)
HS (%)	73.2 ± 1.5 (6)	64.9 ± 7.9 (12)	67.4 ± 8.5 (11)	73.5 ± 5.7 (26)	79.9 ± 2.8 (11)	68.8 ± 5.8 (11)	75.6 ± 3.2 (18)

Analyte	Pacific Maritime 1	Pacific Maritime 2	Montane Cordillera	Boreal Plains	Taiga Plains	Boreal Shield	Atlantic Maritime
BB (%)	10.6 ± 1.2 (6)	12.6 ± 1.5 (12)	14.5 ± 3.1 (11)	13.8 ± 2.3 (26)	11.7 ± 1.2 (11)	12.7 ± 2.8 (11)	9.9 ± 2.0 (18)
LMWA (%)	2.46 ± 0.20 (6)	3.05 ± 0.60 (12)	3.5 ± 1.3 (11)	2.34 ± 0.52 (26)	1.85 ± 0.31 (11)	2.72 ± 0.47 (11)	2.02 ± 0.34 (18)
LMWN (%)	7.4 ± 2.5 (6)	9.0 ± 2.0 (12)	9.6 ± 3.1 (11)	5.9 ± 1.3 (26)	4.97 ± 0.79 (11)	7.2 ± 1.0 (11)	6.0 ± 1.1 (18)
M_p (Da)	1228 ± 65 (9)	1240 ± 150 (24)	1226 ± 81 (29)	1190 ± 140 (56)	1460 ± 230 (13)	1160 ± 170 (23)	1140 ± 130 (30)
Aliphatic (%)	8.4 ± 1.5 (3)	15.6 ± 5.0 (8)	23 ± 12 (6)	5.6 ± 1.7 (13)	3.46 ± 0.20 (2)	8.9 ± 2.4 (6)	7.8 ± 1.6 (8)
Low-O Unsaturated (%)	21.4 ± 3.7 (3)	26.7 ± 9.8 (8)	28.7 ± 5.4 (6)	14.8 ± 2.0 (13)	16.2 ± 4.1 (2)	22.2 ± 5.4 (6)	16.9 ± 3.1 (8)
High-O Unsaturated (%)	53.3 ± 2.4 (3)	46.5 ± 5.8 (8)	43 ± 12 (6)	69.9 ± 2.8 (13)	70.4 ± 4.1 (2)	57.7 ± 2.1 (6)	58.9 ± 2.4 (8)
Aromatic (%)	11.1 ± 3.3 (3)	7.3 ± 2.7 (8)	3.58 ± 0.95 (6)	6.6 ± 1.4 (13)	6.92 ± 0.20 (2)	7.1 ± 2.9 (6)	10.51 ± 0.79 (8)
Condensed Aromatic (%)	3.0 ± 1.1 (3)	2.0 ± 1.5 (8)	0.43 ± 0.23 (6)	1.00 ± 0.45 (13)	0.75 ± 0.32 (2)	2.1 ± 1.3 (6)	3.10 ± 0.35 (8)

Note: an outlier sample S15 from February 2021 (Boreal Plains) is not included in calculation of concentrations for several analytes.

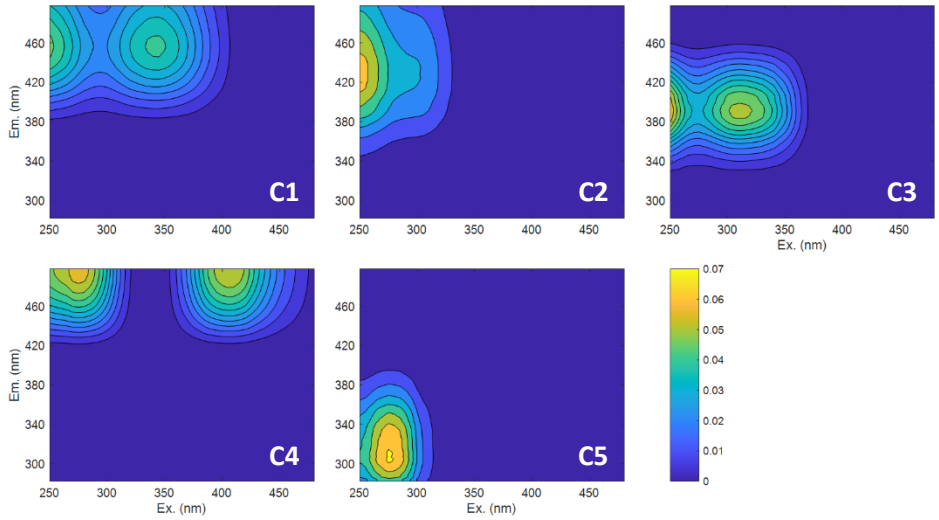

Figure A3. Fluorescence signatures of validated PARAFAC components C1 to C5.

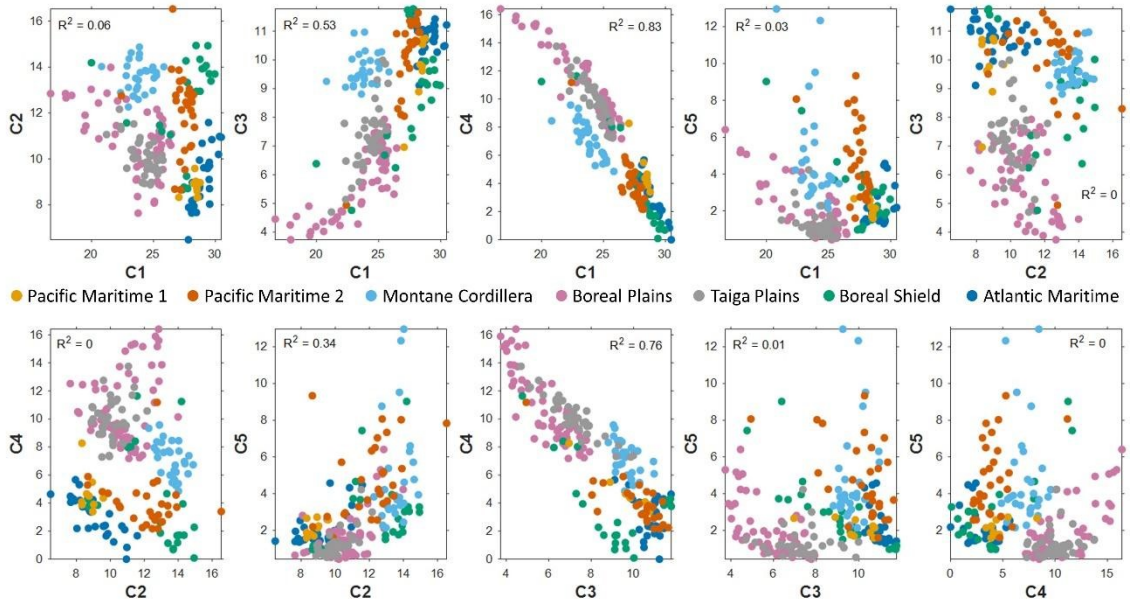

Figure A4. Correlations of PARAFAC components in a 5-component model using a normalized dataset.

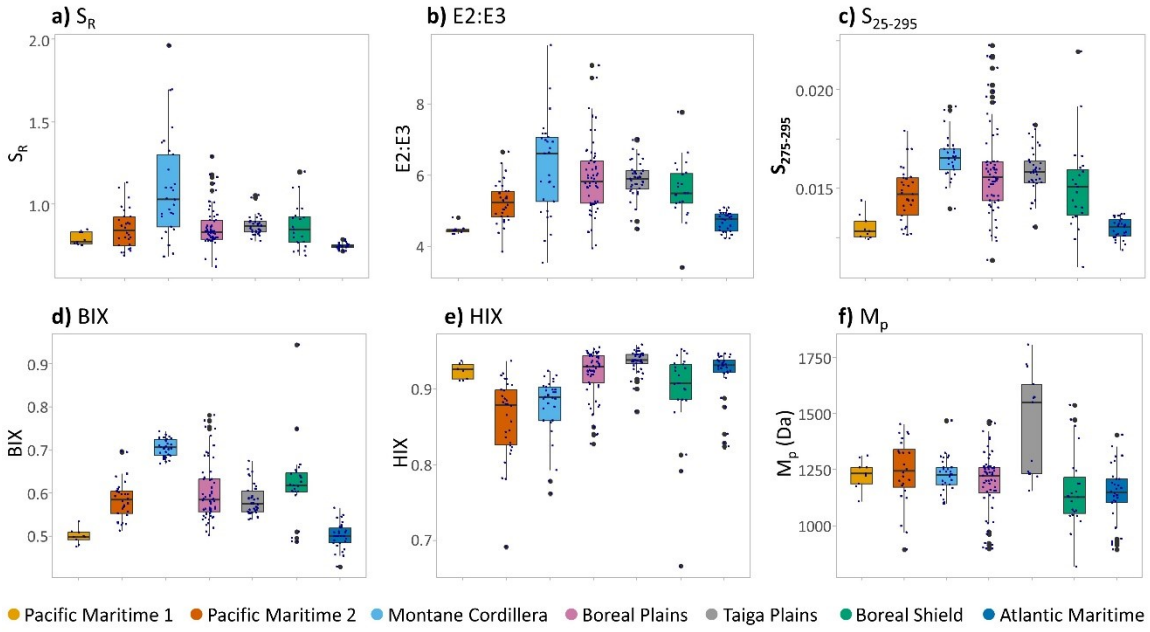

Figure A5. Boxplots of DOM composition indices by research site. Small blue dots indicate individual samples, larger black dots are outliers.

Table A6. PCA on water chemistry (major ions, inorganic nutrients, DOC, TDN, pH). Only data for principal components with eigenvalues >1 are shown.

	PC1	PC2	PC3
Importance of components:			
Eigenvalue	4.34	2.78	1.24
Proportion of variance	0.39	0.25	0.11
Cumulative variance	0.39	0.65	0.76
Loadings:			
DOC	0.43	-0.10	0.06
TDN	0.40	0.16	0.28
NH_4	0.36	0.08	0.17
NO_2+NO_3	-0.18	0.36	0.18
SRP	0.31	0.09	0.41
Cl	0.35	-0.12	-0.49
SO_4	0.02	0.46	-0.36
Ca	0.12	0.54	0.04
Na	0.32	0.15	-0.54
Fe	0.41	-0.17	0.15
pH	-0.05	0.51	0.07

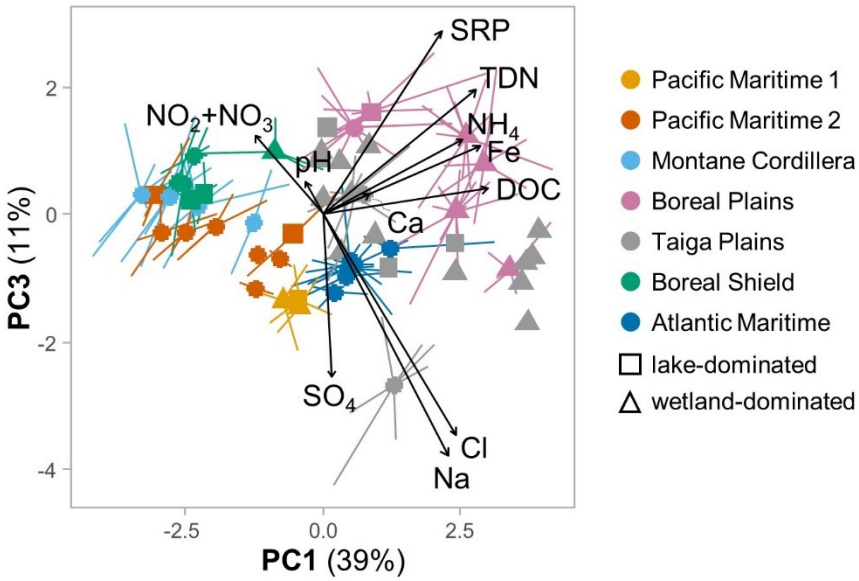

Figure A6. PCA on water chemistry (major ions, inorganic nutrients, DOC, TDN, pH), PC1 and PC3.

Table A7. PCA on absorbance and fluorescence data. Only data for principal components with eigenvalues >1 are shown.

	PC1	PC2	PC3
Importance of components:			
Eigenvalue	5.75	2.32	1.23
Proportion of variance	0.52	0.21	0.11
Cumulative variance	0.52	0.73	0.85
Loadings:			
SUVA	0.34	-0.19	0.30
E2:E3	-0.29	-0.21	-0.30
$S_{275-295}$	-0.37	-0.17	-0.11
S_R	-0.29	-0.01	0.27
HIX	0.23	-0.45	-0.35
BIX	-0.39	0.08	-0.14
C1	0.38	0.08	-0.23
C2	-0.17	-0.54	0.28
C3	-0.28	0.15	-0.54
C4	0.28	0.34	-0.25
C5	-0.21	0.50	0.34

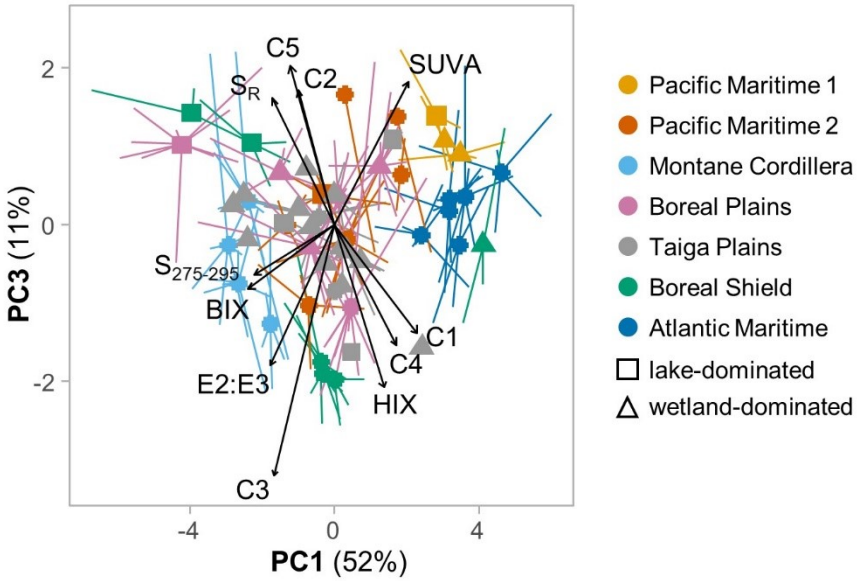

Figure A7. PCA on absorbance and fluorescence data, PC1 and PC3.

Table A8. PCA on FT-ICR-MS and AF4 data. Only data for principal components with eigenvalues >1 are shown.

	PC1	PC2	PC3
Importance of components:			
Eigenvalue	4.29	2.01	1.00
Proportion of variance	0.54	0.25	0.12
Cumulative variance	0.54	0.79	0.91
Loadings:			
Aliphatic	0.39	-0.27	0.06
Low-O Unsaturated	0.41	-0.03	-0.22
High-O Unsaturated	-0.40	0.39	0.05
Aromatics	-0.29	-0.54	-0.10
Condensed Aromatic	-0.21	-0.60	-0.18
H/C	0.44	0.19	0.09
O/C	-0.45	0.21	0.05
M_p	0.00	-0.21	0.94

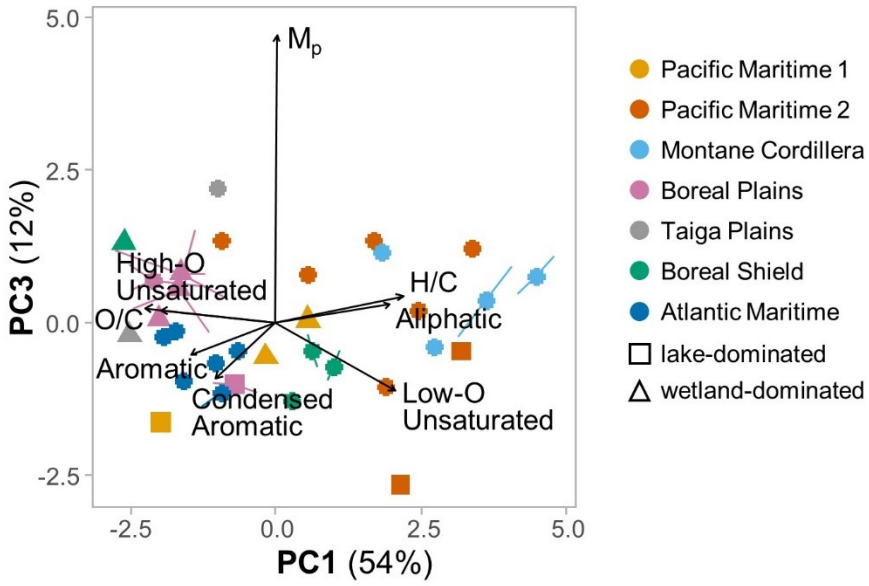

Figure A8. PCA on FT-ICR-MS data, PC1 and PC3.

Table A9. PCA on LC-OCD data. Only data for components with eigenvalues >1 are shown.

	PC1	PC2
Importance of components:		
Eigenvalue	2.75	1.84
Proportion of variance	0.55	0.24
Cumulative variance	0.55	0.79
Loadings:		
BP	0.19	0.75
HS	-0.56	-0.11
BB	0.25	-0.64
LMWA	0.54	-0.01
LMWN	0.54	-0.08

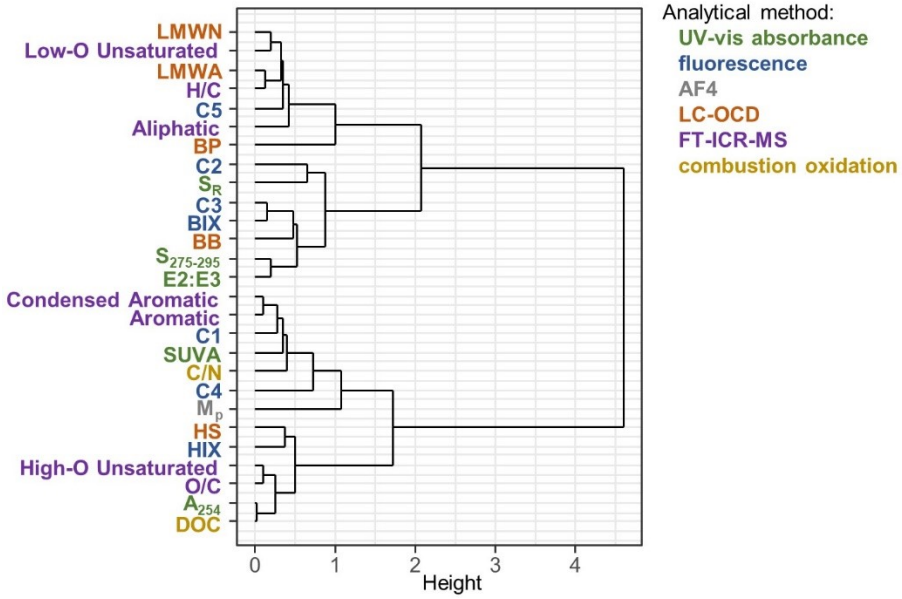

Figure A9. A dendrogram for the cluster analysis in Figure 4 with DOM indices colour-coded based on the analytical method.

Table A10. PCA on the averages for all DOM composition indices. Only data for principal components with eigenvalues >1 are shown.

	PC1	PC2	PC3	PC4
Importance of components:				
Eigenvalue	12.94	5.19	2.66	1.30
Proportion of variance	0.52	0.21	0.11	0.05
Cumulative proportion	0.52	0.73	0.83	0.88
Loadings:				
C/N	-0.23	-0.01	0.11	-0.10
SUVA	-0.25	-0.04	0.16	0.08
S_R	0.24	0.07	0.03	0.32
$S_{275\text{-}295}$	0.21	0.25	0.09	0.06
E2:E3	0.19	0.30	-0.04	-0.03
BIX	0.25	0.15	-0.01	-0.03
HIX	-0.20	0.14	-0.30	-0.12
C1	-0.23	-0.18	-0.16	-0.25
C2	0.02	0.35	0.19	0.30
C3	0.19	0.15	-0.23	-0.34
C4	-0.14	-0.29	-0.27	-0.04
C5	0.21	-0.20	0.23	0.06
H/C	0.25	-0.12	-0.12	0.16
O/C	-0.22	0.24	0.10	-0.12
Aliphatic	0.16	-0.30	-0.03	0.17
High-O Unsaturated	-0.14	0.36	0.00	-0.14
Low-O Unsaturated	0.21	-0.17	-0.06	-0.16
Aromatic	-0.24	-0.11	0.22	0.09
Condensed Aromatic	-0.20	-0.20	0.20	0.02
BP	0.01	0.02	0.59	-0.07
HS	-0.23	0.15	-0.19	0.14
BB	0.18	0.18	-0.12	-0.19
LMWA	0.24	-0.12	0.08	-0.10
LMWN	0.21	-0.23	0.00	-0.14
M_p	-0.08	-0.01	-0.32	0.61

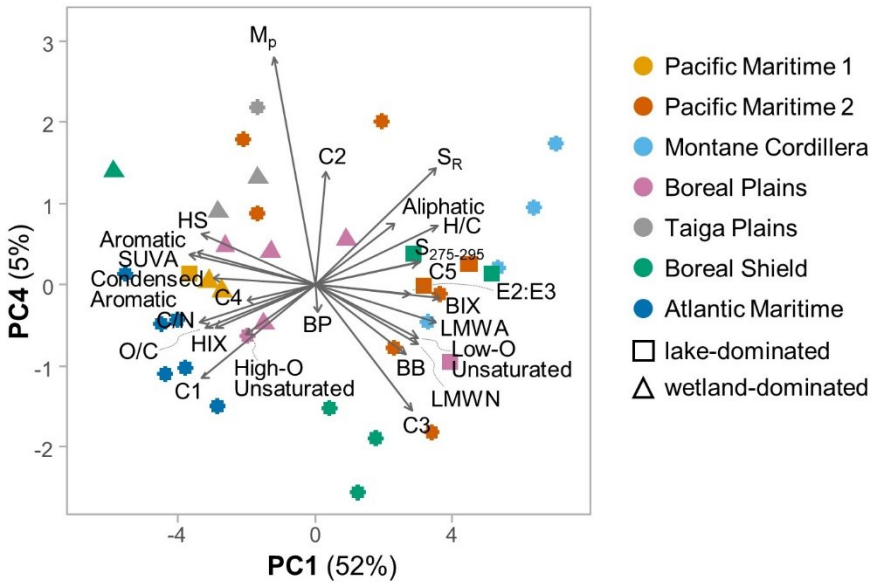

Figure A10. PCA on the averages for all DOM indices, PC1 vs. PC4.

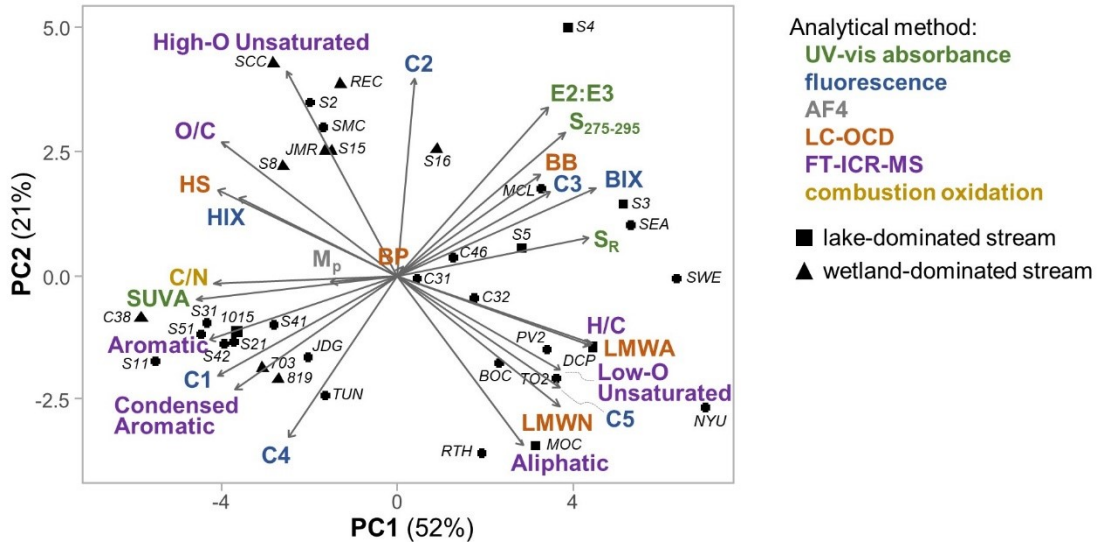

Figure A11. PCA using averages (where applicable) for each stream for all DOM indexes (except BB and HS). DOM indices are colour-coded based on the analytical method. Stream IDs are shown in black cursive.

Appendix B. Supporting information for Chapter 3

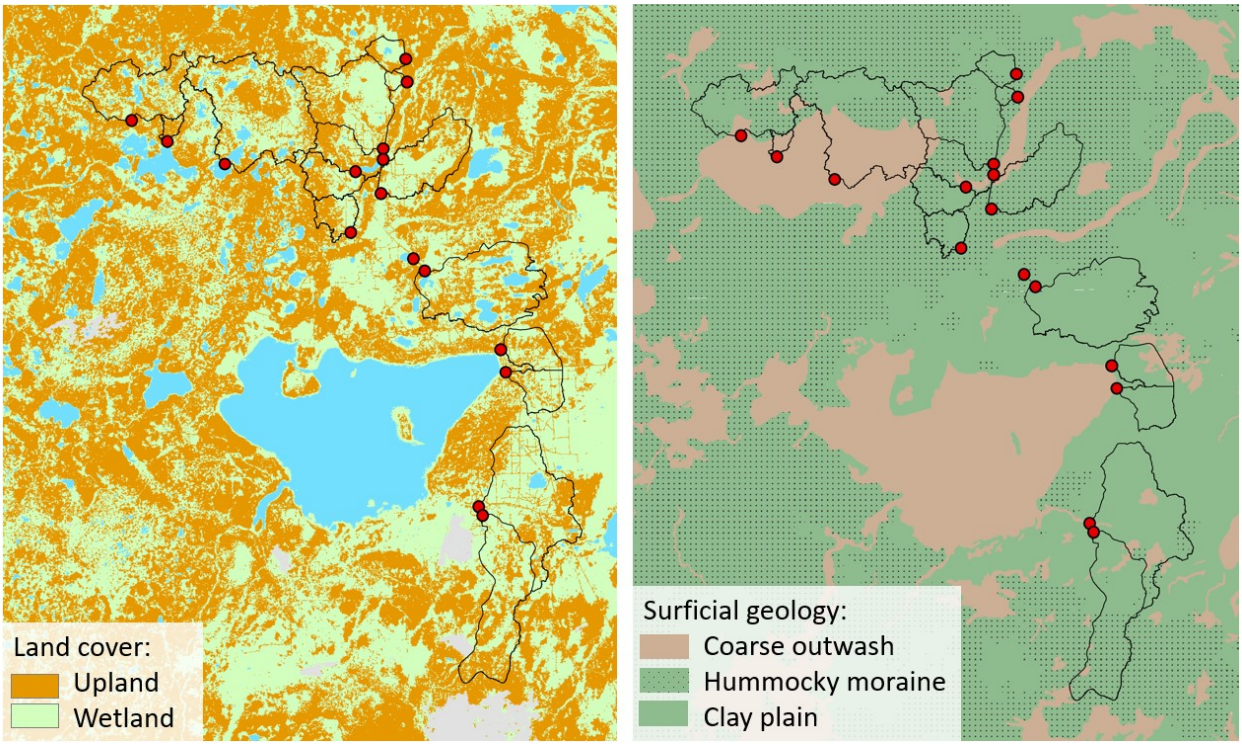

Figure B1. Variations in wetland cover and surficial geology in small catchments at the URSA.

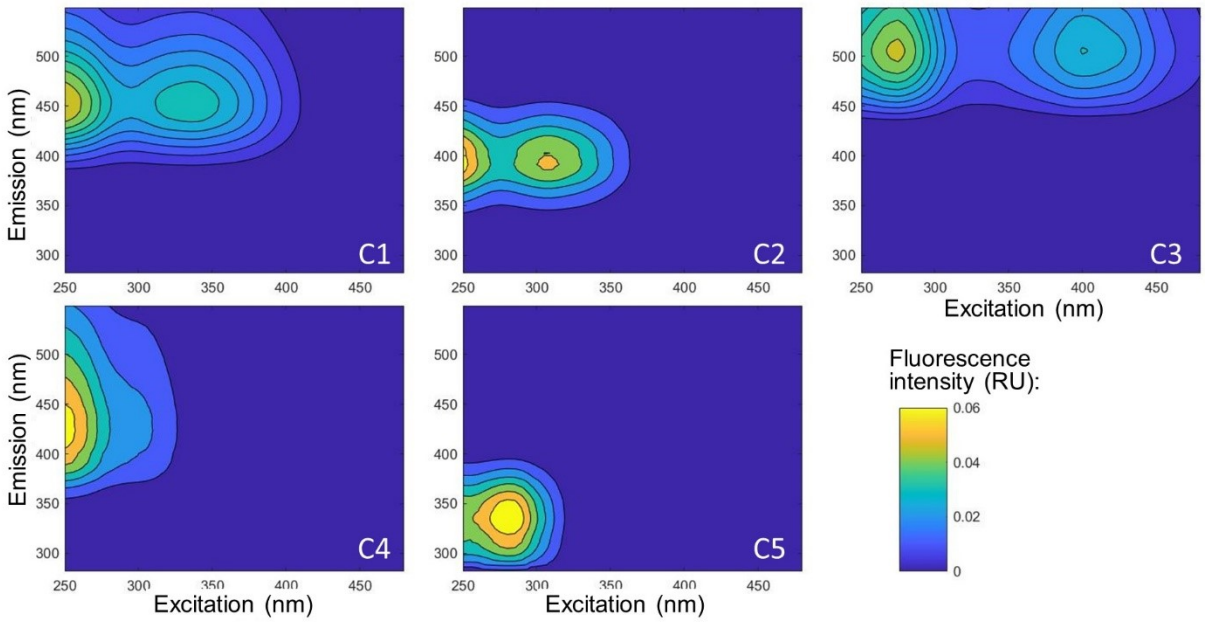

Figure B2. Fingerprint plots for validated PARAFAC components C1 to C5.

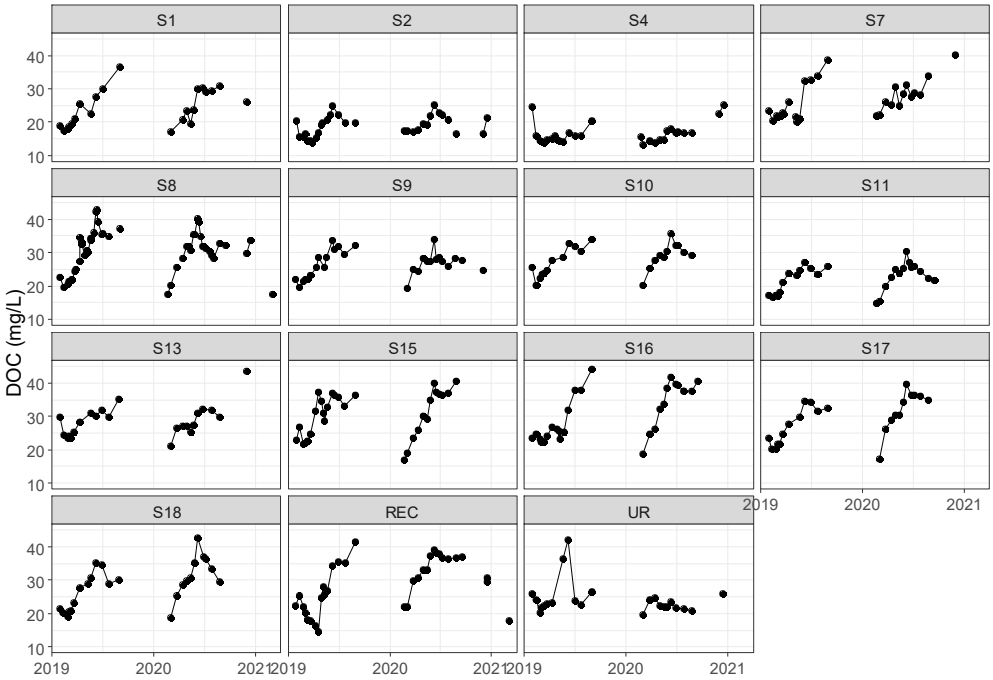

Figure B3a. DOC concentration at URSA streams in 2019-2021.

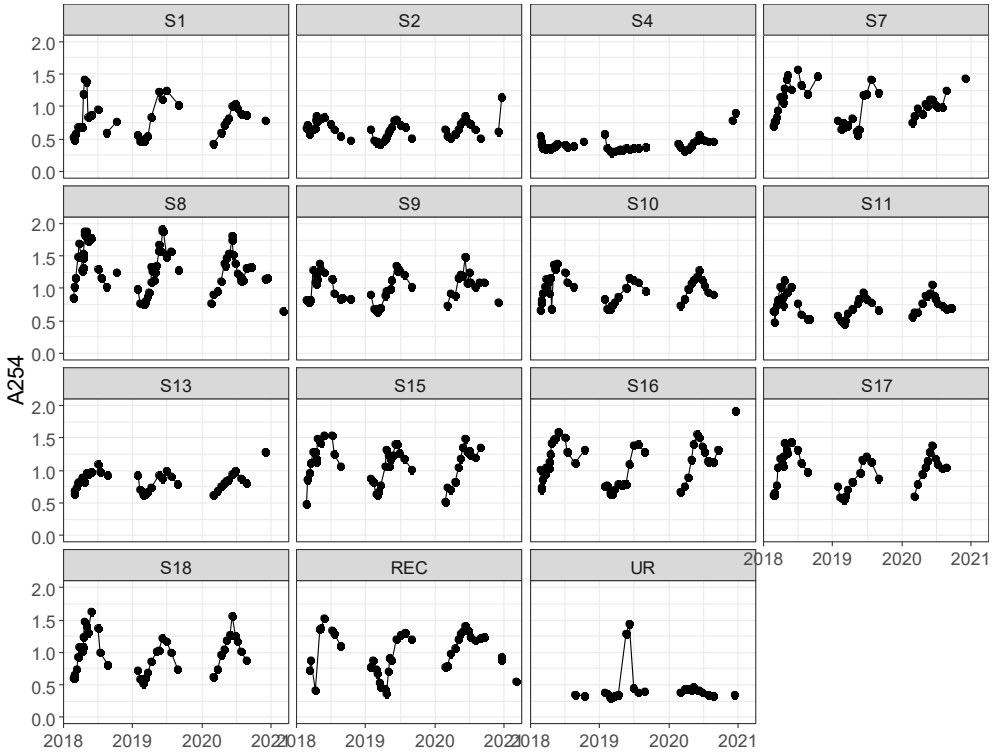

Figure B3b. A_{254} at URSA streams in 2018-2021.

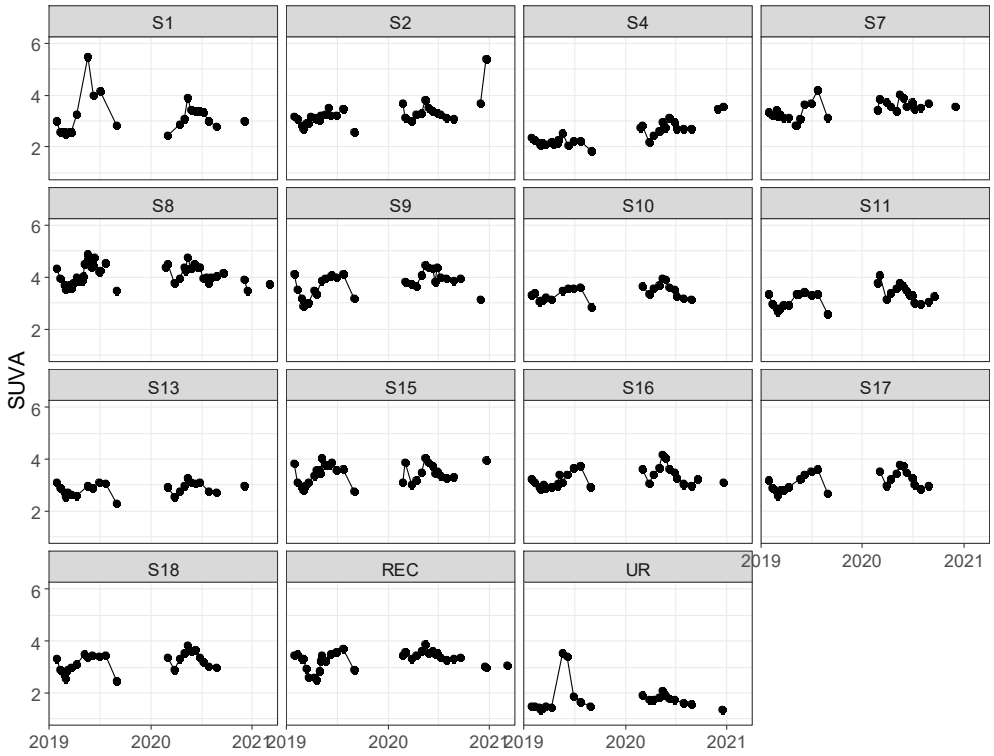

Figure B3c. SUVA at URSA streams in 2019-2021.

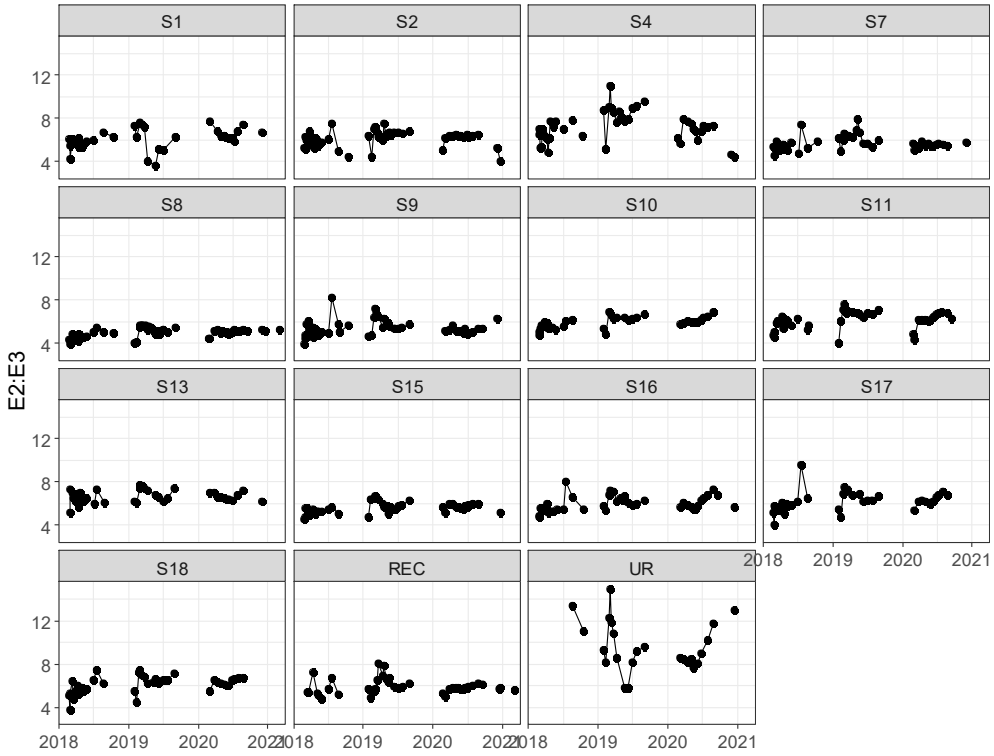

Figure B3d. E2:E3 at URSA streams in 2018-2021.

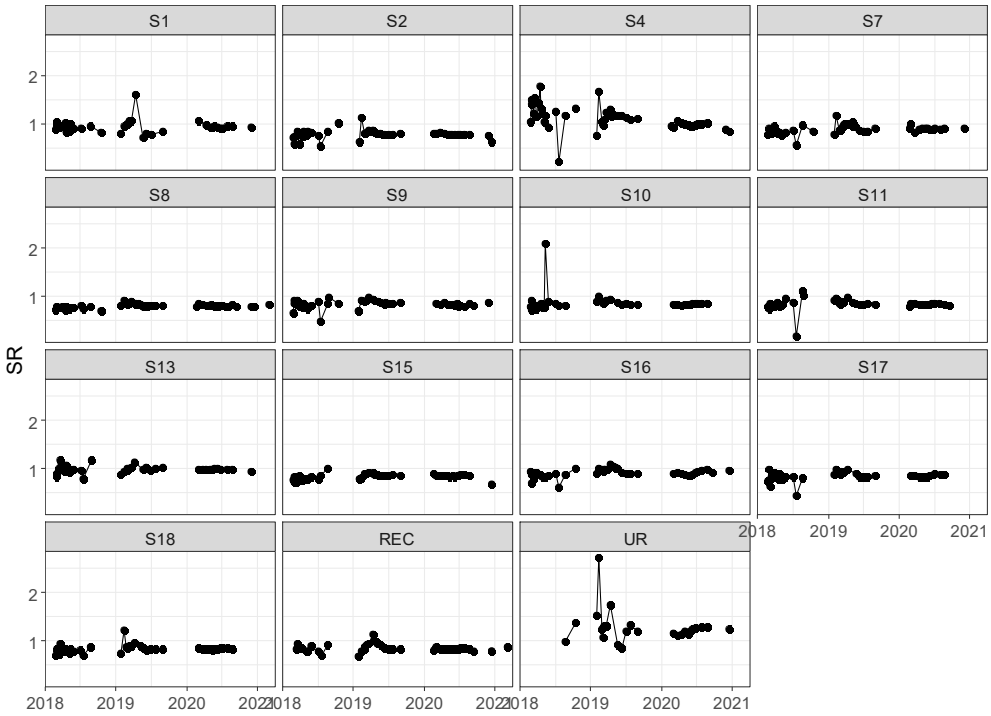

Figure B3e. S_R at URSA streams in 2018-2021.

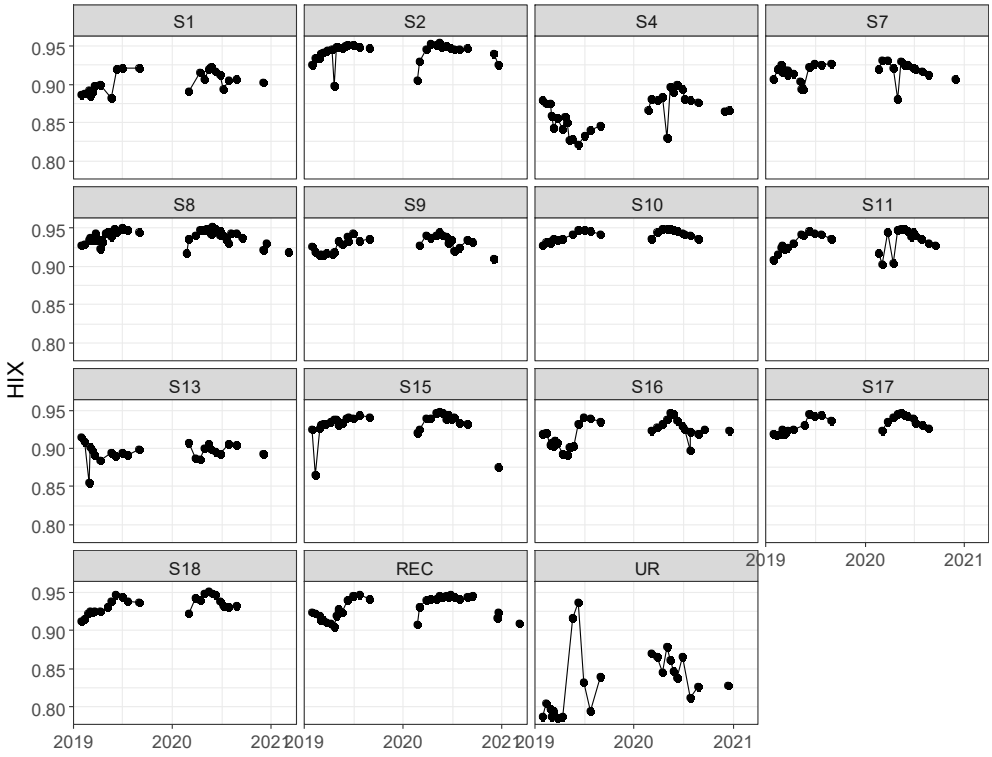

Figure B3f. HIX at URSA streams in 2019-2021.

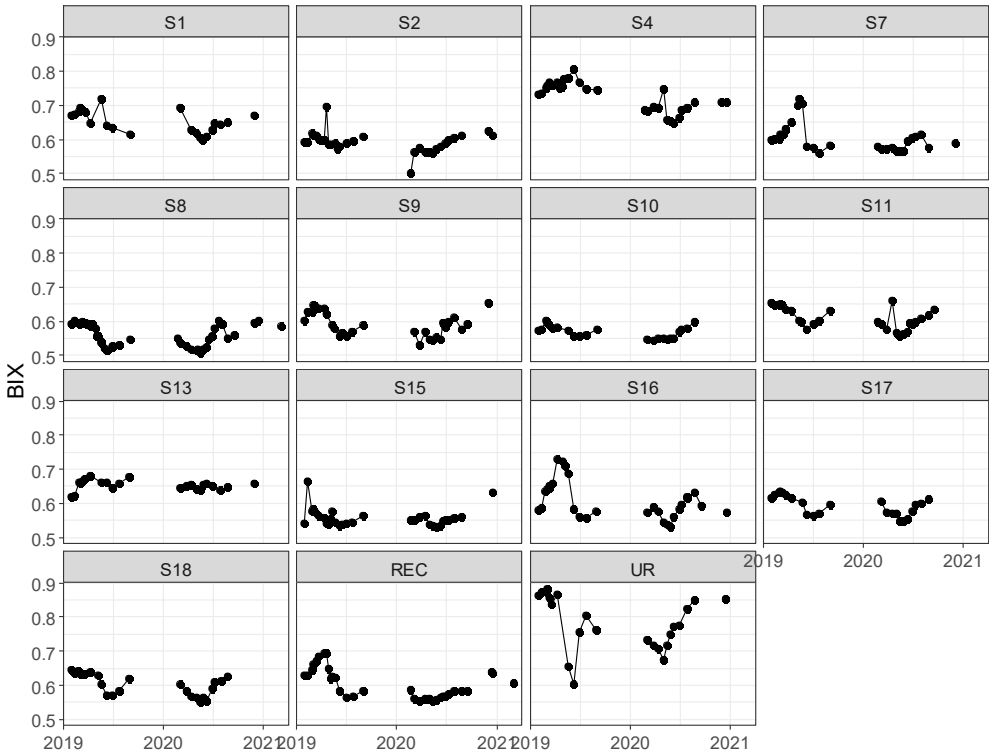

Figure B3g. BIX at URSA streams in 2019-2021.

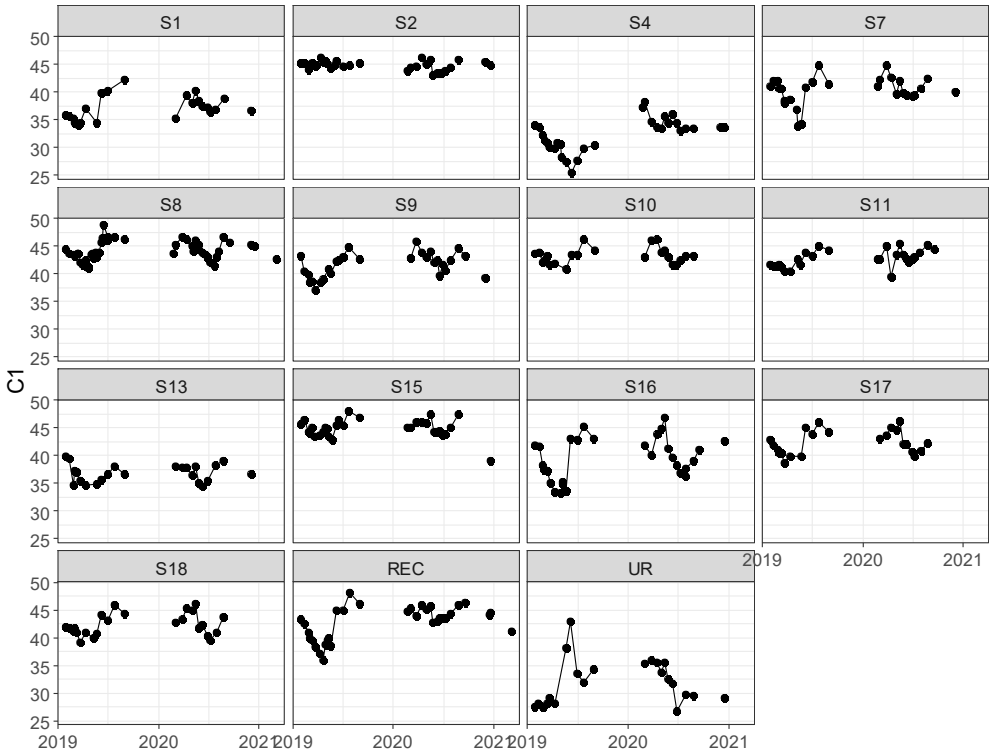

Figure B3h. PARAFAC component C1 at URSA streams in 2019-2021.

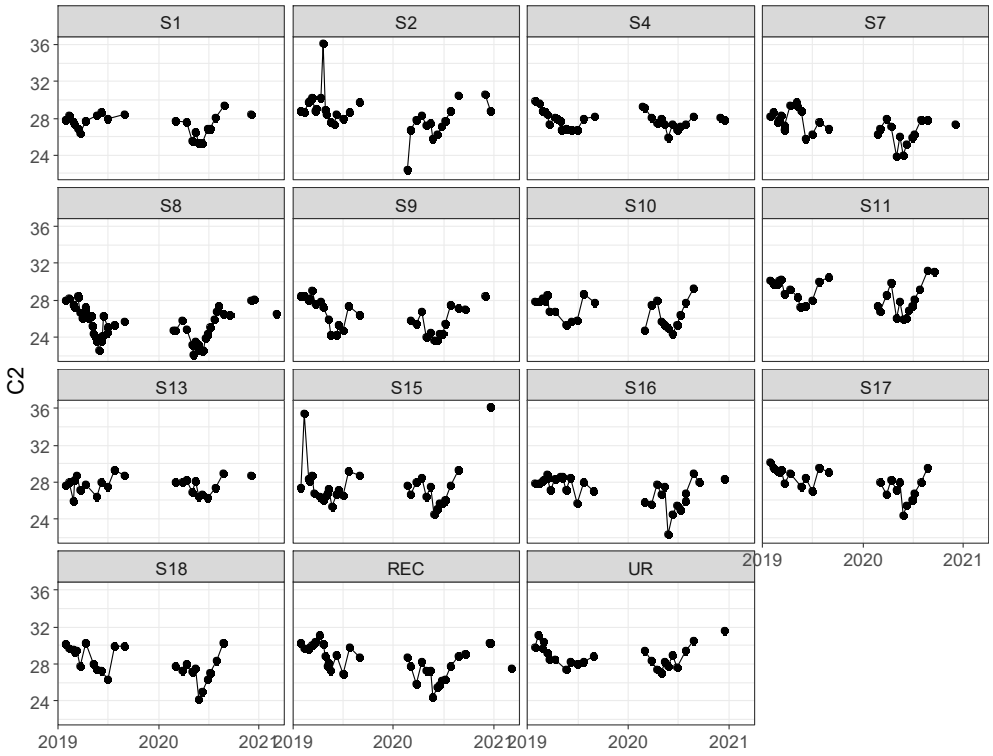

Figure B3i. PARAFAC component C2 at URSA streams in 2019-2021.

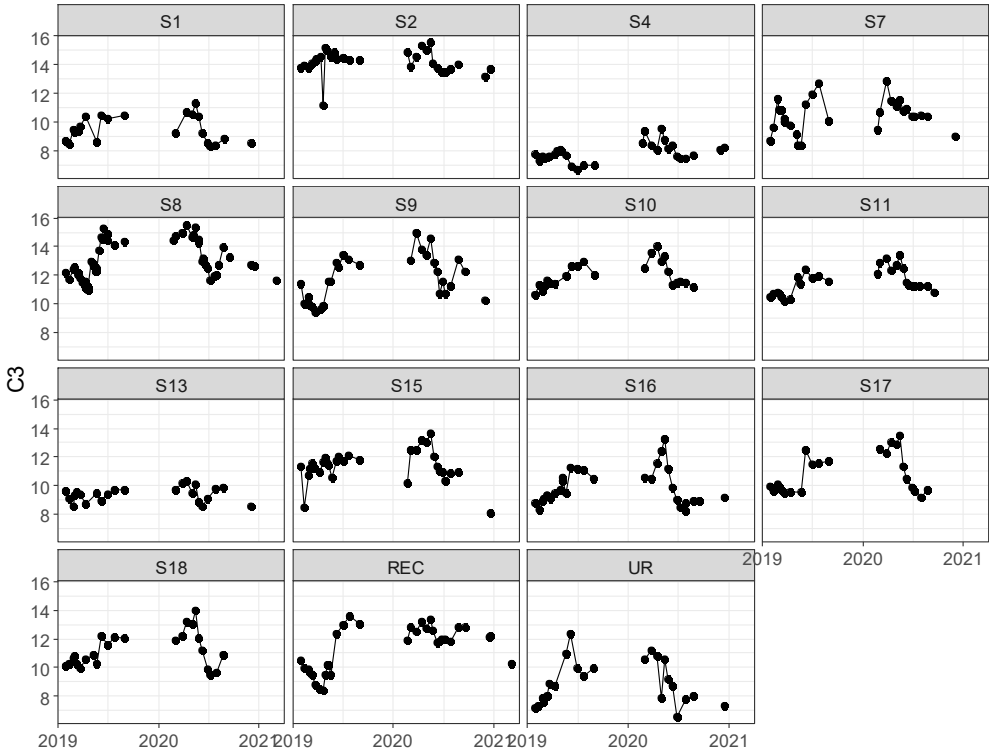

Figure B3j. PARAFAC component C3 at URSA streams in 2019-2021.

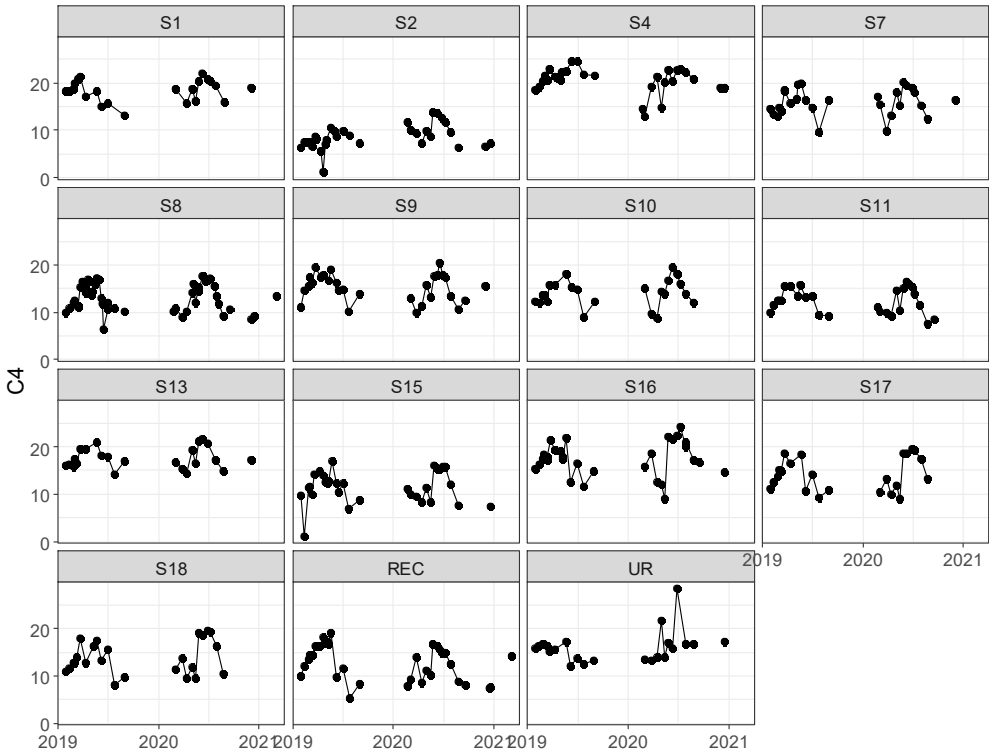

Figure B3k. PARAFAC component C4 at URSA streams in 2019-2021.

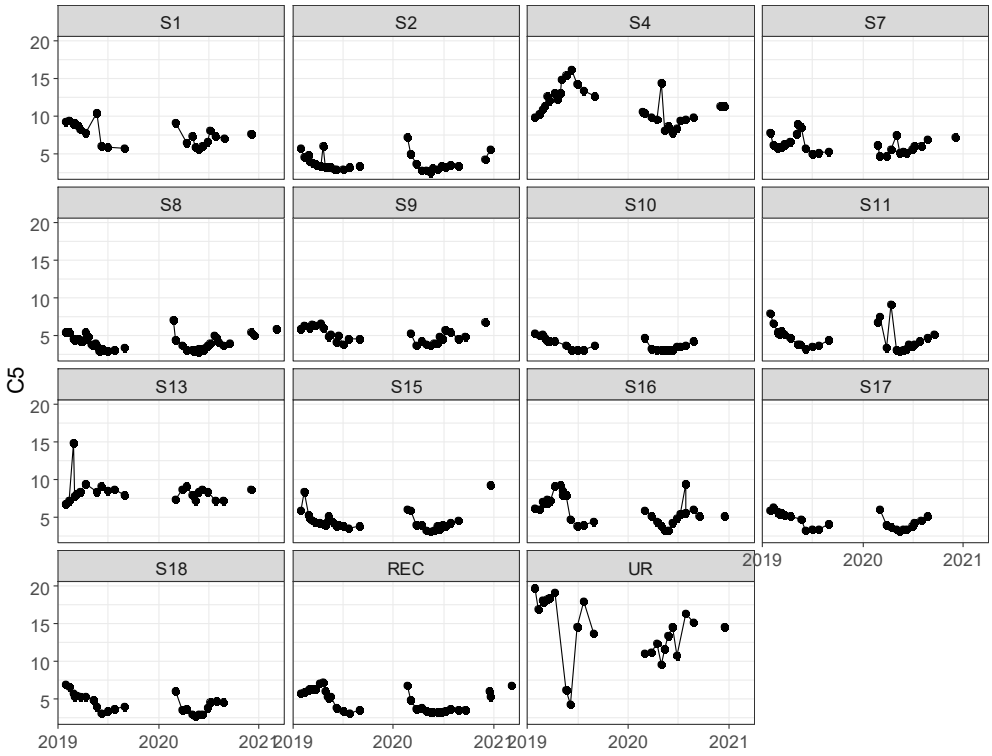

Figure B3l. PARAFAC component C5 at URSA streams in 2019-2021.

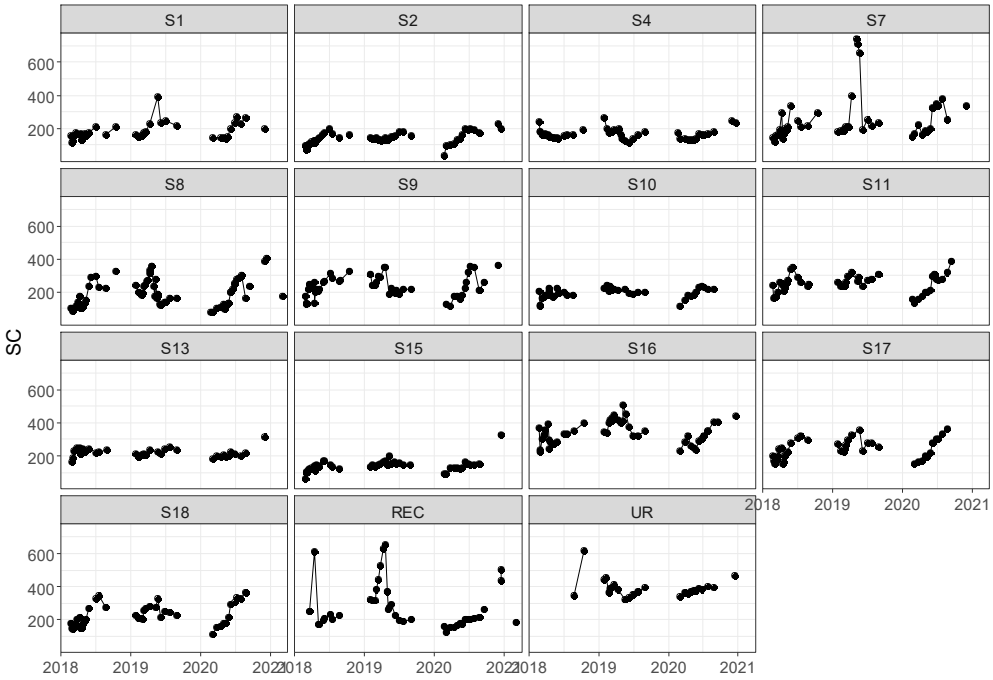

Figure B3m. SC at URSA streams in 2018-2021.

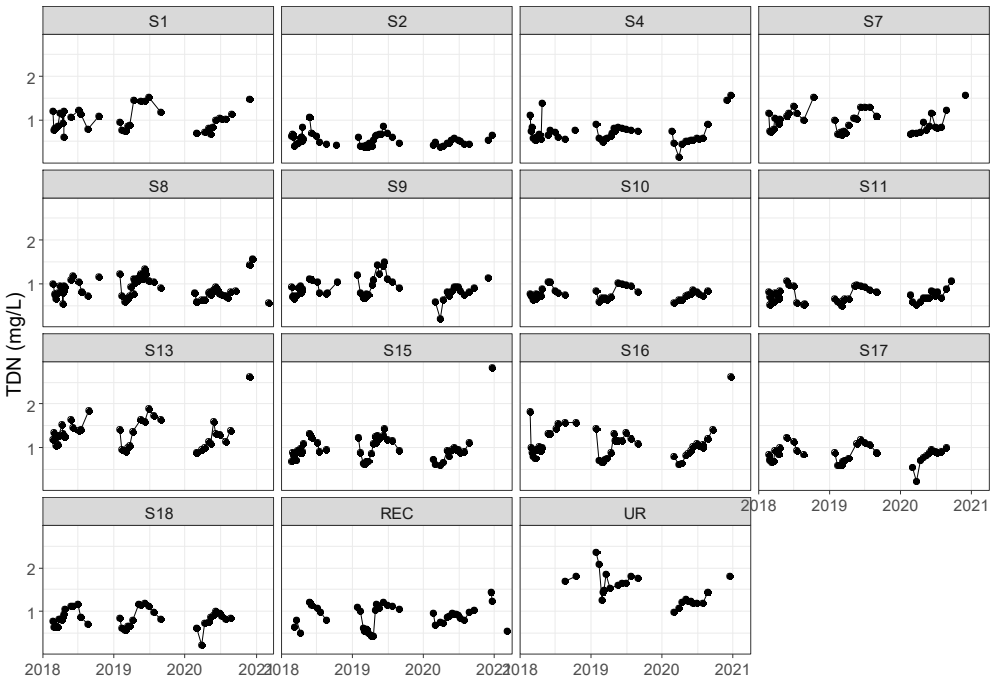

Figure B3n. TDN at URSA streams in 2018-2021.

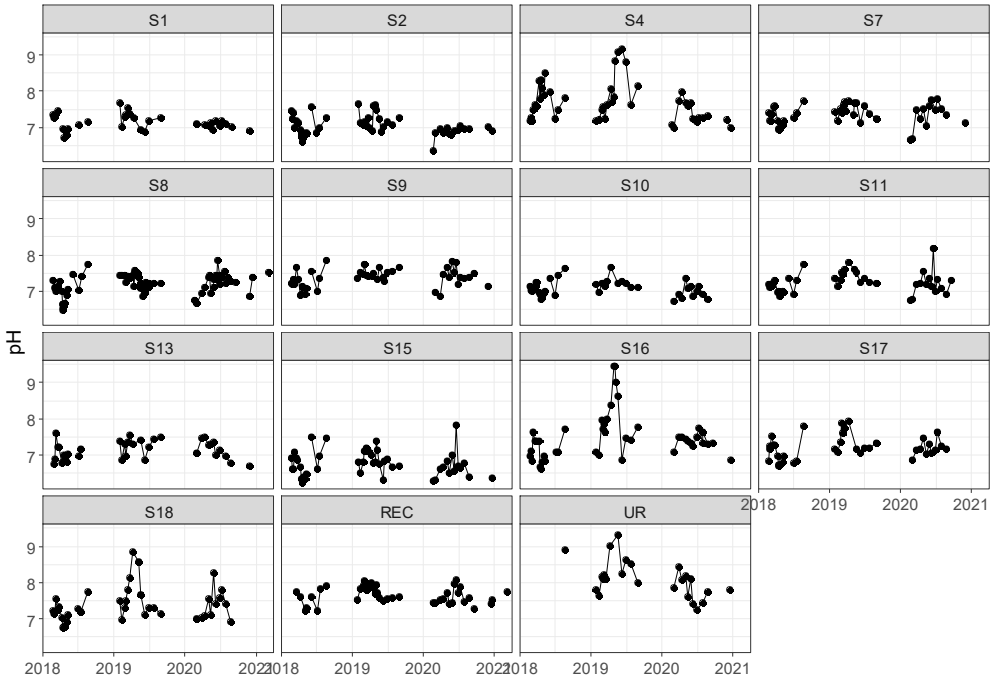

Figure B3o. pH at URSA streams in 2018-2021.

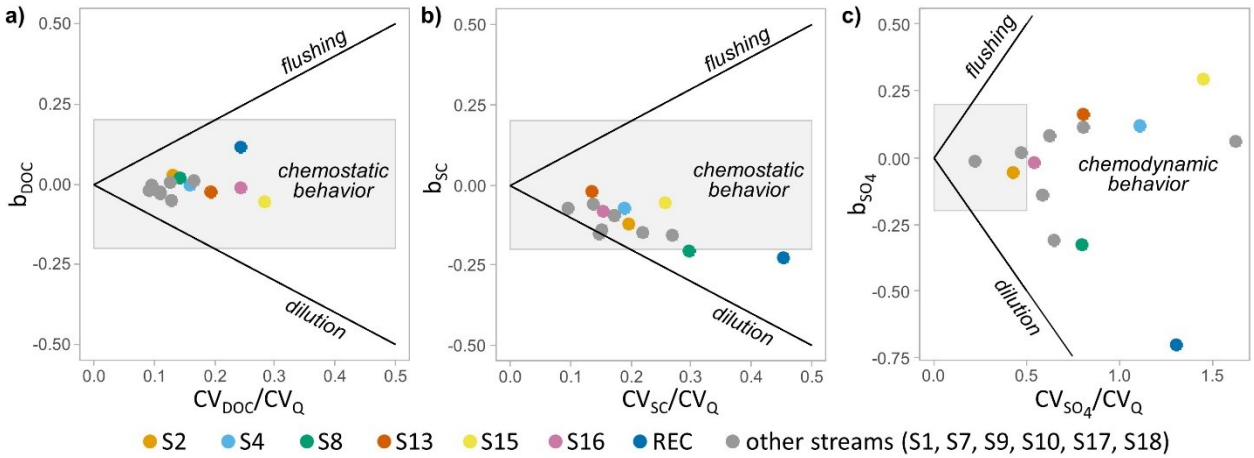

Figure B4. Behavior of solute concentrations in URSA streams. CV_C/CV_Q is the ratio of the coefficients of variance of concentration and discharge; b is the slope of the power law relationship (Cartwright et al., 2020). A chemostatic solute behavior is defined as $-0.2 < b < 0.2$ and $Cv_C/Cv_Q < 0.5$ (shaded rectangle). DOC and TDN behave chemostatically and are similar (a); SC, Ca, Mg and Na behave largely chemostatically, but some dilution can be seen with higher discharge (b); other solutes (Fe, SRP, Cl^-, SO_4^{2-}, NO_2+NO_3-N) show primarily chemodynamic behavior, with no or little trend (c).

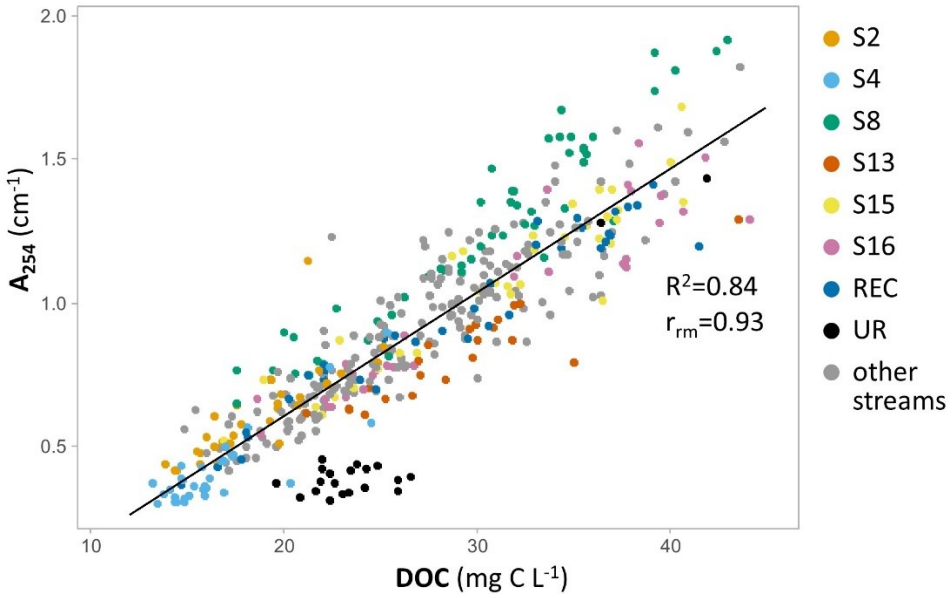

Figure B5. Strong correlation between [DOC] and A_{254}. Three outliers from February 2021 (S21, S15 and S16) are not shown in the plot, but were used to calculate correlation coefficients. R^2 is the coefficient of determination and r_{rm} is the repeated measures correlation coefficient (Bakdash and Marusich, 2017).

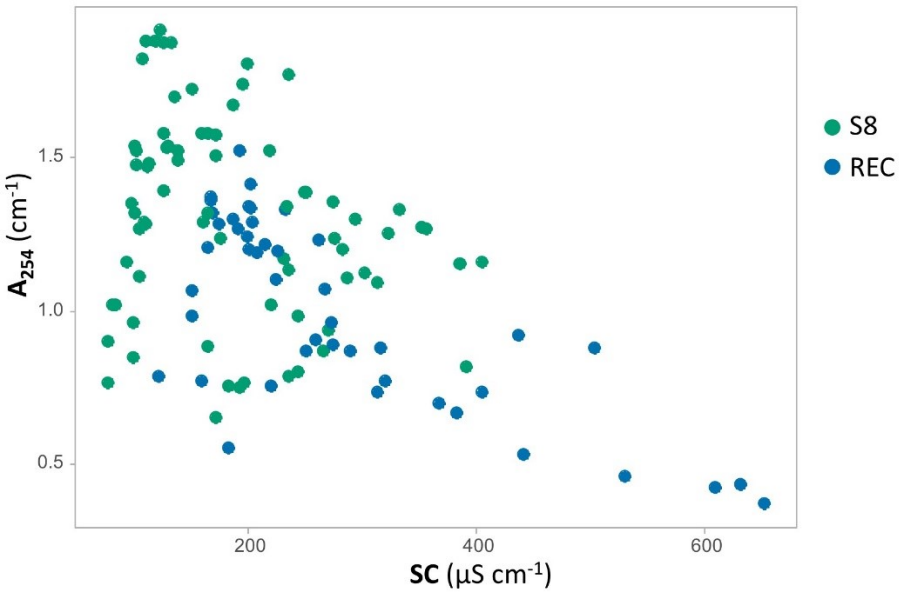

Figure B6. Relationship between A_{254} and SC for two wetland-dominates streams. The highest SC coincides with lower A_{254}, especially for REC.

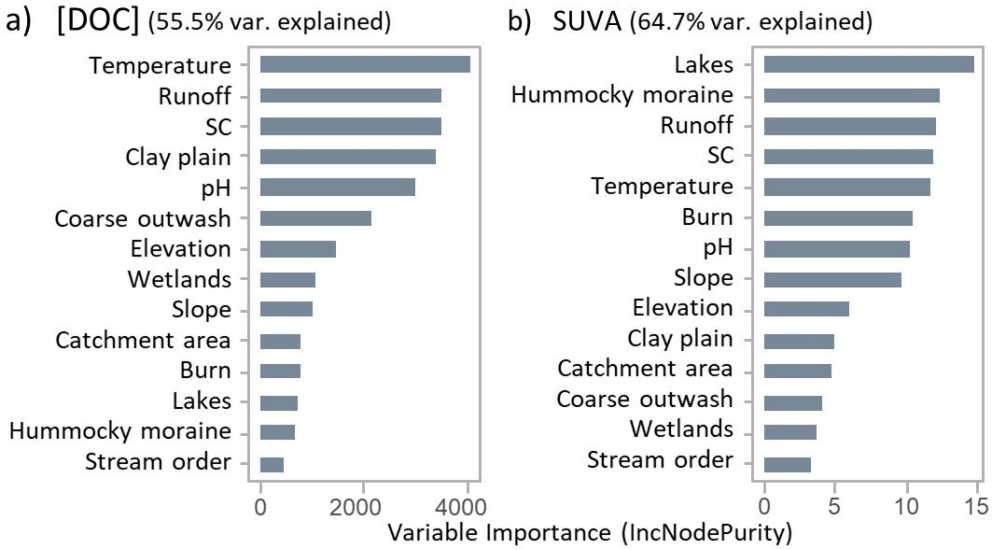

Figure B7. Random forest on [DOC] and SUVA. UR is not included. Catchment area and runoff are log-transformed.

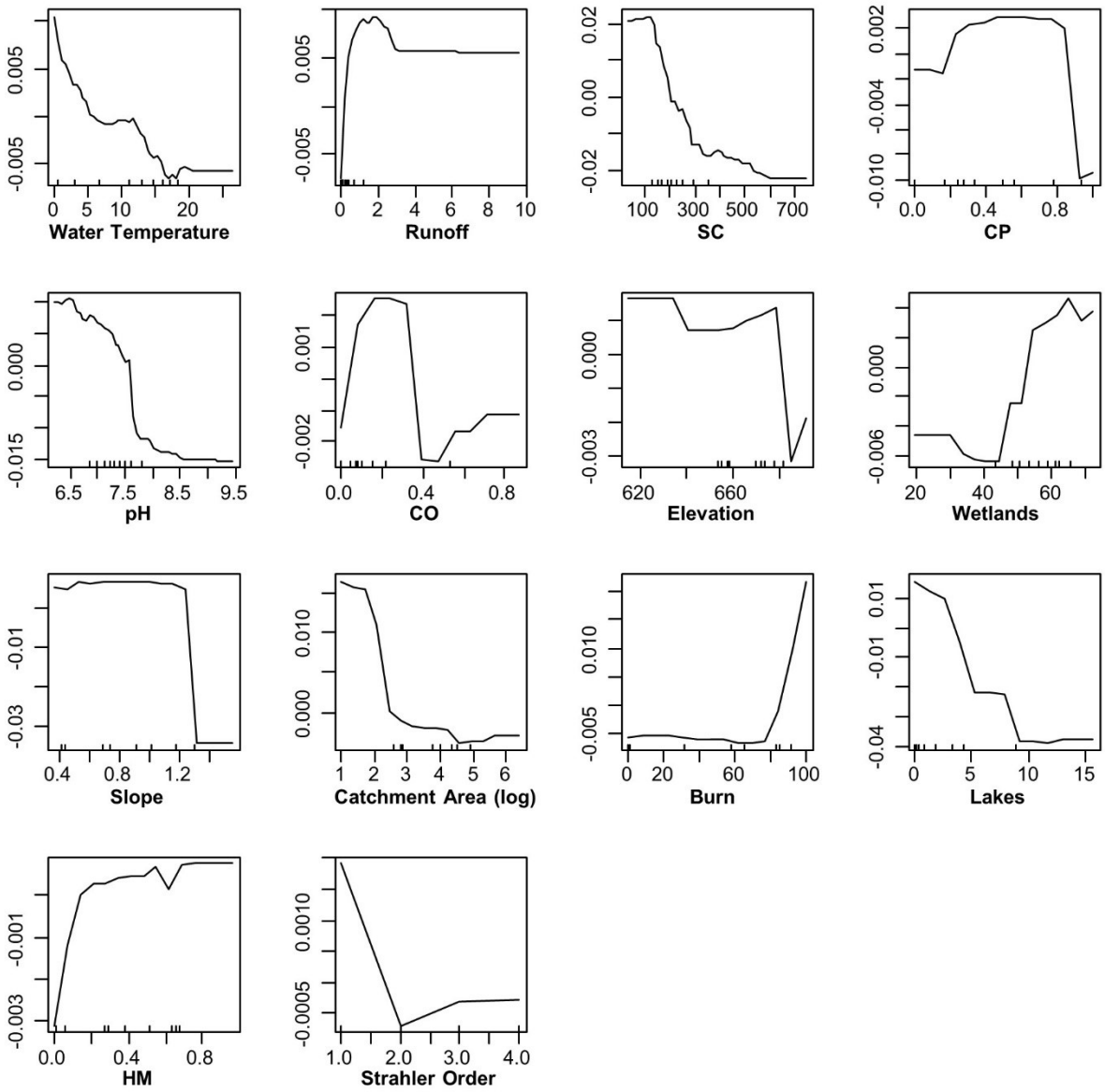

Figure B7a. Partial dependence plots for random forest model using [DOC] data.

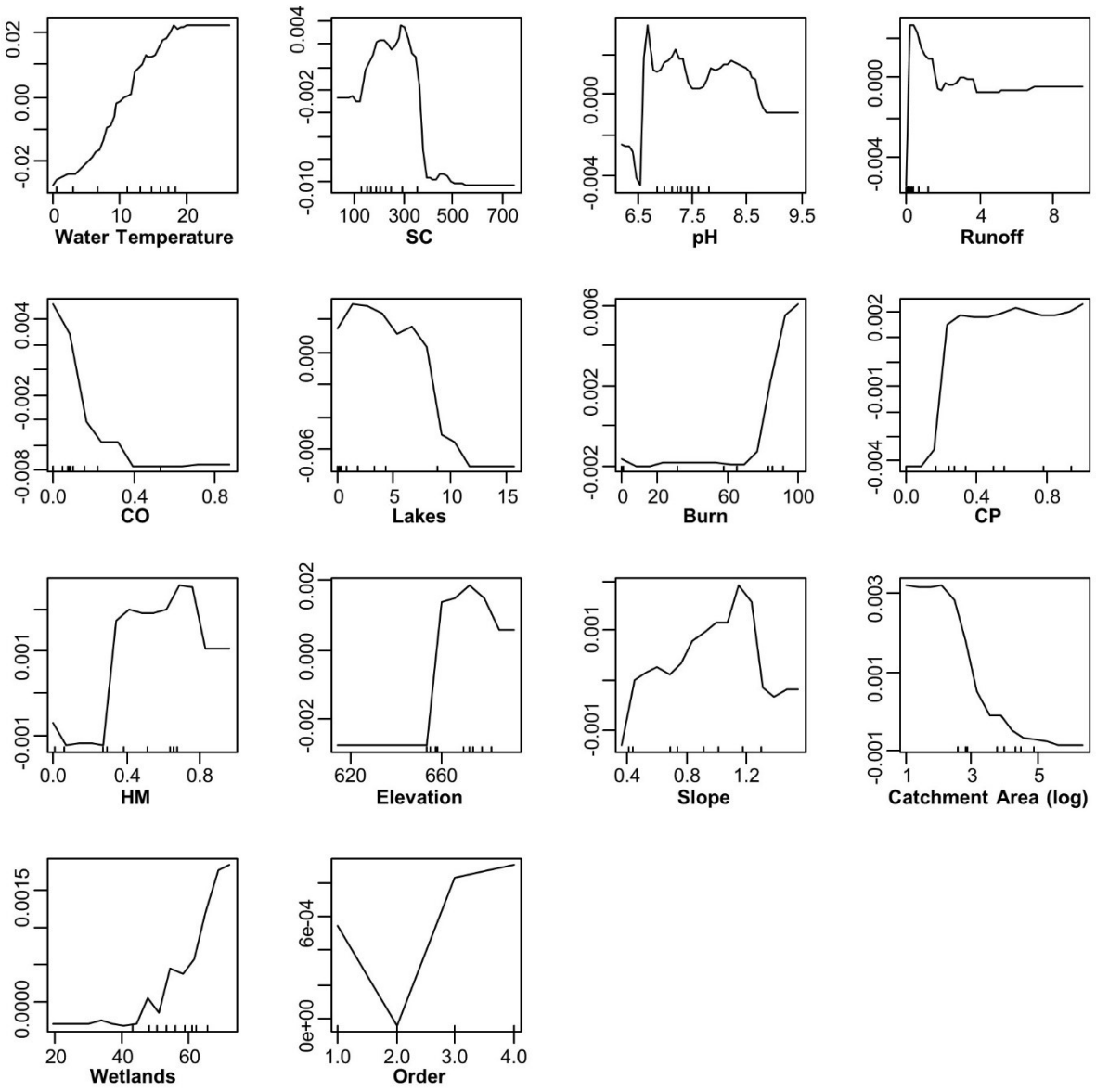

Figure B7b. Partial dependence plots for random forest model using NMDS2 scores from the NMDS on DOM composition data.

Appendix C. Supporting information for Chapter 4

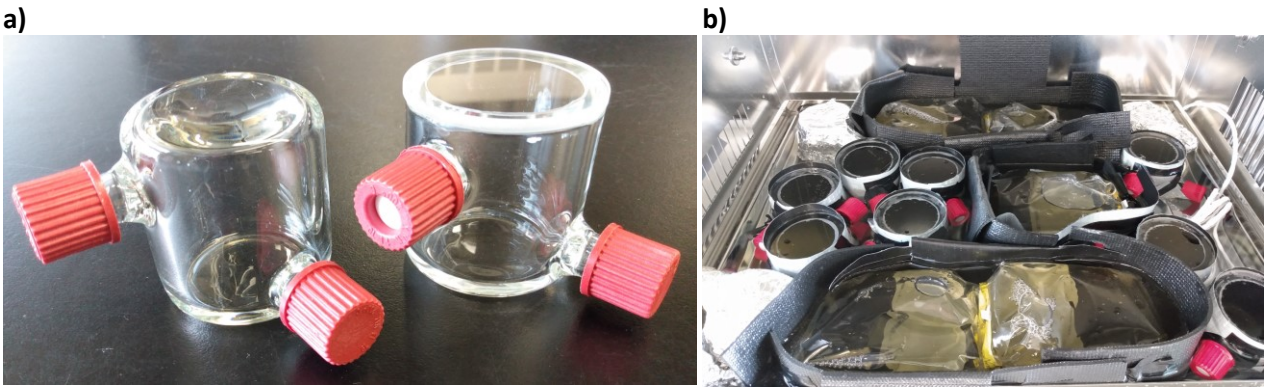

Figure C1. Photograph of the glass vial with glued-on quartz top and dark control glass vial (a) used in photodegradation experiment, following the design in Koehler et al. (2014), and a photograph of the photodegradation experiment using vials and Whirl-Pak® bags (b) used for DBP-FP analysis.

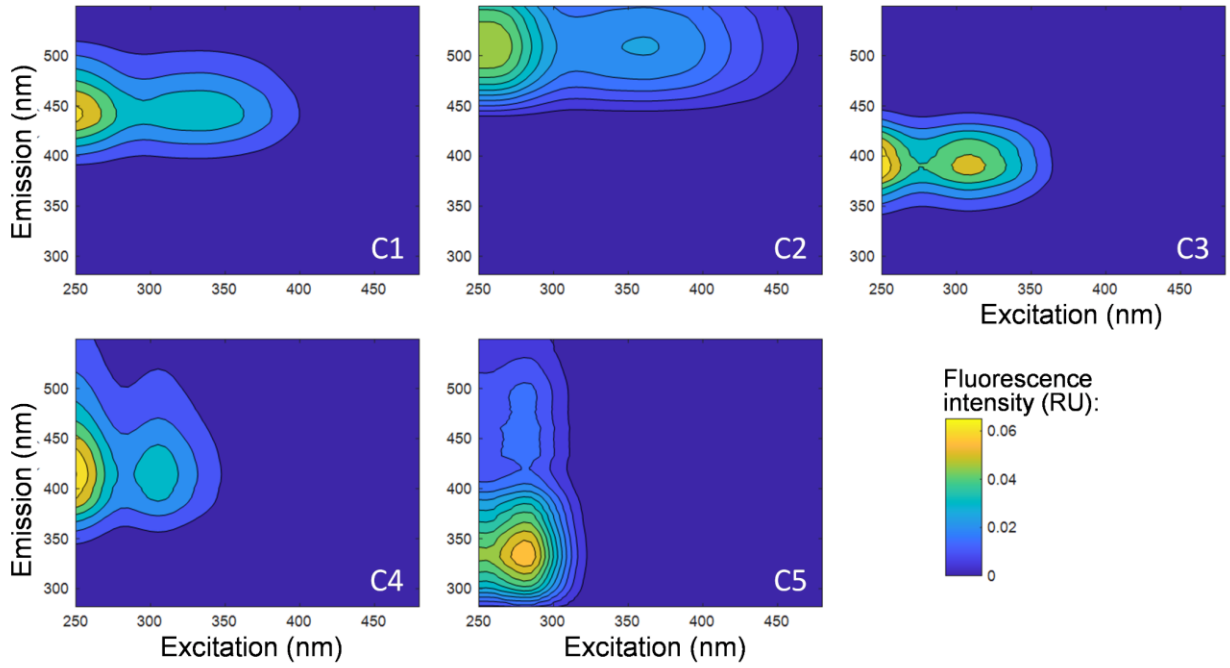

Figure C2. Fingerprint plots for validated PARAFAC components

Table C1. Dark control summary for photodegradation experiments.

	A_{254}		DOC		DIC	
Incubation duration	**24 h**	**72 h**	**24 h**	**72 h**	**24 h**	**72 h**
# of incubations with dark controls / total # of incubations	34/36	30/30	32/36	30/30	34/36	30/30
Median change (%)	-0.6	-0.6	0.1	-0.5	-0.5	-0.6
Min–max change (%)	-3.0–5.3	-1.5–2.3	-4.2–3.8	-4.5–7.8	-3.0–2.6	-8.4–0.4
# of incubations with negative change (loss) in dark control	28	26	14	18	26	19

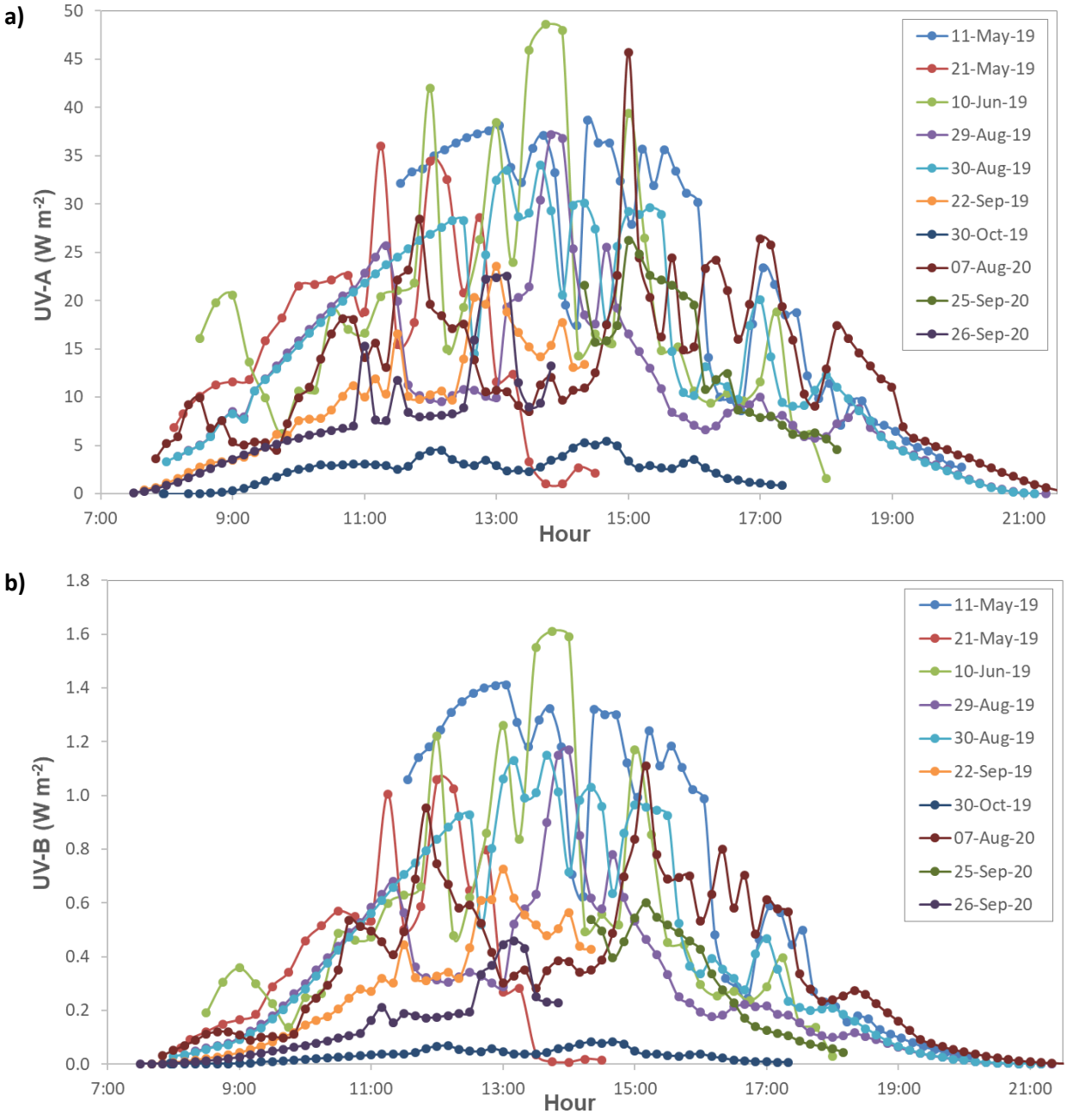

Figure C3. Field UV-A (a) and UV-B (b) measurements in 2019-2020.

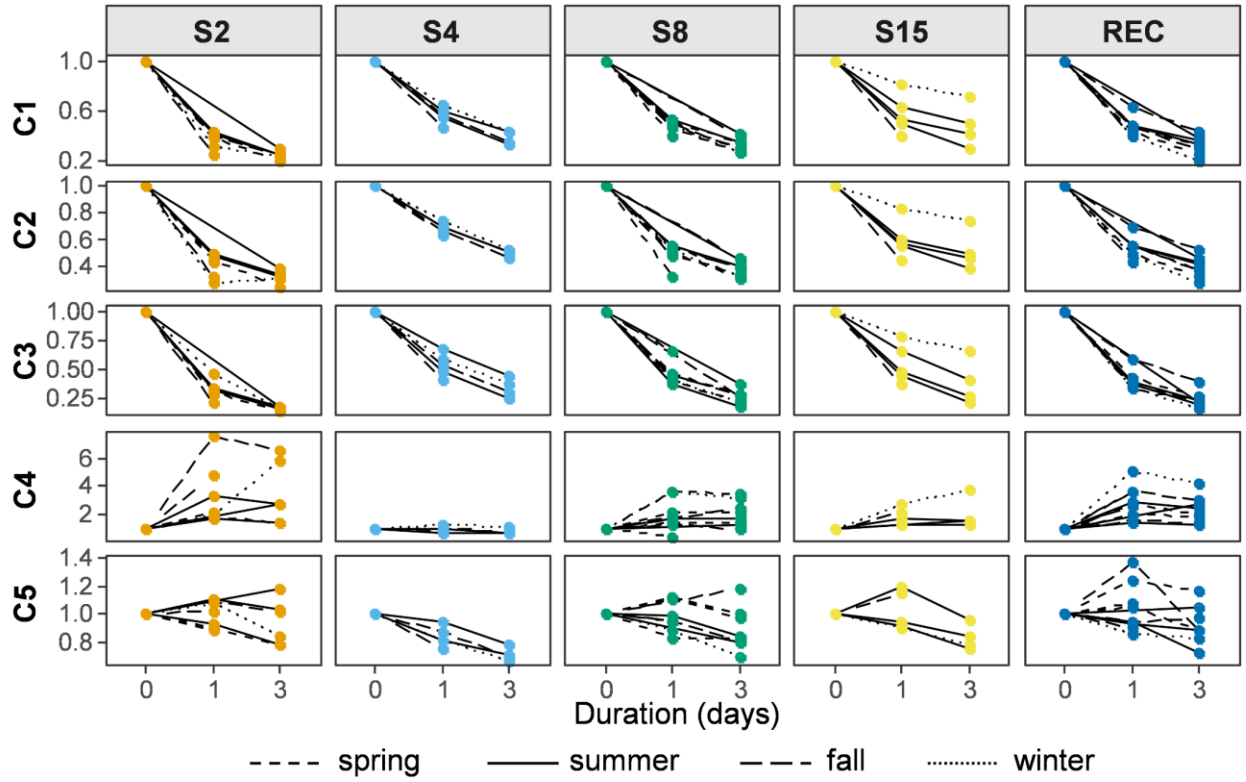

Figure C4. Change in fluorescent intensity of PARAFAC components C1 to C5 during photodegradation incubations relative to the initial concentration of 1.

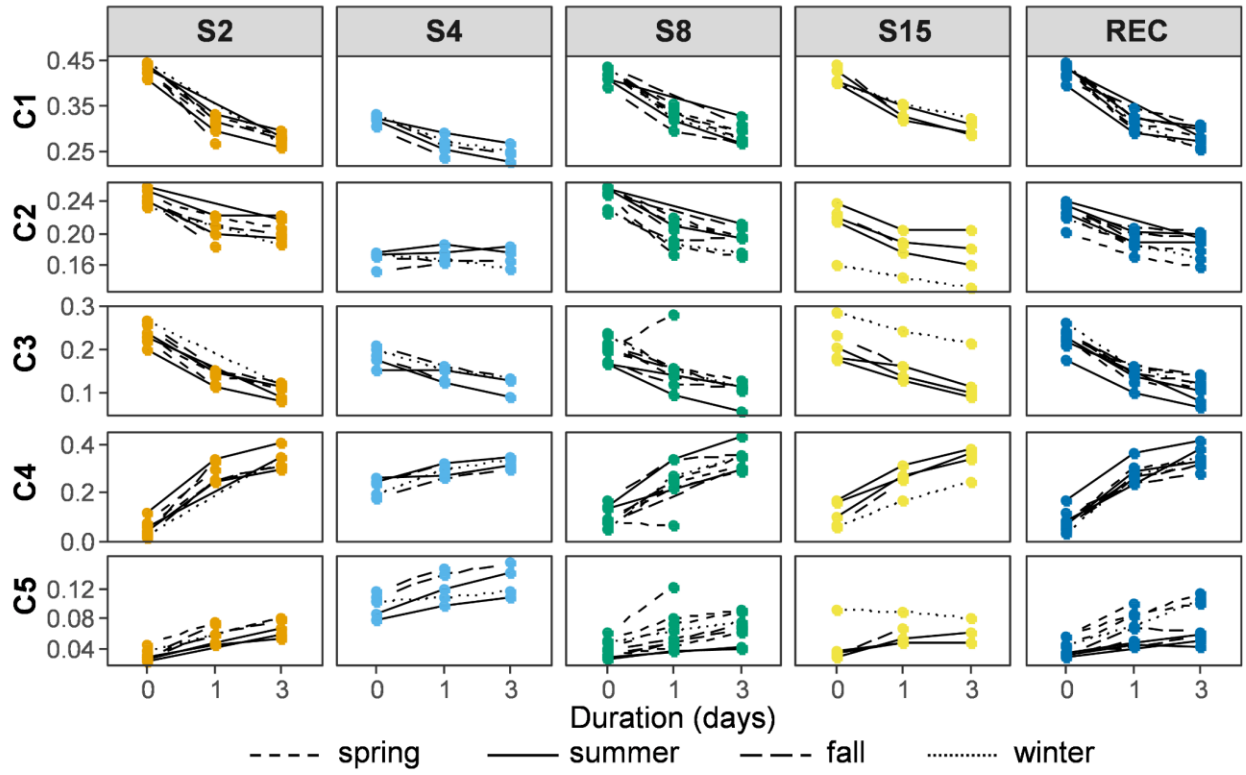

Figure C5. Proportion of PARAFAC components C1 to C5 during photodegradation incubations.

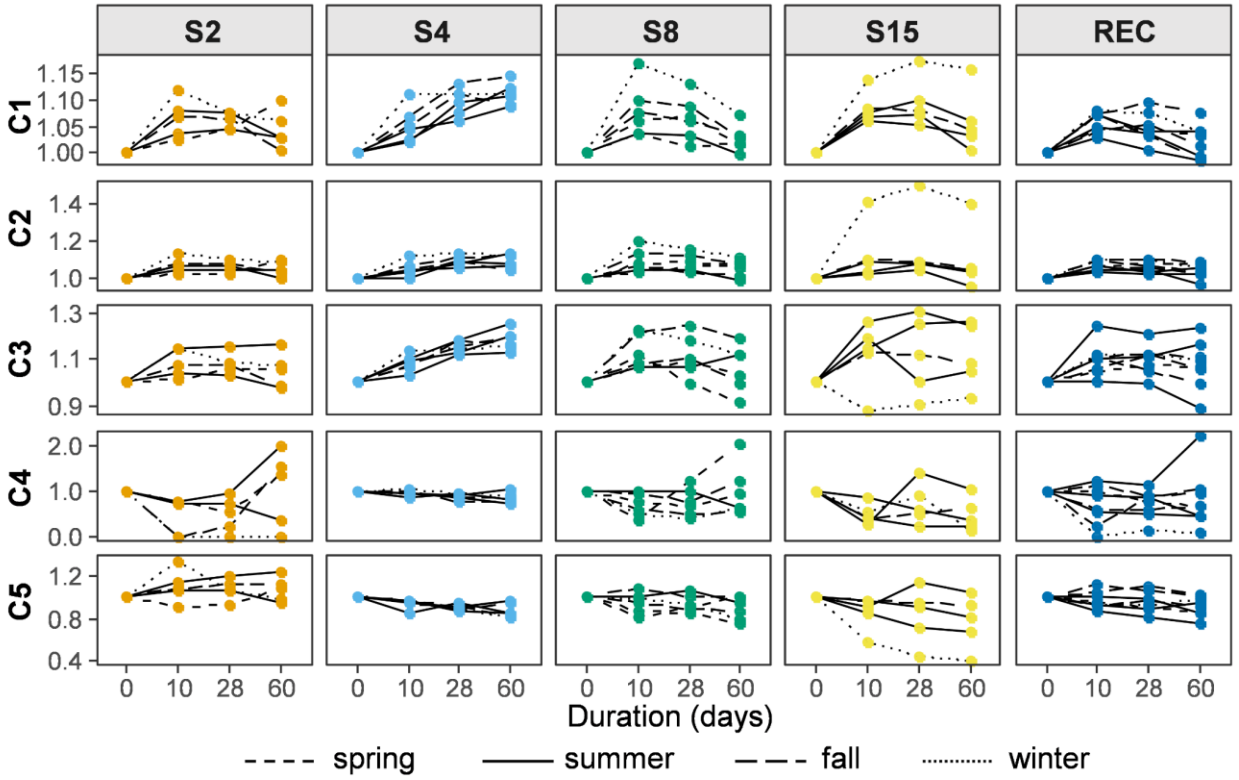

Figure C6. Change in fluorescent intensity of PARAFAC components C1 to C5 during biodegradation incubations relative to the initial concentration of 1.

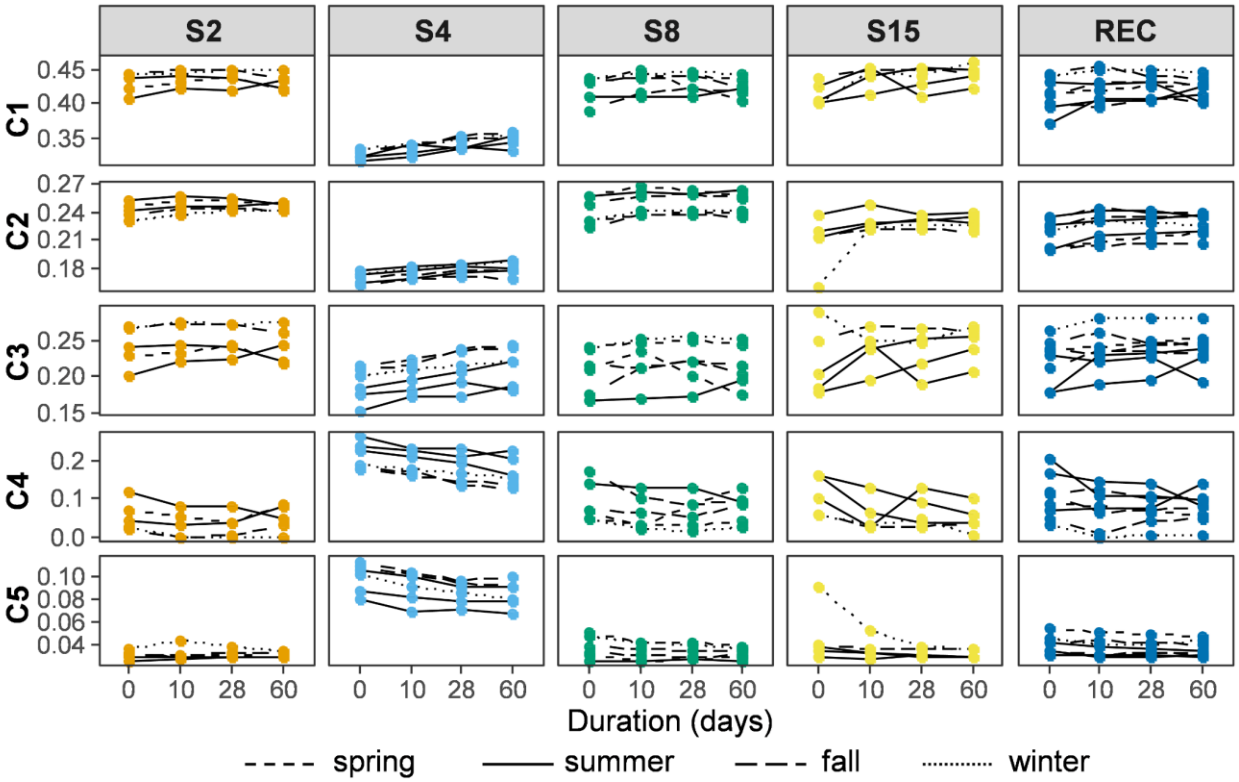

Figure C7. Proportion of PARAFAC components C1 to C5 during biodegradation incubations.

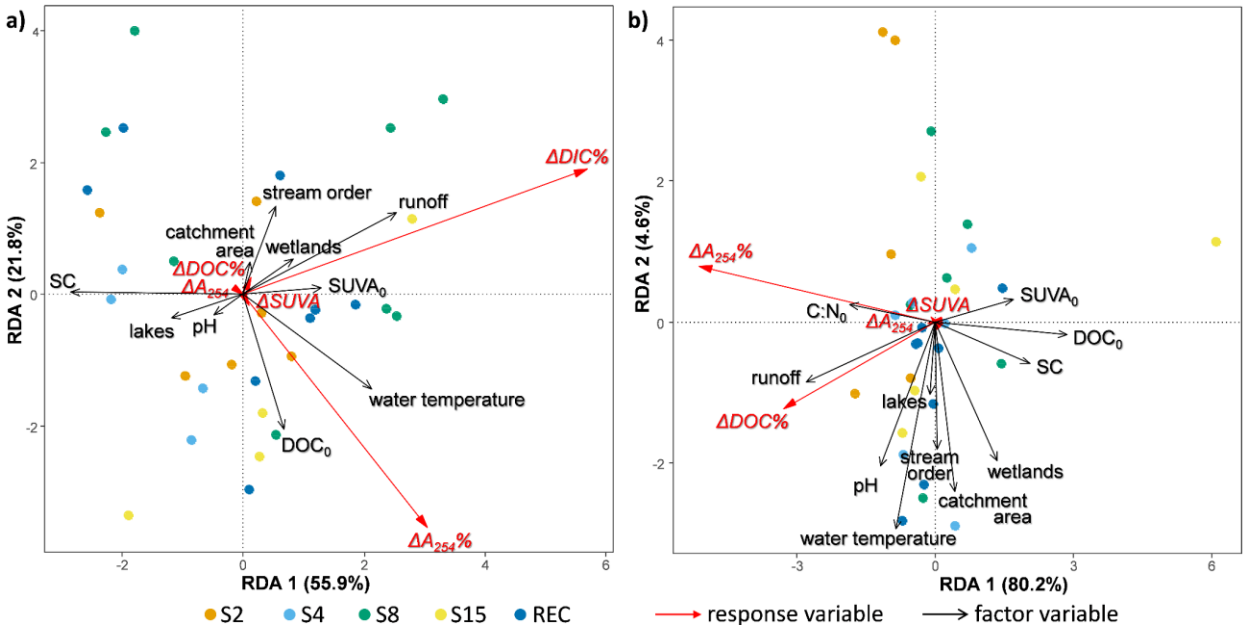

Figure C8. RDA on 3-day photodegradation data (a) and 60-day biodegradation data (b).

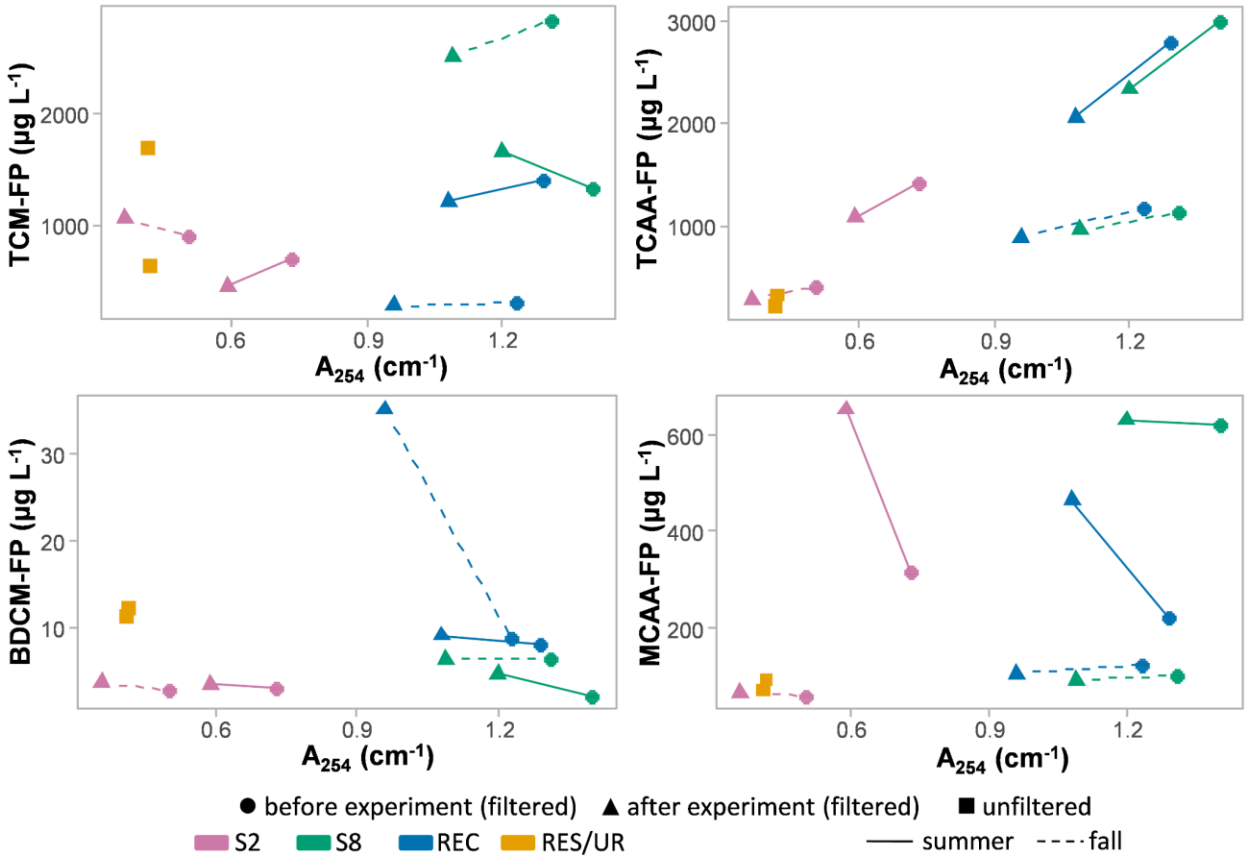

Figure C9. DBPs-FP before and after experiment in S2, S8 and REC (summer and fall 2020), as well as in RES and UR (summer 2020). DCAA-FP is not shown as the pattern is similar to HAAs-FP in Figure 4-6. Other DBPs-FP not shown usually remained below the detection limit.

Table C2. LME models for predicting absolute and relative changes in DOC, DIC, A_{254} and SUVA during photodegradation incubations.

Formula	R^2 (conditional / marginal)	AIC	Fixed effects significance	Random effect significance
All durations:				
ΔDOC% ~ R + Temp + SC + pH + wetlands + lakes + + area + (1 | Duration)	0.499/ 0.198	324.3	lakes *** pH, area * wetlands ·	***
ΔDOC% ~ pH + wetlands + lakes + area + + (1 | Duration)	0.422 / 0.138	325.9	lakes *** pH ·	***
ΔDOC% ~ pH + lakes + (1 | Duration)	0.412 / 0.126	323.1	lakes ***	***
ΔDOC% ~ lakes + $SUVA_0$ + (1 | Duration)	0.439 / 0.128	322.4	lakes ***	***
ΔA_{254}% ~ R + Temp + SC + pH + wetlands + lakes + + area + (1 | Duration)	0.684 / 0.213	418.3	Temp ** SC *	***
ΔA_{254}% ~ Temp + SC + (1 | Duration)	0.672 / 0.202	410.6	Temp, SC ***	***
ΔA_{254}% ~ Temp + SC + $SUVA_0$ + (1 | Duration)	0.672 / 0.202	412.6	Temp, SC ***	***
ΔDIC% ~ R + Temp + SC + pH + wetlands + lakes + + area + (1 | Duration)	0.660 / 0.592	429.2	R, pH, lakes ** Temp ·	**
ΔDIC% ~ R + Temp + pH + wetlands + lakes + + (1 | Duration)	0.658 / 0.591	425.5	R, pH *** wetlands, lakes ** Temp *	**
ΔDIC% ~ R + $SUVA_0$ + lakes + (1 | Duration)	0.615 / 0.558	428.2	R, $SUVA_0$ *** lakes **	*
ΔDIC% ~ R + $SUVA_0$ + (1 | Duration)	0.552 / 0.501	435.2	R, $SUVA_0$ ***	.
ΔSUVA ~ R + Temp + SC + pH + wetlands + lakes + + area + (1 | Duration)	0.594 / 0.164	67.3	Temp * SC, lakes ·	***
ΔSUVA ~ R + Temp + SC + pH + $SUVA_0$ + lakes + + (1 | Duration)	0.605 / 0.186	51.5	Temp ** lakes * SC, $SUVA_0$ ·	***
ΔSUVA ~ Temp + SC + $SUVA_0$ + lakes + + (1 | Duration)	0.603 / 0.177	40.9	Temp *** SC, $SUVA_0$ * lakes ·	***
ΔSUVA ~ Temp + SC + (1 | Duration)	0.580 / 0.134	32.0	Temp ** SC *	***
Duration = 3 days:				
ΔDOC% ~ SC + Temp + pH + R + $SUVA_0$ + (1 | Site)	0.136 / 0.088	167.1		
ΔDOC% ~ SC + Temp + R + (1 | Site)	0.189 / 0.052	170.0		
ΔDOC% ~ SC + R + (1 | Site)	0.225 / 0.048	165.1		
ΔA_{254}% ~ SC + Temp + pH + R + $SUVA_0$ + (1 | Site)	0.407 / 0.391	200.7	Temp*	
ΔA_{254}% ~ SC + R + $SUVA_0$ + (1 | Site)	0.279 / 0.233	207.4	SC ·	
ΔA_{254}% ~ R + $SUVA_0$ + (1 | Site)	0.322 / 0.169	203.5	R *	
ΔA_{254} ~ SC + Temp + pH + R + (1 | Site)	0.678 / 0.315	-28.8	SC *	**
ΔA_{254} ~ SC + Temp + R + (1 | Site)	0.694 / 0.323	-34.8	SC *	***
ΔA_{254} ~ SC + Temp + (1 | Site)	0.694 / 0.329	-44.1	SC ***	***
ΔA_{254} ~ SC + R + (1 | Site)	0.695 / 0.318	-47.4	SC *	***
ΔA_{254} ~ SC + pH + (1 | Site)	0.681/ 0.328	-50.9	SC ***	***
ΔSUVA ~ SC + Temp + pH + R + $SUVA_0$ + (1 | Site)	0.346 / 0.307	54.8	Temp *	
ΔSUVA ~ SC + Temp + pH + R + (1 | Site)	0.337 / 0.307	50.8	Temp *	
ΔSUVA ~ SC + Temp + pH + (1 | Site)	0.344 / 0.315	44.8	Temp *	
ΔSUVA ~ Temp + R + (1 | Site)	0.317 / 0.306	34.0	Temp **	
ΔDIC% ~ SC + Temp + pH + R + $SUVA_0$ + (1 | Site)	0.810 / 0.599	186.7	R ** Temp, pH *	*
ΔDIC% ~ SC + Temp + pH + R + (1 | Site)	0.834 / 0.537	189.7	Temp, pH, R **	***

Formula	R^2 (conditional / marginal)	AIC	Fixed effects significance	Random effect significance
ΔDIC% ~ Temp + pH + R + (1 | Site)	0.838 / 0.544	181.9	Temp, pH ** R ***	***
ΔDIC% ~ R + pH + (1 | Site)	0.786 / 0.418	187.3	R ***	**

Table C3. LME models for predicting absolute and relative changes in DOC, DIC, A_{254} and SUVA during biodegradation incubations.

Formula	R^2 (conditional / marginal)	AIC	Fixed effects significance	Random effect significance
All durations:				
ΔDOC% ~ R + Temp + SC + pH + C/N_0 + $SUVA_0$ + + wetlands + lakes + area + (1|Duration)	0.608 / 0.137	487.0		***
ΔDOC% ~ R + Temp + SC + pH + wetlands + lakes + area + (1 | Duration)	0.592 / 0.122	486.4	SC ** area, Temp ·	***
ΔDOC% ~ Temp + SC + area + (1 | Duration)	0.580 / 0.110	480.9	SC, area ** Temp ·	***
ΔDOC% ~ Temp + SC + (1 | Duration)	0.544 / 0.075	487.8	SC, Temp *	***
ΔDOC% ~ Temp + SC + area + $SUVA_0$ + + (1 | Duration)	0.580 / 0.110	482.8	SC, area ** Temp ·	***
ΔDOC ~ Temp + SC + area + C/N_0 + (1 | Duration)	0.591 / 0.121	480.6	SC, area **	***
ΔDOC ~ Temp + (1 | Duration)	0.519 / 0.051	488.2		***
ΔA_{254}% ~ R + Temp + SC + pH + wetlands + lakes + + area + (1 | Duration)	0.773 / 0.206	431.0	Temp, SC, lakes *** wetlands, pH ·	***
ΔA_{254}% ~ Temp + SC + wetlands + lakes + + (1 | Duration)	0.750 / 0.183	433.2	Temp, SC *** wetlands, lakes *	***
ΔA_{254}% ~ Temp + SC + (1 | Duration)	0.724 / 0.158	437.4	Temp, SC ***	***
ΔA_{254}% ~ Temp + SC + $SUVA_0$ + (1 | Duration)	0.729 / 0.162	438.1	Temp, SC ***	***
ΔA_{254} ~ Temp + SC + lakes + (1 | Duration)	0.738 / 0.171	435.2	Temp, SC *** lakes *	***
ΔA_{254} ~ Temp + (1 | Duration)	0.623 / 0.059	461.6	Temp ***	***
Duration = 60 days:				
BDOC ~ SC + Temp + R + $SUVA_0$ + pH + (1 | Site)	0.317 / 0.269	160.9		
BDOC ~ SC + Temp + R + (1 | Site)	0.292 / 0.249	163.1	Temp ·	
BDOC ~ Temp + SC + C/N_0 + (1 | Site)	0.253 / 0.221	167.6		
BDOC ~ Temp + SC + R + C/N_0 + (1 | Site)	0.302 / 0.261	167.8		
BDOC ~ Temp + R + (1 | Site)	0.282 / 0.257	153.4	R*, Temp ·	
BDOC ~ $SUVA_0$ + R + (1 | Site)	0.204 / 0.181	150.8	R*	
BDOC ~ SC + Temp + (1 | Site)	0.232 / 0.199	163.2	Temp ·	

Notes:

- significance codes: *** $p<0.001$; ** $p<0.01$; * $p<0.05$; · $p<0.1$
- Δ = absolute change in parameter during incubation; Δ% = relative (percent) change in parameter during incubation
- $SUVA_0$ and C/N_0– initial SUVA and C/N
- area and runoff data were log-transformed